University of Nottingham

Doctoral Thesis

The Combinatorics of Lattice Polytopes

Author:
Thomas Francis Hall

Supervisors:
Dr. Alexander Kasprzyk
and Dr. Johannes Hofscheier

A thesis submitted in fulfillment of the requirements for the degree of Doctor of Philosophy

July 1, 2024

Abstract

We first study the nearly Gorensteinness of Ehrhart rings arising from lattice polytopes. We give necessary conditions and sufficient conditions on lattice polytopes for their Ehrhart rings to be nearly Gorenstein. Using this, we give an efficient method for constructing nearly Gorenstein polytopes. Moreover, we determine the structure of nearly Gorenstein 0/1-polytopes.

Next, we introduce a new constant associated to a Fano polygon, called the PCR index, and prove that it is invariant under mutation. We obtain a convenient formula for the PCR index in terms of the lengths and heights of the edges of the polygon and apply this to show that two given Fano polygons with the same singularity content are not mutation-equivalent. Finally, we give an alternative way to classify the minimal Fano triangles which have empty basket of singularities; we accomplish this using Markov-like Diophantine equations.

Then, we study a subclass of Kähler-Einstein Fano polygons and how they behave under mutation. The polygons of interest are Kähler-Einstein Fano triangles and symmetric Fano polygons, which were recently conjectured to constitute all Kähler-Einstein Fano polygons. We show that all polygons in this subclass are minimal and that each mutation-equivalence class has at most one Fano polygon belonging to this subclass. Finally, we provide counterexamples to the aforementioned conjecture and discuss several of their properties.

Finally, we study generalised flatness constants of lattice polytopes. Let $A \in \{\mathbb{Z}, \mathbb{R}\}$ and $X \subset \mathbb{R}^d$ be a bounded set. Affine transformations given by an automorphism of $\mathbb{Z}^d$ and a translation in A^d are called (affine) A-unimodular transformations. The image of X under such a transformation is called an A-unimodular copy of X. It was shown in [7] that every convex body whose width is "big enough" contains an A-unimodular copy of X. The threshold when this happens is called the generalised flatness constant $\mathrm{Flt}_d^A(X)$. It resembles the classical flatness constant if $A = \mathbb{Z}$ and X is a lattice point. We introduce a general framework for the explicit computation of these numerical constants. The approach relies on the study of A-X-free convex bodies generalising lattice-free (also known as hollow) convex bodies. We then focus on the case that $X = P$ is a full-dimensional polytope and show that inclusion-maximal A-P-free convex bodies are polytopes. The study of those inclusion-maximal polytopes provide us with the means to explicitly determine generalised flatness constants. We apply our approach to the case $X = \Delta_2$ the standard simplex in $\mathbb{R}^2$ of normalised volume 1 and compute $\mathrm{Flt}_2^{\mathbb{R}}(\Delta_2) = 2$ and $\mathrm{Flt}_2^{\mathbb{Z}}(\Delta_2) = \frac{10}{3}$.

Acknowledgements

I would first like to thank my wonderful supervisors, Alexander Kasprzyk and Johannes Hofscheier, for their generosity of time and ideas. I am grateful for their enthusiasm and guidance throughout my PhD, and for pushing me to achieve my best. I would also like to thank Akihiro Higashitani for being an accommodating and keen host during my research visit to Osaka.

I'd like to thank all the friends I've met along the way, for adding meaning to the journey and providing an escape when I needed it. I'd finally like to thank my family for their loving support and belief in me while I undertook this challenge.

Contents

Chapter 1

Introduction

1.1 Convex geometry

The main objects of study in this thesis are (convex) lattice polytopes. They crop up in many different areas of mathematics, such as algebra, geometry, optimisation, and physics. In this section, we recall the definitions of several important notions in convex geometry and the geometry of numbers, which include lattices, polytopes, and cones. We also give several of their fundamental properties, which will be useful in the main chapters.

1.1.1 Lattices, cones, and polytopes

Definition 1.1.1. A *d-dimensional lattice* is a free, finitely-generated $\mathbb{Z}$-module of rank d.

So really, a lattice is just isomorphic to the $\mathbb{Z}$-module $\mathbb{Z}^d$. The i-th standard basis vector of the lattice $\mathbb{Z}^d$ is denoted as $\boldsymbol{e}_i$, for $i = 1, 2, \ldots, d$. We also typically denote the lattice point $a_1\boldsymbol{e}_1 + a_2\boldsymbol{e}_2 + \cdots + a_d\boldsymbol{e}_d \in \mathbb{Z}^d$ as the *column vector* $(a_1, a_2, \ldots, a_d)$.

We now recall the notion of duality for lattices. For a lattice L, its dual is defined as $L^* := \mathrm{Hom}(L, \mathbb{Z})$, and is isomorphic to L itself. The i-th standard basis vector of $(\mathbb{Z}^d)^*$ is denoted as e_i^*. We typically denote the lattice point $u_1e_1^* + u_2e_2^* + \cdots + u_de_d^* \in (\mathbb{Z}^d)^*$ as the *row vector* $(u_1, u_2, \ldots, u_d)^t$. Further, we identify the lattice $(L^*)^*$ with L.

A subtle point to make is that matrices act on points in L from the left whereas they act on points in the dual space L^* from the right.

Now, just as the lattice $\mathbb{Z}^d$ lives inside the vector space $\mathbb{Q}^d$ (and also $\mathbb{R}^d$), we would also like to have a $\mathbb{Q}$-or $\mathbb{R}$-vector space for any lattice to live inside. This is because we need a space where our cones and polytopes will live.

Definition 1.1.2. Let L be a lattice and $k \in \{\mathbb{Q}, \mathbb{R}\}$. Then its *k-extension* is the k-vector space $L_k := L \otimes_{\mathbb{Z}} k$. By abuse of notation, we say that $L \subset L_{\mathbb{Q}} \subset L_{\mathbb{R}}$.

We may similarly extend the dual lattice to a vector space: L_k^*, which is isomorphic to k^d.

Remark 1.1.3. If L has dimension d, then L_k also has dimension d, i.e. $L_k \cong k^d$.

Now that we have defined the ambient spaces where our objects will live, let us recall what a cone is. For the rest of this subsection, fix a lattice L and an ordered field $k \in \{\mathbb{Q}, \mathbb{R}\}$. We define $k_{\geq 0} := \{x \in k : x \geq 0\}$. For a subset $S \subset L_k$, we denote by ∂S, $\mathrm{int}(S)$, and $\mathrm{rel}(S)$ as the boundary of S, the (strict) interior of S, and the relative interior of S, respectively, all with respect to the standard Euclidean topology on $L_k \cong k^d$.

Definition 1.1.4. For some subset $S \subseteq L_k$, the *cone over* S is defined as

$$\mathrm{cone}(S) := \left\{ \sum_{i=0}^{n} q_i \boldsymbol{x}_i : q_i \in k_{\geq 0}, \boldsymbol{x}_i \in S, n \in \mathbb{Z}_{\geq 0} \right\} \subseteq L_k,$$

i.e. it is the set of all finite $k_{\geq 0}$-linear combinations of points in S. The set $\sigma \subseteq L_k$ is called a *cone* if there exists some subset $S \subseteq L_k$ such that $\sigma = \mathrm{cone}(S)$. In this case, S is said to *generate* σ. If a set S of generators of a cone σ is minimal with respect to inclusion, then it is called a set of *ray generators* of σ.

In this thesis, unless stated otherwise, we only consider cones having certain nice properties, which we now define.

Definition 1.1.5. Let $\sigma \subseteq L_k$ be a cone. Then σ is called *pointed* (or *strongly convex*) if there is no line contained in it, i.e. $\sigma \cap -\sigma = \{\mathbf{0}\}$. It is called *polyhedral* (or *finitely generated*) if there exists some finite set $S = \{\boldsymbol{x}_0, \boldsymbol{x}_1, \ldots, \boldsymbol{x}_m\}$ such that $\sigma = \mathrm{cone}(S)$. In this case, we may write $\sigma = \mathrm{cone}\{\boldsymbol{x}_0, \boldsymbol{x}_1, \ldots, \boldsymbol{x}_m\}$. Finally, σ is called *rational* if it is generated by a subset of L.

Example 1.1.6. Consider the cone σ generated by the lattice points $(1, 2)$, $(1, 1)$, and $(4, -3)$. It is clearly polyhedral and rational, since it is generated by a finite number of lattice points. As can be seen from Figure 1.1, it is also pointed. A set of ray generators for the cone σ is $\{(1, 2), (4, -3)\}$; the point $(1, 1)$ is redundant as a generator of σ. Finally, we remark that all cones of dimension less than three are polyhedral; the exact notion of dimension for cones is given later on (Definition 1.1.8). Further, in these dimensions, the only non-pointed cones are half-spaces.

From now on, we assume that all cones are pointed, polyhedral and rational. We can now recall what a face of a cone is.

Definition 1.1.7. Let $\sigma, \tau \subset L_k$ be cones. Then τ is a *face of* σ if there exists some $m \in L_k^*$ such that $\tau = \sigma \cap \partial H_m$ and $\sigma \subset H_m$, where $H_m = \{\boldsymbol{x} \in L_k : m(\boldsymbol{x}) \geq 0\}$. Further, if $\tau \neq \sigma$, then τ is called a *proper face of* σ. Note that σ is always a face of itself, via $m = 0$.

It now makes sense to introduce the notion of dimension for cones.

Definition 1.1.8. Let $\sigma \subset L_k$ be a cone. Then its *dimension* is equal to the dimension of the subspace of L_k linearly spanned by the points of σ.

We note that the only zero-dimensional face of a cone is $\{\mathbf{0}\}$. The one-dimensional faces (i.e. the *rays*) of a cone are simply the cones over the ray generators of σ.

Now, just as there is a notion of duality for lattices, there is also one for cones. While we have defined cones in terms of its rays, we may also define them in terms of their *facets*, i.e. their maximal dimensional faces.

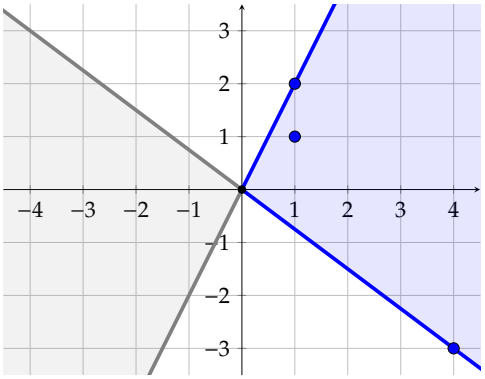

FIGURE 1.1: The cone σ from Example 1.1.6 and one collection of generators for it are in blue. The cone $-\sigma$ is in grey. It is clear that σ and $-\sigma$ intersect only at the origin; thus, σ is pointed.

Definition 1.1.9. Let $\sigma \subset L_k$ be a cone. Then its *dual cone* is defined as

$$\sigma^\vee := \left\{u \in L_k^* : \ u(\boldsymbol{x}) \geq 0, \ \forall \boldsymbol{x} \in \sigma\right\} \subset L_k^*.$$

It can be shown that if σ is *full-dimensional*, i.e. its dimension coincides with the ambient dimension, the dimension d of L_k, then $\sigma^\vee$ is a cone, i.e. a pointed, rational, polyhedral cone. Otherwise, if the dimension of σ is less than d, then the dual cone $\sigma^\vee$ will not be pointed.

Now, there exists a finite collection of lattice points $u_1, u_2, \ldots, u_m \in L^*$ such that $\sigma^\vee = \text{cone}\,\{u_1, u_2, \ldots, u_m\}$. Assuming that σ is full-dimensional, if this collection of lattice points is minimal with respect to inclusion, then each u_i is normal to a facet of σ. Further, each ray generator of σ corresponds to a facet of $\sigma^\vee$. In fact, the duality is even stronger: each i-dimensional face of σ corresponds to a $(d-i)$-dimensional face of $\sigma^\vee$ in a way which we now make precise.

Definition 1.1.10. Let $\sigma \subset L_k$ be a cone and $\boldsymbol{x}$ be a point of σ. Then the *(inner) normal cone of σ at $\boldsymbol{x}$* is defined as

$$N_\sigma(\boldsymbol{x}) := \left\{u \in \sigma^\vee : \ u(\boldsymbol{x}) = 0\right\} \subset L_k^*.$$

Let τ be a face of σ. Then the *(inner) normal cone of σ at τ* is defined as

$$N_\sigma(\tau) := \bigcap_{\boldsymbol{x} \in \tau} N_\sigma(\boldsymbol{x}).$$

Example 1.1.11. Consider the cone $\sigma \subset \mathbb{R}^3$ with ray generators $(2,-1,0)$, $(0,1,0)$, and $(0,0,1)$. Let ρ_0, ρ_1, and ρ_2 be the respective rays of σ. Let τ be the facet of σ spanned by ρ_0 and ρ_1; we aim to compute the normal cone of σ at τ. In order to do so, we must first compute $N_\sigma(\rho_0)$ and $N_\sigma(\rho_1)$.

We note that $N_\sigma(\rho_0) = N_\sigma((2,-1,0))$ and $N_\sigma(\rho_1) = N_\sigma((0,1,0))$. This follows from the fact that σ is invariant under scaling by elements of $k_{\geq 0}$. We show in some detail how to compute $N_\sigma((2,-1,0))$. First, we must find $u \in L_k^*$ satisfying $u(2,-1,0) = 0$.

We obtain that $u = (a, 2a, c)^t$, for some $a, c \in \mathbb{Z}$. Finally, we must determine when u belongs to the dual cone $\sigma^\vee$. We require that u evaluated on the generators of σ are non-negative. On $(2, -1, 0)$, it always evaluates to 0. Next, we have $u(0, 1, 0) = 2a$ and $u(0, 0, 1) = c$. These must be non-negative; thus, it follows that $N_\sigma(\rho_0) = \text{cone}\left\{(1, 2, 0)^t, (0, 0, 1)^t\right\}$.

Similarly, we find that $N_\sigma(\rho_1) = \text{cone}\left\{(1, 0, 0)^t, (0, 0, 1)^t\right\}$. Thus, we may now compute that $N_\sigma(\tau)$ is the ray generated $(0, 0, 1)^t$.

Proposition 1.1.12 (cf. [107, Theorem 1.3])**.** *Let $\sigma \subset L_k$ be a full-dimensional cone, i.e. $\dim(\sigma) = \dim(L_k) = d$. Then there is a one-to-one correspondence between the i-dimensional faces of σ and the $(d - i)$-dimensional faces of its dual $\sigma^\vee$. This is given by $\tau \mapsto N_\sigma(\tau)$. Further, this correspondence is inclusion-reversing.*

Finally, we recall what it means for two cones to be isomorphic.

Definition 1.1.13. Let $\sigma_1, \sigma_2 \subset L_k$ be cones. Then σ_1 is *isomorphic* to σ_2 if there exists some unimodular matrix $U \in \text{GL}_d(\mathbb{Z})$ such that $U\sigma_1 = \sigma_2$.

We will soon recall the notion of a polytope. As with cones, there are two dual ways of defining a polytope: either in terms of its vertices (i.e. its zero-dimensional faces) or in terms of its facets (i.e. its codimension one faces). We first define polytopes in terms of their vertices.

Definition 1.1.14 ([107, Definition 0.1])**.** For some subset $S \subseteq L_k$, the *convex hull of S* is defined as

$$\text{conv}(S) := \left\{ \sum_{i=0}^{n} q_i \boldsymbol{x}_i \ : \ \sum_{i=0}^{n} q_i = 1,\ q_i \in k_{\geq 0}, x_i \in S, n \in \mathbb{Z}_{\geq 0} \right\} \subseteq L_k,$$

The (convex) set $P \subseteq L_k$ is said to be a *polytope* if there exists some finite set $S \subset L_k$ such that $P = \text{conv}(S)$. In this case, if S is the minimal such set with respect to inclusion, then the *vertices of P* are $\mathcal{V}(P) = S$.

The second description of polytopes involves their facets.

Proposition 1.1.15 (cf. [107, Theorem 1.1])**.** *Let $P \subset L_k$ be a polytope. Then there exists a finite collection of points $u_1, u_2, \ldots, u_m \in L_k^*$ and corresponding numbers $h_1, h_2, \ldots, h_m \in k$ such that*

$$P = \{\boldsymbol{x} \in L_k \ : \ u_i(\boldsymbol{x}) \geq -h_i,\ \forall i\}\,.$$

If the collection of points $u_1, u_2, \ldots, u_m$ isn't redundant, then the *facets of P* is the set $\mathcal{F}(P)$ consisting of all the intersections $P \cap \partial H_i$, where

$$H_i := \{\boldsymbol{x} \in L_k \ : \ u_i(\boldsymbol{x}) \geq -h_i\}\,.$$

In order to talk more about the faces of P, their dimensions, and duality, we find it convenient to first introduce the notion of the cone over a polytope. Here, we will associate to a polytope a cone, and the analogous properties of polytopes can then be defined in terms of their associated cones.

Definition 1.1.16. Let $P \subset L_k$ be a polytope. The *cone of* P is defined as

$$C_P \coloneqq \operatorname{cone}\{(1, \boldsymbol{x}) : \ \boldsymbol{x} \in P\} \subset k \times L_k \cong k^{d+1}.$$

In other words, we embed P in one dimension higher, placing it at height one. Then, we take the cone over it. Note that the original polytope can be recovered by intersecting the cone with the hyperplane at height one and then projecting onto the last d coordinates.

Definition 1.1.17. Let $F, P \subset L_k$ be polytopes. Then F is a *(proper) face* of P if C_F is a (proper) face of C_P. The *dimension of* P is defined as $\dim(P) \coloneqq \dim(C_P) - 1$.

Next, we define duality for polytopes.

Definition 1.1.18. Let $P \subset L_k$ be a polytope and assume that $\mathbf{0}$ is in the strict interior of P. Then, the *dual of* P is defined as

$$P^* \coloneqq \left\{u \in L_k^* : \ u(\boldsymbol{x}) \geq -1, \ \forall \boldsymbol{x} \in P\right\} \subset L_k^*.$$

Remark 1.1.19. Alternatively, duality of polytopes can be defined in terms of duality of the cones over them. As such, a precise duality between the $(i-1)$-dimensional faces of P and the $(n-i)$-dimensional faces of P^* can be established via Proposition 1.1.12

Finally, we recall a linear notion of equivalence for polytopes.

Definition 1.1.20. Let $P_1, P_2 \subset L_k$ be polytopes. Then P_1 is *isomorphic* to P_2 if there exists some unimodular matrix $U \in \mathrm{GL}_d(\mathbb{Z})$ such that $UP_1 = P_2$.

1.1.2 Lattice polytopes

So far, lattices haven't been so prevalent in our story, only cropping up in our notation for the vector spaces $L_{\mathbb{Q}}$ and $L_{\mathbb{R}}$ and in the definition of rational cones. So, it is now time to introduce the main combinatorial object of this thesis.

Definition 1.1.21. Let L be a lattice and $P \subset L_k$ be a polytope. Then P is called a *lattice polytope with respect to* L if its vertices are contained in L, i.e. $\mathcal{V}(P) \subset L$.

One nice feature of lattice polytopes is that the complexity can be shifted from the polytope to the lattice, and vice versa. In order to more precisely explain this point, we must first introduce the notion of isomorphism for lattice polytopes.

Definition 1.1.22. Let L, L' be lattices and P, P' be lattice polytopes with respect to L and L', respectively. Then the pair (P, L) is *isomorphic* to (P', L') if there exists a vector space isomorphism $\theta \colon L_{\mathbb{Q}} \to L'_{\mathbb{Q}}$ such that $\theta(P) = P'$ and $\theta(L) = L'$.

Example 1.1.23. In some sense, the simplest polygon is the standard triangle $\Delta_2 = \operatorname{conv}\{\mathbf{0}, \boldsymbol{e}_1, \boldsymbol{e}_2\}$ and the simplest two-dimensional lattice is $\mathbb{Z}^2$. We now consider the following two objects: the lattice $L = \mathbb{Z}^2 + \frac{1}{5}(1,2)\mathbb{Z}$ and the polygon $P = \operatorname{conv}\{(0,0),(5,-2),(0,1)\}$. It can be shown that (Δ_2, L) is isomorphic to $(P, \mathbb{Z}^2)$, using the map $\theta = \left(\begin{smallmatrix} 5 & 0 \\ -2 & 1 \end{smallmatrix}\right)$.

So, we have demonstrated how the complexity of lattice polytopes can be shifted between the polytope and the lattice. We will explore this further when we introduce weights and weight systems of lattice polytopes, later in this subsection. Before that, we will introduce a couple of important subclasses of lattice polytopes, which see use in toric geometry and mirror symmetry.

Definition 1.1.24. Let $P \subset L_k$ be a lattice polytope. Consider the following two conditions.

1. The origin lies in the strict interior of P, i.e. $\mathbf{0} \in \mathrm{int}(P)$;
2. Every vertex $\boldsymbol{v} = (v_1, v_2, \ldots, v_d)$ of P is *primitive*, i.e. $\gcd(v_1, v_2, \ldots, v_d) = 1$.

If P satisfies condition (1), then it is called an *IP polytope*. If P satisfies conditions (1) and (2), then it is called a *Fano polytope*. Note that due to condition (1), all IP (and hence Fano) polytopes must be full-dimensional.

Let us now introduce several lattices which can be associated to cones, Fano polytopes, and their facets.

Definition 1.1.25. Fix a lattice L and let $\sigma \subset L_k$ be a cone. Then the *lattice associated to* σ is defined as the lattice Γ_σ spanned by the primitive ray generators of σ. The *index of* σ is defined as $k_\sigma \coloneqq [L \colon \Gamma_\sigma]$.

This definition can be naturally extended to IP polytopes and their facets.

Definition 1.1.26. Fix a lattice L. Let $P \subset L_{\mathbb{Q}}$ be an IP polytope and F be a facet of P. Then, the *lattice associated to* F is the lattice Γ_F spanned by the vertices of F and the *index of* F is $k_F \coloneqq [L : \Gamma_F]$. Similarly, the *lattice associated to* P is the lattice Γ_P spanned by the vertices of P. The *index of* P is $k_P \coloneqq [L : \Gamma_P]$.

We are now ready to recall the notion of weights and weight matrices.

Definition 1.1.27. Let $P \subset L_{\mathbb{Q}}$ be an IP polytope and fix an ordering of its vertices $\boldsymbol{v}_1, \boldsymbol{v}_2, \ldots, \boldsymbol{v}_m$. Let $\boldsymbol{q} \in \mathbb{Z}^m$ be an integer vector of length m. Then $\boldsymbol{q}$ is a *weight* of P if $\sum_{i=1}^m q_i \boldsymbol{v}_i = \mathbf{0}$. Let $W \in \mathbb{Z}^{(m-d)\times m}$ be an integer matrix of rank $m - d$. Then W is a *weight matrix* for P if $\sum_{i=1}^m W_{ji} \boldsymbol{v}_i = \mathbf{0}$ for all $j = 1, 2, \ldots, m - d$.

Remark 1.1.28. Since a polytope can have many different weight matrices, it is often helpful to conflate W with the space spanned by its length m rows, i.e. the space of all weights of the polytope. If we consider an IP polytope P with respect to its associated lattice Γ_P then, up to isomorphism, this will determine and be determined by the space of weights of P.

It will be important later, when considering mutations, to have the notion of length and height of an edge of an IP polygon.

Definition 1.1.29. Let E be an edge of an IP polygon and let $u \in L^*$ be the unique primitive inner normal vector to E. Then we say that E has *(lattice) length* $\ell_E \coloneqq |E \cap N| - 1$ and *height* $h_E \coloneqq |u(\boldsymbol{v})|$, where $\boldsymbol{v}$ is a vertex of E. Note that the length and the height will be strictly positive integers.

The final notion of this subsection is that of the Minkowski sum of convex sets.

Definition 1.1.30. Let $X, Y \subseteq \mathbb{R}^d$. Then the *Minkowski sum of X and Y* is defined as

$$X + Y := \{x + y : x \in X, y \in Y\}.$$

Note that, $X + \varnothing = \varnothing$.

The Minkowski sum sees use in each chapter of this thesis. It is used in the definition of combinatorial mutation, in the characterisation of nearly Gorenstein polytopes, and to ease the computation of generalised flatness constants.

Example 1.1.31. Consider the following two lattice polytopes.

$$P = \text{conv}\{(0,0),(1,0),(0,2)\} \quad \text{and} \quad Q = \text{conv}\{(0,0),(2,1),(1,2)\}.$$

Their Minkowski sum $P+Q$ has the vertices $(0,0),(1,0),(3,1),(2,3),(1,4),(0,2)$. Due to the convexity of P, we can view $P+Q$ as the convex hull of three copies of Q, which are the translations of Q by the three vertices of P. We can similarly view $P + Q$ as the convex hull of three copies of P. This is shown in Figure 1.2.

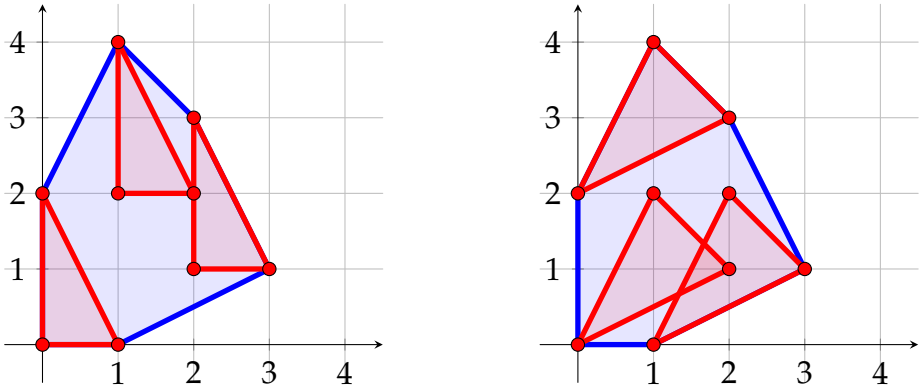

FIGURE 1.2: In blue is the Minkowski sum $P + Q$. On the left, the red polygons are the translations of P by the vertices of Q. On the right, the red polygons are the translations of Q by the vertices of P.

1.1.3 Fans

Another combinatorial object is the fan. These objects find particular use in toric geometry, which we detail in Section 1.2.2

Definition 1.1.32. A collection Σ of cones is called a *fan* if

- Every pair of cones in Σ intersects in a common face, i.e. if $\sigma, \tau \in \Sigma$, then $\sigma \cap \tau$ is a face of σ and a face of τ;
- Σ is closed under taking faces, i.e. if $\sigma \in \Sigma$ and τ is a face of σ, then $\tau \in \Sigma$.

We denote by $\Sigma(i)$ the set of i-dimensional cones in Σ. The *support* of Σ is $|\Sigma| = \bigcup_{\sigma\in\Sigma}\sigma$. If the support of Σ coincides with the entire ambient space, then Σ is called *complete*.

Note that the set of all faces of a cone is itself a fan. As such, we often conflate a cone with its associated fan.

There are two complete fans which can be created from a polytope P.

Definition 1.1.33. Let $P \subset L_{\mathbb{Q}}$ be an IP polytope. Then the *spanning fan (or face fan) of* P is the fan Σ_P consisting of the cones over each face of P.

The rays of Σ_P are the cones over the vertices of P. The full-dimensional cones of Σ_P are the cones over the facets of P.

Definition 1.1.34. Let $P \subset L_{\mathbb{Q}}$ be a polytope and F be a face of P. Then, the *normal cone of* P *at* F is defined as

$$N_P(F) := \left\{u \in L^*_{\mathbb{Q}} : \ \operatorname{face}_u(P) = F\right\},$$

where $\operatorname{face}_u(P) := \left\{\boldsymbol{x} \in P : \ u(\boldsymbol{x}) = \min_{\boldsymbol{y}\in P} u(\boldsymbol{y})\right\}$. The *(inner) normal fan* $\Sigma(P)$ of a polytope P is the fan consisting of the normal cones $N_P(F)$ at each face F of P.

Note that translating P has no effect on the normal fan; thus, the normal fan of P is an affine property of P. Further, if P is an IP polytope, then the normal fan of P coincides with the spanning fan of P^*.

We conclude this section with a result concerning Minkowski sums and normal fans. In order to give the statement, we need the following definition.

Definition 1.1.35. Let Σ, Σ' be two fans lying in the same ambient space. Then the *common refinement of* Σ *and* Σ' is the fan

$$\Sigma \cap \Sigma' := \{\sigma \cap \sigma' : \ \sigma \in \Sigma, \sigma' \in \Sigma'\}.$$

It is straightforward to verify that the common refinement of two fans is indeed a fan.

We can now conclude with this known result.

Proposition 1.1.36 ([107, Proposition 7.12])**.** *Let* $P, Q \subset L_{\mathbb{Q}}$ *be polytopes. Then the normal fan* $\Sigma(P + Q)$ *of their Minkowski sum is equal to the common refinement of the normal fans* $\Sigma(P)$ *and* $\Sigma(Q)$ *of the Minkowski summands.*

Observe that in Example 1.1.31, the normal fan of $P+Q$ is the common refinement of the normal fans of P and Q, since the inner normals to the facets of $P + Q$ are exactly the inner normals to the facets of P and Q.

1.2 Toric geometry

In algebraic geometry, the central idea is a correspondence between geometric objects (such as zero sets of polynomial equations, i.e. *varieties*) and algebraic objects (such as reduced, finitely-generated $\mathbb{C}$-algebras). This allows geometric questions to be studied using algebraic methods. Toric geometry sets up another dictionary of correspondences between algebraic geometry and the combinatorics of polytopes, cones, and fans. The price to pay for this beautiful correspondence is that the varieties must obey a certain symmetry condition involving toruses, hence the name.

1.2.1 Toruses and toric varieties

Throughout this section on toric geometry, we fix the d-dimensional lattice N and refer to its dual lattice as M; we identify the former with $\mathbb{Z}^d$ and the latter with $(\mathbb{Z}^d)^*$. All varieties are over $\mathbb{C}$. We follow the book [29]. We first recall the definition of an algebraic torus.

Definition 1.2.1. A d-dimensional *(algebraic) torus* T is an affine algebraic group, isomorphic to $(\mathbb{C}^\times)^d$. We define $T_N := N \otimes_{\mathbb{Z}} \mathbb{C}^\times \cong (\mathbb{C}^\times)^d$ to be the *torus of* N.

We can now recall what a toric variety is.

Definition 1.2.2 ([29, page 49])**.** Let X be a variety. Then X is a *toric variety* if it is irreducible and contains a torus T as a Zariski-open subset, whose action on itself extends to an action on X.

Example 1.2.3. We provide a (non-exhaustive) list of examples and non-examples of toric varieties.

1. The affine plane $\mathbb{C}^n$ and the torus $(\mathbb{C}^\times)^n$ itself are toric varieties.
2. Let $X = \mathbb{P}^n$ be the projective plane. It contains the torus $T = \mathbb{P}^n \setminus \mathbb{V}(x_0 \cdots x_n)$. An element in T looks like $(1 \colon t_1 \colon \cdots \colon t_n)$, and acts on X by sending $(x_0 \colon \cdots \colon x_n)$ to $(x_0 \colon t_1 x_1 \colon \cdots \colon t_n x_n)$. Thus it is a toric variety.
3. Let $X = \mathbb{V}(y^2 - x^3)$ be the cuspidal cubic. The torus $T = \{(t^2, t^3) : t \in \mathbb{C}^\times\}$ is contained in X, and it acts on X naturally by sending (x, y) to $(t^2 x, t^3 y)$. Thus X is toric.
4. Let $X = \mathbb{V}(y^2 - x^3 + x)$ be an elliptic curve. This is a non-toric variety.

1.2.2 The fan of a toric variety

In this part, we will show how to obtain a fan from a toric variety X. Suppose that T_N is the torus of X, i.e. it is a Zariski-open subset of X whose action on itself extends to an action on X. Associated to the torus T_N is its *group of characters* $\mathrm{Hom}(T_N, \mathbb{C}^\times)$ and its *group of one-parameter subgroups* $\mathrm{Hom}(\mathbb{C}^\times, T_N)$. It turns out that all characters have the form $\chi^m \colon (t_1, \ldots, t_n) \mapsto t_1^{m_1} \cdots t_n^{m_n}$, for $m \in M$. Thus, the group of characters

is isomorphic to the lattice M. Moreover, all one-parameter subgroups have the form $\lambda^v : t \mapsto (t^{v_1}, \ldots, t^{v_n})$, for $v \in N$. Thus, the group of one-parameter subgroups is isomorphic to the lattice N. Finally, notice that the characters and one-parameter subgroups inherit the natural pairing from M and N, i.e. $\chi^m \circ \lambda^v : t \mapsto t^{m(v)}$.

Consider $\lambda_0^v := \lim_{t\to 0} \lambda^v(t)$, for $v \in N$. If λ_0^v exists, then it will be a point of the toric variety X. We can define an equivalence relation on $\{v \in N : \lambda_0^v \text{ exists}\}$, by identifying all v which have the same limit λ_0^v. This partitions N into the origin $\mathbf{0}$, the lattice points in the relative interiors of cones, and a (possibly empty) region where λ_0^v is undefined. This partition corresponds bijectively with a fan. Further, each cone in the fan corresponds to an orbit of a point in X under the group action by T_N.

Example 1.2.4. Let $X = \mathbb{C}^2$ be the affine plane, which is a toric variety with torus $T = (\mathbb{C}^\times)^2$. For $v = (a, b) \in N_\mathbb{Q}$, we have

$$\lambda_0^v = \lim_{t\to 0}(t^a, t^b) = \left\{ \begin{array}{ll} (1,1), & \text{for } a = b = 0 \\ (1,0), & \text{for } a = 0, b > 0 \\ (0,1), & \text{for } a > 0, b = 0 \\ (0,0), & \text{for } a, b > 0 \\ \text{undefined}, & \text{else} \end{array} \right\}.$$

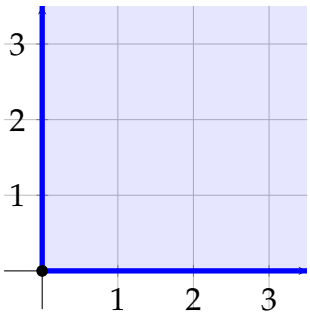

FIGURE 1.3: The fan of $X = \mathbb{C}^2$.

Thus the fan of X consists of $\sigma = \text{cone}\{e_1, e_2\}$ and its lower dimensional faces.

Example 1.2.5. Let $X = \mathbb{V}(xy - z^2)$. This is the surface of a cone, and is an affine toric variety. It has torus $T = \{(t_1, t_1^{-1}t_2^2, t_2) : t_1, t_2 \in \mathbb{C}^\times\}$. Thus, for $v = (a, b) \in N_\mathbb{Q}$, we have that

$$\lambda_0^v = \lim_{t\to 0}(t^a, t^{-a+2b}, t^b) = \left\{ \begin{array}{ll} (1,1,1), & \text{for } a = b = 0 \\ (1,0,0), & \text{for } a = 0, b > 0 \\ (0,1,0), & \text{for } a = 2b > 0 \\ (0,0,0), & \text{for } 0 < a < 2b \\ \text{undefined}, & \text{else} \end{array} \right\}.$$

So, the fan of X consists of $\sigma = \text{cone}\{e_2, (2,1)\}$ and its lower dimensional faces.

We will now look at a non-affine example.

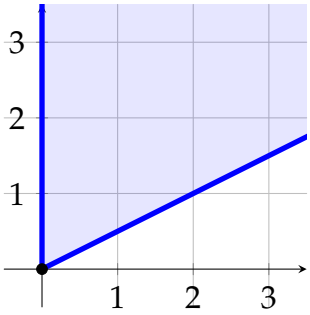

FIGURE 1.4: The fan of $X = \mathbb{V}(xy - z^2)$.

Example 1.2.6. Let $X = \mathbb{P}^2$ be the projective plane. Recall that it contains the torus $T = \mathbb{P}^2 \setminus \mathbb{V}(x_0x_1x_2)$. Since X is compact, λ_0^v always exists. We get that

$$\lambda_0^v = \lim_{t\to 0}(1 : t^a : t^b) = \left\{ \begin{array}{ll} (1:1:1), & \text{for } a = b = 0 \\ (1:1:0), & \text{for } a = 0, b > 0 \\ (1:0:1), & \text{for } a > 0, b = 0 \\ (0:1:1), & \text{for } a = b < 0 \\ (1:0:0), & \text{for } a, b > 0 \\ (0:1:0), & \text{for } a < 0, a < b \\ (0:0:1), & \text{for } a > b, b < 0 \end{array} \right\}.$$

Note that the computation of these limits follows immediately from the fact that

$$(1 : t^a : t^b) = (t^{-a} : 1 : t^{b-a}) = (t^{-b} : t^{a-b} : 1).$$

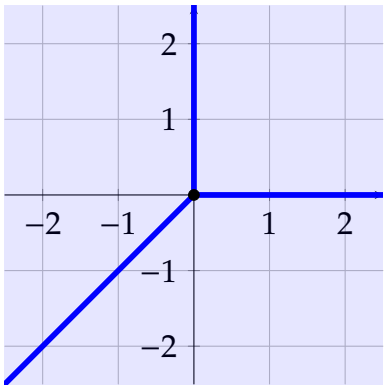

FIGURE 1.5: The fan of $X = \mathbb{P}^2$.

The fan of X consists of 3 full-dimensional cones, 3 rays, and the origin. Notice how one of the full-dimensional cones is the full-dimensional cone in the fan of $\mathbb{C}^2$. In fact, all of the full-dimensional cones in the fan of $\mathbb{P}^2$ are isomorphic to the cone from the fan of $\mathbb{C}^2$. This makes sense, since $\mathbb{P}^2$ can be covered by three copies $U_i = \mathbb{P}^2 \setminus \mathbb{V}(x_i)$ of $\mathbb{C}^2$.

Definition 1.2.7. Let X be an irreducible affine variety. X is *normal* if its coordinate ring $\mathbb{C}[X]$ is integrally closed, i.e. if $f \in \mathbb{C}(X)$ is a root of a monic polynomial in $\mathbb{C}[X][t]$, then $f \in \mathbb{C}[X]$.

Example 1.2.8. Let $X = \mathbb{V}(y^2 - x^3)$ be the cuspidal cubic. It has coordinate ring $\mathbb{C}[X] = \mathbb{C}[x] \oplus y\mathbb{C}[x]$. Consider $\frac{y}{x} \in \mathbb{C}(X)$. This is a root of the monic polynomial $t^2 - x \in \mathbb{C}[X][t]$. But $\frac{y}{x} \notin \mathbb{C}[X]$. Thus, X is not a normal variety. Now we will also compute the fan of this non-normal toric variety X. Recall that the torus $T = \left\{(t^2, t^3) : t \in \mathbb{C}^\times\right\}$ is contained in X. Then, for $a \in N_\mathbb{Q}$, we have that

$$\lambda_0^a = \lim_{t \to 0}(t^{2a}, t^{3a}) = \left\{ \begin{array}{ll} (1,1), & \text{for } a = 0 \\ (0,0), & \text{for } a > 0 \\ \text{undefined}, & \text{else} \end{array} \right\}.$$

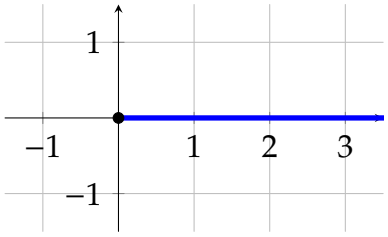

FIGURE 1.6: The fan of $X = \mathbb{V}(y^2 - x^3)$.

The fan of X just consists of the ray $\rho = \text{cone}\{\boldsymbol{e}_1\}$ and its lower-dimensional face $\{\mathbf{0}\}$. This fan is the same as the fan of $\mathbb{C}^1$. It should be noted that $X' = \mathbb{C}^1$ is the *normalisation* of X, i.e. the integral closure $\mathbb{C}[X]'$ of the coordinate ring of X is the coordinate ring $\mathbb{C}[\mathbb{C}^1]$ of $\mathbb{C}^1$.

Because of this, we restrict our attention to normal toric varieties. This way, the correspondence between fans and such varieties will be one-to-one.

1.2.3 The toric variety of a fan

We start by looking at a special case of a fan – a cone. Take $\sigma \subset N_\mathbb{Q}$. Now, we define $S_\sigma := \sigma^\vee \cap M$ to be the semigroup of the lattice points of the dual of σ. We call the minimal set of generators of S_σ the *Hilbert basis of* $\sigma^\vee$, and denote it by $\text{Hilb}(\sigma^\vee)$. Gordon's Lemma [29, Proposition 1.2.17] tells us that S_σ is finitely generated, i.e. $\text{Hilb}(\sigma^\vee)$ is finite. We can construct a $\mathbb{C}$-algebra associated to the semigroup S_σ, defined as follows:

$$\mathbb{C}[S_\sigma] := \left\{ \sum_{i=1}^{k} a_i \chi^{m_i} \; : \; a_i \in \mathbb{C}, m_i \in S_\sigma \right\},$$

where addition is formal, and multiplication is inherited from the semigroup operation, i.e. $\chi^m \cdot \chi^{m'} := \chi^{m+m'}$.

As a consequence of Gordon's Lemma, this $\mathbb{C}$-algebra is finitely generated. Its ring structure is also an integral domain. Thus, by Hilbert's Nullstellensatz, it corresponds to an irreducible affine variety $U_\sigma := \operatorname{Spec}(\mathbb{C}[S_\sigma])$.

Example 1.2.9. Consider $\sigma = \operatorname{cone}\{e_1, e_2\} \subset N_\mathbb{Q}$. Then we get the semigroup $S_\sigma = \sigma^\vee \cap M = \operatorname{span}_{\mathbb{Z}_{\geq 0}}\{e_1^*, e_2^*\}$. Thus, we obtain the $\mathbb{C}$-algebra $\mathbb{C}[S_\sigma] = \mathbb{C}[x, y]$, and its associated irreducible affine variety $U_\sigma = \mathbb{C}^2$.

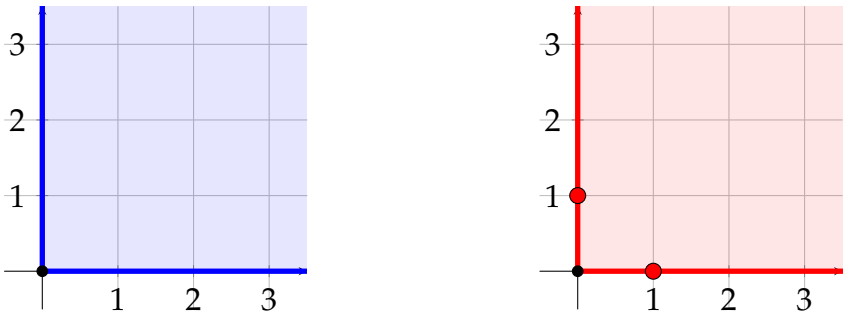

(A) $\sigma \subset N_\mathbb{Q}$. (B) $\sigma^\vee \subset M_\mathbb{Q}$ and its Hilbert basis.

FIGURE 1.7: The two cones involved in constructing $U_\sigma = \mathbb{C}^2$.

Example 1.2.10. Let $\sigma = \operatorname{cone}\{(2,1),(0,1)\} \subset N_\mathbb{Q}$. Then its dual cone is $\sigma^\vee = \operatorname{cone}\{(1,0)^t, (-1,2)^t\} \subset M_\mathbb{Q}$. We obtain that $\operatorname{Hilb}(\sigma^\vee) = \{(1,0)^t, (0,1)^t, (-1,2)^t\}$. The variety U_σ will have coordinate ring $\mathbb{C}[S_\sigma] = \mathbb{C}[x, xy, xy^2]$. Thus $U_\sigma = \mathbb{V}(xy - z^2) \subset \mathbb{C}^3$, after a change of variables. Notice that this is the same variety as in Example 1.2.5, and the cone σ isomorphic to the cone featured there.

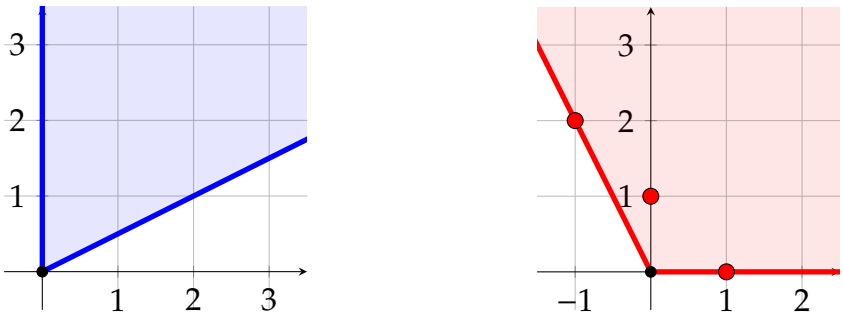

(A) $\sigma \subset N_\mathbb{Q}$. (B) $\sigma^\vee \subset M_\mathbb{Q}$ and its Hilbert basis.

FIGURE 1.8: The cones involved in the construction of $U_\sigma = \mathbb{V}(xy - z^2)$.

Now that we have shown how to recover the variety in the case of a cone, we can discuss it in the case of a fan in general.

Let Σ be a fan whose cones lie in the vector space $N_\mathbb{Q}$. Each cone $\sigma \in \Sigma$ corresponds to an affine toric variety U_σ with coordinate ring $\mathbb{C}[S_\sigma]$. The variety X_Σ is constructed by gluing these S_σ together in a way given by the fan.

Consider $\sigma_1, \sigma_2 \in \Sigma$ with corresponding affine toric varieties U_{σ_1} and U_{σ_2}. We glue U_{σ_1} and U_{σ_2} together along U_τ, where $\tau = \sigma_1 \cap \sigma_2$ is the common face of σ_1 and

σ_2. We may write the common face τ in two different ways: $\tau = \sigma_1 \cap H_m = \sigma_2 \cap H_{-m}$, for some $m \in -\sigma_1^\vee \cap \sigma_2^\vee$, where $H_m = \{\boldsymbol{x} \in N_\mathbb{Q} : m(\boldsymbol{x}) \geq 0\}$ is a half-space at height 0. Then, we get the semigroup S_τ, which consequently can be written in the following two ways: $S_\tau = S_{\sigma_1} + (-m)\mathbb{Z}_{\geq 0} = S_{\sigma_2} + m\mathbb{Z}_{\geq 0}$. Thus, we can write its associated $\mathbb{C}$-algebra in two ways: $\mathbb{C}[S_\tau] = \mathbb{C}[S_{\sigma_1}]_{\chi^m} = \mathbb{C}[S_{\sigma_2}]_{\chi^{-m}}$. So, there exist embeddings ι_1 and ι_2 from U_τ into U_{σ_1} and U_{σ_2}, respectively. There is also an isomorphism g_{12} from $\iota_1(U_\tau)$ to $\iota_2(U_\tau)$. The variety X_Σ is finally defined to be

$$X_\Sigma := \left(\bigsqcup_{\sigma \in \Sigma} U_\sigma \right) / \sim,$$

where $a \in U_{\sigma_1}$ and $b \in U_{\sigma_2}$ are identified if, for the common face $\tau = \sigma_1 \cap \sigma_2$, we have that $a \in \iota_1(U_\tau)$, $b \in \iota_2(U_\tau)$, and $g_{12}(a) = b$.

Note that X_Σ is a toric variety, with torus $T = U_{\{\mathbf{0}\}}$ corresponding to the 0-dimensional cone $\{\mathbf{0}\} \in \Sigma$. Furthermore, this construction and the main construction of §1.2.2 are inverse to each other, forming a bijection between fans and normal toric varieties.

Example 1.2.11. Let Σ be the fan determined by the full-dimensional cones $\sigma_1 = \text{cone}\,\{\boldsymbol{e}_1, \boldsymbol{e}_2\}$ and $\sigma_2 = \text{cone}\,\{\boldsymbol{e}_1, -\boldsymbol{e}_2\}$. The two cones intersect in the face $\tau = \mathbb{Q}_{\geq 0}\boldsymbol{e}_1 = \sigma_1 \cap H_{-e_2^*} = \sigma_2 \cap H_{e_2^*}$.

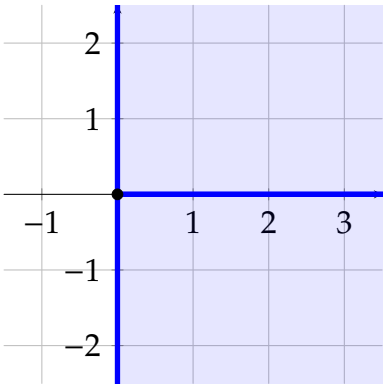

FIGURE 1.9: The fan Σ.

We get the following $\mathbb{C}$-algebras: $\mathbb{C}[S_{\sigma_1}] = \mathbb{C}[x, y]$, $\mathbb{C}[S_{\sigma_2}] = \mathbb{C}[x, y^{-1}]$, and $\mathbb{C}[S_\tau] = \mathbb{C}[x, y, y^{-1}]$.

Thus U_{σ_1} and U_{σ_2} are two copies of $\mathbb{C}^2$ glued together along U_τ. If we give U_{σ_i} coordinates (x_i, y_i), then we can describe the gluing map as follows:

$$\begin{aligned} g_{12} \colon \iota_1(U_\tau) &\longrightarrow \iota_2(U_\tau) \\ (x_1, y_1) &\longmapsto (x_1, y_1^{-1}). \end{aligned}$$

Thus, $X_\Sigma = (U_{\sigma_1} \sqcup U_{\sigma_2})/\sim$ where, for $(x_i, y_i) \in U_{\sigma_i}$, we define the equivalence $(x_1, y_1) \sim (x_2, y_2)$ if and only if $y_1, y_2 \neq 0$ and $g_{12}(x_1, y_1) = (x_2, y_2)$.

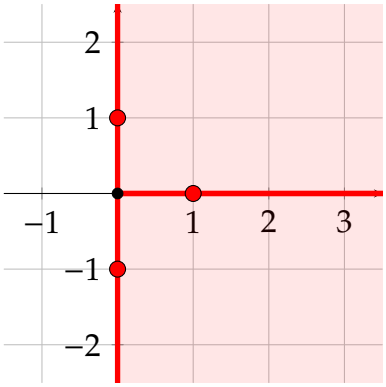

(A) The dual cones $\sigma_i^\vee \subset M_\mathbb{Q}$ and their Hilbert bases.

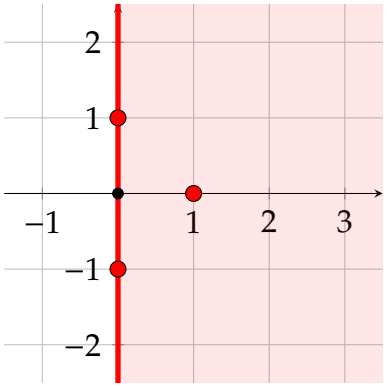

(B) $\tau^\vee \subset M_\mathbb{Q}$ and one choice of $\mathbb{Z}_{\geq 0}$-generators.

FIGURE 1.10: The cones involved in the construction of X_Σ.

We now identify each patch like follows:

$$(x_1, y_1) \in U_{\sigma_1} \longmapsto (x_1, (1 : y_1)),\ (x_2, y_2) \in U_{\sigma_2} \longmapsto (x_2, (y_2 : 1)),$$

where $(a : b)$ is a point in $\mathbb{P}^1$, expressed in homogeneous coordinates. Since these maps agree on U_τ, we can identify the variety $X_\Sigma = \mathbb{C}^1 \times \mathbb{P}^1$.

Example 1.2.12. Let Σ be the fan determined by the full-dimensional cones $\sigma_0 = \text{cone}\{e_1, e_2\}$, $\sigma_1 = \text{cone}\{e_2, (-1,-1)\}$. and $\sigma_3 = \text{cone}\{(-1,-1), e_1\}$.

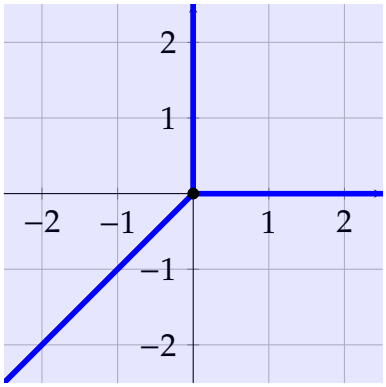

(A) The fan Σ.

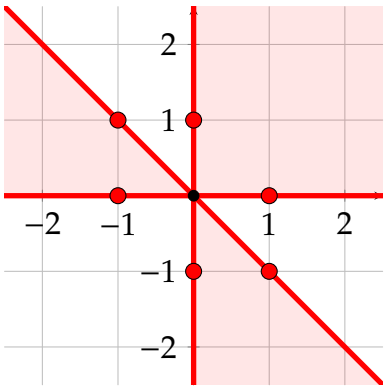

(B) The dual cones $\sigma_i^\vee \subset M_\mathbb{Q}$ and their Hilbert bases.

FIGURE 1.11: The cones involved in the construction of X_Σ.

We get the following $\mathbb{C}$-algebras:

$$\mathbb{C}[S_{\sigma_0}] = \mathbb{C}[x_1, x_2], \quad \mathbb{C}[S_{\sigma_1}] = \mathbb{C}\left[\frac{1}{x_1}, \frac{x_2}{x_1}\right], \quad \mathbb{C}[S_{\sigma_2}] = \mathbb{C}\left[\frac{1}{x_2}, \frac{x_1}{x_2}\right].$$

Thus, the U_{σ_i} are all copies of $\mathbb{C}^2$.

Letting $\tau_{ij} \coloneqq \sigma_i \cap \sigma_j$, we get three faces. Their duals $\tau_{ij}^\vee$ are half-spaces, so their corresponding varieties $U_{\tau_{ij}}$ are copies of $\mathbb{C}^1 \times \mathbb{C}^\times$. For each face, we obtain a gluing map. Let ι_{ij} embed $U_{\tau_{ij}}$ into U_{σ_i}, and define g_{ij} identifying $\iota_{ij}(U_{\tau_{ij}}) \subset U_{\sigma_i}$ with $\iota_{ji}(U_{\tau_{ij}}) \subset U_{\sigma_j}$, via

$$g_{01} \colon (s,t) \longmapsto \left(\frac{1}{s}, \frac{t}{s}\right)$$
$$g_{12} \colon (s,t) \longmapsto \left(\frac{s}{t}, \frac{1}{t}\right)$$
$$g_{20} \colon (s,t) \longmapsto \left(\frac{t}{s}, \frac{1}{s}\right).$$

We can finally make the following identifications:

$$(s,t) \in U_{\sigma_0} \longmapsto (1 : s : t),\ (s,t) \in U_{\sigma_1} \longmapsto (s : 1 : t),\ (s,t) \in U_{\sigma_2} \longmapsto (s : t : 1),$$

where $(a : b : c)$ is a point in $\mathbb{P}^2$ given by homogeneous coordinates. These agree on each intersection, and therefore $X_\Sigma = \mathbb{P}^2$.

1.2.4 Toric divisors

Fix a normal projective toric variety X with corresponding (complete) fan Σ over $N_\mathbb{Q}$. To each ray ρ of Σ, there is a corresponding torus-invariant irreducible divisor D_ρ. A *T-Weil divisor D of X* is a formal sum $\sum_{\rho \in \Sigma(1)} a_\rho D_\rho$, where the a_ρ are integers. We refer to the lattice of all T-Weil divisors of X as $\mathrm{Div}_T(X)$.

We now discuss several properties and types of T-Weil divisors. We begin with Cartier divisors.

Proposition 1.2.13 (c.f. [29, Theorem 4.2.8])**.** *Let $D = \sum_{\rho \in \Sigma(1)} a_\rho D_\rho$ be a T-Weil divisor on X. Then D is Cartier if and only if for all maximal cones $\sigma \in \Sigma(d)$, there exists some lattice point $u_\sigma \in M$ such that, for all rays $\rho \in \sigma(1)$, we have that $u_\sigma(\boldsymbol{v}_\rho) = -a_\rho$, where $\boldsymbol{v}_\rho$ is the primitive ray generator of ρ.*

The collection $\{u_\sigma\}_{\sigma \in \Sigma(d)}$ is called the *Cartier data* of D. The lattice of all Cartier T-Weil divisors of X is referred to as $\mathrm{CDiv}_T(X)$.

Let χ^m be a character of the torus T_N, with $m \in M$. Then we may associate to it a T-Weil divisor defined as follows:

$$\mathrm{div}(\chi^m) \coloneqq \sum_{\rho \in \Sigma(1)} m(\boldsymbol{v}_\rho) D_\rho,$$

where $\boldsymbol{v}_\rho$ is the primitive ray generator of ρ. These are the principle T-Weil divisors on X. Note that $\mathrm{div}(\chi^m)$ is Cartier as its Cartier data is simply $u_\sigma = -m$ for all $\sigma \in \Sigma(d)$. Thus, we obtain a surjection from M into $\mathrm{CDiv}_T(X)$.

Next, the divisor class group of X is $\mathrm{Cl}(X) \coloneqq \mathrm{Div}(X)/\mathrm{Div}_0(X)$ and the Picard group of X is $\mathrm{Pic}(X) \coloneqq \mathrm{CDiv}(X)/\mathrm{Div}_0(X)$, where $\mathrm{Div}_0(X)$ is the set of principal

divisors of X. In fact, by [29, Theorem 4.1.3], we obtain an exact sequence:

$$M \longrightarrow \mathrm{Div}_T(X) \longrightarrow \mathrm{Cl}(X) \longrightarrow 0.$$

The analogous statement holds for the torus-invariant Cartier divisors and the Picard group.

Next, we may also associate to a T-Weil divisor a polytope.

Definition 1.2.14. Let $D = \sum_{\rho\in\Sigma(1)} a_\rho D_\rho$ be a T-Weil divisor on X. Then the *polytope of sections of* D is the polytope in $M_\mathbb{Q}$ defined as follows:

$$P_D := \left\{u \in M_\mathbb{Q} : \ u(v_\rho) \geq -a_\rho, \ \forall \rho \in \Sigma(1)\right\},$$

where v_ρ is the primitive ray generator of ρ.

We now discuss basepoint-free divisors and ample divisors, which can be characterised in terms the polytope of sections.

Proposition 1.2.15. *Let D be a T-Weil divisor on X that is Cartier. Then, the following statements hold.*

(i) [29, Theorem 6.1.10] D is basepoint free if and only if the vertices of P_D are the lattice points u_σ forming the Cartier data of D.

(ii) [29, Proposition 6.1.4, Corollary 6.1.15] D is ample if and only if D is basepoint free and the normal fan of P_D is Σ.

Let D be a T-Weil divisor on X. It is called $\mathbb{Q}$-Cartier if some multiple of it is Cartier. It can be seen that if D is $\mathbb{Q}$-Cartier, then it is ample if and only if the normal fan of P_D is Σ. Note that the vertices of such a P_D are not necessarily lattices points.

This naturally brings us onto the definition of several important types of varieties, Gorenstein varieties and Fano varieties, which we cover in the next subsection.

1.2.5 Toric Fano varieties

Fano varieties are an important class of varieties, which have been extensively studied in algebraic geometry. In some sense, they are the building blocks of all other varieties. It has been proven that, in each dimension, there are finitely many smooth Fano varieties, up to deformation. In low dimensions (i.e. $d \leq 3$), these varieties have been completely classified. We recall their general definition below.

Definition 1.2.16. Let X be a normal projective variety. Then X is called *Fano* if the anticanonical divisor $-K_X$ is ample.

Later, in §1.3, we discuss one recent approach to the classification of Fano varieties. But for the rest of this subsection, we focus on toric Fano varieties. Let Σ be a complete fan in $N_\mathbb{Q}$ and $X = X_\Sigma$ be the corresponding projective toric variety. The anticanonical divisor on X is simply the sum of the T-divisors of X, i.e. $-K_X = \sum_{\rho\in\Sigma(1)} D_\rho$. Let $P \subset$

$N_{\mathbb{Q}}$ be the convex hull of the primitive ray generators of Σ. Then, the polytope of sections of $-K_X$ is simply the dual of P, i.e. $P_{-K_X} = P^*$.

Now, for X to be Fano, we need $-K_X$ to be ample. It can be seen that $-K_X$ is ample if and only if the normal fan of P^* coincides with Σ. But, this is equivalent to the vertices of P being exactly the primitive ray generators of Σ. Such fans Σ are in one-to-one correspondence with Fano polytopes P. Thus, toric Fano varieties (up to isomorphism) are in one-to-one correspondence with Fano polytopes (up to $\mathrm{GL}_2(\mathbb{Z})$-equivalence).

We now introduce several classes of Fano polytopes. In many cases, it is convenient to define a property locally first, at the level of the maximal cones in the corresponding fan.

Definition 1.2.17. Let $\sigma \subset N_{\mathbb{Q}}$ be a cone. Then, σ is called $\mathbb{Q}$-*Gorenstein* if all its primitive ray generators lie on a common hyperplane. Furthermore, if σ is $\mathbb{Q}$-Gorenstein then its *Gorenstein index* is the height of the common hyperplane of its primitive ray generators. Moreover, σ is called *Gorenstein* if it has Gorenstein index 1.

All Fano polytopes are $\mathbb{Q}$-Gorenstein. A Fano polytope is Gorenstein if all its maximal cones are Gorenstein. This is equivalent to P being *reflexive*, i.e. the dual polytope P^* is a lattice polytope, i.e. each facet of P is supported by a hyperplane of height 1.

Definition 1.2.18. Let $\sigma \subset N_{\mathbb{Q}}$ be a cone. Then, σ is called *smooth* if its primitive ray generators extend to a basis of N. It is called *simplicial* if the number of primitive ray generators of σ is equal to its dimension. A Fano polytope is *smooth* (resp. *simplicial*) if all its maximal cones are smooth (resp. simplicial).

Definition 1.2.19. Let $\sigma \subset N_{\mathbb{Q}}$ be a $\mathbb{Q}$-Gorenstein cone, with common hyperplane H. Then, σ is called *terminal* if the only lattice points of σ on or below H are exactly its primitive ray generators and the origin. It is called *canonical* if the only lattice point strictly below H is the origin. A Fano polytope is *terminal* (resp. *canonical*) if all its maximal cones are terminal (resp. canonical).

Remark 1.2.20. An equivalent condition for the Fano polytope P being terminal is if the only lattice points of P are the origin and its vertices, i.e. $P \cap N = \{\mathbf{0}\} \cup \mathcal{V}(P)$. An equivalent condition for the Fano polytope P being canonical is if the only lattice point in the interior of P is the origin, i.e. $\mathrm{int}(P) \cap N = \{\mathbf{0}\}$.

Finally, these properties form a nice chain of implications, as shown in Figure 1.12. We remark that for dimension $d = 2$, some of these properties coincide:

1. All two-dimensional cones are simplicial; thus, they are also all $\mathbb{Q}$-Gorenstein.
2. All terminal cones are smooth.
3. All canonical cones are Gorenstein.

The first coincidence follows from the fact that all one-dimensional polytopes are simplices (as they are line segments). The last two follow from the fact that there is a unique empty lattice simplex, up to isomorphism.

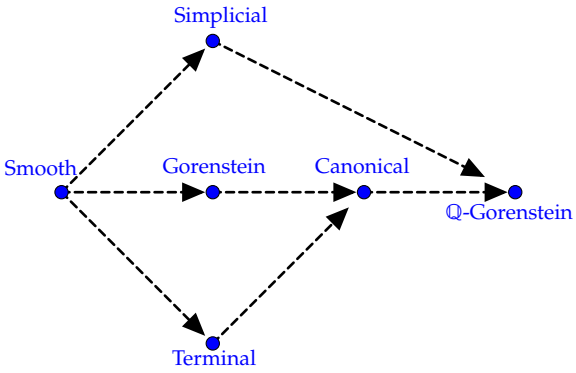

FIGURE 1.12: Chain of implications.

1.3 Mirror symmetry

1.3.1 Overview

A new approach to the classification of Fano manifolds was initiated by Coates–Corti–Galkin–Golyshev–Kasprzyk [23], which has become known as the *Fanosearch programme*. Following this programme, a Laurent polynomial f is said to be *mirror dual* to a Fano manifold X if the classical period π_f of f agrees with the regularized quantum period $\widehat{G}_X$ of X; see [23] for details. This correspondence is not unique: a Fano manifold can have (infinitely) many different mirror dual Laurent polynomials, and these Laurent polynomials are expected to be related via a combinatorial process called *mutation* [2]. It is conjectured that Fano manifolds, up to $\mathbb{Q}$-Gorenstein-deformation, are in bijective correspondence with certain Laurent polynomials, up to mutation.

Crucial to this approach is the Newton polytope P of the Laurent polynomial f. This polytope P is *Fano*, i.e. it is a convex lattice polytope containing the origin in its strict interior, and has primitive vertices [64]. We thus enter the world of toric geometry. The polytope P corresponds to a (possibly singular) toric Fano variety X_P, which is expected to be a toric degeneration of the original Fano manifold X. The notion of mutation can be extended from Laurent polynomials to Fano polytopes, which we detail in §1.3.2. Ilten showed that if two Fano polytopes P and Q are related by mutation, then the corresponding toric varieties X_P and X_Q are deformation-equivalent [56].

In [3], the Fanosearch programme was specialised to orbifold del Pezzo surfaces; that is, del Pezzo surfaces with at worst cyclic quotient singularities. There are infinitely many of these surfaces, even up to $\mathbb{Q}$-Gorenstein-deformation; however, bounding the possible basket of singularities results in a finite classification. For example, an empty basket recovers the classical 10 smooth del Pezzo surfaces, up to $\mathbb{Q}$-Gorenstein-deformation.

Kasprzyk–Nill–Prince [66] introduced the notion of *minimality* for Fano polygons. A Fano polygon is called *minimal* if, out of all polygons related to it by a single mutation, its number of lattice points is minimal. That is, minimality is a

local property, and there can be multiple minimal polygons in a single mutation-equivalence class. Using this purely combinatorial definition, they found exactly 26 mutation-equivalence classes of Fano polygons whose baskets contain only $\frac{1}{3}(1,1)$ singularities; these agree with 26 of the del Pezzo surfaces with $\frac{1}{3}(1,1)$ singularities classified by Corti–Heuberger [28].

One of the main results of [66] is the following:

Theorem 1.3.1 ([66, Theorem 6.3])**.** *There are finitely many minimal Fano polygons, up to isomorphism, with a given basket of singularities.*

As a consequence, the problem of classifying Fano polygons (up to mutation) with a given basket can be reduced to classifying finitely many minimal Fano polygons; this has been implemented algorithmically by Cavey–Kutas [17]. The final problem in the classification is then to tease apart the minimal Fano polygons which are in different mutation-equivalence classes.

1.3.2 Combinatorial mutation

In this subsection, we will introduce in more detail the notion of combinatorial mutation. We follow [3] and give the simplified definition for dimension two. First, we find it useful to distinguish between several types of edges when studying mutations of polygons.

Definition 1.3.2. Let E be an edge of an IP polygon. Denote by ℓ_E the (lattice) length of E and by h_E the height of E. If $\ell_E \geq h_E$, then E is called *long*; otherwise, we call E *short*. Further, if the lattice length ℓ_E divides the height h_E, then E is called *pure*.

As an operation, (combinatorial) mutation takes a polygon and some data, and then outputs another polygon. We first recall what sort of compatible data can be chosen for a given polygon.

Definition 1.3.3 ([3, page 2])**.** Let $P \subset N_{\mathbb{Q}}$ be an IP polygon. Let $w \in M$ be a primitive vector and $\boldsymbol{d} \in N$ be a non-zero lattice point. Suppose that the following two conditions hold:

1. There is a long edge of P with primitive *inner* normal vector w;
2. $w(\boldsymbol{d}) = 0$.

Then the tuple $(w, \boldsymbol{d})$ is *mutation data* for P.

We may now recall the definition of mutation for polygons.

Definition 1.3.4 ([3, pages 2-3])**.** Let $P \subset N_{\mathbb{Q}}$ be an IP polygon and let $(w, \boldsymbol{d})$ be some mutation data for P. Let $\boldsymbol{v}_1, \boldsymbol{v}_2, \ldots$ be the vertices of P, labelled so that each pair of adjacent vertices forms an edge of P and so that $\boldsymbol{v}_1$ is maximal over P with respect to w. Let $1 < i < m + 1$ be such that $[\boldsymbol{v}_i, \boldsymbol{v}_{i+1}]$ is the long edge of P with primitive inner normal w. We may assume that $\boldsymbol{v}_{i+1} - \boldsymbol{v}_i$ is a positive multiple of $\boldsymbol{d}$; otherwise, we reverse the order for labelling the vertices. We distinguish two cases:

(i) P has m vertices and $\boldsymbol{v}_1$ is the unique maximiser for w over P.

(ii) P has $m+1$ vertices and $\boldsymbol{v}_1$ and $\boldsymbol{v}_{m+1}$ are maximiser for w over P.

In case (i), we set $\boldsymbol{v}_{m+1} \coloneqq \boldsymbol{v}_1$. Then, in both cases, the *mutation* of P with respect to the mutation data $(w, \boldsymbol{d})$ is the polygon $\mathrm{mut}_w(P, \boldsymbol{d})$ with vertices

$$\begin{cases} \boldsymbol{v}_j, & 1 \leq j \leq i \\ \boldsymbol{v}_j + w(\boldsymbol{v}_j) \cdot \boldsymbol{d}, & i < j \leq m+1. \end{cases} \tag{1.1}$$

We now collect some relevant facts about mutations.

Lemma 1.3.5. *Let $P \subset N_{\mathbb{Q}}$ be an IP polygon and $(w, \boldsymbol{d})$ be mutation data for P. Then the following hold.*

1. *[2, Proposition 3.11] Being Fano is preserved under mutation, i.e. P is Fano if and only if $\mathrm{mut}_w(P, \boldsymbol{d})$ is Fano;*
2. *[2, Lemma 3.6] Mutation is invertible; in particular, we have*
$$\mathrm{mut}_w(\mathrm{mut}_{-w}(P, \boldsymbol{d}), \boldsymbol{d}) = P;$$
3. *[3] Mutations can be broken down into primitive mutations, i.e. if $(w, (n+1)\boldsymbol{d})$ is mutation data for P, for some positive integer n, then*
$$\mathrm{mut}_w(P, (n+1)\boldsymbol{d}) = \mathrm{mut}_w(\mathrm{mut}_w(P, n\boldsymbol{d}), \boldsymbol{d}).$$

Definition 1.3.6. Let $P, Q \subset N_{\mathbb{Q}}$ be Fano polygons. They are *mutation-equivalent* if there exists a sequence of mutations connecting them, i.e. there exists $P_0, \ldots, P_s$ such that $P_0 = P$, $P_s = Q$, and $P_{i+1} = \mathrm{mut}_{w_i}(P_i, \boldsymbol{d}_i)$, where $(w_i, \boldsymbol{d}_i)$ is mutation data for P_i, for all $i = 0, \ldots, s-1$.

1.3.3 Mutation invariants

The first invariant of this subsection is the singularity content. We recall what a cyclic quotient singularity is for surfaces.

Definition 1.3.7 ([88])**.** Let r and a be coprime integers. Consider the affine variety $U = \mathbb{C}^2/\mathbb{Z}_r$, where $\mathbb{Z}_r$ is the cyclic group of order r generated by the r-th roots of unity in $\mathbb{C}^\times$ and $\eta \in \mathbb{Z}_r$ acts on $(x, y) \in \mathbb{C}^2$ via

$$\eta \cdot (x, y) = (\eta^1 x, \eta^a y).$$

Then the orbit of $(0, 0)$ in U is a called a *cyclic quotient singularity of type* $1/r(1, a)$.

Remark 1.3.8. The variety U in the above definition is in fact toric. It corresponds, up to isomorphism, to the cone generated by $(1, 0)$ and $(-a, r)$.

We now begin defining singularity content at the local level, i.e. at the level of cones/edges.

Definition 1.3.9 ([62, Definition 2.4])**.** Let $\sigma \subset N_{\mathbb{Q}}$ be a cone with singularity type $1/r(1,a)$. Set $\ell = \gcd(r, a+1)$. Thus, we can write $r = \ell h$ and $a = \ell\alpha - 1$, for some positive coprime integers h and α. Now, by the division algorithm, $\ell = n_\sigma h + \tilde{\ell}$, for some unique integers $n_\sigma \geq 0$ and $0 \leq \tilde{\ell} < h$. The quantity n_σ is referred to as the number of *primitive T-singularities* of σ. The *residue* of σ is defined as

$$\operatorname{res}(\sigma) := \begin{cases} \varnothing, & \tilde{\ell} = 0 \\ \frac{1}{\tilde{\ell}h}(1, \tilde{\ell}\alpha - 1), & \tilde{\ell} > 0. \end{cases}$$

The *singularity content* of σ is defined as $\operatorname{SC}(\sigma) := (n_\sigma, \operatorname{res}(\sigma))$.

We can now define it at the global level, i.e. at the level of fans/polygons.

Definition 1.3.10 ([62, Definition 3.1])**.** Let $P \subset N_{\mathbb{Q}}$ be a Fano polygon. The number n_P of primitive T-singularities of P is the sum over all edges E of P of the number n_{σ_E} of primitive T-singularities of σ_E. The *basket of R-singularities* $\mathcal{B}_P$ of P is the cyclically ordered set of non-empty residues $\operatorname{res}(\sigma_E)$, running over all edges E of P. The *singularity content* of P is $\operatorname{SC}(P) := (n_P, \mathcal{B}_P)$.

Theorem 1.3.11 ([62, Proposition 3.6])**.** *The singularity content of two mutation-equivalent Fano polygons are identical.*

The next invariant to consider is the Ehrhart series of the dual polygon.

Definition 1.3.12. Let $P \subset N_{\mathbb{Q}}$ be a polygon. The *Ehrhart series* $\operatorname{Ehr}_P(t)$ of P is defined as the formal power series

$$\operatorname{Ehr}_P(t) := \sum_{k=0}^{\infty} |kP \cap N|\, t^k.$$

In [2], it was shown that if we apply a mutation to a Fano polytope P, its dual polytope P^* is transformed by a piecewise linear function. Thus, it follows that the Ehrhart series of the dual polytope is invariant under mutation. It also follows that the volume of P^*, i.e. the anticanonical degree of X_P, is invariant under mutation.

Proposition 1.3.13 (cf. [2, Proposition 3.15])**.** *Let $P \subset N_{\mathbb{Q}}$ be a Fano polygon. Then the Ehrhart series $\operatorname{Ehr}_{P^*}(t)$ of its dual polygon P^* is invariant under mutation of P.*

In [62, Corollary 3.5], it was shown that the Ehrhart series $\operatorname{Ehr}_{P^*}(t)$ is completely determined by the singularity content of P.

Chapter 2

Nearly Gorenstein Polytopes

This chapter is based on joint work with Max Kölbl, Koji Matsushita, and Sora Miyashita, which appears in [38].

2.1 Introduction

Let $P \subset \mathbb{R}^d$ be a lattice polytope and $C_P \subset \mathbb{R}^{d+1}$ be the cone of P. Then the *Ehrhart ring* $A(P)$ of P is defined by $\mathbb{C}[C_P \cap \mathbb{Z}^{d+1}]$, where each lattice point $(x_1, \ldots, x_d, k) \in \mathbb{Z}^{d+1}$ is identified with a Laurent monomial $t_1^{x_1} \cdots t_d^{x_d} s^k$. This classical construction allows for the study of ring theoretic notions via polytopes and combinatorics.

Cohen-Macaulay rings and Gorenstein rings play a central role in commutative algebra. In the study of rings which are Cohen-Macaulay but not Gorenstein, it has been useful to water down the strong property of being Gorenstein; in fact, many generalised notions of Gorensteinness have been explored. There are *nearly Gorenstein* rings, *level* rings, and *almost Gorenstein* rings, to name just a few examples.

In this chapter, we primarily focus on the nearly Gorenstein property, as introduced in [42]. Let R be a Cohen-Macaulay ring which is a finitely generated $\mathbb{N}$-graded $\mathbb{C}$-algebra. The definition of nearly Gorenstein arises from studying the non-Gorenstein locus of R, which is determined by the *trace* $\mathrm{tr}(\omega_R)$ of the canonical module ω_R of R (see Definition 2.2.1). Explicitly, R is Gorenstein if and only if this trace coincides with the ring itself, i.e. $\mathrm{tr}(\omega_R) = R$. We call R *nearly Gorenstein* if this trace contains the (unique) maximal graded ideal $\mathfrak{m}$ of R, i.e. $\mathfrak{m} \subseteq \mathrm{tr}(\omega_R)$.

Recently, the nearly Gorenstein property has been studied for certain special cases, such as Hibi rings [42, Theorem 5.4], edge rings associated to edge polytopes [46], numerical semigroup rings [41], and projective monomial curves [80]. Moreover, h-vectors of nearly Gorenstein homogeneous affine semigroup rings are also studied [79, Theorem 4.4].

It is a classical result that the lattice polytopes whose Ehrhart rings are Gorenstein are those for which there exists an integer k such that kP is reflexive [11], after an appropriate translation. In this chapter, we study the nearly Gorensteinness of the Ehrhart rings arising from general lattice polytopes.

In Section 2.3, we discuss some relations between nearly Gorensteinness of Ehrhart rings and their polytopes. Before we discuss the main results of this section, we must fix some notation and recall a few notions. We fix a lattice polytope P and

its facet presentation:

$$P = \left\{x \in \mathbb{R}^d : \ n_F(x) \geq -h_F \text{ for all } F \in \mathcal{F}(P)\right\},$$

where each height h_F is an integer and each inner normal vector $n_F \in (\mathbb{Z}^d)^*$ is a primitive lattice point. For a lattice polytope $P \subset \mathbb{R}^d$, we define its *floor polytope* as $\lfloor P \rfloor := \text{conv}(\text{int}(P) \cap \mathbb{Z}^d)$. We also introduce the *remainder polytope* $\{P\}$ of P, whose definition involves the pushing in and out of its facets in a particular way (see Definition 2.3.3 for the explicit details). These polytopes are central to our study of nearly Gorenstein polytopes. Also of importance is the *codegree* a_P of a lattice polytope P, which is defined as $a_P := \min\left\{k \in \mathbb{N} : \ \text{int}(kP) \cap \mathbb{Z}^d \neq \varnothing\right\}$, i.e. the minimum positive integer you have to dilate P by until its interior contains lattice points [10].

We now give the main results of Section 2.3. We say that a lattice polytope is *nearly Gorenstein* if its Ehrhart ring is nearly Gorenstein. Our first theorem gives a necessary condition and a sufficient condition for a lattice polytope to be nearly Gorenstein.

Theorem 2.1.1 (Proposition 2.3.5 and Theorem 2.3.8)**.** *Let $P \subset \mathbb{R}^d$ be a lattice polytope with codegree a.*

1. *If P is nearly Gorenstein, then it has the Minkowski decomposition $P = \lfloor aP \rfloor + \{P\}$.*
2. *Conversely, if $P = \lfloor aP \rfloor + \{P\}$, then there exists some K such that, for all integers $k \geq K$, the polytope kP is nearly Gorenstein.*

The next main theorem gives facet presentations for the floor and remainder polytopes appearing in the Minkowski decomposition of a nearly Gorenstein polytope.

Theorem 2.1.2 (Theorem 2.3.13)**.** *Let $P \subset \mathbb{R}^d$ be a lattice polytope with codegree a. Suppose that $P = \lfloor aP \rfloor + \{P\}$. Then*

$$\lfloor aP \rfloor = \left\{x \in \mathbb{R}^d : \ n_F(x) \geq 1 - a\,h_F \text{ for all } F \in \mathcal{F}(P)\right\} \text{ and}$$
$$\{P\} = \left\{x \in \mathbb{R}^d : \ n_F(x) \geq (a-1)h_F - 1 \text{ for all } F \in \mathcal{F}(P)\right\}.$$

Furthermore, if $\lfloor P \rfloor \neq \varnothing$, then $\{P\}$ is reflexive.

These results allow us to prove the final main theorem of Section 2.3. It reveals that the primitive inner normal vectors of a nearly Gorenstein polytope come from boundary points of reflexive polytopes.

Theorem 2.1.3. *Let $P \subset \mathbb{R}^d$ be a nearly Gorenstein polytope. Then there exists a reflexive polytope $Q \subset \mathbb{R}^d$ such that*

$$P = \left\{x \in \mathbb{R}^d : \ n(x) \geq -h_n \text{ for all } n \in \partial Q^* \cap (\mathbb{Z}^d)^*\right\},$$

where h_n are integers. Moreover, the inequalities defined by $n \in \mathcal{V}(Q^*)$ are irredundant. Furthermore, the number of facets of a nearly Gorenstein polytope is bounded by a constant depending on the dimension d.

We then use Theorem 2.1.3 to derive an efficient method for constructing nearly Gorenstein polytopes. Using this method, we find an example of a nearly Gorenstein polytope which does not have a Minkowski decomposition into Gorenstein polytopes (Example 2.3.19). We conclude the section by studying Minkowski indecomposable nearly Gorenstein polytopes; in particular, we show that they are in fact Gorenstein.

In Section 2.4, we study nearly Gorenstein 0/1-polytopes. This family of polytopes includes many subfamilies of polytopes which arise in combinatorics, such as order polytopes of posets and base polytopes from graphic matroids. Previous work has studied nearly Gorensteinness of Hibi rings [42] and of Ehrhart rings of stable set polytopes arising from perfect graphs [46, 81]. The main result of this section generalises these previous results by characterising a large class of nearly Gorenstein 0/1-polytopes:

Theorem 2.1.4 (Theorem 2.4.2)**.** *Let P be a 0/1-polytope which has the integer decomposition property. Then, P is nearly Gorenstein if and only if $P = P_1 \times \cdots \times P_s$, for some Gorenstein 0/1-polytopes $P_1, \ldots, P_s$ which satisfy $|a_{P_i} - a_{P_j}| \leq 1$, where a_{P_i} and a_{P_j} are the respective codegrees of P_i and P_j, for $1 \leq i < j \leq s$.*

In Subsection 2.4.1, we go into more detail how Theorem 2.1.4 extends previous results which appear in the literature. Subsequently, we obtain a number of our own interesting corollaries from Theorem 2.1.4. For example, we show that every nearly Gorenstein 0/1-polytope which has the integer decomposition property is level (Corollary 2.4.4). Furthermore, we characterise nearly Gorenstein edge polytopes which have the integer decomposition property (Corollary 2.4.5) and nearly Gorenstein base polytopes arising from graphic matroids (Corollary 2.4.11).

2.2 Preliminaries and auxiliary lemmas

2.2.1 Nearly Gorenstein $\mathbb{C}$-algebras

Let R be a finitely generated $\mathbb{N}$-graded $\mathbb{C}$-algebra with unique graded maximal ideal $\mathfrak{m}$. We will always assume that R is Cohen-Macaulay and admits a canonical module ω_R. We call $a(R)$ the a-invariant of R, i.e.

$$a(R) = -\min\{i \in \mathbb{N} : (\omega_R)_i \neq 0\},$$

where $(\omega_R)_i$ is the i-th graded piece of ω_R.

Definition 2.2.1. For a graded R-module M, let $\mathrm{tr}_R(M)$ be the sum of the ideals $\phi(M)$ over all $\phi \in \mathrm{Hom}_R(M, R)$, i.e.

$$\mathrm{tr}_R(M) = \sum_{\phi \in \mathrm{Hom}_R(M,R)} \phi(M).$$

When there is no risk of confusion about the ring, we simply write $\mathrm{tr}(M)$.

Definition 2.2.2 ([42, Definition 2.2])**.** We say that R is *nearly Gorenstein* if $\mathrm{tr}(\omega_R) \supseteq \mathbf{m}$. In particular, R is Gorenstein if and only if $\mathrm{tr}(\omega_R) = R$.

Proposition 2.2.3 ([42, Lemma 1.1]). *Let R be a ring and I an ideal of R containing a non-zero divisor of R. Let $Q(R)$ be the total quotient ring of fractions of R and set $I^{-1} := \{x \in Q(R) : xI \subseteq R\}$. Then*

$$\mathrm{tr}(I) = I \cdot I^{-1}.$$

Definition 2.2.4 ([95, Chapter III, Proposition 3.2]). We say that R is *level* if all the degrees of the minimal generators of ω_R are the same.

Let $R = \bigoplus_{n\geq 0} R_n$ and $S = \bigoplus_{n\geq 0} S_n$ be standard $\mathbb{C}$-algebras and define their *Segre product* $R\#S$ as the graded algebra:

$$R\#S = (R_0 \otimes_{\mathbb{C}} S_0) \oplus (R_1 \otimes_{\mathbb{C}} S_1) \oplus \cdots \subseteq R \otimes_{\mathbb{C}} S.$$

We denote a homogeneous element $x \otimes_{\mathbb{C}} y \in R_i \otimes_{\mathbb{C}} S_i$ by $x\#y$.

Proposition 2.2.5 ([43, Proposition 2.2 and Theorem 2.4]). *Let $R_1, \cdots, R_s$ be standard graded Cohen-Macaulay toric $\mathbb{C}$-algebras which have Krull dimension at least 2. Let $R = R_1\#R_2\#\cdots\#R_s$ be the Segre product. Then the following is true.*

$$\omega_R = \omega_{R_1}\#\omega_{R_2}\#\cdots\#\omega_{R_s} \quad \text{and} \quad \omega_R^{-1} = \omega_{R_1}^{-1}\#\omega_{R_2}^{-1}\#\cdots\#\omega_{R_s}^{-1}.$$

Lemma 2.2.6. *Let $R_1, \ldots, R_s$ be homogeneous normal affine semigroup rings over infinite field $\mathbb{C}$ which have Krull dimension at least 2. Let $R = R_1\#\cdots\#R_s$ be the Segre products. Then the following are true:*

(1) If R is nearly Gorenstein, then R_i is nearly Gorenstein for all i.

(2) If R_i is level for all i, then R is level.

Proof. It suffices to prove the case $s = 2$. Let $\boldsymbol{x}_1, \ldots, \boldsymbol{x}_n$ be $\mathbb{C}$-basis of $(R_1)_1$ and $\boldsymbol{y}_1, \ldots, \boldsymbol{y}_m$ be a $\mathbb{C}$-basis of$(R_2)_1$.

(1): In this case, by using Proposition 2.2.5, we get $\omega_R \cong \omega_{R_1}\#\omega_{R_2}$ and $\omega_R^{-1} \cong \omega_{R_1}^{-1}\#\omega_{R_2}^{-1}$. Then we may identify ω_R and ${\omega_R}^{-1}$ with $\omega_{R_1}\#\omega_{R_2}$ and $\omega_{R_1}^{-1}\#\omega_{R_2}^{-1}$, respectively.

It is enough to show that $\boldsymbol{x}_i \in \mathrm{tr}(\omega_{R_1})$ for any $1 \leq i \leq n$. Since R is nearly Gorenstein, there exist homogeneous elements $\boldsymbol{v}_1\#\boldsymbol{v}_2 \in \omega_{R_1}\#\omega_{R_2}$ and $\boldsymbol{u}_1\#\boldsymbol{u}_2 \in \omega_{R_1}^{-1}\#\omega_{R_2}^{-1}$ such that $\boldsymbol{x}_i\#\boldsymbol{y}_1 = (\boldsymbol{v}_1\#\boldsymbol{v}_2)(\boldsymbol{u}_1\#\boldsymbol{u}_2) = (\boldsymbol{v}_1\boldsymbol{u}_1\#\boldsymbol{v}_2\boldsymbol{u}_2)$, by [79, Proposition 4.2]. Thus, we get $\boldsymbol{x}_i = \boldsymbol{v}_1\boldsymbol{u}_1 \in \mathrm{tr}(\omega_{R_1})$, so R_1 is nearly Gorenstein. In the same way as above, we can show that R_2 is also nearly Gorenstein.

(2): First, $\omega_R = \omega_{R_1}\#\omega_{R_2}$ by Proposition 2.2.5. Let a_1 and a_2 be the a-invariants of R_1 and R_2, respectively, and assume that $a_1 \leq a_2$. Since R_1 and R_2 are level, $\omega_{R_1} \cong \langle f_1, \cdots, f_r\rangle R_1$ and $\omega_{R_2} \cong \langle g_1, \cdots, g_l\rangle R_2$ where $\deg f_i = -a_1$ and $\deg g_j = -a_2$ for all $1 \leq i \leq r$, $1 \leq j \leq l$. Thus, since $\omega_R = \omega_{R_1}\#\omega_{R_2}$, we may identify ω_R with $\langle f_1, \cdots, f_r\rangle R_1\#\langle g_1, \cdots, g_l\rangle R_2$. We set

$$V := \left\{ \boldsymbol{y}^{\boldsymbol{b}} g_j : 1 \leq j \leq l,\ \boldsymbol{a} \in \mathbb{N}^m,\ \sum_{i=1}^{m} b_i = a_2 - a_1 \right\},$$

where $\boldsymbol{y}^{\boldsymbol{a}} := \boldsymbol{y}_1^{a_1} \cdots \boldsymbol{y}_m^{a_m}$. Then $\omega_R = \langle f_i \# v \,:\, 1 \leq i \leq r, v \in V \rangle R$. Therefore, R is level. □

2.2.2 Lattice polytopes and Ehrhart rings

Throughout this subsection, let $P \subset \mathbb{R}^d$ be a lattice polytope, $\mathcal{F}(P)$ be the set of facets of P, and $\mathcal{V}(P)$ be the set of vertices of P. Moreover, recall that we always assume P is full-dimensional and has the facet presentation

$$P = \left\{ x \in \mathbb{R}^d \,:\, n_F(x) \geq -h_F \text{ for all } F \in \mathcal{F}(P) \right\}, \tag{2.1}$$

where each height h_F is an integer and each inner normal vector $n_F \in (\mathbb{Z}^d)^*$ is a *primitive* lattice point, i.e. a lattice point such that the greatest common divisor of its coordinates is 1.

Let C_P be the *cone of* P, that is,

$$C_P = \mathbb{R}_{\geq 0}(P \times \{1\}) = \left\{ (x,k) \in \mathbb{R}^{d+1} \,:\, n_F(x) \geq -kh_F \text{ for all } F \in \mathcal{F}(P) \right\}.$$

We define the *Ehrhart ring* of P as

$$A(P) = \mathbb{C}[C_P \cap \mathbb{Z}^{d+1}] = \mathbb{C}[\boldsymbol{t}^x s^k : k \in \mathbb{N} \text{ and } x \in kP \cap \mathbb{Z}^d],$$

where $\boldsymbol{t}^x = t_1^{x_1} \cdots t_d^{x_d}$ and $x = (x_1, \ldots, x_d) \in kP \cap \mathbb{Z}^d$. Note that the Ehrhart ring of P is a normal affine semigroup ring, and hence it is Cohen-Macaulay. Moreover, we can regard $A(P)$ as an $\mathbb{N}$-graded $\mathbb{C}$-algebra by setting $\deg(\boldsymbol{t}^x s^k) = k$ for each $x \in kP \cap \mathbb{Z}^d$.

We also define another affine semigroup ring, the *toric ring* of P, as

$$\mathbb{C}[P] = \mathbb{C}[\boldsymbol{t}^x s : x \in P \cap \mathbb{Z}^d].$$

The toric ring of P is a standard $\mathbb{N}$-graded $\mathbb{C}$-algebra.

It is known that $\mathbb{C}[P] = A(P)$ if and only if P has the integer decomposition property. Here, we say that P has the *integer decomposition property* (i.e. P is *IDP*) if for all positive integers k and all $x \in kP \cap \mathbb{Z}^d$, there exist $y_1, \ldots, y_k \in P \cap \mathbb{Z}^d$ such that $x = y_1 + \cdots + y_k$.

In order to describe the canonical module and the anti-canonical module of $A(P)$ in terms of P, we prepare some notation.

For a polytope or cone K, we denote the strict interior of σ by $\mathrm{int}(\sigma)$. Note that

$$\mathrm{int}(C_P) = \left\{ (x,k) \in \mathbb{R}^{d+1} \,:\, n_F(x) > -kh_F \text{ for all } F \in \mathcal{F}(P) \right\}.$$

Moreover, we define

$$\mathrm{ant}(C_P) := \left\{ (x,k) \in \mathbb{R}^{d+1} \,:\, n_F(x) \geq -kh_F - 1 \text{ for all } F \in \mathcal{F}(P) \right\}.$$

Then the following is true.

Proposition 2.2.7 (see [43, Proposition 4.1 and Corollary 4.2]). *The canonical module of $A(P)$ and the anti-canonical module of $A(P)$ are given by the following, respectively:*

$$\omega_{A(P)} = \left\langle \boldsymbol{t}^x s^k : (x,k) \in \mathrm{int}(C_P) \cap \mathbb{Z}^{d+1} \right\rangle \text{ and } \omega_{A(P)}^{-1} = \left\langle \boldsymbol{t}^x s^k : (x,k) \in \mathrm{ant}(C_P) \cap \mathbb{Z}^{d+1} \right\rangle.$$

Further, the negated a-invariant of $A(P)$ coincides with the codegree of P, i.e.

$$a(A(P)) = -\min\left\{k \in \mathbb{Z}_{\geq 1} : \mathrm{int}(kP) \cap \mathbb{Z}^d \neq \emptyset\right\}.$$

We recall that the *(direct) product* of two polytopes $P \subset \mathbb{R}^d$ and $Q \subset \mathbb{R}^e$ is denoted by $P \times Q \subset \mathbb{R}^{d+e}$. Note that we can regard $P \times Q$ as the Minkowski sum of polytopes, as follows. Let

$$P' = \left\{ (p, \underbrace{0, \ldots, 0}_{e}) \in \mathbb{R}^{d+e} : p \in P \right\} \text{ and } Q' = \left\{ (\underbrace{0, \ldots, 0}_{d}, q) \in \mathbb{R}^{d+e} : q \in Q \right\}.$$

Then, we can see that $P \times Q = P' + Q'$. Conversely, suppose two polytopes $P', Q' \subset \mathbb{R}^d$ satisfy the following condition: for all $i \in [d] := \{1, \ldots, d\}$, we have that $\pi_i(P') = \{0\}$ or $\pi_i(Q') = \{0\}$, where $\pi_i : \mathbb{R}^d \to \mathbb{R}$ is the projection onto the i-th coordinate. Then we can regard $P' + Q'$ as the product of two polytopes. Moreover, let P and Q be two lattice polytopes. It is known that $\mathbb{C}[P \times Q]$ is isomorphic to the Segre product $\mathbb{C}[P] \# \mathbb{C}[Q]$.

2.3 Nearly Gorensteinness of lattice polytopes

Throughout this section, the lattice polytope P has the facet presentation (2.1).

Definition 2.3.1. We say that P is *Gorenstein* (resp. *nearly Gorenstein*) if the Ehrhart ring $A(P)$ is Gorenstein (resp. nearly Gorenstein).

There are well-known equivalent conditions of Gorensteinness in terms of the lattice polytope P itself. For instance, P is Gorenstein if and only if there exists a positive integer a such that a *lattice translation* of aP is *reflexive*, i.e. aP has a unique interior lattice point which has lattice distance 1 to all facets of aP.

In this section, we will determine a necessary condition for P to be nearly Gorenstein, in terms of the polytope P itself. This condition demands that P has a particular Minkowski decomposition. By taking a dual perspective, we see exactly the connection to reflexive polytopes. Next, we will show that if P satisfies the aforementioned necessary condition and is in some sense "big enough", then P will be nearly Gorenstein. We end the section by investigating the nearly Gorensteinness of Minkowski indecomposable lattice polytopes.

2.3.1 Necessary conditions

The main aim of this subsection is to show the first half of Theorem 2.1.1. Before we proceed, let us first introduce some helpful notation. For a subset X of $\mathbb{R}^{d+1}$ and $k \in \mathbb{Z}$, let $X_k = \left\{x \in \mathbb{R}^d : (x,k) \in X\right\}$ be the k-th *piece* of X. Note the subtlety in our notation: while X is a subset of $\mathbb{R}^{d+1}$, its k-th piece X_k is a subset of $\mathbb{R}^d$. Moreover, for a lattice polytope P, we denote its *codegree* by a_P – see Proposition 2.2.7 for the definition. When it is clear from context, we simply write a instead of a_P.

Proposition 2.3.2. *Let $P \subset \mathbb{R}^d$ be a lattice polytope with codegree a. Then P is nearly Gorenstein if and only if*

$$(C_P \cap \mathbb{Z}^{d+1}) \setminus \{0\} \subseteq \mathrm{int}(C_P) \cap \mathbb{Z}^{d+1} + \mathrm{ant}(C_P) \cap \mathbb{Z}^{d+1}. \tag{2.2}$$

In particular, if P is nearly Gorenstein, then

$$P \cap \mathbb{Z}^d = \mathrm{int}(C_P)_a \cap \mathbb{Z}^d + \mathrm{ant}(C_P)_{1-a} \cap \mathbb{Z}^d. \tag{2.3}$$

The converse also holds if P is IDP.

Proof. By definition, P is nearly Gorenstein if and only if the trace $\mathrm{tr}(\omega)$ of the canonical ideal ω of $A(P)$ contains the maximal ideal $\mathfrak{m}$ of $A(P)$. By Proposition 2.2.3, this trace is exactly the product $\omega_{A(P)} \cdot \omega_{A(P)}^{-1}$. Then, Proposition 2.2.7 tells us the monomial generators of ω and ω^{-1} in terms of the lattice points of $\mathrm{int}(C_P)$ and $\mathrm{ant}(C_P)$. We finally note that the maximal ideal $\mathfrak{m}$ can be generated by the monomials $\boldsymbol{t}^x s^k$, where (x,k) are lattice points in $C_P \setminus \{0\}$. From this, it is clear to see that P is nearly Gorenstein if and only if (2.2) holds.

We next prove that (2.3) follows from nearly Gorensteinness of P. First, note that the right hand side of (2.2) is contained in $C_P \cap \mathbb{Z}^{d+1}$ by definition. Therefore, when we take the 1st piece of both sides in (2.2), we obtain the equality

$$P \cap \mathbb{Z}^d = (\mathrm{int}(C_P) \cap \mathbb{Z}^{d+1} + \mathrm{ant}(C_P) \cap \mathbb{Z}^{d+1})_1.$$

Note that when P is Gorenstein, $\mathrm{int}(C_P)_a \cap \mathbb{Z}^d$ and $\mathrm{ant}(C_P)_{-a} \cap \mathbb{Z}^d$ are singleton sets; therefore, the result easily follows. Otherwise, we claim that $\mathrm{ant}(C_P)_{1-b} \cap \mathbb{Z}^d$ is empty for all $b \geq a+1$. Since $\mathrm{int}(C_P)_b$ is empty for $b < a$, we obtain the desired result.

Finally, we show that the converse holds when P is IDP. Let $(x,k) \in C_P \cap \mathbb{Z}^d \setminus \{0\}$. Since P is IDP, there are $x_1, \ldots, x_k \in P \cap \mathbb{Z}^d$ such that $(x,k) = (x_1,1) + \cdots + (x_k,1)$. Further, each $x_i \in P \cap \mathbb{Z}^d$ can be written as the sum of lattice points in $\mathrm{int}(C_P)$ and $\mathrm{ant}(C_P)$. Therefore, (2.2) holds and so P is nearly Gorenstein. □

Definition 2.3.3. Let $P \subset \mathbb{R}^d$ be a lattice polytope with codegree a. We define its *floor polytope* and *remainder polytopes* as

$$\lfloor P \rfloor := \mathrm{conv}(\mathrm{int}(P) \cap \mathbb{Z}^d) \qquad \text{and} \qquad \{P\} := \mathrm{conv}(\mathrm{ant}(C_P)_{1-a} \cap \mathbb{Z}^d),$$

respectively. Note that $\lfloor P \rfloor$ coincides with $\operatorname{conv}(\operatorname{int}(C_P)_1 \cap \mathbb{Z}^d)$.

We collate a couple of easy facts about these polytopes and reformulate part of Proposition 2.3.2 into the following statement.

Lemma 2.3.4. *Let $P \subset \mathbb{R}^d$ be a lattice polytope with codegree a. Then:*

1. $\lfloor aP \rfloor \subseteq \left\{x \in \mathbb{R}^d : n_F(x) \geq 1 - ah_F \text{ for all } F \in \mathcal{F}(P)\right\}$;
2. $\{P\} \subseteq \left\{x \in \mathbb{R}^d : n_F(x) \geq (a-1)h_F - 1 \text{ for all } F \in \mathcal{F}(P)\right\}$;
3. *If P is nearly Gorenstein, then $P \cap \mathbb{Z}^d = \lfloor aP \rfloor \cap \mathbb{Z}^d + \{P\} \cap \mathbb{Z}^d$;*
4. *If P is IDP and $P \cap \mathbb{Z}^d = \lfloor aP \rfloor \cap \mathbb{Z}^d + \{P\} \cap \mathbb{Z}^d$, then P is nearly Gorenstein.*

Proof. Statements (1) and (2) follow immediately from the definition of the floor and remainder polytope. To prove statements (3) and (4), notice that the lattice points of $\operatorname{int}(C_P)_a$ coincide with those of $\lfloor aP \rfloor$ and the lattice points of $\operatorname{ant}(C_P)_{1-a}$ coincide with those of $\{P\}$. Then simply substitute this into Proposition 2.3.2. □

The following proposition is the first half of Theorem 2.1.1:

Proposition 2.3.5. *If P is nearly Gorenstein, then $P = \lfloor aP \rfloor + \{P\}$, where a is the codegree of P.*

Proof. Let $x \in \lfloor aP \rfloor$ and $y \in \{P\}$. By statements (1) and (2) of Lemma 2.3.4, we have that, for all facets F of P, $n_F(x+y) \geq 1 - ah_F + (a-1)h_F - 1 = -h_F$. So, $x + y \in P$. Therefore, we obtain that $\lfloor aP \rfloor + \{P\} \subseteq P$.

On the other hand, let v be a vertex of P. Since P is a lattice polytope, $v \in P \cap \mathbb{Z}^d$. Thus, by statement (3) of Lemma 2.3.4, can write v as the sum of an element of $\lfloor aP \rfloor \cap \mathbb{Z}^d$ and an element of $\{P\} \cap \mathbb{Z}^d$. This implies $P \subseteq \lfloor aP \rfloor + \{P\}$. □

Example 2.3.6. Consider the stop sign polytope, given by

$$P = \operatorname{conv}\{(1,0),(2,0),(3,1),(3,2),(2,3),(1,3),(0,2),(0,1)\}.$$

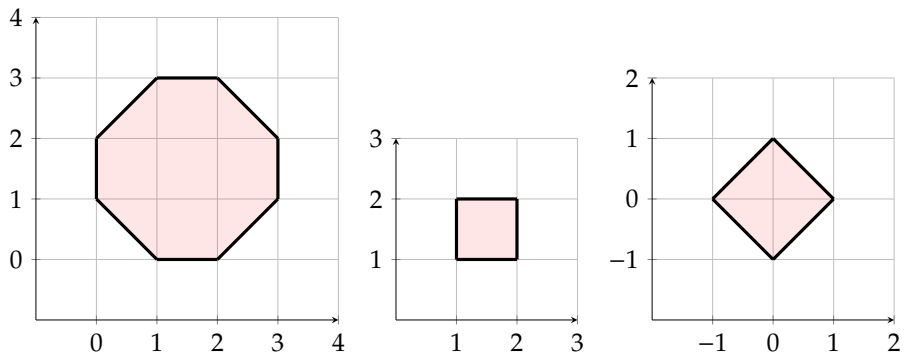

FIGURE 2.1: The stop sign polytope P (left) with its floor polytope $\lfloor P \rfloor$ (middle) and remainder polytope $\{P\}$ (right).

First, we note that $a_P = 1$. Next, we may compute the floor and remainder polytopes:

$$\lfloor P \rfloor = \text{conv}\{(1,1),(2,1),(1,2),(2,2)\} \quad \text{and} \quad \{P\} = \text{conv}\{(1,0),(0,1),(-1,0),(0,-1)\}.$$

By taking the Minkowski sum of these polytopes, we see that P satisfies the necessary condition to be nearly Gorenstein given by Proposition 2.3.5, i.e. $P = \lfloor P \rfloor + \{P\}$. On the other hand, it is straightforward to verify that every lattice point of P can be written as the sum of a lattice point of $\lfloor P \rfloor$ and a lattice point of $\{P\}$. Since P is IDP (as is true for all *polygons*), statement (4) of Lemma 2.3.4 informs us that P is nearly Gorenstein.

Finally, we remark that the remainder polytope $\{P\}$ is reflexive. This is not coincidence, as we will prove in Proposition 2.3.13.

2.3.2 A sufficient condition

In this subsection, we will explore sufficient conditions for a lattice polytope to be nearly Gorenstein; in particular, we will prove the second half of Theorem 2.1.1.

We first note that the converse of Proposition 2.3.5 does not hold in general.

Example 2.3.7 (compare [82, Example 1.1])**.** Let $f = \frac{1}{3}(e_1 + \cdots + e_6) \in \mathbb{R}^6$, where $e_1, \ldots, e_6$ is a basis of the lattice $\mathbb{Z}^6$. Define a new lattice $L := \mathbb{Z}^6 + f \cdot \mathbb{Z}$, and consider the lattice polytope

$$Q := \text{conv}\{e_1, \ldots, e_6, e_1 - f, \ldots, e_6 - f\}$$

with respect to the lattice L. Set $P := 2Q$. Since $\lfloor P \rfloor = \{P\} = Q$, it's easy to see that $P = \lfloor P \rfloor + \{P\}$, meeting the necessary condition of Proposition 2.3.5 for nearly Gorensteinness.

On the other hand, Q is not IDP. In particular, $2Q \cap L \neq (Q \cap L) + (Q \cap L)$. Thus, $P = 2Q$ fails the necessary condition of statement (3) in Lemma 2.3.4, and so P is not nearly Gorenstein.

So, we need to make more assumptions about P in order to be guaranteed nearly Gorensteinness. This brings us to the following result, which is the second half of Theorem 2.1.1:

Theorem 2.3.8. *Let $P \subset \mathbb{R}^d$ be a lattice polytope satisfying $P = \lfloor aP \rfloor + \{P\}$, where a is the codegree of P. Then there exists some integer $K \geq 1$ (depending on P) such that for all $k \geq K$, the polytope kP is nearly Gorenstein.*

In order to prove the above, we rely on a few key ingredients. The first ingredient is an extension of known results from the reflexive case, which appear in [45].

Lemma 2.3.9. *Let $P \subset \mathbb{R}^d$ be a lattice polytope satisfying $P = \lfloor aP \rfloor + \{P\}$, where a is the codegree of P. Then the following statements hold:*

1. $kP = \lfloor (k + a - 1)P \rfloor + \{P\}$, *for all* $k \geq 1$;
2. $\lfloor k'P \rfloor = \lfloor aP \rfloor + (k' - a)P$, *for all* $k' \geq a$.

Before we give the proof, we will restrict these statements to the reflexive case for the sake of comparison. First, we have $a = 1$. Next, since $\lfloor P \rfloor$ is the origin, $P = \{P\}$. So, for reflexive polytopes, the statement (1) is equivalent to $kP = \lfloor kP \rfloor + P$. After cancellation by P, we obtain the reflexive version of statement (2): $\lfloor kP \rfloor = (k-1)P$.

Proof of Lemma 2.3.9. Let $k \geq 1$ be an integer. Throughout this proof, we repeatedly use the two inequalities appearing in statements (1) and (2) of Lemma 2.3.4. We also use the inequalities appearing in the facet presentations for P and its dilates.

We first prove the "$\supseteq$" part of statement (1), i.e. that

$$kP \supseteq \lfloor (k+a-1)P \rfloor + \{P\}\,, \text{ for all } k \geq 1. \tag{2.4}$$

Let $x \in \lfloor (k+a-1)P \rfloor$ and $y \in \{P\}$. Then $n_F(x+y) \geq (1-(k+a-1)h_F)+((a-1)h_F-1) = -kh_F$, for all facets F of P. Thus, $x+y \in kP$.

Next, we note that $kP = (k-1)P + \lfloor aP \rfloor + \{P\}$. We substitute this into (2.4), then cancel $\{P\}$ from both sides to obtain $\lfloor (k+a-1)P \rfloor \subseteq (k-1)P + \lfloor aP \rfloor$.

We now prove the reverse inclusion of the above. Let $x \in (k-1)P$ and $y \in \lfloor aP \rfloor$. Then, $n_F(x+y) \geq -(k-1)h_F+(1-ah_F) = 1-(k+a-1)h_F$. Therefore, $x+y \in \lfloor (k+a-1)P \rfloor$. Thus, we obtain the equality $\lfloor (k+a-1)P \rfloor = (k-1)P + \lfloor aP \rfloor$. Setting $k' := k+a-1$ then gives us statement (2). Adding $\{P\}$ to both sides gives us statement (1). □

The main ingredient in proving Theorem 2.3.8 is a result of Haase and Hofmann, which allows us to guarantee that the second condition of statement (4) of Lemma 2.3.4 holds.

Theorem 2.3.10 ([35, Theorem 4.2]). *Let $P, Q \subset \mathbb{R}^d$ be rational polytopes such that the normal fan $\mathcal{N}(P)$ of P is a refinement of the normal fan $\mathcal{N}(Q)$ of Q. Suppose also that for each edge E of P, the corresponding face E' of Q has lattice length $\ell_{E'}$ satisfying $\ell_E \geq d\ell_{E'}$. Then $(P+Q) \cap \mathbb{Z}^d = (P \cap \mathbb{Z}^d) + (Q \cap \mathbb{Z}^d)$.*

In order to guarantee the first condition of statement (4) of Lemma 2.3.4, we need this next result:

Theorem 2.3.11 ([102, Theorem 1.3.3]). *Let $P \subset \mathbb{R}^d$ be a lattice polytope. Then $(d-1)P$ is IDP.*

We are now ready to give the proof.

Proof of Theorem 2.3.8. We first wish to find a suitable K which satisfies

$$kP \cap \mathbb{Z}^d = \lfloor kP \rfloor \cap \mathbb{Z}^d + \{kP\} \cap \mathbb{Z}^d, \text{ for all } k \geq K.$$

Let a be the codegree of P. Looking at statement (2) of Lemma 2.3.9, we see that $(k-a)P$ is a Minkowski summand of $\lfloor kP \rfloor$; thus, we get a crude lower bound on the length of the edges of $\lfloor kP \rfloor$: for $k \geq a$, every edge E of $\lfloor kP \rfloor$ has lattice length $\ell_E \geq k-a$. Denote by L the maximum edge length of $\{aP\}$ and set $K := dL + a$. Note that for $k \geq a$, the polytopes $\{kP\}$ and $\{aP\}$ coincide. So, for all $k \geq K$, every edge E of $\lfloor kP \rfloor$ will have lattice length $\ell_E \geq k-a \geq dL$.

Further, statement (2) of Lemma 2.3.9 implies that, for $k \geq a+1$, the normal fan $\mathcal{N}(\lfloor kP \rfloor)$ coincides with $\mathcal{N}(P)$. Hence, $\mathcal{N}(\lfloor kP \rfloor)$ is a refinement of the normal fan of $\{kP\}$. Thus, we may apply Theorem 2.3.10, obtaining that $kP \cap \mathbb{Z}^d = \lfloor kP \rfloor \cap \mathbb{Z}^d + \{kP\} \cap \mathbb{Z}^d$.

Finally, since $a, L \geq 1$, we see that $K \geq d-1$. Thus, by Theorem 2.3.11, we have that kP is IDP. Therefore, by statement (4) of Lemma 2.3.4, we can conclude that kP is nearly Gorenstein for all $k \geq K$. □

Remark 2.3.12. We say that a graded ring R is *Gorenstein on the punctured spectrum* [42] if $\mathrm{tr}(\omega_R)$ contains $\mathfrak{m}^k$ for some integer $k \geq 0$. If $k = 0$, this is just the Gorenstein condition; if $k = 1$, it is the nearly Gorenstein condition. Now, for a lattice polytope $P \subset \mathbb{R}^d$, it can be shown that its Ehrhart ring $A(P)$ is Gorenstein on the punctured spectrum if there exists a positive integer K such that $kP \cap \mathbb{Z}^d$ coincides with $(\mathrm{int}(C_P) \cap \mathbb{Z}^{d+1} + \mathrm{ant}(C_P) \cap \mathbb{Z}^{d+1})_k$, for all $k \geq K$. Therefore, using Theorem 2.3.8, it's straightforward to show that all lattice polytopes P satisfying $P = \lfloor aP \rfloor + \{P\}$ are Gorenstein on the punctured spectrum.

2.3.3 Decompositions of nearly Gorenstein polytopes

In this subsection, we first prove Theorem 2.1.2. This naturally leads to an investigation of whether nearly Gorenstein polytopes decompose into the Minkowski sum of Gorenstein polytopes (Questions 2.3.15 and 2.3.16). We prove Theorem 2.1.3, which leads to a way to systematically construct examples of nearly Gorenstein polytopes. This is then used to find a counterexample to Questions 2.3.15 and 2.3.16. Finally, we conclude the section with a result about indecomposable nearly Gorenstein polytopes.

Theorem 2.3.13 (Theorem 2.1.2)**.** *Let $P \subset \mathbb{R}^d$ be a lattice polytope which satisfies $P = \lfloor aP \rfloor + \{P\}$, where a is the codegree of P. Then we have*

$$\lfloor aP \rfloor = \left\{ x \in \mathbb{R}^d : \ n_F(x) \geq 1 - ah_F \text{ for all } F \in \mathcal{F}(P) \right\} \text{ and}$$

$$\{P\} = \left\{ x \in \mathbb{R}^d : \ n_F(x) \geq (a-1)h_F - 1 \text{ for all } F \in \mathcal{F}(P) \right\}.$$

In particular, the right hand sides of the equalities are lattice polytopes. Furthermore, if $a = 1$, then $\{P\}$ is a reflexive polytope.

Proof. Label the two polytopes on the right-hand sides as Q_1 and Q_2, respectively. It's straightforward to see that $\lfloor aP \rfloor = \mathrm{conv}(Q_1 \cap \mathbb{Z}^d)$ and $\{P\} = \mathrm{conv}(Q_2 \cap \mathbb{Z}^d)$. Thus, $\lfloor aP \rfloor \subseteq Q_1$ and $\{P\} \subseteq Q_2$. Ultimately, we want to prove the reverse inclusions but first, we must show an intermediate equality: $P = Q_1 + Q_2$. Let $x \in Q_1$ and $y \in Q_2$. Then, for all facets F of P, we have $n_F(x+y) \geq 1 - ah_F + (a-1)h_F - 1 = -h_F$. Thus, $x + y \in P$ and so, $Q_1 + Q_2 \subseteq P$. Conversely, if we combine this with our assumption that $P = \lfloor aP \rfloor + \{P\}$, we obtain that, in fact, $P = Q_1 + Q_2$.

We now use the above equality to obtain that $\lfloor aP \rfloor = Q_1$ and $\{P\} = Q_2$, as follows. Assume towards a contradiction that $Q_1 \not\subseteq \lfloor aP \rfloor$, i.e. there exists a vertex v of Q_1 which doesn't belong to $\lfloor aP \rfloor$. Choose a normal vector $n \in (\mathbb{R}^d)^*$ which achieves its

minimal value h_1 over Q_1 *only* at v (i.e. n lies in the interior of the cone σ_v in the (inner) normal fan $\mathcal{N}(Q_1)$ which corresponds to v). Denote by h_2 the minimal evaluation of n over Q_2. Then, the minimal evaluation of n over P is $h_1 + h_2$. However, for all $x \in \lfloor aP \rfloor$ and $y \in \{P\}$, we have that $n(x + y) > h_1 + h_2$. This contradicts the fact that $P = \lfloor aP \rfloor + \{P\}$. Therefore, the vertices of Q_1 coincide with the vertices of $\lfloor aP \rfloor$; in particular, $\lfloor aP \rfloor = Q_1$. We similarly obtain that $\{P\} = Q_2$.

Next, since $\lfloor aP \rfloor$ and $\{P\}$ are lattice polytopes by definition, we note that Q_1 and Q_2 are lattice polytopes in this situation.

Finally, suppose we are in the case when P has an interior lattice point, i.e. $a = 1$. By substituting this into the second equality, we see that the remainder polytope $\{P\}$ is indeed reflexive as all its facets lie at height 1.

□

In contrast, when P has no interior points, the remainder polytope $\{P\}$ is not necessarily even Gorenstein.

Example 2.3.14. Consider the polytope

$$P = \text{conv}\{(0,0,0),(2,0,0),(1,1,0),(0,1,0),(0,0,1),(2,0,1),(1,1,1),(0,1,1)\}.$$

We can verify that P is nearly Gorenstein and IDP, but the remainder polytope $\{P\}$ is not Gorenstein. However, $\{P\}$ can be written as the Minkowski sum of

$$\text{conv}\{(0,0,0),(1,0,0),(0,1,0)\} \quad \text{and} \quad \text{conv}\{(-1,-1,-1),(-1,-1,0)\},$$

which are both Gorenstein.

We see similar behavior when studying the nearly Gorensteinness for certain restricted classes of polytopes. This motivated us to pose the following question.

Question 2.3.15. If P is nearly Gorenstein, then can we write $P = P_1 + \cdots + P_s$ for some Gorenstein lattice polytopes $P_1, \ldots, P_s$?

We recall that P is (*Minkowski*) *indecomposable* if P is not a singleton and if there exist lattice polytopes P_1 and P_2 with $P = P_1 + P_2$, then either P_1 or P_2 is a singleton. Note that if P is not a singleton, then we can write $P = P_1 + \cdots + P_s$ for some indecomposable lattice polytopes $P_1, \ldots, P_s$. Then, a stronger version of Question 2.3.15 can be posed:

Question 2.3.16. If P has an indecomposable non-Gorenstein lattice polytope as a Minkowski summand, then is P not nearly Gorenstein?

This question has a positive answer for IDP 0/1-polytopes, which is shown in Section 2.4. For the remainder of this section, we will build up some machinery which allows for the efficient construction of nearly Gorenstein polytopes. We then use this in Example 2.3.19 to give an answer to Questions 2.3.15 and 2.3.16.

Theorem 2.3.17 (Theorem 2.1.3)**.** *Let $P \subset \mathbb{R}^d$ be a nearly Gorenstein polytope. Then there exists a reflexive polytope $Q \subset \mathbb{R}^d$ such that*

$$P = \left\{x \in \mathbb{R}^d \,:\, n(x) \geq -h_n \text{ for all } n \in \partial Q^* \cap (\mathbb{Z}^d)^*\right\},$$

where h_n are integers. Moreover, the inequalities defined by $n \in \mathcal{V}(Q^*)$ are irredundant. Furthermore, the number of facets of a nearly Gorenstein polytope is bounded by a constant depending on the dimension d.

Before we dive into the proof, it will be useful to have the following lemma.

Lemma 2.3.18. *Let P be a lattice polytope satisfying $P = \lfloor aP \rfloor + \{P\}$, where a is the codegree of P. Then $aP = \lfloor aP \rfloor + \{aP\}$. Moreover, $\{aP\} = (a-1)P + \{P\}$.*

Proof. We first wish to show that $(a-1)P + \{P\} \subseteq \{aP\}$. Let $x \in (a-1)P$ and $y \in \{P\}$. Then, by Lemma 2.3.4 (2), $n_F(x+y) \geq -(a-1)h_F + (a-1)h_F - 1 = -1$, for all facets F of P. So, $x + y \in \{aP\}$. Thus, $(a-1)P + \{P\} \subseteq \{aP\}$.

We can add $\lfloor aP \rfloor$ to both sides of the inclusion to get $aP \subseteq \lfloor aP \rfloor + \{aP\}$.

We next wish to show the reverse inclusion of the above. Let $z \in \lfloor aP \rfloor$ and $w \in \{aP\}$. Then $n_F(z+w) \geq (1 - ah_F) - 1 = -ah_F$, for all facets F of P. So, $z + w \in aP$. Therefore, $\lfloor aP \rfloor + \{aP\} \subseteq aP$. Combining the two inclusions gives the desired equality: $aP = \lfloor aP \rfloor + \{aP\}$.

Moreover, we obtain that $\lfloor aP \rfloor + \{P\} + (a-1)P = \lfloor aP \rfloor + \{aP\}$. Since Minkowski addition of convex sets satisfies the cancellation law, we may cancel both sides by $\lfloor aP \rfloor$ to obtain the equality $\{aP\} = (a-1)P + \{P\}$. □

Proof of Theorem 2.3.17. We wish to study the (inner) normal fan $\mathcal{N}(P)$ of P, as it's enough to show that its primitive ray generators all lie in $\partial Q^* \cap (\mathbb{Z}^d)^*$, for some reflexive polytope $Q \subset \mathbb{R}^d$. Let a be the codegree of P. Since dilation has no effect on the normal fan, we may pass to the normal fan of aP. Now, by Lemma 2.3.18, aP has a Minkowski decomposition into $\lfloor aP \rfloor$ and $\{aP\}$. Thus, $\mathcal{N}(aP)$ is the common refinement of $\mathcal{N}(\lfloor aP \rfloor)$ and $\mathcal{N}(\{aP\})$. By Proposition 2.3.13, we obtain that $Q := \{aP\}$ is a reflexive polytope. Hence, the primitive ray generators of $\mathcal{N}(Q)$ are vertices of the reflexive polytope $Q^* \subset (\mathbb{R}^d)^*$; in particular, they are lattice points lying in the boundary of Q^*.

We next look at the contribution to $\mathcal{N}(aP)$ coming from $\lfloor aP \rfloor$. Let $n \in (\mathbb{Z}^d)^*$ be a primitive ray generator of $\mathcal{N}(\lfloor aP \rfloor)$. Then, by definition of the remainder polytope, $n(x) \geq -1$, for all $x \in Q$. But now, this means that n lies in Q^*. So, since $n \neq 0$ and Q is reflexive, we obtain that $n \in \partial Q^* \cap (\mathbb{Z}^d)^*$. Therefore, we have now shown that the primitive ray generators of $\mathcal{N}(P) = \mathcal{N}(aP)$ contain the vertices of Q^*, and that they all lie in $\partial Q^* \cap (\mathbb{Z}^d)^*$.

Finally, we note that the number of facets of a nearly Gorenstein polytope $P \subset \mathbb{R}^d$ is bounded by $c_d := \sup_Q |\partial Q^* \cap (\mathbb{Z}^d)^*|$, where Q runs over all d-dimensional reflexive polytopes. Since there are only finitely reflexive polytopes in each dimension d, and all polytopes only have a finite number of boundary points, we see that c_d is a finite number. □

We will now detail how to construct nearly Gorenstein polytopes. First, choose a reflexive polytope $Q \subset \mathbb{R}^d$. Then, choose a (possibly empty) subset S' of the boundary lattice points of Q^* which are not vertices of Q^*. Now, for each $n \in S := S' \cup \mathcal{V}(Q^*)$, choose the height $h_n \in \mathbb{Z}$. Construct a polytope P' defined by $n(x) \geq -h_n$ for all $n \in S$, and assert that none of these inequalities are redundant. Next, we can dilate P' to rP' so that it's a lattice polytope which contains an interior lattice point. By construction, its remainder polytope $\{rP'\}$ coincides with the reflexive polytope Q. In practice, rP' has a Minkowski decomposition into $\lfloor rP' \rfloor$ and $\{rP'\}$, but we don't yet have a proof that this always holds. Finally, we can use Theorem 2.3.8 to dilate rP' even further to $P := krP'$ so that $P = \lfloor P \rfloor + \{P\}$ is nearly Gorenstein.

Example 2.3.19. Consider the polytope

$$P = \operatorname{conv}\{(-4,-3,-4),(-3,-1,-3),(-2,-2,-3),(0,1,4),(0,4,1),(3,1,1)\}.$$

Note that P has many interior lattice points, it has codegree 1. Its floor polytope is

$$\lfloor P \rfloor = \operatorname{conv}\{(-3,-2,-3),(0,3,1),(0,1,3),(2,1,1)\}.$$

This is an indecomposable simplex, which is not Gorenstein. Its remainder polytope is

$$\{P\} = \operatorname{conv}\{(-1,-1,-1),(1,0,0),(0,1,0),(0,0,1)\},$$

which is clearly reflexive. We have $P = \lfloor P \rfloor + \{P\}$. We use Magma [16] to verify that $P \cap \mathbb{Z}^3 = (\lfloor P \rfloor \cap \mathbb{Z}^3) + (\{P\} \cap \mathbb{Z}^3)$ and that P is IDP. Thus, we may conclude by Lemma 2.3.4 that P is a nearly Gorenstein polytope.

It can be shown that $P = \lfloor P \rfloor + \{P\}$ is the only non-trivial Minkowski decomposition of P. Thus, we may conclude that the nearly Gorenstein polytope P cannot be decomposed into Gorenstein polytopes. Therefore, we may answer Questions 2.3.15 and 2.3.16 in the negative.

It now remains to show that P has no other Minkowski decompositions. But first, we need a way to measure the $\mathbb{Z}$-translations of one polytope which are contained in another. We define the *(lattice) Minkowski difference* of two lattice polytopes $P, Q \subset \mathbb{R}^d$ as $P \div Q := \operatorname{conv}\left\{x \in \mathbb{Z}^d : x + Q \subseteq P\right\}$. Thus, $(P \div Q) + Q \subseteq P$.

Let $P = P_1 + P_2$ be a Minkowski decomposition of P into two lattice polytopes. Now, consider the following facet of P.

$$F = \operatorname{conv}\{(-4,-3,-4),(-2,-2,-3),(0,1,4),(3,1,1)\}.$$

We can compute that $P \div F = \{(0,0,0)\}$. So, it follows that if F is a face of P_1 or P_2, then $P_1 = P$ or $P_2 = P$, respectively. The facet F has only one non-trivial decomposition $F = F_1 + F_2$, where

$$F_1 = \operatorname{conv}\{(-3,-2,-3),(0,1,3),(2,1,1)\} \quad \text{and} \quad F_2 = \operatorname{conv}\{(-1,-1,-1),(1,0,0),(0,0,1)\}.$$

Without loss of generality, we may assume that F_1 is a face of P_1 and F_2 is a face of P_2. Let $P_1' := P \div F_2$ and $P_2' := P \div F_1$. By definition, we must have $P_1 \subseteq P_1'$ and $P_2 \subseteq P_2'$. So, $P = P_1 + P_2 \subseteq P_1' + P_2' \subseteq P$. This implies that $P_1 = P_1'$ and $P_2 = P_2'$. But now, if

we compute the Minkowski differences, we see that P_1' and P_2' (and hence P_1 and P_2) coincide with $\lfloor P \rfloor$ and $\{P\}$, respectively. Thus, $P = \lfloor P \rfloor + \{P\}$ is the only non-trivial Minkowski decomposition of P.

We end this section by giving the following theorem about nearly Gorensteinness of indecomposable polytopes, which plays an important role in the characterisation of nearly Gorenstein 0/1-polytopes in Section 2.4.

Theorem 2.3.20. *Let P be an indecomposable lattice polytope. Then, P is nearly Gorenstein if and only if P is Gorenstein.*

Proof. It is already clear that Gorensteinness implies nearly Gorensteinness, so we just have to treat the converse implication. Suppose that P is nearly Gorenstein. By Proposition 2.3.5, we have that $P = \lfloor aP \rfloor + \{P\}$, where a is the codegree of P. Since P is indecomposable, either (i) $\lfloor aP \rfloor$ is a singleton or (ii) $\{P\}$ is a singleton.

We first deal with case (i). Consider aP. By Lemma 2.3.18, $aP = \lfloor aP \rfloor + \{aP\}$. Thus, aP is a translation of $\{aP\}$. By Proposition 2.3.13, $\{aP\}$ is reflexive. Thus, P is Gorenstein.

The argument for case (ii) is similar. We consider $\{aP\}$. By Lemma 2.3.18, $\{aP\} = (a-1)P + \{P\}$. Proposition 2.3.13 tells us that $\{aP\}$ is reflexive; therefore, $(a-1)P$ is a translation of a reflexive polytope. But this is an absurdity as it implies that $(a-1)P$ has an interior lattice point, contradicting that the codegree of P is a. Thus, this case cannot occur.

□

2.4 Nearly Gorenstein 0/1-polytopes

In this section, we consider the case of 0/1-polytopes. We provide the characterisation of nearly Gorenstein 0/1-polytopes which are IDP. Moreover, we also characterise nearly Gorenstein edge polytopes of graphs satisfying the odd cycle condition and characterise nearly Gorenstein graphic matroid polytopes.

2.4.1 The characterisation of nearly Gorenstein 0/1-polytopes

Lemma 2.4.1. *Let $P \subset \mathbb{R}^d$ be a 0/1-polytope. Then, after a change of coordinates, we can write $P = P_1 \times \cdots \times P_s$ for some indecomposable 0/1-polytopes $P_1, \ldots, P_s$.*

Proof. As mentioned in Section 2.3, we can write $P = P_1' + \cdots + P_s'$ for some indecomposable lattice polytopes $P_1', \ldots, P_s'$.

First, we show that we can choose $P_1', \ldots, P_s'$ so that these are 0/1-polytopes. Suppose that we can write $P = P_1' + P_2'$ for some lattice polytopes P_1' and P_2'. Then, for any $v \in P_1' \cap \mathbb{Z}^d$ and for any $u \in P_2' \cap \mathbb{Z}^d$, $v + u$ is a 0/1-vector. Therefore, for any $i \in [d]$, $\pi_i(P_1' \cap \mathbb{Z}^d)$ can take one of the following forms: (i) $\{w_i\}$ or (ii) $\{w_i, w_i + 1\}$

for some $w_i \in \mathbb{Z}$. In case (i), $\pi_i(P_2' \cap \mathbb{Z}^d)$ is equal to $\{-w_i\}$, $\{-w_i+1\}$ or $\{-w_i, -w_i+1\}$. In case (ii), $\pi_i(P_2' \cap \mathbb{Z}^d)$ is equal to $\{-w_i\}$. Thus, in all cases, $P_1' - w$ and $P_2' + w$ are 0/1-polytopes and we have $P = (P_1' - w) + (P_2' + w)$, where $w = (w_1, \ldots, w_d)$.

Moreover, if we can write $P = P_1' + P_2'$ for some 0/1-polytopes P_1' and P_2', then we can see that either $\pi_i(P_1')$ or $\pi_i(P_2')$ is equal to $\{0\}$ for any $i \in [d]$. Therefore, after a change of coordinates, we can write $P = P_1 \times P_2$ for some 0/1-polytopes P_1 and P_2. □

Now, we provide the main theorem of this section.

Theorem 2.4.2. *Let P be an IDP 0/1-polytope. Then, P is nearly Gorenstein if and only if you can write $P = P_1 \times \cdots \times P_s$ for some Gorenstein 0/1-polytopes $P_1, \ldots, P_s$ with $|a_{P_i} - a_{P_j}| \leq 1$, where a_{P_i} and a_{P_j} are the respective codegrees of P_i and P_j, for $1 \leq i < j \leq s$.*

Proof. It follows from Lemma 2.4.1 that we can write $P = P_1 \times \cdots \times P_s$ for some indecomposable 0/1-polytopes $P_1, \ldots, P_s$. Thus, we have $\mathbb{C}[P] \cong \mathbb{C}[P_1] \# \cdots \# \mathbb{C}[P_s]$. Note that if P is IDP, then so is P_i for each $i \in [s]$, and $A(P)$ (resp. $A(P_i)$) coincides with $\mathbb{C}[P]$ (resp. $\mathbb{C}[P_i]$). Therefore, since P is nearly Gorenstein, $\mathbb{C}[P]$ is nearly Gorenstein, and hence $\mathbb{C}[P_i]$ is also nearly Gorenstein from Lemma 2.2.6 (1). Furthermore, P_i is nearly Gorenstein. Since P_i is indecomposable, P_i is Gorenstein by Theorem 2.3.20. Moreover, it follows from [43, Corollary 2.8] that $|a_{P_i} - a_{P_j}| \leq 1$ for $1 \leq i < j \leq s$.

The converse also holds from [43, Corollary 2.8]. □

From this theorem, we immediately obtain the following corollaries:

Corollary 2.4.3. *Question 2.3.15 is true for IDP 0/1-polytopes.*

Corollary 2.4.4. *Let P be an IDP 0/1-polytope. If $\mathbb{C}[P]$ is nearly Gorenstein, then $\mathbb{C}[P]$ is level.*

Proof. It follows immediately from Lemma 2.2.6 (2) and Theorem 2.4.2. □

The result of Theorem 2.4.2 can be applied to many classes of 0/1-polytopes such as order polytopes and stable set polytopes.

Order polytopes, which were introduced by Stanley [96], arise from posets. Let Π be a poset equipped with a partial order $\preceq$. The Ehrhart ring of the order polytope of a poset Π is called the Hibi ring of Π, denoted by $\mathbb{C}[\Pi]$. It is known that Hibi rings are standard graded ([44]). For a subset $I \subset P$, we say that I is a *poset ideal* of P if $p \in I$ and $q \preceq p$ then $q \in I$. According to [96], the characteristic vectors of poset ideals in $\mathbb{R}^\Pi$ are precisely the vertices of the order polytope of Π (hence order polytopes are 0/1-polytopes). By this fact, we can see that the order polytope of a poset Π is indecomposable if and only if Π is connected. Nearly Gorensteinness of Hibi rings have been studied in [42]. It is shown that $\mathbb{C}[\Pi]$ is nearly Gorenstein if and only if Π is the disjoint union of pure connected posets $\Pi_1, \ldots, \Pi_q$ such that their ranks of any two also can only differ by at most 1. Moreover, in this case, $\mathbb{C}[\Pi_i]$ is Gorenstein and $\mathbb{C}[\Pi] \cong \mathbb{C}[\Pi_1] \# \cdots \# \mathbb{C}[\Pi_s]$. Therefore, its characterisation can be derived from Theorem 2.4.2.

Stable set polytopes, which were introduced by Chvátal [21], arise from graphs. For a finite simple graph G on the vertex set $V(G)$ with the edge set $E(G)$, the stable set polytope of G, denoted by Stab_G, is defined as the convex hull of the characteristic vectors of stable sets of G in $\mathbb{R}^{V(G)}$, hence Stab_G is a 0/1-polytope. Here, we say that a subset S of $V(G)$ is a *stable set* if $\{v, u\} \notin E(G)$ for any $v, u \in S$. This implies that Stab_G is indecomposable if and only if G is connected. Stable set polytopes behave well for perfect graphs. For example, Stab_G is IDP if G is perfect (cf.[84]). Moreover, the characterisation of nearly Gorenstein stable set polytopes of perfect graphs has been given in [46, 81]. Let G be a perfect graph with connected components $G_1, \ldots, G_s$ and let δ_i denote the maximal cardinality of cliques of G_i. Then, it is known that Stab_G is nearly Gorenstein if and only if the maximal cliques of each G_i have the same cardinality and $|\delta_i - \delta_j| \leq 1$ for $1 \leq i < j \leq s$. In this case, as in the case of order polytopes, $\mathbb{C}[\mathrm{Stab}_{G_i}]$ is Gorenstein and $\mathbb{C}[\mathrm{Stab}_G] \cong \mathbb{C}[\mathrm{Stab}_{G_1}]\# \cdots \#\mathbb{C}[\mathrm{Stab}_{G_s}]$. Therefore, its characterisation can also follow from Theorem 2.4.2.

Furthermore, by using this theorem, we can study the nearly Gorensteinness of other classes of 0/1-polytopes.

2.4.2 Nearly Gorenstein edge polytopes

First, we define the edge polytope and edge ring of a graph. We refer the reader to [40, Section 5] and [103, Chapters 10 and 11] for an introduction to edge rings.

Let G be a finite simple graph on the vertex set $V(G) = \{1, \ldots, d\}$ with the edge set $E(G)$. Given an edge $e = \{i, j\} \in E(G)$, let $\rho(e) := \boldsymbol{e}_i + \boldsymbol{e}_j$, where $\boldsymbol{e}_i$ denotes the i-th unit vector of $\mathbb{R}^d$ for $i \in [d]$. We define the *edge polytope* P_G of G as follows:

$$P_G = \mathrm{conv}\left\{\rho(e) : \ e \in E(G)\right\}.$$

The toric ring of P_G is called the *edge ring* of G, denoted by $\mathbb{C}[G]$ instead of $\mathbb{C}[P_G]$.

Let $G_1, \ldots, G_s$ be the connected components of G. From the definition of edge polytope, we can see that $\mathbb{C}[G] \cong \mathbb{C}[G_1] \otimes \cdots \otimes \mathbb{C}[G_s]$. Therefore, in considering the characterisation of nearly Gorenstein edge polytopes, we may assume that G is connected.

Moreover, for a connected graph G, P_G is IDP if and only if G satisfies the *odd cycle condition*, in other words, for each pair of odd cycles C and C' with no common vertex, there is an edge $\{v, v'\}$ with $v \in V(C)$ and $v' \in V(C')$ (see [85, 94]).

Gorenstein edge polytopes have been investigated in [86]. We now state the characterisation of nearly Gorenstein edge polytopes.

Corollary 2.4.5. *Let G be a connected simple graph satisfying the odd cycle condition. Then, the edge polytope P_G of G is nearly Gorenstein if and only if P_G is Gorenstein or G is the complete bipartite graph $K_{n,n+1}$ for some $n \geq 2$.*

Proof. If P_G is nearly Gorenstein, then Theorem 2.4.2 allows us to write $P_G = P_1 \times \cdots \times P_s$ for some indecomposable Gorenstein 0/1-polytopes $P_1, \ldots, P_s$. Then, we have $s \leq 2$ since $P_G \subset \{(x_1, \ldots, x_d) \in \mathbb{R}^d : x_1 + \cdots + x_d = 2\}$, where $d = |V(G)|$. In the case $s = 1$, P_G is Gorenstein. If $s = 2$, we can see that $P_1 = \mathrm{conv}\{\boldsymbol{e}_1, \ldots, \boldsymbol{e}_n\} \subset \mathbb{R}^n$

and $P_2 = \text{conv}\{\boldsymbol{e}_1, \ldots, \boldsymbol{e}_{d-n}\} \subset \mathbb{R}^{d-n}$ for some $1 < n < d-1$. Therefore, we have $G = K_{n,d-n}$, and it is shown by [46, Proposition 1.5] that for any $1 < n < d-1$, $P_{K_{n,d-n}}$ is nearly Gorenstein if and only if $d - n \in \{n, n+1\}$. Since $P_{K_{n,n}}$ is Gorenstein, we get the desired result. □

2.4.3 Nearly Gorenstein graphic matroid polytopes

We start by giving one of several equivalent definitions of a matroid.

Definition 2.4.6. Let E be a finite set and let $\mathcal{B}$ be a subset of the power set of E satisfying the following properties:

1. $\mathcal{B} \neq \emptyset$.
2. If $A, B \in \mathcal{B}$ with $A \neq B$ and $a \in A \setminus B$, then there exists some $b \in B \setminus A$ such that $(A \setminus \{a\}) \cup \{b\} \in \mathcal{B}$.

Then the tuple $M = (E, \mathcal{B})$ is called a *matroid* with *ground set* E and *set of bases* $\mathcal{B}$.

Let now $G = (V, E)$ be a multigraph. The *graphic matroid* associated to G is the matroid M_G whose ground set is the set of edges E and whose bases are precisely the subsets of E which induce a spanning tree of G. Given two matroids $M_E = (E, \mathcal{B}_E)$ and $M_F = (F, \mathcal{B}_F)$, their *direct sum* $M_E \oplus M_F$ is the matroid with ground set $E \sqcup F$ such that for each basis B of $M_E \oplus M_F$, there exist bases $B_E \in \mathcal{B}_E$ and $B_F \in \mathcal{B}_F$ with $B = B_E \sqcup B_F$. If such a decomposition is not possible for a matroid M, we call it *irreducible*.

A graphic matroid with underlying multigraph G is irreducible if and only if its underlying graph is 2-connected. If it is not irreducible, its irreducible components correspond precisely to the 2-connected components of G.

For any matroid $M = (E, \mathcal{B})$, we can define its *matroid base polytope* (or simply *base polytope*) by

$$B_M = \text{conv}\left\{\sum_{b \in B} e_b : B \in \mathcal{B}\right\} \subset \mathbb{R}^{|E|}$$

where e_b is the incidence vector in $\mathbb{R}^{|E|}$ corresponding to the basis b. If B_M comes from a graphic matroid M_G, we will call it B_G.

An alternative definition of matroid base polytopes is as follows.

Definition 2.4.7 ([33, Section 4])**.** A 0/1-polytope $P \subset \mathbb{R}^d$ is called *(matroid) base polytope* if there is a positive integer h such that every vertex $v = (v_1, \ldots, v_n)$ satisfies $\sum_{i=1}^{d} v_i = h$ and every edge (i.e. dimension 1 face) of P is a translation of a vector $e_i - e_j$ with $i \neq j$.

It is shown in [33, Theorem 4.1] that this definition is indeed equivalent to that of a base polytope as given above and that the underlying matroid is uniquely determined. This gives us the following two lemmas.

Lemma 2.4.8. *Let G be a multigraph and let $G_1, \dots G_n$ be its 2-connected components. Then B_G can be written as a direct product of the base polytopes $B_{G_1}, \dots, B_{G_n}$. Conversely, if B_G can be written as a direct product of polytopes $P_1, \dots, P_n$, where no P_i is itself a direct product, then these polytopes correspond to the base polytopes of the 2-connected components $G_1, \dots, G_n$ of G.*

Proof. The first statement is trivially satisfied.

The converse follows from two key insights. Firstly, the fact that if a base polytope B_M associated to a (not necessarily graphic) matroid M can be written as a direct product $P_1 \times P_2$, then P_1 and P_2 are again base polytopes. Secondly, if a graphic matroid M_G can be written as a direct sum $M_1 \oplus M_2$, then M_1 and M_2 are again graphic matroids corresponding to subgraphs of G which have at most one vertex in common.

The first insight follows from the alternative definition of a base polytope: Every edge of B_M is given by an edge in P_1 and a vertex of P_2, or vice versa. Hence, P_1 and P_2 must satisfy the definition as well, making them base polytopes with unique underlying matroids M_1 and M_2. The second insight is a classical result and can be found, among other places, in [101, Lemma 8.2.2]. □

The following proposition is the polytopal version of a classical result due to White.

Lemma 2.4.9 ([105, Theorem 1])**.** *Matroid base polytopes are IDP.*

We can now define Gorensteinness, nearly Gorensteinness, and levelness of a matroid by identifying it with its base polytope. In [47] and [69], a constructive, graph-theoretic criterion of Gorensteinness for graphic matroids was found. Since the direct product of two Gorenstein polytopes that have the same codegree is again Gorenstein, the characterisation is presented in terms of 2-connected graphs.

Proposition 2.4.10 ([69, Theorems 2.22 and 2.25])**.** *Let G be a 2-connected multigraph. Then the following are equivalent.*

1. *B_G is Gorenstein with codegree $a = 2$*
2. *Either G is the 2-cycle or G can be obtained from copies of the clique K_4 and Construction 2.15 in [69].*

The following are also equivalent.

1. *B_G is Gorenstein with codegree $a > 2$*
2. *G can be obtained from copies of the cycle C_a and Constructions 2.15, 2.17, 2.18 in [69] with $\delta = a$.*

The full characterisation of nearly Gorenstein graphic matroids is thus an immediate corollary of Theorem 2.4.2 and Proposition 2.4.10.

Corollary 2.4.11. *Let G be a multigraph with 2-connected components $G_1, \dots, G_n$, then the following are equivalent.*

1. B_G *is nearly Gorenstein*
2. $B_{G_1}, \ldots, B_{G_n}$ *are Gorenstein with codegrees* $a_1, \ldots, a_n$*, where* $|a_i - a_j| \leq 1$ *for* $1 \leq i < j \leq s$.

Chapter 3

A New Mutation Invariant of Fano Polygons

3.1 Introduction

Recall that the mirror symmetry approach to the classification of Fano manifolds was specialised in two dimensions in [3]. Here, the conjectural correspondence is between orbifold del Pezzo surfaces having a toric degeneration (up to qG-deformation) and Fano polygons (up to mutation). Because there is an infinite number of these surfaces, the basket of (residual) cyclic quotient singularities must be fixed in order to get a finite classification. The conjecture has been verified in the smooth case [66] and in the case where the surfaces have at worst $\frac{1}{3}(1,1)$ singularities [28, 66]. Crucial to the classification on the polygon side was the notion of minimal Fano polygons. In [66, Theorem 6.3], it was shown that each mutation-equivalence class of Fano polygons has a finite number of minimal polygons. Using [17], all minimal polygons with a given basket of singularities can be classified.

The final step in obtaining a conjectural classification of these varieties is to remove the redundant minimal polygons. This is because some of the minimal polygons may be mutation-equivalent to each other. There are already several tools available which can be used to show that two polygons are not mutation-equivalent; for example, the Ehrhart series of the dual polygon and the singularity content are known to be invariant under mutation [2, 62]. However, this is sometimes not enough to distinguish polygons up to mutation.

In Section 3.2, we introduce a new constant $\tilde{k}_P$ associated to a Fano polygon P, called the *partial crepant resolution (PCR) index*. We prove in Theorem 3.2.10 that the PCR index is invariant under mutation. Computation of this invariant is cheap, and so it can be used to easily distinguish more mutation-equivalence classes of Fano polygons; see Examples 3.2.13 and 3.2.14. Finally, in Corollary 3.2.9, we derive a formula for the PCR index which is in terms of the singularities of X_P.

In Section 3.3, we revisit the classification of minimal polygons from [66] which correspond to the smooth del Pezzo surfaces. In particular, we use the Markov-like diophantine equations similar to those appearing in [1] in order to classify all minimal Fano triangles.

3.2 The Partial Crepant Resolution Index

3.2.1 A natural definition of the PCR index

We first highlight a known behaviour of the (standard) index under mutation, whose definition we recall below.

Definition 3.2.1. Let $P \subset N_{\mathbb{Q}}$ be a lattice polygon. Its *index* is $k_P := [N : \Gamma_P]$, where Γ_P is the sublattice of N spanned by the vertices of P.

Example 3.2.2. Let $P = \operatorname{conv}\{(-1,-1),(2,-1),(-1,2)\} \subset N_{\mathbb{Q}}$. This has index $k_P = 3$. Now consider $Q = \operatorname{conv}\{(-1,-1),(2,-1),(2,1),(-1,1)\}$. In particular, Q has index $k_Q = 1$. Further, we note that $Q = \operatorname{mut}_w(P, \boldsymbol{d})$, where $w = (1,0)^t$ and $\boldsymbol{d} = (0,1)$. Thus, the index is not invariant under mutation.

So, in order to create a mutation-invariant, we need to add more points to the sublattice. Really, we want it to contain the vertices of all the polygons in the mutation-equivalence class. Of course, this will trivially be a mutation-invariant; however, at first sight, it seems that it would be wholly inefficient to compute.

We can decorate the edges of a Fano polygon P in a way that encodes the possible non-trivial mutations of P. This was first described in [62].

Definition 3.2.3. Let $E = [\boldsymbol{v}, \boldsymbol{v}+\ell\boldsymbol{d}]$ be an edge of an IP polygon; the edge has length ℓ and height h, so that $\boldsymbol{d}$ is primitive. By the division algorithm, we have $\ell = nh + \tilde{\ell}$ for some unique integers $n \geq 0$ and $0 \leq \tilde{\ell} < h$. Thus, we can subdivide the edge E into n segments of length and height h and one (possibly empty) segment of length $\tilde{\ell}$ and height h. One choice of subdivision of E is the ordered set $\{\boldsymbol{v} + ih\boldsymbol{d} : 0 \leq i \leq n\} \cup \{\boldsymbol{v} + \ell\boldsymbol{d}\}$. We call any choice of subdivision an (ordered) set of *PCR points for* E.

Lemma 3.2.4. *Let E be an edge of an IP polygon with height h and primitive direction vector $\boldsymbol{d}$. Let $V_E \subset N$ be a choice of PCR points for E. Then the lattice $\widetilde{\Gamma}_E$ spanned by V_E is generated by the vertices of E and, if E is long, the point $h\boldsymbol{d}$. In particular, $\widetilde{\Gamma}_E$ is independent of the choice of PCR points for E.*

Proof. We may write $E = [\boldsymbol{v}, \boldsymbol{v} + \ell\boldsymbol{d}]$, where ℓ is the length of E. Further, we have that $\ell = nh + \tilde{\ell}$ for some unique integers $n \geq 0$ and $0 \leq \tilde{\ell} < h$. So, the PCR points V_E must subdivide E into i segments of length and height h, one (possibly empty) segment of length $\tilde{\ell}$ and height h, and then $n - i$ segments of length and height h, for some $0 \leq i \leq n$. So, the set of PCR points V_E is the union of $\{\boldsymbol{v} + jh\boldsymbol{d} : 0 \leq j \leq i\}$ and $\{\boldsymbol{v} + (\ell - jh)\boldsymbol{d} : 0 \leq j \leq n - i\}$.

It clearly follows that when E isn't long, i.e. $n = 0$, the lattice $\widetilde{\Gamma}_E$ is spanned by $\{\boldsymbol{v}, \boldsymbol{v} + \ell\boldsymbol{d}\}$. Further, it is clear that when E *is* long, i.e. $n \geq 1$, the lattice $\widetilde{\Gamma}_E$ is spanned by $\{\boldsymbol{v}, \boldsymbol{v} + \ell\boldsymbol{d}, h\boldsymbol{d}\}$. Since these generators are independent of the choice of i, the lattice $\widetilde{\Gamma}_E$ is independent of the choice of PCR points for E. □

Definition 3.2.5. The sublattice $\widetilde{\Gamma}_P$ is defined as the smallest lattice containing $\widetilde{\Gamma}_E$ for all edges E of P. We call $\tilde{k}_P := [N : \widetilde{\Gamma}_P]$ the *PCR index* of P.

3.2.2 A formula for the PCR index

We now describe a convenient formula for the PCR index of a Fano polygon. We do this by switching to the point of view of fans, which correspond one-to-one with Fano polygons by definition.

Definition 3.2.6. Let Σ be a fan whose cones lie in $N_{\mathbb{Q}}$. For a ray $\rho \subset N_{\mathbb{Q}}$, we denote by $\boldsymbol{v}_\rho$ its primitive ray generator. We now define $N_\Sigma \coloneqq \operatorname{span}_{\mathbb{Z}} \{\boldsymbol{v}_\rho : \rho \in \Sigma(1)\}$ as the sublattice of N spanned by the primitive ray generators $\boldsymbol{v}_\rho$ of the rays ρ in Σ. The index of this sublattice is denoted $k_\Sigma \coloneqq [N : N_\Sigma]$.

Note that a cone can be naturally endowed with the structure of a fan by taking all of its faces. Thus, we often conflate σ with its associated fan; for example, we use the notation $\sigma(1)$ to mean the one-dimensional faces of σ, and k_σ to mean the index of the sublattice of N spanned by its primitive ray generators.

In the case of 2-dimensional cones, it is straightforward to compute the index: $k_\sigma = |\det(\boldsymbol{x}, \boldsymbol{y})|$, where $\boldsymbol{x}$ and $\boldsymbol{y}$ are the primitive ray generators of σ. More generally, for a fan Σ, we have $k_\Sigma = \gcd(\det(\boldsymbol{v}_{\rho_1}, \boldsymbol{v}_{\rho_2}) : \rho_1, \rho_2 \in \Sigma(1))$. The following result simplifies this formula so that we only look at the maximal dimensional cones of Σ.

Lemma 3.2.7. *Let Σ be a fan over $N_{\mathbb{Q}}$. Then $k_\Sigma = \gcd(k_\sigma : \sigma \in \Sigma(2))$.*

Proof. Before demonstrating the general statement, we must first consider the case when there are three rays in the fan. For distinct primitive lattice points $\boldsymbol{x}, \boldsymbol{y}, \boldsymbol{z} \in N$, set

$$k_0 \coloneqq \det(\boldsymbol{x}, \boldsymbol{y}), \qquad k_1 \coloneqq \det(\boldsymbol{y}, \boldsymbol{z}), \qquad k_2 \coloneqq \det(\boldsymbol{z}, \boldsymbol{x}).$$

We claim that $\gcd(k_0, k_1, k_2) = \gcd(k_0, k_1)$. To see this, we consider the sublattice Γ spanned by $\boldsymbol{x}, \boldsymbol{y}, \boldsymbol{z}$. First, apply an $\mathrm{SL}_2(\mathbb{Z})$-transformation U which sends $\boldsymbol{y}$ to $(0, 1)$. Since determinants are preserved under this transformation, $\boldsymbol{x}$ is sent to $(k_0, -a_0)$ and $\boldsymbol{z}$ is sent to $(-k_1, -a_1)$, for some integers a_0, a_1. It is straightforward to see that the sublattice $U\Gamma$ has index $\gcd(k_0, k_1)$. Thus, the claim is proven.

We now demonstrate the statement for a general fan Σ. Label its primitive ray generators as $\boldsymbol{v}_0, \boldsymbol{v}_1, \ldots, \boldsymbol{v}_m$ in anticlockwise order. Then, each maximal dimensional cone of Σ will have primitive ray generators $\boldsymbol{v}_i$ and $\boldsymbol{v}_{i+1}$, for some i, where indices are taken modulo $m + 1$. As before, we apply an $\mathrm{SL}_2(\mathbb{Z})$-transformation sending $\boldsymbol{v}_0$ to $(0, 1)$ and all other $\boldsymbol{v}_i$ to $\boldsymbol{v}_i'$. It is clear to see that k_Σ coincides with $\gcd(k_{01}, k_{02}, \ldots, k_{0m})$, where $k_{0i} \coloneqq \det(\boldsymbol{v}_0, \boldsymbol{v}_i) = \det((0, 1), \boldsymbol{v}_i')$.

We may apply our claim twice to get that $\gcd(k_{01}, k_{02}) = \gcd(k_{01}, k_{02}, k_{12}) = \gcd(k_{01}, k_{12})$. In total, we may apply our claim $2(m - 1)$ times to obtain that $k_\Sigma = \gcd(k_{01}, k_{12}, k_{13}, \ldots, k_{1m})$. Then, we may apply the claim $2(m - 2)$ times to obtain that $k_\Sigma = \gcd(k_{01}, k_{12}, k_{23}, \ldots, k_{2m})$. We may proceed inductively, until we obtain that $k_\Sigma = \gcd(k_{01}, k_{12}, k_{23}, \ldots, k_{(m-1)m})$.

If Σ is a complete fan, then we may also include k_{m0} inside the gcd at no extra cost. In either case, we obtain the desired result. □

From the above lemma, we obtain formulas for the usual and PCR indices. The latter can be obtained by refining the spanning fan of a Fano polygon, as will be explained now.

Definition 3.2.8. Let $P \subset N_{\mathbb{Q}}$ be a Fano polygon. For each edge E of P, choose a set of PCR points V_E. Then, $\widetilde{\Sigma}_P$ is defined to be a *standard partial crepant resolution* of P if its rays are generated by the points in V_E, for all edges E of P.

Corollary 3.2.9. *Let $P \subset N_{\mathbb{Q}}$ be a Fano polygon. Then the following hold.*

1. *P has (usual) index $k_P = \gcd(k_E : E \text{ an edge of } P)$;*
2. *P has PCR index $\tilde{k}_P = \gcd(\{k_\sigma : \sigma \in \mathcal{B}_P\} \cup \{h_E^2 : E \text{ is a long edge of } P\})$.*

Proof. The first statement follows immediately from Lemma 3.2.7. We now deal with the second statement. Consider the fan $\widetilde{\Sigma}_P$, which is a standard partial crepant resolution of Σ_P. If an edge E is not long, then it contributes $\tilde{\ell}_E h_E$ towards the PCR index. Otherwise, by Lemma 3.2.7, it contributes h_E^2 and $\tilde{\ell}_E h_E$ to the PCR index. Therefore, the formula holds. □

3.2.3 Mutation-invariance of the PCR index

In this subsection, we aim to prove that the PCR index of a Fano polygon is invariant under mutation.

Theorem 3.2.10. *Let $P, Q \subset N_{\mathbb{Q}}$ be mutation-equivalent Fano polygons. Then the sublattices $\widetilde{\Gamma}_P$ and $\widetilde{\Gamma}_Q$ coincide. Moreover, the PCR indices are equal, i.e. $\tilde{k}_P = \tilde{k}_Q$.*

We start by observing that this theorem does not hold for non-Fano polygons.

Example 3.2.11. Consider the non-Fano lattice polytope $P = \text{conv}\{(0,1), (-2,-2), (2,-2)\}$. We may extend our definition of PCR index, keeping the labelling. We obtain $\tilde{k}_P = 2$. Now consider $Q = \text{mut}_w(P, \boldsymbol{d})$, where $w = (0,1)^t$ and $\boldsymbol{d} = (1,0)$. Then $Q = \text{conv}\{(0,1), (1,1), (-2,-2), (0,-2)\}$. This has PCR index $\tilde{k}_Q = 1$. So, PCR index is not invariant under mutation for non-Fano polygons.

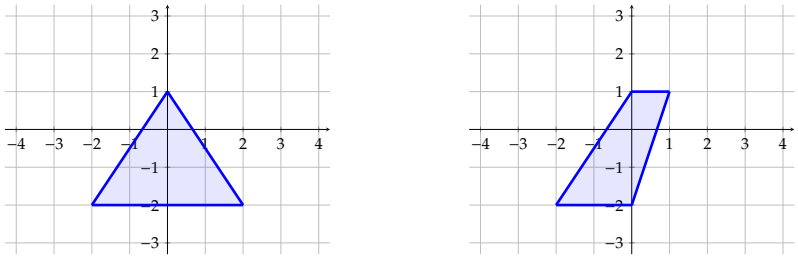

FIGURE 3.1: The polygons P and Q from Example 3.2.11.

The primitive vertex condition is thus essential for the invariance of the PCR index under mutation. This motivates the following lemma, which we will be needed to prove Theorem 3.2.10.

Lemma 3.2.12. *Let L be the sublattice of N spanned by the lattice points $(x, h), (x', h'), (h, 0)$. Suppose that (x, h) is primitive. Then $(h', 0) \in L$.*

Proof. To show that $(h', 0)$ belongs to L, we will express it as a $\mathbb{Z}$-linear combination of the generators of L. Since x and h are coprime, there exist integers p and q such that $px + qh = 1$. Thus, we may write

$$(h', 0) = ph' \cdot (x, h) - ph \cdot (x', h') + (px' + qh') \cdot (h, 0) \in L.$$

And so, we are done. □

We can now prove the main theorem of the section.

Proof of Theorem 3.2.10. By Lemma 1.3.5 (3), it is enough to consider the case when P and Q are related by a single primitive mutation, i.e. $Q = \mathrm{mut}_w(P, \boldsymbol{d})$ for some mutation data $(w, \boldsymbol{d})$ for P, where $\boldsymbol{d}$ is primitive. Further, by Lemma 1.3.5 (2), it is enough to prove that $\widetilde{\Gamma}_P \geq \widetilde{\Gamma}_Q$.

Without loss of generality, $w = (0, 1)^t$ and $\boldsymbol{d} = (1, 0)$. Label the vertices of P as in Definition 1.3.4. Now, the vertices of Q will be

$$\boldsymbol{v}_1, \boldsymbol{v}_2, \ldots, \boldsymbol{v}_i, A\boldsymbol{v}_{i+1}, \ldots, A\boldsymbol{v}_{m+1}, \tag{3.1}$$

where A is the w-shear sending $(x, h) \in N$ to $(x + h, h)$. Further, if V is a set of PCR points for an edge E, then AV is a set of PCR points for the edge AE.

Now, since there is a long edge with primitive vertices and with normal vector w, Lemma 3.2.12 tells us that $\widetilde{\Gamma}_P$ is invariant under w-shears. Thus, the PCR points for all edges of Q whose primitive inner normals aren't $\pm w$ are contained in $\widetilde{\Gamma}_P$.

So, it remains to consider the PCR points of the edges of Q which have primitive inner normal $\pm w$. In fact, we only have to consider those PCR points which aren't vertices (3.1), since their vertices have already been accounted for by their adjacent edges.

Let $E'_{m+1} := [\boldsymbol{v}_1, A\boldsymbol{v}_{m+1}]$ and $E'_i := [\boldsymbol{v}_i, A\boldsymbol{v}_{i+1}]$. The former is the long edge of Q maximising w and the latter is the face of Q minimising w. By Lemma 3.2.4, E'_{m+1} contributes $h_{m+1}\boldsymbol{d}$ to $\widetilde{\Gamma}_Q$, where h_{m+1} is the height of E'_{m+1}. If E'_i is a long edge then, by Lemma 3.2.4, it contributes $h_i\boldsymbol{d}$ to $\widetilde{\Gamma}_Q$, where h_i is the height of E'_i; otherwise, it doesn't contribute anything. Now, we already have that $h_i\boldsymbol{v}_i \in \widetilde{\Gamma}_P$. Since $\boldsymbol{v}_i$ is primitive and $w(\boldsymbol{v}_1) = h_{m+1}$, Lemma 3.2.12 gives us that $h_{m+1}\boldsymbol{d} \in \widetilde{\Gamma}_P$.

We have now shown that the generators of $\widetilde{\Gamma}_Q$ are contained in the lattice $\widetilde{\Gamma}_P$; so, $\widetilde{\Gamma}_P \geq \widetilde{\Gamma}_Q$. By the invertibility of mutations, it follows that $\widetilde{\Gamma}_P = \widetilde{\Gamma}_Q$ and $\tilde{k}_P = \tilde{k}_Q$. □

3.2.4 Applying the PCR index

Now that we have proved the PCR index is invariant under mutation, we can use it to distinguish between mutation-inequivalent polygons which have the same singularity content.

Example 3.2.13. Let $P = \mathrm{conv}\{(3, 4), (-6, 1), (3, -2)\}$ and $Q = \mathrm{conv}\{(-6, 1), (3, 4), (-1, -4)\}$ be Fano polygons whose corresponding toric varieties are the fake weighted projective planes $X_P = \mathbb{P}(1, 2, 3)/\mathbb{Z}_9$ and $X_Q = \mathbb{P}(8, 25, 27)$. These polygons can be

seen in Figure 3.2. They both have anticanonical degree 2/3 and singularity content $\left(3, \left\{\frac{1}{27}(1,20)\right\}\right)$. However, their respective PCR indices are $\tilde{k}_P = 9$ and $\tilde{k}_Q = 1$. Thus, by Theorem 3.2.10, P and Q are not mutation-equivalent.

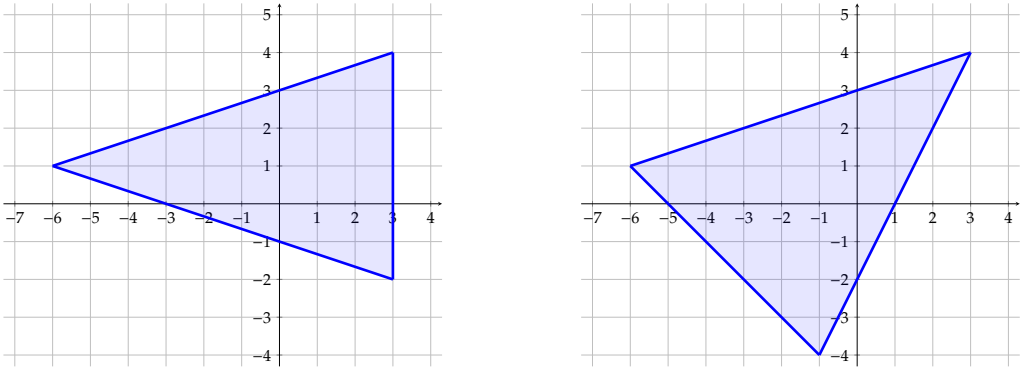

FIGURE 3.2: The polygons P and Q from Example 3.2.13.

Example 3.2.14. We consider another pair of Fano triangles which have the same singularity content but different PCR indices. Set $P = \text{conv}\{(-2,-17),(-2,3),(6,-1)\}$ and $Q = \text{conv}\{(13,-80),(-2,-5),(13,45)\}$. Their corresponding toric varieties are the fake weighted projective planes $X_P = \mathbb{P}(2,5,13)/\mathbb{Z}_8$ and $X_Q = \mathbb{P}(1,9,65)/\mathbb{Z}_{25}$. They both have anticanonical degree 5/13 and singularity content $\left(11, \left\{\frac{1}{104}(1,55)\right\}\right)$. However, their respective PCR indices are $\tilde{k}_P = 4$ and $\tilde{k}_Q = 1$. So, by Theorem 3.2.10, the Fano polygons P and Q are not mutation-equivalent.

3.3 The Existence of Fano Triangles in a Mutation-Equivalence Class

We begin with a motivating example and some questions, which we aim to answer in this section.

Example 3.3.1. Consider the Fano polygon with vertices $\pm(1,0)$ and $\pm(0,1)$. It corresponds to the toric Fano variety $\mathbb{P}^1 \times \mathbb{P}^1$, which has degree 8. Now, it is known that this polygon is mutation-equivalent to the triangle corresponding to $\mathbb{P}(1,1,2)$.

Next, consider the Fano polygon with vertices $(-1,-1)$, $(1,0)$, $(1,1)$, and $(0,1)$. It corresponds to the Hirzebruch surface $\mathbb{F}_1$, which is a toric Fano variety also of degree 8. Is its corresponding Fano polygon mutation-equivalent to a triangle, i.e. does $\mathbb{F}_1$ have a qG-deformation to a fake weighted projective plane?

In fact, we want to answer the more general question: given any Fano polygon, does there exist a triangle that is mutation equivalent to it?

3.3.1 Markov-like Diophantine equations

In [1], they described one-step mutations of Fano triangles. In particular, they described how the weights and the index of the triangle changed under mutation.

Proposition 3.3.2 ([1, Proposition 3.12]). *Let $P, Q \subset N_{\mathbb{Q}}$ be a Fano triangles with respective weights $(\lambda_0, \lambda_1, \lambda_2)$ and $(\lambda'_0, \lambda'_1, \lambda'_2)$ and respective (usual) indices k and k'. Write $\lambda_i = c_i a_i^2$, where the a_i are positive integers and the c_i are square-free positive integers. Suppose that P and Q are related by a sequence of one-step mutations. Then Q has weights satisfying $\lambda'_i = c_i b_i^2$, where the b_i are positive integers. Furthermore, (a_0, a_1, a_2) and (b_0, b_1, b_2) are solutions to the same Diophantine equation*

$$dxyz = e(c_0x^2 + c_1y^2 + c_2z^2), \tag{3.2}$$

for some positive integers d and e. Moreover, the indices of P and Q coincide, i.e. $k = k'$.

This connection to Markov-like Diophantine equations allows us to describe one-step mutations of Fano polygons with index one, i.e. those corresponding to weighted projective spaces.

Example 3.3.3. Consider the Fano triangle $P \subset N_{\mathbb{Q}}$ with corresponding to the weighted projective plane $\mathbb{P}(1,1,2)$. By Proposition 3.3.2, if a triangle is related to P by a sequence of one-step mutations, then it corresponds to the weighted projective space $\mathbb{P}(a_0^2, a_1^2, 2a_2^2)$, for some positive integers a_0, a_1, a_2 satisfying

$$4a_0a_1a_2 = a_0^2 + a_1^2 + 2a_2^2.$$

From one solution (x, y, z) to the above equation, three other solutions can be obtained:

$$(4yz - x, y, z), \qquad (x, 4xz - y, z), \qquad (x, y, 2xy - z).$$

These solutions form a tree, with the fundamental (or minimal) solution $(1,1,1)$ as the parent of the tree; see Figure 3.3. It can be shown that this Markov-like equation has only the one fundamental solution. However, as shown in [1, Section 4], there also exist Markov-like equations with infinitely many fundamental solutions.

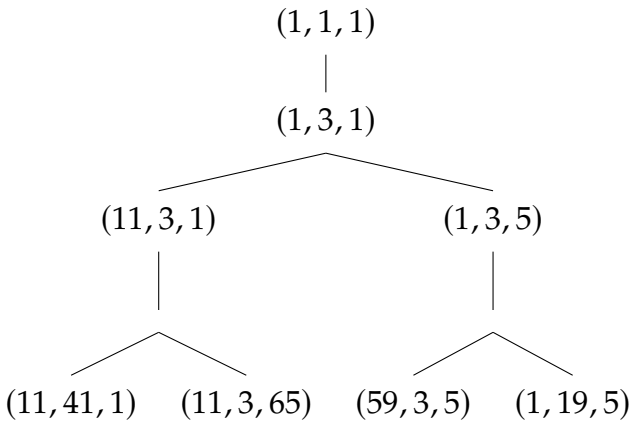

FIGURE 3.3: The tree of solutions of $4xyz = x^2 + y^2 + 2z^2$, up to permutation of x and y, displayed to a depth of four.

3.3.2 Method to produce all equations and their solutions

We can modify the approach of [1] in order to describe all one-step mutation families with a given singularity content. We get a finite number of equations which each have a finite number of fundamental solutions. What we present in this section is the specialisation of this approach to the case when the basket of R-singularities is empty.

Theorem 3.3.4. *Let $P \subset N_{\mathbb{Q}}$ be a Fano polygon with an empty basket of R-singularities. Suppose that P is mutation-equivalent to a triangle Q. Then, the following statements hold:*

(i) Q has edges with length $n_i h_i$ and height h_i, where n_i and h_i are some positive integers, for $i = 0, 1, 2$, and $n_0 \geq n_1 \geq n_2$.

(ii) n_0, n_1, n_2 appear in a row of Table 3.1 and the tuple of heights (h_0, h_1, h_2) is a solution to the Markov-like equation

$$dxyz = n_0x^2 + n_1y^2 + n_2z^2, \tag{3.3}$$

where d is given in Table 3.1.

(iii) Q is related by a sequence of one-step mutations to a fundamental triangle, whose heights are given in Table 3.1.

Before we proceed with the proof of Theorem 3.3.4, we need to recall a couple of formulas for the anticanonical degree of a toric Fano surface. The first formula is a classical result which holds for fake weighted projective planes.

Proposition 3.3.5. *Let $P \subset N_{\mathbb{Q}}$ be a Fano triangle with weights $(\lambda_0, \lambda_1, \lambda_2)$ and index k. Then,*

$$\mathrm{Vol}(P^*) = \frac{(\lambda_0 + \lambda_1 + \lambda_2)^2}{k\lambda_0\lambda_1\lambda_2}.$$

This next formula is for general toric Fano surfaces.

Proposition 3.3.6 ([62, Proposition 3.3])**.** *Let $P \subset N_{\mathbb{Q}}$ be a Fano polygon with singularity content $(n, \mathcal{B})$. Then the anticanonical degree of X_P is*

$$\mathrm{Vol}(P^*) = 12 - n - \sum_{\sigma \in \mathcal{B}} A_\sigma,$$

where A_σ is a rational number depending only on the singularity type σ.

Remark 3.3.7. An exact formula for A_σ in terms of Hirzebruch-Jung continued fractions is given in [62], but we omit it here.

We are now ready to prove the first main theorem of the section.

Proof of Theorem 3.3.4. We first prove (i). Let E_0, E_1, E_2 be the edges of Q. Since P has empty basket and is mutation-equivalent to Q, then Q must also have empty basket by Theorem 1.3.11. Thus, if h_0, h_1, h_2 are the respective heights of the edges of Q,

Equation ID	d	n_0	n_1	n_2	Fundamental solution(s)	Corresponding Surface
3	3	1	1	1	$(1,1,1)$	$\mathbb{P}^2$
4	4	2	1	1	$(1,1,1)$	$\mathbb{P}(1,1,2)$
6	6	3	2	1	$(1,1,1)$	$\mathbb{P}(1,2,3)$
7	5	5	1	1	$(1,2,1), (1,1,2)$	$\mathbb{P}(1,4,5)$
8	8	4	2	2	$(1,1,1)$	$\mathbb{P}(1,1,2)/\mathbb{Z}_2$
9a	6	6	2	1	$(1,1,2)$	$\mathbb{P}(1,2,3)/\mathbb{Z}_2$
9b	9	3	3	3	$(1,1,1)$	$\mathbb{P}^2/\mathbb{Z}_3$
10a	4	8	1	1	$(1,2,2)$	$\mathbb{P}(1,1,2)/\mathbb{Z}_4$
10b	6	6	3	1	$(1,1,3)$	$\mathbb{P}(1,2,3)/\mathbb{Z}_3$
10c	8	4	4	2	$(1,1,2)$	$\mathbb{P}(1,1,2)/\mathbb{Z}_4$
11a	3	9	1	1	$(1,3,3)$	$\mathbb{P}^2/\mathbb{Z}_9$
11b	4	8	2	1	$(1,2,4)$	$\mathbb{P}(1,1,2)/\mathbb{Z}_8$
11c	5	5	5	1	$(1,2,5), (2,1,5)$	$\mathbb{P}(1,4,5)/\mathbb{Z}_5$
11d	6	6	3	2	$(1,2,3)$	$\mathbb{P}(1,2,3)/\mathbb{Z}_6$

TABLE 3.1: Solutions to the Diophantine equations $dxyz = n_0x^2 + n_1y^2 + n_2z^2$, along with their corresponding fake weighted projective planes. The first number of each equation ID is the number of primitive T-singularities $n_0 + n_1 + n_2$ of each Fano triangle represented by the equation. The weights and index of each corresponding surface can be computed directly from n_0, n_1, n_2 and the solution. In equations 7 and 11c, there are two fundamental solutions; both correspond to the same surface.

then the lengths must be of the form n_ih_i, for some positive integers n_i, for $i = 0, 1, 2$. Without loss of generality, we may assume that $n_0 \geq n_1 \geq n_2 \geq 1$.

We now prove (ii). Let $(\lambda_0, \lambda_1, \lambda_2)$ be the weights and k be the index of Q. We note that the index of each edge of Q can be written in two ways:

$$k\lambda_i = n_ih_i^2,$$

for $i = 0, 1, 2$. We now compute the degree of X_Q in two different ways, and apply the above identity. By Propositions 3.3.5 and 3.3.6, we obtain that

$$12 - n_0 - n_1 - n_2 = \frac{(n_0h_0^2 + n_1h_1^2 + n_2h_2^2)^2}{n_0h_0^2 \cdot n_1h_1^2 \cdot n_2h_2^2}.$$

Now, we can compare the square-free parts of both sides of the above identity to get that $(12 - n_0 - n_1 - n_2)n_0n_1n_2$ is a square d^2, for some positive integer d. It now follows from comparing the squared parts of both sides that (h_0, h_1, h_2) is a solution to Equation (3.3).

Finally, we prove (iii). We first note that the degree of X_Q must be positive, so our coefficients satisfy the bounds $3 \leq n_0 + n_1 + n_2 \leq 11$. A simple brute-force algorithm can loop through all possible tuples (n_0, n_1, n_2) satisfying the above

bounds, returning only those such that $(12 - n_0 - n_1 - n_2)n_0n_1n_2$ is a square. This produces the list of values of n_0, n_1, n_2 given in Table 3.1.

It now remains to show that each equation has the given fundamental solution(s). Previous work of [90, Satz] gives the fundamental solutions for the first four equations in Table 3.1. The remaining equations can be solved by reducing them to one of the first four, as we now demonstrate.

We first deal with Equation 8. Reading the coefficients off the table, the equation is $8xyz = 4x^2 + 2y^2 + 2z^2$. Clearly, if we divide both sides by 2, then we obtain Equation 4. So, (x, y, z) is a fundamental solution to Equation 8 if and only if it is a fundamental solution to Equation 4. Thus, Equation 8 has one fundamental solution: $(1, 1, 1)$.

Next, we look at Equation 9a, which is $6xyz = 6x^2 + 2y^2 + z^2$. We see that z must be even; so, let $z = 2\hat{z}$ for some $\hat{z} \in \mathbb{Z}$. Substituting this back into Equation 9a and dividing both sides by 2, we obtain $6xy\hat{z} = 3x^2 + y^2 + 2\hat{z}^2$. This is just Equation 6. So, $(x, y, 2\hat{z})$ is a fundamental solution to Equation 9a if and only if $(x, \hat{z}, y)$ is a fundamental solution to Equation 6. Thus, Equation 9a has one fundamental solution: $(1, 1, 2)$.

We now skip to consider Equation 10a, which is $4xyz = 8x^2 + y^2 + z^2$. Looking modulo 4, we see that y and z must be even; so, let $y = 2\hat{y}$ and $z = 2\hat{z}$, for some $\hat{y}, \hat{z} \in \mathbb{Z}$. Substituting this back into Equation 10a and dividing both sides by 4, we obtain $4x\hat{y}\hat{z} = 2x^2 + \hat{y}^2 + \hat{z}^2$. This is just Equation 4. Thus, Equation 10a has one fundamental solution: $(1, 2, 2)$.

Using similar such reasoning, the fundamental solutions appearing in Table 3.1 can be produced for the rest of the equations. □

We can now make a statement about the PCR indices of such Fano polygons.

Corollary 3.3.8. *Let $P \subset N_{\mathbb{Q}}$ be a Fano polygon with empty basket of R-singularities. If P is mutation-equivalent to a Fano triangle, then it has PCR index $\tilde{k}_P = 1$.*

Proof. From Table 3.1, we see that all Fano triangles with empty basket have an edge of height one. Thus, by Corollary 3.2.9 (2), all Fano triangles with empty basket have PCR index one. Since P is mutation-equivalent to a Fano triangle with empty basket, by Theorem 3.2.10, P must also have PCR index one. □

3.3.3 Realisation

While Table 3.1 presents a list of invariants that a Fano triangle with an empty basket must satisfy, it still remains to show that such polygons are actually realisable. Of course, they all appear in [66], but we wish to verify this independently from their classification, using methods specific to triangles.

Theorem 3.3.9. *Let d and (n_0, n_1, n_2) be the coefficients appearing in a row of Table 3.1. Let (h_0, h_1, h_2) be a corresponding fundamental solution. Then, up to $\mathrm{GL}_2(\mathbb{Z})$-equivalence, there is exactly one Fano triangle $P_{(p_0,p_1)}$ whose edges E_i have length n_ih_i and height h_i, for $i = 0, 1, 2$. This triangle $P_{(p_0,p_1)}$ has the vertices:*

$$(-n_1h_1^2, 1 - n_1h_1p_1), \quad (n_0h_0^2, 1 - n_0h_0p_0), \quad (0, 1).$$

The realisation (p_0, p_1) *is listed in Table 3.2.*

Equation ID	Equation	p_0	p_1	h_0	h_1
3	$p_0 + p_1 = 3$	1	2	1	1
4	$p_0 + p_1 = 2$	1	1	1	1
6	$p_0 + p_1 = 1$	1	0	1	1
7	$p_0 + p_1 = 2$	1	1	1	1
8	$p_0 + p_1 = 1$	1	0	1	1
9a	$p_0 + p_1 = 1$	1	0	1	1
9b	$p_0 + p_1 = 1$	1	0	1	1
10a	$2p_0 + p_1 = 1$	0	1	1	2
10b	$p_0 + p_1 = 1$	1	0	1	1
10c	$p_0 + p_1 = 1$	1	0	1	1
11a	$3p_0 + p_1 = 1$	0	1	1	3
11b	$2p_0 + p_1 = 1$	0	1	1	2
11c	$2p_0 + p_1 = 1$	0	1	1	2
11d	$2p_0 + p_1 = 1$	0	1	1	2

TABLE 3.2: Realisations of the fundamental solutions of Table 3.1. The equation must be satisfied by (p_0, p_1) to ensure that the edge E_2 has index $n_2 h_2^2$. We include the heights h_0 and h_1 so that it is convenient to check that p_i and h_i are coprime for $i = 0, 1$.

Before we proceed with the proof, we need a couple of technical results.

Lemma 3.3.10. *Let* $\sigma = 1/r(1, a)$ *be a cyclic quotient singularity, so that* a *and* r *are positive coprime integers, with* $0 < a \leq r$. *Then* $A_\sigma \equiv -m/r \mod \mathbb{Z}$, *for some integer* m *satisfying*

$$am \equiv (1 + a)^2 \mod r. \tag{3.4}$$

Proof. We prove by induction. The base case $r = a = 1$ is immediate.

Now suppose that the statement is true for $\sigma = 1/r(1, a)$. For the induction step, we must prove that it holds for $\sigma' = 1/r'(1, r)$, where $r' \equiv a \mod r$. We compute the degree of $\mathbb{P}(1, r, r')$ in two ways, using Propositions 3.3.5 and 3.3.6, and compare in order to find $A_{\sigma'}$:

$$\frac{(1 + r + r')^2}{rr'} \equiv -A_\sigma - A_{\sigma'} \mod \mathbb{Z}.$$

By the induction assumption, we have that

$$A_{\sigma'} \equiv \frac{r'm - (1 + r + r')^2}{rr'} \mod \mathbb{Z}.$$

By Equation (3.4), and since $r' \equiv a \mod r$, we have that $r'm - (1 + r + r')^2 = rm'$, for some integer m. Furthermore, we can see that m' satisfies the congruence relation analogous to Equation (3.4), i.e. $rm' \equiv (1 + r)^2 \mod r'$. Thus, the result now follows by induction. □

The following statement will be necessary in the proof of Theorem 3.3.9. In particular, we will use it to show that our triangles $P_{(p_0,p_1)}$ do indeed have empty baskets.

Corollary 3.3.11. *Let $\sigma = 1/r(1,a)$ be a cyclic quotient singularity, so that a and r are positive coprime integers. Then the denominator of A_σ is $r/\gcd(r,(1+a)^2)$.*

Proof. From Lemma 3.3.10, the denominator of A_σ is $r/\gcd(r,m)$. Since a and r are coprime, this is equal to $r/\gcd(r,am)$. Finally, the result follows by applying Equation (3.4). □

We are now ready to prove the second main theorem of this section.

Proof of Theorem 3.3.9. Suppose that P is a Fano triangle whose edges E_i have length n_ih_i and height h_i. Then, all its vertices are primitive and so, after an appropriate $\mathrm{GL}_2(\mathbb{Z})$-transformation, we may assume that the common vertex of E_0 and E_1 is $(0,1)$. Further, since the index of E_i is $n_ih_i^2$ for $i=0,1$, we may assume that the other vertex of E_0 is $(n_0h_0^2, a_0)$ while the other vertex of E_1 is $(-n_1h_1^2, a_1)$, for some integers a_0 and a_1. Since E_0 has length n_0h_0, we must have that $a_0 = 1 - n_0h_0p_0$, for some integer p_0 coprime to h_0. Similarly, $a_1 = 1 - n_1h_1p_1$, for some integer p_1 coprime to h_1. So, $P = P_{(p_0,p_1)}$. It remains to prove that (p_0,p_1) must appear in the corresponding row of Table 3.2 and that E_2 has the correct length and height.

Since the index of E_2 is $n_2h_2^2$, and then by the Markov-like equation, we obtain that

$$n_0h_0n_1h_1(h_1p_0 + h_0p_1) = n_0h_0^2 + n_1h_1^2 + n_2h_2^2 = dh_0h_1h_2.$$

So, it follows that

$$n_0n_1(h_1p_0 + h_0p_1) = dh_2. \tag{3.5}$$

Let $g := \gcd(h_0,h_1)$ and $h_i = g\hat{h}_i$, for $i=0,1$. If (p_0,p_1) is a solution, then $(p_0 + m\hat{h}_0, p_1 - m\hat{h}_1)$ is a solution for all $m \in \mathbb{Z}$. In fact, these are all the solutions to Equation (3.5). Note that $P_{(p_0,p_1)}$ and $P_{(p_0+m\hat{h}_0,p_1-m\hat{h}_1)}$ are related by a shear whenever the integer m is divisible by g. Thus, since we only care about enumerating our triangles up to $\mathrm{GL}_2(\mathbb{Z})$-equivalence, we may assume that $0 \le m < g$. But now, since h_0 and h_1 are coprime in each row of Table 3.2, we have that $g = 1$. Therefore, there is at most one realisation (p_0,p_1), up to the transformation.

Finally, we must check that the length ℓ and height h of E_2 do indeed coincide with the prescribed length n_2h_2 and height h_2. By Theorem 3.3.4 and Proposition 3.3.5, the dual triangle $P^*_{(p_0,p_1)}$ has volume $12 - n_0 - n_1 - n_2$. Since we know that E_0 and E_1 have $n_0 + n_1$ primitive T-singularities between them (and no residual singularity), it follows from Proposition 3.3.6 that the degree contribution of E_2 is n_2.

In particular, the degree contribution of E_2 has denominator 1. So, by Corollary 3.3.11, we must have that $r = \gcd(r,(1+a)^2)$, where the singularity associated to E_2 is $1/r(1,a)$. This implies that r divides $(1+a)^2$. Now, we may write $a = \ell p - 1$, for some integer p coprime to h. Thus, we obtain that h divides ℓ. In particular, E_2 has empty residue and, by Proposition 3.3.6, it has exactly n_2 primitive T-singularities. So, because each realisation (p_0,p_1) in Table 3.2 satisfies $\gcd(h_0,p_0) = 1$ and $\gcd(h_1,p_1) = 1$, then the result follows. □

Remark 3.3.12. At the start of the section, we wanted to know whether the Hirzebruch surface $\mathbb{F}_1$ was qG-deformation-equivalent to a fake weighted projective space; we can now answer such a question. First, note that $X_P = \mathbb{P}^1 \times \mathbb{P}^1$ and $X_Q = \mathbb{F}_1$ both have the same degree 8. The corresponding Fano polygons P and Q are not mutation-equivalent, by [66, Example 3.12]. Now, P is mutation-equivalent to the triangle corresponding to $\mathbb{P}(1,1,2)$. Since there are no other Fano triangles in Table 3.1, it is impossible for Q to be mutation-equivalent to a triangle.

We further note that there are no Fano triangles in Table 3.1 with 5 primitive T-singularities, i.e. whose corresponding toric variety has degree 7. Now, since Theorem 3.3.9 tells us that all the solutions in Table 3.1 are indeed realisable, we can conclude that exactly eight of the mutation-equivalence classes of Fano polygons with empty basket contain a triangle.

Chapter 4

On the Uniqueness of Kähler-Einstein Polygons up to Mutation

This chapter is based on the work appearing in my paper [37].

4.1 Introduction

One of the main motivations for this chapter is to study minimal Fano polygons, which are important objects appearing in Mirror Symmetry for orbifold del Pezzo surfaces (see our discussion of these in Section 1.3).

Another concept in algebraic geometry which has seen much recent interest is K-stability. It was initially formulated by Tian [100] as a way to characterise the existence of Kähler–Einstein metrics on Fano manifolds. K-stability has since been expanded by Donaldson [30] to polarised varieties. The Yau–Tian–Donaldson conjecture predicts that a Fano variety X is K-polystable if and only if it admits a Kähler–Einstein metric. This was proven in the smooth case by Chen–Donaldson–Sun [19, 20] and Tian [99]; the singular case has seen recent progress [14, 72], but remains open. Its main application is the construction of well-behaved moduli spaces, called K-moduli spaces, of Fano varieties [73, 58, 15].

We study toric Kähler–Einstein Fano varieties. Following Hwang–Kim [53], a Fano polygon P is called *Kähler–Einstein* if its corresponding toric variety X_P admits a Kähler–Einstein metric. A related class, introduced by Batyrev–Selivanova [13], are *symmetric polygons*: these are polygons whose automorphism group fixes only the origin.

Theorem 4.1.1 ([13, Theorem 1.1], [54, Theorem 1.3])**.** *All symmetric polytopes are Kähler–Einstein.*

The converse to Theorem 4.1.1 holds for smooth Fano polytopes in dimension less than seven. Nill–Paffenholz [83] found that exactly one smooth Fano polytope in dimension seven, and exactly two smooth Fano polytopes in dimension eight, are Kähler–Einstein but not symmetric.

In this chapter, we study symmetric Fano polygons and Kähler–Einstein Fano triangles. These were conjectured by Hwang–Kim [54] to constitute all Kähler–Einstein Fano polygons.

Conjecture 4.1.2 ([54, Conjecture 1.6])**.** All Kähler–Einstein polygons are either symmetric or triangles.

We prove that symmetric Fano polygons and Kähler–Einstein Fano triangles are minimal (see, respectively, Lemmas 4.3.15 and 4.4.3). So, in each mutation-equivalence class, there is a finite number of these polygons. The main result of this chapter is the following:

Theorem 4.1.3. *In each mutation-equivalence class, there is at most one Fano polygon which is either symmetric or a Kähler–Einstein triangle.*

Both behaviours are exhibited: there are examples of mutation-equivalence classes with no symmetric Fano polygons or Kähler–Einstein triangles (Example 4.3.2) and examples with exactly one (Example 4.3.3).

In §4.5.1 we provide a counterexample to Conjecture 4.1.2:

Proposition 4.1.4. *The Fano polygon*

$$P := \operatorname{conv}\{(-9,-190),(19,27),(15,113),(-13,112)\} \subset N_{\mathbb{Q}}$$

is a Kähler–Einstein Fano quadrilateral. In particular, Conjecture 4.1.2 does not hold.

All Fano quadrilaterals with barycentre zero are described in Proposition 4.5.5. This allows us to present a method for systematically producing non-symmetric Kähler–Einstein quadrilaterals; see Remark 4.5.7.

As noted above, both symmetric Fano polygons and Kähler–Einstein Fano triangles are minimal. Furthermore, all the non-symmetric Kähler–Einstein Fano quadrilateral examples we have found are minimal. It is natural to ask whether this holds more generally for all Kähler–Einstein Fano polygons; however, this is not the case:

Proposition 4.1.5 (see Proposition 4.5.11)**.** *There exist Kähler–Einstein Fano polygons which are not minimal.*

We now summarise the structure of this chapter. In §4.2, we fix our notation for the objects of study: polygons and mutation. We then extend the notion of basket of singularities to suit our needs. The next two sections are dedicated to proving Theorem 4.1.3. In §4.3, we prove Theorem 4.3.1, which states that there is at most one symmetric Fano polygon in each mutation-equivalence class. In §4.4, we prove the rest of Theorem 4.1.3. In particular, we prove that there is at most one Kähler–Einstein Fano triangle in each mutation-equivalence class and that if a symmetric Fano polygon is mutation-equivalent to a Kähler–Einstein triangle, then they are isomorphic. We conclude with §4.5, where we provide a counterexample to Conjecture 4.1.2. We compute iterated barycentric transformations of P, and show that it has strict type B_2. Finally, we describe an alternative method for constructing non-symmetric Kähler–Einstein Fano polygons and use it to show that there are Kähler–Einstein Fano polygons which are not minimal (Proposition 4.5.11).

4.2 Preliminaries

Throughout, we refer to the lattice $N \cong \mathbb{Z}^2$ and its dual lattice $M := \mathrm{Hom}(N, \mathbb{Z})$. We also refer to their $\mathbb{Q}$-extensions as $N_{\mathbb{Q}} := N \otimes \mathbb{Q}$ and $M_{\mathbb{Q}} := M \otimes \mathbb{Q}$. For elements $u \in M_{\mathbb{Q}}$ and $\boldsymbol{x} \in N_{\mathbb{Q}}$, we denote their natural pairing as $u(\boldsymbol{x})$.

4.2.1 The Hermite normal form of a cone

In toric geometry, we typically consider cones and polytopes up to $\mathrm{GL}_2(\mathbb{Z})$-equivalence. A subtle point used throughout this chapter is to sometimes consider these objects up to the slightly weaker $\mathrm{SL}_2(\mathbb{Z})$-equivalence, since several properties relevant to mutation are only invariant under $\mathrm{SL}_2(\mathbb{Z})$-transformations and not $\mathrm{GL}_2(\mathbb{Z})$-transformations.

A classical way to describe a cone or an edge of a Fano polygon is by its singularity type $\frac{1}{r}(1, a)$, which is equivalently a matrix in Hermite normal form $\left(\begin{smallmatrix} 1 & r-a \\ 0 & r \end{smallmatrix}\right)$. It is invariant under $\mathrm{GL}_2(\mathbb{Z})$-transformations. So, it throws away information; in particular, the orientation of the edge. But knowing how the edges of our polygons are oriented will be vital in several proofs in this chapter. Thus, we modify the notion of Hermite normal form so that it keeps the orientation information.

Definition 4.2.1. Let $\sigma \subset N_{\mathbb{Q}}$ be a (pointed, full-dimensional) cone. Denote the primitive ray generators of σ by $\boldsymbol{v}_0$ and $\boldsymbol{v}_1$, going anticlockwise. Let A_σ be the matrix with left column $\boldsymbol{v}_0$ and right column $\boldsymbol{v}_1$. Let H_σ be the (row-style) Hermite normal form of A_σ. We call H_σ the *Hermite normal form* of the cone σ. Equivalently, we can speak of the *Hermite normal form* H_E of an edge E of a Fano polygon by passing to the cone over E.

Note that the Hermite normal form of σ will be of the form $H_\sigma = \left(\begin{smallmatrix} 1 & a \\ 0 & r \end{smallmatrix}\right)$, for some $r, a \in \mathbb{Z}$ with $0 \leq a < r$. We know that the first column of H_σ must be $(1, 0)$, since the ray generators of σ are primitive. For the same reason, a and r must be coprime.

We now describe the exact behaviour of our orientation-preserving Hermite normal form; in particular, we describe how it behaves when we apply unimodular transformations to the cone (or edge).

Lemma 4.2.2. *Let $\sigma \subset N_{\mathbb{Q}}$ be a pointed, full-dimensional cone with Hermite normal form $H_\sigma = \left(\begin{smallmatrix} 1 & a \\ 0 & r \end{smallmatrix}\right)$. Let G be a unimodular matrix. If G has determinant 1, then $G\sigma$ has Hermite normal form $H_{G\sigma} = H_\sigma$. Instead suppose that G has determinant -1. Then $G\sigma$ has Hermite normal form $H_{G\sigma} = \left(\begin{smallmatrix} 1 & a^* \\ 0 & r \end{smallmatrix}\right)$, where $aa^* \equiv 1 \mod r$.*

Proof. First, suppose that G has determinant 1. So, G preserves the orientation of the ray generators of σ. Thus, $A_{G\sigma} = GA_\sigma$. Since the Hermite normal form of matrices is invariant under unimodular transformation, it follows that $H_{G\sigma} = H_\sigma$.

Now, suppose that G has determinant -1. Consider the cone $\sigma' := \left(\begin{smallmatrix} 0 & 1 \\ 1 & 0 \end{smallmatrix}\right) G\sigma$. This is $\mathrm{SL}_2(\mathbb{Z})$-equivalent to σ, and thus has the same Hermite normal form H_σ. In particular, σ' can be transformed so that its primitive ray generators are the columns

of H_σ, which are $(1,0)$ and (a,r). Applying the matrix $\left(\begin{smallmatrix}0&1\\1&0\end{smallmatrix}\right)$ again, we see that $G\sigma$ can be transformed so that it has primitive ray generators (r,a) and $(0,1)$.

We now aim to compute the Hermite normal form of the matrix $A := \left(\begin{smallmatrix}r&0\\a&1\end{smallmatrix}\right)$. Setting $U := \left(\begin{smallmatrix}r&-a^*\\a&\frac{1-aa^*}{r}\end{smallmatrix}\right)$, for the unique integer $0 \leq a^* < r$ satisfying $aa^* \equiv 1 \mod r$, we see that $A = U\left(\begin{smallmatrix}1&a^*\\0&r\end{smallmatrix}\right)$. Thus, since $G\sigma$ is $SL_2(\mathbb{Z})$-equivalent to A and U is unimodular, the Hermite normal form of $G\sigma$ is as described. □

We can recover the singularity type of σ from its associated Hermite normal form $\left(\begin{smallmatrix}1&a\\0&r\end{smallmatrix}\right)$. The singularity type is simply $\frac{1}{r}(1,-a)$. Since cones are usually considered only up to $\mathrm{GL}_2(\mathbb{Z})$-equivalence, we can also get a Hermite normal form of $\left(\begin{smallmatrix}1&a^*\\0&r\end{smallmatrix}\right)$, where $aa^* \equiv 1 \mod r$, which results in a singularity type of $\frac{1}{r}(1,-a^*)$. This is consistent, since these two singularities are in fact indistinguishable in the world of algebraic geometry.

4.2.2 The directed singularity content of a polygon

In [62], they introduced the important notion of singularity content of a Fano polygon. They proved that the singularity content of a Fano polygon is invariant under mutation. Here, we will introduce a modified version of this invariant. In particular, while the classical singularity content keeps track of singularity types of cones, we keep track of Hermite normal forms of cones. This modification will be vital to the success of later proofs.

We first define the notion locally, i.e. at the level of the edge (or cone).

Definition 4.2.3. Let E be an edge of a Fano polygon with length ℓ and height h. Then $\ell = nh + \widetilde{\ell}$, for some integers $n \geq 0$ and $0 \leq \widetilde{\ell} < h$. So, we can subdivide E into n segments of length h and a (possibly empty) segment $\mathrm{res}(E)$ of length $\widetilde{\ell}$. We call $\mathrm{res}(E)$ the *residue* of E. Each segment of length and height h corresponds to a *primitive T-singularity*. If $\widetilde{\ell} > 0$, then the segment $\mathrm{res}(E)$ corresponds to an *R-singularity*. We define the *directed singularity content* $\mathrm{SC}(E)$ of E as the tuple $(n_E, \mathrm{res}(H_E))$, where $\mathrm{res}(H_E)$ is the *residue* of the Hermite normal form of E, i.e. if $\widetilde{\ell} > 0$, then $\mathrm{res}(H_E) = H_{\mathrm{res}(E)}$; else, $\mathrm{res}(H_E) = \varnothing$.

We now define the notion globally, i.e. at the level of the polygon.

Definition 4.2.4. Let $P \subset N_{\mathbb{Q}}$ be a Fano polygon. The number n_P of primitive T-singularities of P is defined as the sum over all edges E of P of the number n_E of primitive T-singularities of E. The *directed basket* $\overrightarrow{\mathcal{B}}_P$ of P is defined as the cyclically ordered set of non-empty residues of the Hermite normal forms of the edges of P (ordered anticlockwise). We define the *directed singularity content* $\mathrm{SC}(P)$ of P as the tuple $(n_P, \overrightarrow{\mathcal{B}}_P)$. The subscript P's are often omitted when clear from context.

Next, we prove that this modified version of singularity content is indeed a mutation-invariant of Fano polygons.

Proposition 4.2.5. *Let $P, Q \subset N_{\mathbb{Q}}$ be Fano polygons. Suppose that they are related by a mutation, i.e. $Q = \mathrm{mut}_w(P, \boldsymbol{d})$ for some mutation data $(w, \boldsymbol{d})$ of P. Then, the directed singularity contents of P and Q coincide, i.e.* $\mathrm{SC}(P) = \mathrm{SC}(Q)$.

Proof. Let $\overrightarrow{\mathcal{B}}_P \coloneqq \{H_1, H_2, \ldots, H_m\}$ be the directed basket of P and $\overrightarrow{\mathcal{B}}_Q \coloneqq \{H'_1, H'_2, \ldots, H'_{m'}\}$ be the directed basket of Q. By [62, Proposition 3.6], the usual singularity content is invariant under mutation; therefore, we have $m = m'$ and $H'_i \in \{H_i, H_i^*\}$, for all $i = 1, 2, \ldots, m$. It remains to show that $H'_i = H_i$ for all $i = 1, 2, \ldots, m$. But this follows from the fact that Hermite normal forms of edges are invariant under $\mathrm{SL}_2(\mathbb{Z})$-transformations; from P to Q, the normals of the edges undergo one of two linear transformations which have determinant 1. □

Before we discuss minimality of Fano polygons, we will introduce some minor notation. Fix an edge E of a Fano polygon P. Then $h_{\min}(E) \coloneqq \min_{\boldsymbol{x} \in P} u_E(\boldsymbol{x})$ and $h_{\max}(E) \coloneqq \max_{\boldsymbol{x} \in P} u_E(\boldsymbol{x})$, where u_E is the primitive inner normal to E. Note that we simply write $h_{\min}$ and $h_{\max}$ when the edge E is clear from context.

There are several equivalent conditions for a Fano polygon to be minimal (see [66, Lemma 4.2]). We can now summarise the main characterisation that we use.

Lemma 4.2.6 ([66, Corollary 4.5])**.** *Let $P \subset N_{\mathbb{Q}}$ be a Fano polygon. Then P is minimal if and only if $|h_{\min}| \leq h_{\max}$, for each long edge E of P.*

Remark 4.2.7. There are two properties of reflexive polygons relevant to minimality which we wish to highlight. First, it follows by Lemma 4.2.6 that all reflexive polygons are minimal (see [66, Example 4.4]). Second, their edges are all long and pure. In particular, all reflexive polygons have an empty basket.

We finally introduce the notion of edge data, which is instrumental in the proof of Theorem 4.3.1.

Definition 4.2.8. Let $P \subset N_{\mathbb{Q}}$ be a Fano polygon. Order its edges anticlockwise: $E_1, E_2, \ldots, E_m$. The *edge data* $\mathcal{E}(P)$ of P is defined as the cyclically ordered set $\{H_1, H_2, \ldots, H_m\}$, where H_i is the Hermite normal form of the edge E_i.

In general, the edge data is not a mutation-invariant. Note that if we take the residue of the edge data, and remove the empty entries, then we recover the directed basket, which *is* invariant under mutation.

Example 4.2.9. Consider the Fano polygon

$$P = \mathrm{conv}\left\{\pm(5,1), \pm(5,6), \pm(4,7), \pm(-3,7), \pm(-4,5)\right\},$$

which is shown in Figure 4.1. This has edge data

$$\mathcal{E}(P) = \left\{\left(\begin{smallmatrix}1 & 6\\ 0 & 25\end{smallmatrix}\right), \left(\begin{smallmatrix}1 & 3\\ 0 & 11\end{smallmatrix}\right), \left(\begin{smallmatrix}1 & 36\\ 0 & 49\end{smallmatrix}\right), \left(\begin{smallmatrix}1 & 10\\ 0 & 13\end{smallmatrix}\right), \left(\begin{smallmatrix}1 & 23\\ 0 & 29\end{smallmatrix}\right), \left(\begin{smallmatrix}1 & 6\\ 0 & 25\end{smallmatrix}\right), \left(\begin{smallmatrix}1 & 3\\ 0 & 11\end{smallmatrix}\right), \left(\begin{smallmatrix}1 & 36\\ 0 & 49\end{smallmatrix}\right), \left(\begin{smallmatrix}1 & 10\\ 0 & 13\end{smallmatrix}\right), \left(\begin{smallmatrix}1 & 23\\ 0 & 29\end{smallmatrix}\right)\right\}.$$

Finally, we remark that edge data is invariant under $\mathrm{SL}_2(\mathbb{Z})$-transformation. Further, applying a transformation in $\mathrm{GL}_2(\mathbb{Z})$ with determinant -1 to the polygon P changes the edge data in a predictable way. Write the edge data of P as $\mathcal{E}(P) = \{H_1, H_2, \ldots, H_m\}$ and let $U \in \mathrm{GL}_2(\mathbb{Z}) \setminus \mathrm{SL}_2(\mathbb{Z})$. Then, $\mathcal{E}(UP) = \{H_m^*, \ldots, H_2^*, H_1^*\}$. Of course, the analogous fact holds for the directed basket $\overrightarrow{\mathcal{B}}$ of P.

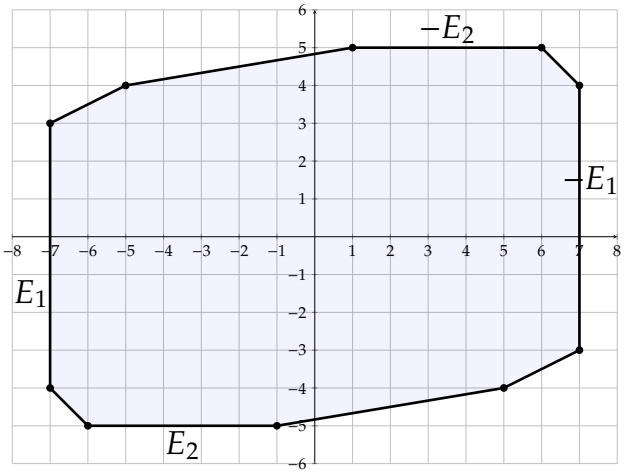

FIGURE 4.1: An example of a centrally symmetric Fano polygon with exactly two pairs of long edges $\pm E_1, \pm E_2$ whose primitive normals span the dual lattice M. Its edge data is described in Example 4.2.9.

4.2.3 Symmetric and Kähler–Einstein polygons

The main objects of study in this chapter are symmetric and Kähler–Einstein Fano polygons. In this subsection, we state their definitions and several basic results concerning them.

Definition 4.2.10. Let $P \subset N_{\mathbb{Q}}$ be a Fano polygon. It's called *Kähler–Einstein* if the barycentre of its dual polytope P^* is the origin. It's called *symmetric* if its automorphism group $\mathrm{Aut}(P)$ only fixes the origin, i.e. $\{\boldsymbol{x} \in N_{\mathbb{Q}} : G \cdot \boldsymbol{x} = \boldsymbol{x}, \forall G \in \mathrm{Aut}(P)\} = \{\mathbf{0}\}$.

Definition 4.2.11. Let $P \subset N_{\mathbb{Q}}$ be a polygon. We call it *centrally symmetric* if for all $\boldsymbol{x} \in P$, we also have $-\boldsymbol{x} \in P$. We call it 3-*symmetric* if there exists an element $G \in \mathrm{Aut}(P)$ of order 3.

It is straightforward to see that if a polygon is centrally symmetric or 3-symmetric, then it is also symmetric. We show that the converse also holds.

Proposition 4.2.12. *Let $P \subset N_{\mathbb{Q}}$ be a symmetric polygon. Then P is either centrally symmetric or 3-symmetric.*

Proof. Consider the automorphism group of P, which is a finite subgroup of $\mathrm{GL}_2(\mathbb{Z})$. Since P is symmetric, $\mathrm{Aut}(P)$ must contain a rotation G. By [75, Theorem 3], $\mathrm{Aut}(P)$ is isomorphic to a subgroup of D_4 or D_6, the dihedral groups of order 8 and 12, respectively. Thus, the rotation G has order in $\{2, 3, 4, 6\}$. If G has order 3, then P is 3-symmetric. Otherwise, G has even order $2g$. Since the element G^g, which belongs to $\mathrm{Aut}(P)$, is $\left(\begin{smallmatrix} -1 & 0 \\ 0 & -1 \end{smallmatrix}\right)$, it follows that P is centrally symmetric. □

Remark 4.2.13. The polygon of Example 4.2.9 is centrally symmetric. For cyclically ordered sets like directed baskets and edge data, let us introduce the notation $\times g$ to indicate that the objects are repeated g times. For example, $\{H_1, H_2, H_3\} \times 2$

means $\{H_1, H_2, H_3, H_1, H_2, H_3\}$. It is a fact that the directed basket (and edge data) of a centrally symmetric polygon can always be written as $C \times 2$, for some cyclically ordered set C. The analogous fact holds for 3-symmetric polygons (replace $\times 2$ with $\times 3$).

Next, let us recall the definition of weights and weight matrices of polygons. As we will immediately see, Kähler-Einstien Fano triangles have a nice description in terms of weights. Further, we will give a description in §4.5 of a Kähler–Einstein quadrilateral P in terms of the weight system of P^*.

Remark 4.2.14. The toric variety corresponding to a Fano polygon $P \subset N_{\mathbb{Q}}$ is a fake weighted projective plane $X_P = \mathbb{P}(\lambda_0\lambda_1, \lambda_2)/G$, where $(\lambda_0, \lambda_1, \lambda_2)$ are the weights of P and G is the group N/N_P and N_P is the sublattice of N generated by the vertices of P. Since we are in dimension two, G is a cyclic group of order k.

There are typically several different fake weighted projective planes with the same weights $(\lambda_0, \lambda_1, \lambda_2)$ and index k. In some cases, though, there is only one such variety up to isomorphism. In these cases, we are safe to write $X_P = \mathbb{P}(\lambda_0, \lambda_1, \lambda_2)/\mathbb{Z}_k$. For instance, throughout the chapter we will write $X_P = \mathbb{P}^2$ when P is isomorphic to the triangle with vertices $(-1, -1)$, $(1, 0)$, and $(0, 1)$. We will also write $X_P = \mathbb{P}^2/\mathbb{Z}_3$ when P is isomorphic to the triangle with vertices $(-1, -1)$, $(2, -1)$, and $(-1, 2)$.

We prove the following statement, which will be useful in both §4.3.3 and §4.4.

Lemma 4.2.15. *Let $P \subset N_{\mathbb{Q}}$ be a Fano triangle. Then P is Kähler–Einstein if and only if P has weights $(1, 1, 1)$.*

Proof. It is well-known that the barycentre of a triangle is the average of its vertices. Therefore, a triangle has barycentre zero if and only if the sum of its vertices is the origin. Equivalently, a triangle has barycentre zero if and only if it has weights $(1, 1, 1)$. By [27, Lemma 3.5], the weights of a Fano triangle coincide with the weights of its dual. Thus, a Fano triangle is Kähler–Einstein if and only if it has weights $(1, 1, 1)$. □

We can also use the above to give an alternative proof for the following statement, which was proven in [54] using direct computation of the barycentre of the dual.

Lemma 4.2.16 ([54, Proposition 4.1])**.** *Let $P \subset N_{\mathbb{Q}}$ be a Fano triangle. Then P is Kähler–Einstein if and only if P is isomorphic to a triangle with vertices $(-k, a-1)$, $(k, -a)$, and $(0, 1)$, for some integers $k, a \geq 1$ satisfying $\gcd(k, a) = \gcd(k, a-1) = 1$.*

Proof. Since P is Fano, we may assume without loss of generality that one of its vertices $(0, 1)$. We label its other vertices as $(-m, b)$ and $(k, -a)$, for some integers $a, b, k, m \geq 1$. By Lemma 4.2.15, since P is Kähler–Einstein, the sum of its vertices must be the origin. So, $(k - m, 1 + b - a) = (0, 0)$. Thus, $m = k$, $b = a - 1$, and the result follows. □

Finally, we must give the following lemma, which again is used in both §4.3.3 and §4.4.

Lemma 4.2.17. *Let $P \subset N_{\mathbb{Q}}$ be a Kähler–Einstein Fano triangle. Suppose that all the edges of P have the same height h and are long. Then, either $X_P = \mathbb{P}^2$ or $X_P = \mathbb{P}^2/\mathbb{Z}_3$.*

Proof. By Lemma 4.2.16, we may apply an appropriate transformation so that P has vertices $(-k, a-1)$, $(k, -a)$, and $(0, 1)$, for some integers $a, k \geq 1$. For each edge E of P, consider the triangle with base E and peak $\mathbf{0}$. It has (normalised) volume k. It also has volume $\ell_E h_E$, where ℓ_E is the length of E and h_E is the height of E. But by assumption, all the edges of P have the same height h. Thus, all edges have the same length ℓ and so we obtain the following condition:

$$\ell = \gcd(k, a+1) = \gcd(k, a-2) = \gcd(2k, 2a-1). \tag{4.1}$$

We see that ℓ divides $a+1$ and $a-2$; thus, ℓ divides 3.

If $\ell = 1$ then, since each edge of P is long, we have $h = 1$. We may write $a = 1$. It follows that $X_P = \mathbb{P}^2$. Otherwise, $\ell = 3$. We may write $a = 3b - 1$, for some integer $b \geq 1$. Plugging this into (4.1), we obtain:

$$1 = \gcd(h, b) = \gcd(h, b-1) = \gcd(2h, 2b-1). \tag{4.2}$$

Since the edges of P are long, we have $h \leq 3$. If $h = 1$, then we may write $b = 1$. It follows that $X_P = \mathbb{P}^2/\mathbb{Z}_3$. If $h = 2$, then (4.2) implies that $b \not\equiv 0, 1 \mod 2$, which cannot hold. Else $h = 3$, and (4.2) implies that $b \not\equiv 0, 1, 2 \mod 3$, which also cannot hold. □

4.3 At most one symmetric

We dedicate this section to proving part of Theorem 4.1.3. Namely, we prove the following statement.

Theorem 4.3.1. *There is at most one symmetric Fano polygon in each mutation-equivalence class.*

As we will see later in Proposition 4.3.16, the above theorem holds for symmetric Fano polygons with empty basket $\mathcal{B}$. Thus, the next few subsections will mainly focus on the case $\mathcal{B} \neq \varnothing$.

4.3.1 Observation of both behaviours

Before we prove Theorem 4.3.1, we will first demonstrate that both possibilities occur. More precisely, we show that there exists a mutation-equivalence class with no symmetric Fano polygons or Kähler–Einstein Fano triangles and that there exists a mutation-equivalence class with exactly one of them.

Example 4.3.2. Consider the Fano polygon $P := \operatorname{conv}\{(2, -3), (1, 5), (-1, -2)\} \subset N_{\mathbb{Q}}$. Since P is a triangle with weights $(3, 7, 13)$, it is not Kähler–Einstein by Lemma 4.2.15. Further, the edges of P all have length 1 while their heights are 3, 7, and 13 — all greater than 1. Thus, none of the edges of P are long. Therefore, P is the only polygon in its mutation-equivalence class. So, the mutation-equivalence class of P contains no Kähler–Einstein polygons. In particular, it contains no symmetric Fano polygons or Kähler–Einstein Fano triangles.

We now show that the other possibility can occur.

Example 4.3.3. Consider the Fano polygon $P := \operatorname{conv}\{(\pm(1,-2), \pm(2,-1), \pm(1,1)\} \subset N_{\mathbb{Q}}$. Clearly, P is centrally symmetric (and thus symmetric). The edges of P all have length 1 and height 3; thus, none of the edges of P are long. Therefore, P is the only polygon in its mutation-equivalence class. So, the mutation-equivalence class of P contains exactly one Kähler–Einstein polygon. In particular, it contains exactly one symmetric Fano polygon or Kähler–Einstein Fano polygon.

In the following subsections, we will show that for symmetric Fano polygons, no other possibility can occur, i.e. that if two symmetric Fano polygons are mutation-equivalent, then they are isomorphic.

4.3.2 Constraints on centrally symmetric Fano polygons

When mutating polygons, it's the long edges (in particular, the T-singularities) which move and change, while the short edges (i.e. the R-singularities) stay the same. Generally speaking, if a polygon has more long edges, then its behaviour under mutation will be richer. As we saw in Example 4.3.2 and Example 4.3.3, if a polygon has no long edges, then its mutation-equivalence class is trivial; we can conclude that Theorem 4.1.3 holds in this case. For centrally symmetric polygons, the next simplest case is when the polygon has exactly one pair of parallel long edges.

Proposition 4.3.4. *Let $P \subset N_{\mathbb{Q}}$ be a centrally symmetric polygon with exactly one pair of long edges $\pm E$. Let $Q \subset N_{\mathbb{Q}}$ be a symmetric polygon. Suppose P is mutation-equivalent to Q. Then $P \cong Q$.*

Proof. Let $w \in M$ be the primitive inner normal to E. Then $-w$ is the primitive inner normal to $-E$. Consider $\operatorname{mut}_w(P, \boldsymbol{d})$, where $(w, \boldsymbol{d})$ is mutation data for P. Then again, this polygon will have at most two long edges, whose primitive inner normals are in $\{w, -w\}$. Thus, by induction, all polygons mutation-equivalent to P will have at most two long edges with inner normals in $\{w, -w\}$.

Now consider the symmetric polygon Q, which is mutation-equivalent to P. Since the number of primitive T-singularities is invariant under mutation, and P has at least one primitive T-singularity, it follows that Q has at least one long edge. If Q were 3-symmetric, then it would have at least three long edges. So, since Q has at most two long edges, it must be centrally symmetric. In particular, the number of primitive T-singularities on its two long edges must be equal. Thus, Q is isomorphic to P. □

Now, we are left to consider centrally symmetric Fano polygons with at least two pairs of parallel long edges. The rest of the subsection is dedicated to constraining the combinatorics of these polygons. In fact, in Corollary 4.3.10, we discover that these polygons must have *exactly* two pairs of parallel long edges with at most 8 primitive T-singularities in total. This restricts the complexity of their behaviour under mutation, making the study of these objects under mutation realistic.

Lemma 4.3.5. *Let $P \subset N_{\mathbb{Q}}$ be a centrally symmetric Fano polygon with non-empty basket $\mathcal{B}$ and two pairs of opposite long edges $\pm E_1$ and $\pm E_2$. Then the primitive normals to E_1 and E_2 span the dual lattice M.*

Proof. We may apply an appropriate unimodular transformation so that the primitive inner normal to E_1 is $u_1 = e_1^*$. We may also assume that the edge E_2 is on the bottom. Thus, its primitive inner normal vector $u_2 := (a, b)^t \in M$ will have $b > 0$, as in Figure 4.2. We obtain $\det(u_1, u_2) = b$. Thus, u_1 and u_2 span M if and only if $b = 1$. So, assume towards a contradiction that $b \geq 2$.

Let ℓ_1 and ℓ_2 be the (lattice) lengths of E_1 and E_2, respectively, and let h_1 and h_2 be the respective heights of E_1 and E_2. Consider the primitive direction vector for E_2, which is $(b, -a)$. We can see that the starting vertex of E_2 uses up one lattice point, and each unit segment of E_2 uses up b lattice points. Since there are $2h_1 + 1$ lattice points between E_1 and $-E_1$ for E_2 to go through, we obtain the inequality $b\ell_2 \leq 2h_1$. We can similarly derive that $b\ell_1 \leq 2h_2$. Now, since E_2 is a long edge and E_1 has a smaller height than E_2, we obtain that $bh_1 \leq 2h_1$. Thus, $b = 2$ and the inequalities become equalities, giving $\ell_1 = h_1 = h_2 = \ell_2$. Further, all $2h_1 + 1$ lattice points were used up by E_2. This means that no more lattice points are left for any other edges going from E_1 to $-E_1$ to go through. So, no more pairs of edges exist other than $\pm E_1$ and $\pm E_2$. Thus, P is a centrally symmetric quadrilateral with only T-singularities, which contradicts our assumption that the basket $\mathcal{B}$ is non-empty. □

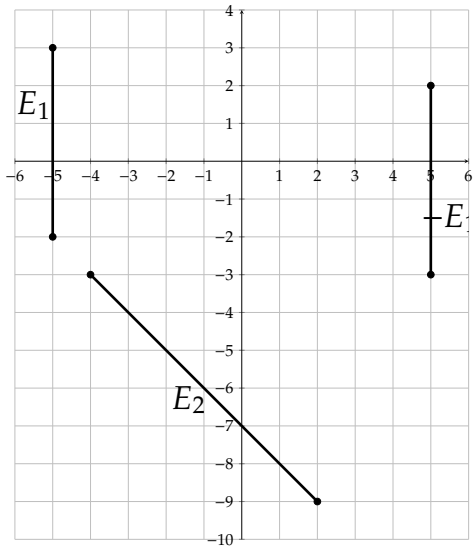

FIGURE 4.2: A configuration of two long edges of a centrally symmetric polygon; see the proof of Lemma 4.3.5

Remark 4.3.6. 1. Let $P \subset N_{\mathbb{Q}}$ be a centrally symmetric Fano polygon with two pairs of long edges $\pm E_1$ and $\pm E_2$ whose primitive inner normal vectors are $\pm u_1$ and $\pm u_2$, respectively. If $\mathcal{B}_P \neq \emptyset$ then, by Lemma 4.3.5, $\det(u_1, u_2) = 1$. The matrix V with rows u_1 and u_2 is invertible in $\mathrm{GL}_2(\mathbb{Z})$. Thus, we can apply a unimodular transformation to P so that the primitive inner normals to E_1 and E_2 become e_1^* and e_2^*, respectively.

2. Later, in §4.3.4, we will be working with the edge data $\mathcal{E}(P)$ and directed basket $\overrightarrow{\mathcal{B}}_P$ of P. Thus, we will want to only transform P by elements of $\mathrm{SL}_2(\mathbb{Z})$ so that this data stays the same. If the matrix V has determinant -1, we instead simply consider the matrix V' with rows u_1 and $-u_2$. This now has determinant 1, and so we can apply an $\mathrm{SL}_2(\mathbb{Z})$-transformation to P so that the primitive inner normals to E_1 and $-E_2$ become e_1^* and e_2^*, respectively.

We now give the following lemma, which helps us to prove Proposition 4.3.8.

Lemma 4.3.7. *Let $P \subset N_{\mathbb{Q}}$ be a centrally symmetric Fano polygon with non-empty basket $\mathcal{B} \neq \varnothing$. Suppose that P has two pairs of opposite long edges $\pm E_1$ and $\pm E_2$ with heights $h_1 \leq h_2$. Then, $2 \leq h_1 \leq h_2 < 2h_1$.*

Proof. We may assume without loss of generality that the primitive inner normals to E_1 and E_2 are e_1^* and e_2^*, respectively. We first show that $h_1 \geq 2$. Assume towards a contradiction that $h_1 = 1$. Then P is contained in the strip $\{-1 \leq x \leq 1\}$. So, E_2 has length at most 2. Now, since E_2 is long, it must have height $h_2 = 1$ or $h_2 = 2$. We explore both possibilities.

Suppose that $h_2 = 1$. Then P is contained in the box $\{-1 \leq x, y \leq 1\}$. Up to isomorphism, there are two polygons in this box which have long edges E_1 and E_2 with the prescribed heights: either $P = \mathrm{conv}\{\pm(1,1), \pm(-1,1)\}$ or $P = \mathrm{conv}\{\pm(1,0), \pm(1,1), \pm(0,1)\}$. In either case, P has an empty basket $\mathcal{B} = \varnothing$, which is a contradiction.

Now suppose that $h_2 = 2$. Then P must be the quadrilateral $\mathrm{conv}\{\pm(1,2), \pm(-1,2)\}$. This has empty basket $\mathcal{B} = \varnothing$, so we again reach a contradiction. Thus, we have shown that $h_1 \geq 2$.

Finally, we show that $h_2 < 2h_1$. Note that P is contained in the strip $\{-h_1 \leq x \leq h_1\}$, which implies that E_2 has length $\ell_2 \leq 2h_1$. Since E_2 is a long edge, we obtain that $h_2 \leq 2h_1$. We see that it now remains to show that $h_2 \neq 2h_1$.

Suppose towards a contradiction that $h_2 = 2h_1$. Then P must be the rectangle with vertices $\pm(h_1, 2h_1)$ and $\pm(-h_1, 2h_1)$. Since P is Fano, its vertices must be primitive, i.e. $\gcd(h_1, 2h_1) = 1$. Thus, $h_1 = 1$. But we have already seen above that this results in a contradiction. Therefore, $h_2 < 2h_1$. □

In order to decide whether two polygons P and Q are mutation-equivalent, we can compare their mutation-invariants. One such invariant is the Ehrhart series of the dual polygon, i.e. $\mathrm{Ehr}_{P^*}(t) = \mathrm{Ehr}_{Q^*}(t)$. We find a striking pattern in the coefficients of the Ehrhart series.

Proposition 4.3.8. *Let $P \subset N_{\mathbb{Q}}$ be a centrally symmetric Fano polygon with non-empty basket of R-singularities. Suppose P has two non-parallel long edges E_1 and E_2, which have primitive inner normals u_1 and u_2 and heights h_1 and h_2, respectively, with $h_1 \leq h_2$. Then,*

$$kP^* \cap M = \begin{cases} \{0\}, & 0 \leq k < h_1 \\ \{0, \pm u_1\}, & h_1 \leq k < h_2 \\ \{0, \pm u_1, \pm u_2\}, & k = h_2. \end{cases}$$

Proof. The inclusion "$\supseteq$" is clear; thus, it is enough to show that $h_2P^* \cap M \subseteq \{0, \pm u_1, \pm u_2\}$. By Lemma 4.3.5, we may assume that $u_1 = (1,0)^t$ and $u_2 = (0,1)^t$. We first show that $\pm(1,1)^t \notin h_2P^*$. This is equivalent to showing that there exists a point $(x,y) \in P$ satisfying $x + y < -h_2$. Let $(a, -h_2)$ be the left vertex of E_2, where a is an integer satisfying $-h_1 \leq a \leq h_1 - h_2 \leq 0$. In fact, $a < 0$. Otherwise, $(0, -h_2)$ would be a vertex of P. By Lemma 4.3.7, $h_2 \geq 2$. On the other hand, since P is Fano, its vertices must be primitive. So, we must have that $h_2 = 1$, which is a contradiction. Thus, we have $(a, -h_2) \in P$ satisfying $a < 0$. Equivalently, $a - h_2 < -h_2$. We can conclude that $(1,1)^t$ is not in h_2P^*.

Using the same logic as above, we can also show that $\pm(-1,1)^t \notin h_2P^*$. Furthermore, since $(1,1)^t \notin h_2P^*$, we can rule out from h_2P^* all points in the region $(1,1)^t + \text{cone}((1,0)^t, (0,1)^t)$. We can rule out similarly defined regions from the other 3 quadrants; see Figure 4.3. It now remains to treat the points on the axes.

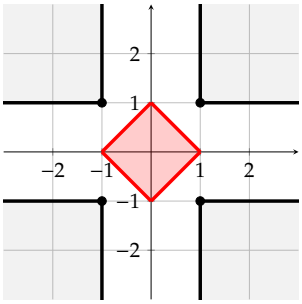

FIGURE 4.3: In red: the polygon conv $\{\pm u_1, \pm u_2\}$. In grey: the regions which can be ruled out from h_2P^* given that their apexes are not in h_2P^*.

Clearly, the only points of h_2P^* on the y-axis are 0 and $\pm u_2$. By Lemma 4.3.7, we have $h_2 < 2h_1$. Therefore, the only points of h_2P^* on the x-axis are 0 and $\pm u_1$. Thus, we now have the desired result. □

An immediate implication of Proposition 4.3.8 is that the heights of the long edges can be read off the Ehrhart series.

Example 4.3.9. Consider the polygon $P \subset N_{\mathbb{Q}}$ from Example 4.2.9. Let $Q \subset N_{\mathbb{Q}}$ be a centrally symmetric Fano polygon mutation-equivalent to P. Then it must also have at least two pairs of opposite long edges whose primitive normals span the lattice M. The dual polygon P^* has Ehrhart series $\text{Ehr}_{P^*}(t) = 1+t+t^2+t^3+t^4+3t^5+3t^6+5t^7+O(t^8)$. Since Q is mutation-equivalent to P, its dual Q^* has the same Ehrhart series. Since the coefficient jumps from 1 to 3 at the t^5 term and then to 5 at the t^7 term, it follows that Q has long edges with heights 5 and 7, just as P does. This is because, by Proposition 4.3.8, the non-origin lattice points in $7Q^* \cap M$ must be primitive normals to the long edges of Q.

The main implications of Proposition 4.3.8 are summarised in the following corollary.

Corollary 4.3.10. *Let P be a centrally symmetric Fano polygon with non-empty basket. Suppose that P has at least two pairs of long edges $\pm E_1$ and $\pm E_2$. Then the long edges of P are*

exactly $\pm E_1$ *and* $\pm E_2$*. Moreover, if* P *has an R-singularity* $H_\sigma \in \overrightarrow{\mathcal{B}}_P$ *with the same height as one of the long edges, then* σ *will be on a long edge of* P*, i.e.* $H_\sigma = \operatorname{res}(H_{E_i})$ *for some* $i = 1, 2$*. In particular, the number of edges is fixed.*

Proof. Without loss of generality, suppose that the height h_1 of E_1 is the smallest out of all long edges of P and the height h_2 of E_2 is the largest out of all long edges of P. By Proposition 4.3.8, there are no edges of P other than $\pm E_1$ and $\pm E_2$ which have height between 1 and h_2, inclusively; otherwise, the primitive inner normal of such an edge would be a lattice point of $h_2 P^* \cap M$. Thus, we may conclude that $\pm E_1$ and $\pm E_2$ are the only long edges of P and that all other edges of P must have height strictly greater than h_2. It now follows that if an R-singularity of P has height h_1 or h_2, then it must be on one of the long edges of P. □

4.3.3 Constraints on 3-symmetric Fano polygons

As stated at the beginning of §4.3.2, the more long edges a polygon has, the richer its behaviour under mutation will be. The simplest non-trivial case for 3-symmetric polygons is when there is *at least one* triple of long edges. In fact, similarly to the centrally symmetric case, we see that these polygons must have *exactly one* triple of long edges (Corollary 4.3.13).

Before we proceed with the first lemma of the subsection, we reiterate a subtle distinction regarding the action of matrices on points of $N_\mathbb{Q}$ and $M_\mathbb{Q}$. First recall that points in $N_\mathbb{Q}$ are regarded as column vectors and that points in the dual space $M_\mathbb{Q}$ are regarded as row vectors. Now, matrices in $\mathrm{GL}_2(\mathbb{Z})$ act on the left for points in $N_\mathbb{Q}$ and on the right for points in $M_\mathbb{Q}$. As a consequence, if $P \subset N_\mathbb{Q}$ is an IP polytope and $G \in \mathrm{GL}_2(\mathbb{Z})$, then we have that $(GP)^* = P^* G^{-1}$.

Since we will reuse the following result in the general setting, we emphasise that P can have either empty or non-empty basket of R-singularities in the following lemma.

Lemma 4.3.11. *Let* $P \subset N_\mathbb{Q}$ *be a 3-symmetric Fano polygon with* $G \in \mathrm{Aut}(P)$ *having order 3. Suppose* P *has a long edge* E *with primitive inner normal* u*. Then, one of the following must hold:*

(i) $\det(u, uG) = 3$ *and* $X_P = \mathbb{P}^2$*;*

(ii) $\det(u, uG) = 1$*.*

Proof. Denote by h_E the height of E. Consider the (not necessarily lattice) triangle Q which is the intersection of the supporting half-spaces of E, GE, and G^2E, i.e.

$$Q := \left\{ \boldsymbol{x} \in N_\mathbb{Q} : \; u(\boldsymbol{x}) \geq -h_E, (uG)(\boldsymbol{x}) \geq -h_E, (uG^2)(\boldsymbol{x}) \geq -h_E \right\}.$$

Due to the action of G on Q, there exists a unique $t \in \mathbb{Q}_{>0}$ such that tQ has primitive vertices. Since Q contains the origin, we can conclude that tQ is Fano. Now, consider the sum of the vertices of tQ. This is fixed by G, so it must equal the origin. Thus, tQ has weights $(1, 1, 1)$.

Let F be an edge of tQ. Then the other two edges of tQ are GF and G^2F. In particular, the edges of tQ all have the same height. Further, since the original edge E of P is long, the edges F, GF, and G^2F must also be long. So, we may apply Lemma 4.2.17 to tQ. We obtain that either (i) $X_{tQ} = \mathbb{P}^2$ or (ii) $X_{tQ} = \mathbb{P}^2/\mathbb{Z}_3$.

In case (i), the result follows from the observation that $t = 1$ and $P = Q$. In case (ii), the result follows after noticing that E and F have the same primitive inner normal vector. □

The above lemma is enough to prove that 3-symmetric Fano polygons are minimal, which we do later in Lemma 4.3.15. For the rest of this subsection, we again focus on 3-symmetric Fano polygons with *non-empty* baskets. The above lemma also constrains the dual polygon P^*. As in §4.3.2, we next describe the mutation-invariants $|kP^* \cap M|$ for relevant k.

Proposition 4.3.12. *Let $P \subset N_{\mathbb{Q}}$ be a 3-symmetric Fano polygon with element $G \in \mathrm{Aut}(P)$ of order 3. Suppose that P has a non-empty basket of singularities and that P has a long edge E with primitive inner normal u and height h. Then*

$$kP^* \cap M = \begin{cases} \{0\}, & 0 \leq k < h \\ \{0, u, uG, uG^2\}, & k = h. \end{cases}$$

Proof. Since the basket of R-singularities is non-empty, we are in case (ii) of Lemma 4.3.11. Thus, we may assume, after applying a suitable linear transformation to P, that $u = (0,1)^t$ and $uG = (1,0)^t$. This determines G, and so $uG^2 = (-1,-1)^t$. Now, since the edges E, GE, and G^2E all have height h, we see that $u, uG, uG^2 \notin kP^*$, for $0 \leq k < h$, and $\{0, u, uG, uG^2\} \subseteq hP^* \cap M$.

In order to show the reverse inclusion, it is enough to show that $(1,1)^t \notin hP^*$, as we will now explain. Consider the cone C in $M_{\mathbb{Q}}$ generated by $(1,0)^t$ and $(0,1)^t$. It is clear that, for $m > 1$, the points $(m,0)^t$ and $(0,m)^t$ do not belong to hP^*. Now let $w \in (1,1)^t + C$. It is clear that $(1,1)^t$ is contained in $\mathrm{conv}\{(1,0)^t, (0,1)^t, w\}$. So, if $w \in hP^*$, then $(1,1)^t \in hP^*$. Therefore, if we can show that $(1,1)^t \notin hP^*$, then $hP^* \cap C \cap M = \{0, u, uG\}$. We can treat CG and CG^2 similarly, and reach the desired conclusion.

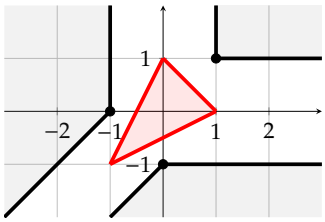

FIGURE 4.4: In red: the polygon $\mathrm{conv}\{u, uG, uG^2\}$. In grey: the regions which can be ruled out from hP^* given that their apexes are not in hP^*.

It remains to prove that $(1,1)^t$ is not contained in hP^*. This is equivalent to showing that there exists a point $(x,y) \in P$ such that $x + y < -h$. Let $(a,-h)$ be a vertex of E. Without loss of generality, and due to E being a long edge, we know

that $(a+h,-h) \in E$. So, we get the point $G \cdot (a+h,-h) = (-h,-a)$ of P. Then, we may set

$$(x,y) \coloneqq \begin{cases} (a,-h), & a < 0 \\ (-h,-a), & a > 0. \end{cases}$$

The case $a = 0$ cannot occur. Otherwise, since P is a Fano polytope, its vertex $(a,-h)$ must be primitive. It follows that $h = 1$. Now, P has exactly one interior lattice point, i.e. it is reflexive. But this implies that P has an empty basket of R-singularities, which contradictions our starting assumption. Thus, we may conclude that indeed $(1,1)^t$ does not belong to hP^*. □

Let us now summarise the main implications of Proposition 4.3.12. Note that this is analogous to Corollary 4.3.10.

Corollary 4.3.13. *Let P be a 3-symmetric Fano polygon with non-empty basket. Suppose that P has at least one triple of long edges E, GE, and G^2E, where $G \in \mathrm{Aut}(P)$ is an element of order 3. Then the long edges of P are exactly E, GE, and G^2E. Moreover, if P has an R-singularity $H_\sigma \in \overrightarrow{\mathcal{B}}_P$ with the same height as one of the long edges, then σ will be on a long edge of P, i.e. $H_\sigma = \mathrm{res}(H_E)$. In particular, the number of edges is fixed.*

Proof. Without loss of generality, take E to be a long edge of P achieving the maximal height h among all long edges of P. By Proposition 4.3.12, the only edges of P which have height $h' \leq h$ are in $\{E, GE, G^2E\}$; otherwise, the primitive inner normal of such an edge would be a lattice point of $hP^* \cap M$. Thus, we may conclude that E, GE, and G^2E are the only long edges of P and that all other edges of P must have height strictly greater than h. It now follows that if an R-singularity of P has height h, then it must be on one of the long edges of P. □

Finally, we give the following lemma specific to 3-symmetric polygons which will be of use in the following subsection.

Lemma 4.3.14. *Let $P \subset N_{\mathbb{Q}}$ be a 3-symmetric polygon with non-empty basket $\mathcal{B}$. Suppose E is an edge of P with height h. Then $h \geq 2$.*

Proof. Suppose towards a contradiction that $h = 1$. Then E is a long edge. Since $\mathcal{B} \neq \emptyset$, case (ii) of Lemma 4.3.11 applies. Therefore, P is contained in a reflexive triangle Q with $X_Q = \mathbb{P}^2/\mathbb{Z}_3$. In particular, P itself is reflexive. This is a contradiction, since it implies that $\mathcal{B} = \emptyset$. □

4.3.4 The proof for symmetric Fano polygons

In this subsection, the aim is to prove Theorem 4.3.1. We first prove it for the case when the basket of R-singularities is empty. Then, we prove the non-empty basket case.

So, we begin by proving that all symmetric Fano polygons are minimal.

Lemma 4.3.15. *Let $P \subset N_{\mathbb{Q}}$ be a symmetric Fano polygon. Then P is minimal.*

Proof. If P is centrally symmetric, then minimality of P is clear. It remains to treat the case when P is 3-symmetric. If P has no long edges, then we are done. Otherwise, let E be a long edge of P with length ℓ and height h. In order to demonstrate minimality of P, we need to prove that there is a point x of P satisfying $u(x) \geq h$.

We can apply Lemma 4.3.11. In case (i), it's straightforward to see that P is minimal. We now consider case (ii). Without loss of generality, $u = (0,1)^t$ is the inner normal to E and $(1,0)^t$ is the inner normal to GE, where $G \in \mathrm{Aut}(P)$ is an element of order 3. Thus, $G = \left(\begin{smallmatrix} -1 & -1 \\ 1 & 0 \end{smallmatrix}\right)$. We may write $E = \mathrm{conv}\{(a,-h),(a+\ell,-h)\}$ for some integer a. Since E is long, the point $(a+h,-h)$ is in E.

Consider the points $G \cdot (a,-h) = (-h, h-a)$ and $G^2 \cdot (a+h,-h) = (-a, h+a)$, which belong to P. If we evaluate them at u, we obtain $h-a$ and $h+a$, respectively. At least one of these is greater than or equal to h. Thus, we are done. □

Previous work of [66] already contains the answer for symmetric Fano polygons whose baskets of R-singularities are empty.

Proposition 4.3.16. *Let $P, Q \subset N_{\mathbb{Q}}$ be symmetric Fano polygons with empty basket $\mathcal{B}$. If P and Q are mutation-equivalent, then P is isomorphic to Q.*

Proof. In [66, Theorem 5.4], all minimal Fano polygons with $\mathcal{B} = \varnothing$ are classified up to isomorphism. Since symmetric Fano polygons are minimal by Lemma 4.3.15, the ones with empty basket all appear in their list.

We display all 6 symmetric Fano polygons with empty baskets in Figure 4.5. They each have a different number of primitive T-singularities. So, none are mutation-equivalent to each other. Therefore, no two non-isomorphic symmetric Fano polygons are mutation-equivalent to each other.

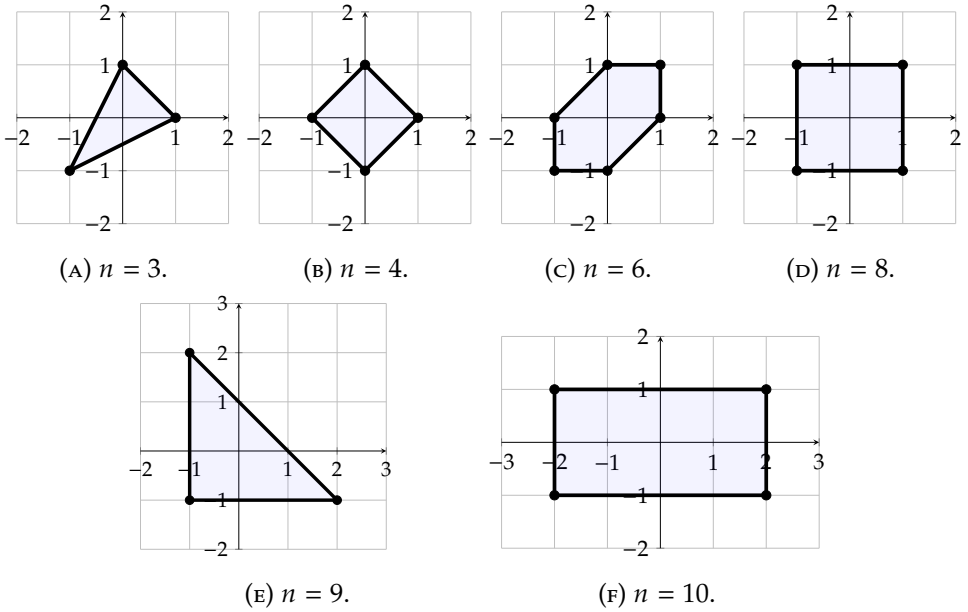

(A) $n = 3$. (B) $n = 4$. (C) $n = 6$. (D) $n = 8$.

(E) $n = 9$. (F) $n = 10$.

FIGURE 4.5: The six symmetric Fano polygons with n primitive T-singularities and empty basket $\mathcal{B} = \varnothing$.

□

So, we can restrict our attention to symmetric Fano polygons which have a non-empty basket $\mathcal{B}$ of R-singularities. We prove the remainder of Theorem 4.3.1 in two big steps. In the first step, we prove that two symmetric Fano polygons with the same edge data are isomorphic (Proposition 4.3.19). In the second step, we prove that if two symmetric Fano polygons are mutation-equivalent, then their edge data is the same (Proposition 4.3.21). Thus, Theorem 4.3.1 would then follow.

In order to complete the first step, we need the following two lemmas.

Lemma 4.3.17. *Let $H = \left(\begin{smallmatrix} 1 & a \\ 0 & r \end{smallmatrix}\right)$ be a Hermite normal form satisfying $\gcd(a, r) = 1$. Fix an edge E with primitive vertices $\boldsymbol{v}_0$ and $\boldsymbol{v}_1$ in N, which are ordered anticlockwise. Let $u_E \in M$ be the primitive inner normal of E and let h_E be the height of E. Let $\mathcal{F}$ be the set of all edges F which satisfy the following conditions:*

(i) F has Hermite normal form H;

(ii) The first vertex of F is the second vertex $\boldsymbol{v}_1$ of E;

(iii) The second vertex $\boldsymbol{v}_2$ of F satisfies $-h_E < u_E(\boldsymbol{v}_2) \leq (r-1)h_E$.

Then, $|\mathcal{F}| \leq 1$.

Proof. Since the vertices are primitive, we may assume without loss of generality that $\boldsymbol{v}_0 = (b, -s)$ and $\boldsymbol{v}_1 = (1, 0)$, for some coprime integers $b, s > 0$. If $\mathcal{F} = \varnothing$, then we are done. Otherwise, let $F, F' \in \mathcal{F}$ so that, by (ii), F has vertices $\boldsymbol{v}_1$ and $\boldsymbol{v}_2$ and F' has vertices $\boldsymbol{v}_1$ and $\boldsymbol{v}_2'$, ordered anticlockwise. We aim to show that $F = F'$.

Write $\boldsymbol{v}_2 = (x, y)$ and $\boldsymbol{v}_2' = (x', y')$. By (i), there exists some $U, U' \in \mathrm{SL}_2(\mathbb{Z})$ such that $F = UH$ and $F' = U'H$. It follows that $y = y' = r$ and $x \equiv x' \equiv a \mod r$. Thus, $x' = x + dr$ for some $d \in \mathbb{Z}$.

It remains to show that $d = 0$. To do this, we apply condition (iii). An important observation is that the half-open strip $S := \{\boldsymbol{x} \in N_{\mathbb{Q}} : \ -h_E < u_E(\boldsymbol{x}) \leq (r-1)h_E\}$ is the Minkowski sum of the half-open segment $\{(x, 0) : \ 1 - r \leq x < 1\}$ and a line with non-horizontal slope. From this, we can see that at each fixed y-coordinate, there are at most r lattice points in S. The vertices $\boldsymbol{v}_2$ and $\boldsymbol{v}_2'$ both lie in S and share the same y-coordinate; consequently, $|x - x'| < r$, i.e. $|dr| < r$. Thus, $d = 0$. Therefore, $\boldsymbol{v}_2 = \boldsymbol{v}_2'$, and so $F = F'$. It now follows that $|\mathcal{F}| \leq 1$.

□

This next lemma generalises a behaviour shared by centrally symmetric polygons and 3-symmetric polygons.

Lemma 4.3.18. *Let $P \subset N_{\mathbb{Q}}$ be a symmetric polygon and E be an edge of P. Then, P is contained in the strip supported by E and $-2E$.*

Proof. Let S be the strip supported by E and $-2E$, i.e. $S := \{\boldsymbol{x} \in N_{\mathbb{Q}} : \ -h \leq u(\boldsymbol{x}) \leq 2h\}$, where u is the primitive inner normal to E and h is the height of E. If P is centrally symmetric, then $-E$ is an edge of P. So, by convexity, $P \subseteq S$. Otherwise, P is 3-symmetric. Now, as in the proof of Lemma 4.3.11, consider the triangle $Q := \left\{\boldsymbol{x} \in N_{\mathbb{Q}} : \ (uG^k)(\boldsymbol{x}) \geq -h, \text{ for } k = 0, 1, 2\right\}$. It has weights $(1, 1, 1)$. Thus, Q

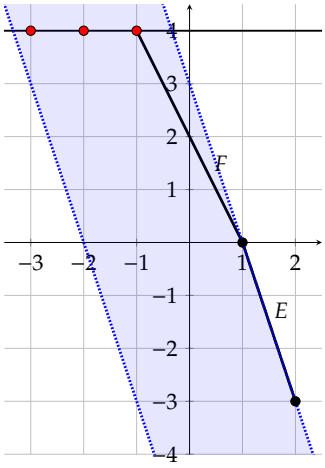

FIGURE 4.6: An example to demonstrate Lemma 4.3.17. Here, $E = \text{conv}\{(2,-3),(1,0)\}$ and $H = \left(\begin{smallmatrix}1 & 3\\ 0 & 4\end{smallmatrix}\right)$. The red points are the three choices for the second vertex v_2 of F; the only valid choice for v_2 is $(-1,4)$.

is isomorphic to the triangle with vertices $(-a,-h)$, $(\ell-a,-h)$, and $(2a-\ell,2h)$, for some $a,\ell > 0$. So, Q is contained in the strip S and, since $P \subseteq Q$, the result follows. □

We can now use the above two lemmas to complete the first step, which was to prove the following statement.

Proposition 4.3.19. *Let $P, Q \subset N_{\mathbb{Q}}$ be symmetric Fano polygons with non-empty basket of R-singularities. Suppose they have the same edge data, i.e. $\mathcal{E}(P) = \mathcal{E}(Q)$. Then P is isomorphic to Q.*

Proof. Let $\mathcal{E}(P) = \mathcal{E}(Q) = \{H_1, H_2, \ldots, H_m\}$. To get the desired result, we aim to repeatedly apply Lemma 4.3.17. In order to do so, we must show that all the hypotheses of the lemma hold. Let E and F be two consecutive edges of P, ordered anticlockwise. Let H be the Hermite normal form of F. Since P is Fano, the vertices of F are primitive; hence, H satisfies the requirements of Lemma 4.3.17. We next show that F belongs to the set $\mathcal{F}$ of Lemma 4.3.17.

Condition (i) is satisfied by the definition of H. Since E is adjacent to F, condition (ii) is satisfied. It remains to show condition (iii). Consider the second vertex v_2 of F. Since v_2 does not lie on E, the first inequality $u_E(v_2) > -h$ holds. In order to prove the second inequality, we must use the fact that P is symmetric. By Lemma 4.3.18, we have $u_E(v_2) \leq 2h$. Now, it remains to show that $2h \leq (r-1)h$, i.e. that $r \geq 3$.

We note that $r = \ell_F h_F$. Since P is symmetric and has non-empty empty basket, it follows from Lemma 4.3.7 and Lemma 4.3.14 that $h_F \geq 2$. If $h_F \geq 3$, then $r \geq 3$ and we are done. Otherwise, F has height $h_F = 2$. Since the vertices of P are primitive, the length ℓ_F of F must be even; hence, $\ell_F \geq 2$. So, $r \geq 4$, and we are done.

We may now prove the statement of the proposition. Label anticlockwise the edges of P and Q as $E_1, E_2, \ldots, E_m$ and $E'_1, E'_2, \ldots, E'_m$, respectively, so that E_i and E'_i have Hermite normal form H_i. So, there exists some $U \in \mathrm{SL}_2(\mathbb{Z})$ such that $UE'_1 = E_1$. The next edge of UQ is UE'_2. We may apply Lemma 4.3.17 to obtain $UE'_2 = E_2$. By

induction, we obtain that $UE_i' = E_i$ for all $i = 1, 2, \ldots, m$. Therefore, $Q = UP$, and we are done. □

We now move onto the final step in order to prove Theorem 4.3.1. Before we proceed with the final proposition of the section, we require the following small result.

Lemma 4.3.20. *Let $P \subset N_{\mathbb{Q}}$ be a polygon. Let $u \in M$ be primitive and let $n \geq 2$ be an integer. Suppose there are exactly n vertices $\boldsymbol{v}$ of P which satisfy $u(\boldsymbol{v}) \leq 0$. If P is centrally symmetric, then P has at most $2n$ vertices. If P is 3-symmetric, then P has at most $3n$ vertices.*

Proof. Without loss of generality, we may take $u = (0, 1)^t$. Let $\boldsymbol{v}_1, \boldsymbol{v}_2, \ldots, \boldsymbol{v}_n$ be the n vertices of P satisfying $u(\boldsymbol{v}_i) \leq 0$, i.e. they lie on or below the x-axis. We assume that the vertices are ordered anticlockwise.

First, suppose that P is centrally symmetric. Then P has either 0 or 2 vertices on the x-axis and either n or $n-2$ vertices strictly below it, respectively. By the central symmetry of P, it has either n or $n-2$ vertices strictly above it, respectively. So, P has either $2n$ or $2n-2$ vertices in total. In particular, P has at most $2n$ vertices.

Instead, suppose that P is 3-symmetric. Let $G \in \mathrm{Aut}(P)$ be an element of order 3. Let $\boldsymbol{v}_0$ be the vertex of P immediately before $\boldsymbol{v}_1$ and let $\boldsymbol{v}_{n+1}$ be the vertex of P immediately after $\boldsymbol{v}_n$. By assumption, these two vertices lie strictly above the x-axis. Consider the triangle $T = \mathrm{conv}\left\{\boldsymbol{v}_0, G\boldsymbol{v}_0, G^2\boldsymbol{v}_0\right\}$ and the line L passing through $\boldsymbol{v}_0$ and the origin $\mathbf{0}$. Without loss of generality, $G\boldsymbol{v}_0$ lies below L and $G^2\boldsymbol{v}_0$ lies above L. By convexity of P, $G\boldsymbol{v}_0$ in fact lies below the x-axis. Thus, $G\boldsymbol{v}_0 = \boldsymbol{v}_i$ for some $i = 1, 2, \ldots, n$. This means that the vertices of P are $\boldsymbol{v}_0, \boldsymbol{v}_1, \ldots, \boldsymbol{v}_{i-1}, G\boldsymbol{v}_0, G\boldsymbol{v}_1, \ldots, G\boldsymbol{v}_{i-1}, G^2\boldsymbol{v}_0, G^2\boldsymbol{v}_1, \ldots, G^2\boldsymbol{v}_{i-1}$. Therefore, P has $3i \leq 3n$ vertices.

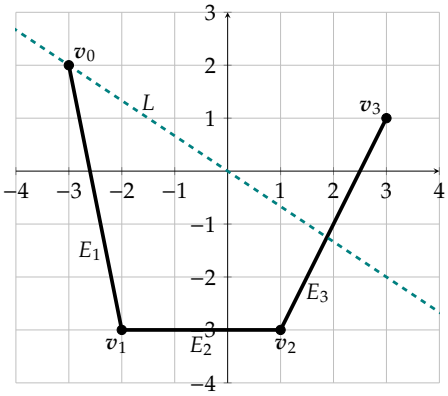

FIGURE 4.7: An example with $n = 2$ and P is assumed to be 3-symmetric. The points $\boldsymbol{v}_1$ and $\boldsymbol{v}_2$ are the only two vertices of P below the x-axis. One of these must also be a vertex of the triangle T.

□

We may now complete the final step, which was to prove the following statement.

Proposition 4.3.21. *Let P and Q be symmetric Fano polygons with non-empty baskets. If they are mutation-equivalent, then their edge data is equal.*

Proof. If P and Q are isomorphic, then their edge data is equal and we are done. So, let us assume that P is not isomorphic to Q. Thus, P must have at least one long edge; otherwise, P has no mutations and $P \cong Q$ – a contradiction. If P is centrally symmetric then, by Proposition 4.3.4, P is isomorphic to Q – a contradiction. Thus, either P is centrally symmetric with two pairs of long edges or P is 3-symmetric with one triple of long edges. The same holds for Q. Applying Proposition 4.3.8 and Proposition 4.3.12, we see that P and Q must either both be centrally symmetric or both be 3-symmetric; otherwise, the Ehrhart series $\mathrm{Ehr}_{P^*}(t)$ and $\mathrm{Ehr}_{Q^*}(t)$ would differ – this is a contradiction because the Ehrhart series of the dual polygon is a mutation-invariant, and P and Q are assumed to be mutation-equivalent. Moreover, by Corollary 4.3.10 and Corollary 4.3.13, we see that the number of edges is fixed, i.e. $|\mathcal{E}(P)| = |\mathcal{E}(Q)|$.

So, let's write $\mathcal{E}(P) = \{H_1, H_2, \ldots, H_m\} \times g$ and $\mathcal{E}(Q) = \{H'_1, H'_2, \ldots, H'_m\} \times g$, for some integer $m \geq 1$ and where $g = 2$ if P is centrally symmetric and $g = 3$ if P is 3-symmetric (see Remark 4.2.13 for notation). The (directed) basket of P and Q can be written $\mathcal{B} = \{S_1, S_2, \ldots, S_b\} \times g$. We may insist that $\mathcal{E}(P)$ is *aligned* with $\mathcal{B}$, i.e. that $\mathrm{res}(H_1) = S_1$ and $\mathrm{res}(H_{i_j}) = S_j$, for $1 = i_1 < i_2 < \cdots < i_b \leq m$. We may also insist that $\mathcal{E}(Q)$ is aligned with $\mathcal{B}$.

The strategy of the remainder of the proof is by induction on the elements of $\mathcal{E}(P)$. In particular, we want to show that $H_1 = H'_1$ and that if $H_n = H'_n$ for $1 \leq n \leq k$, where $1 \leq k < m$, then $H_{k+1} = H'_{k+1}$. Given these two statements, it immediately follows that $\mathcal{E}(P) = \mathcal{E}(Q)$.

Base case: We first prove that H_1 and H'_1 coincide. Suppose towards a contradiction that all the edges of P are long. If P is centrally symmetric, then P is isomorphic to the box with vertices $\pm(h_1, h_2)$ and $\pm(h_1, -h_2)$, for some integers $2 \leq h_1 \leq h_2$. By Corollary 4.3.10, Q is also a quadrilateral. By Lemma 4.3.5, Q is isomorphic to the box with vertices $\pm(h'_1, h'_2)$ and $\pm(h'_1, -h'_2)$, for some integers $2 \leq h'_1 \leq h'_2$. By Proposition 4.3.8, its edges have heights h_1 and h_2, i.e. $h_1 = h'_1$ and $h_2 = h'_2$. Thus, $P \cong Q$, a contradiction. Otherwise, P is 3-symmetric. So, since all its edges are long, it is isomorphic to the triangle with vertices $(-h, -h)$, $(2h, -h)$, and $(-h, 2h)$. Since P is Fano, its vertices must be primitive. Thus, $h = 1$, which implies that $\mathcal{B} = \varnothing$, another contradiction.

So, we may conclude that there is an edge of P which is short. Since the edge data $\mathcal{E}(P)$ is cyclically ordered, we may relabel its elements so that H_1 represents a short edge; thus, $H_1 = \mathrm{res}(H_1) = S_1$. Now, this implies that S_1 has height strictly greater than the heights of the long edges of P and Q. Since $\mathrm{res}(H'_1) = S_1$, it follows that H'_1 is also short. Thus, $H_1 = H'_1 = S_1$.

Inductive step: Let $1 \leq k < m$ and suppose that $H_n = H'_n$ for all $1 \leq n \leq k$. Let $1 \leq j \leq b$ be the index of the previous R-singularity S_j in $\{\mathrm{res}(H_1), \ldots, \mathrm{res}(H_k)\}$, i.e. $i_j \leq k$ and either $j = b$ or $k < i_{j+1}$. Consider H_{k+1} and H'_{k+1}. We split into three cases: (i) both are short; (ii) both are long; and (iii) one is short and one is long.

Case (i). If both forms represent short edges, then $H_{k+1} = S_{j+1}$ and $H'_{k+1} = S_{j+1}$, i.e. they coincide.

Case (ii). Now suppose that H_{k+1} and H'_{k+1} both represent long edges. Fix the edge of P and Q represented by H_k so that its second vertex is $(1,0)$. Now, the primitive inner normal vectors of the next edges of P and Q, which are represented by H_{k+1} and H'_{k+1}, respectively, are forced to be the same; otherwise, we would violate Proposition 4.3.8 or Proposition 4.3.12. In order to show that H_{k+1} and H'_{k+1} coincide, we show that the next edges have the same length.

Since the edges represented by H_{k+1} and H'_{k+1} share a vertex and have the same primitive inner normal, they must have the same height. Hence, they have the same number of primitive T-singularities. If they have the same residue, then we are done. Otherwise, due to the directed basket being a mutation invariant, we must have that, without loss of generality, H_{k+1} has a residue while H'_{k+1} has no residue. Now, consider the Hermite normal form H'_{k+2} in $\mathcal{E}(Q)$. H'_{k+2} must represent a long edge with the same residue as H_{k+1}. The long edges represented by H'_{k+1} and H'_{k+2} have the same height h. By Lemma 4.3.5 and Lemma 4.3.11, we can transform Q so that the common vertex of these long edges is (h,h). Since Q is Fano, its vertices must be primitive. Thus, $h = 1$. But this is a contradiction; for example, the residue of H_{k+1} is now empty. So, $H_{k+1} = H'_{k+1}$.

Case (iii). Finally, we suppose that one of H_{k+1} and H'_{k+1} is short and the other is long. Without loss of generality, we may assume that the former is long and the latter is short. So, $H_{k+1} = T$ represents a *pure* long edge, i.e. $\mathrm{res}(H_{k+1}) = \varnothing$, and $H'_{k+1} = S_{j+1}$ is short. Now, consider the next edge represented in $\mathcal{E}(P)$. There are two subcases: either (a) $H_{k+2} = S_{j+1}$ represents a short edge or (b) $H_{k+2} = T'$ represents a pure long edge. We aim to show that both subcases are impossible to achieve.

Subcase (a): As in Figure 4.8, transform P so that the edge E represented by T has inner normal $(0,1)^t$. Denote by F_1 and F_2 the edges adjacent to E which are represented by H_k and S_{j+1}, respectively. Let $v_0, v_1, v_2, v_3 \in N$ be the vertices which form the edges F_1, E, and F_2, ordered anticlockwise. Consider the shear A which maps v_1 to v_2. The edge AF_1 is now adjacent to F_2. We may also transform Q so that its edge represented by S_{j+1} is also F_2. The aim is to show that AF_1 must be the edge of Q represented by H_k. If that is the case then, by convexity, Q is contained in the half-space $\{y \geq -h\}$, i.e. $(0,1)^t \in hQ^*$, where h is the height of E. But now, this contradicts Proposition 4.3.8 and Proposition 4.3.12, since $(0,1)^t$ is not an inner normal vector to an edge of Q. So, we can conclude that subcase (a) is impossible to achieve. It remains to show that AF_1 and F_2 are indeed edges of Q. To do this, we want to apply Lemma 4.3.17. In order to apply it, we must show its condition (iii) is satisfied, i.e. we want to show that Av_0 satisfies the chain of inequalities: $-h_{F_2} < u_{F_2}(Av_0) \leq 2h_{F_2}$.

By the assumption of subcase (a), if P is centrally symmetric, it has at least 6 edges and if P is 3-symmetric, it has at least 9 edges. So, in order to not contradict Lemma 4.3.20, it follows that at least one of v_0 and v_3 lies on or below the x-axis. Without loss of generality, v_0 lies on or below the x-axis.

We may now write $v_0 = \lambda v_1 - (\mu, 0)$, for some $0 \leq \lambda < 1$ and $\mu > 0$. Thus, $Av_0 = \lambda v_2 - (\mu, 0)$. So, $u_{F_2}(Av_0) = -\lambda h_{F_2} - \mu u_{F_2}(1,0)$. Since $u_{F_2}(1,0) < 0$, the first inequality holds. On the other hand, $Av_0 = v_0 + (x,0)$ for some $x \in \mathbb{Z}$. Since v_0 lies on or below the x-axis, it follows that $x \geq 0$. Furthermore, by Lemma 4.3.18, we

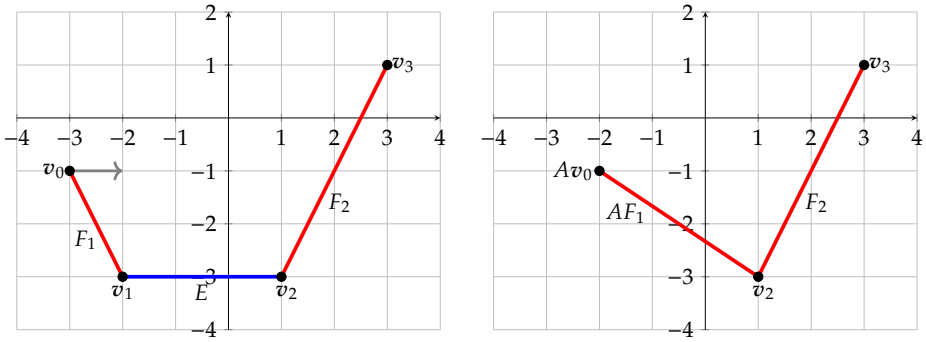

FIGURE 4.8: The situation of subcase (a) in the proof of Proposition 4.3.21. In this example, E has length equal to its height; thus, A is the shear $\left(\begin{smallmatrix} 1 & -1 \\ 0 & 1 \end{smallmatrix}\right)$.

have $u_{F_2}(v_0) \leq 2h_{F_2}$. Thus, the second inequality follows. As set out above, this is now enough to conclude that subcase (a) cannot occur.

Subcase (b): We first note that P (and Q) must be centrally symmetric, since there are two long edges between H_1 and H_m. Thus, it follows that H_{k+3} must be short, i.e. $H_{k+3} = S_{j+1}$. As in Figure 4.9, transform P so that the edge E represented by T has inner normal $(0,1)^t$ and the edge E' represented by T' has inner normal $(-1,0)^t$. Denote by F_1 and F_2 the edges adjacent to E which are represented by H_k and S_{j+1}, respectively. Let $v_0, v_1, \ldots, v_4 \in N$ be the vertices which form the edges F_1, E, E', and F_2, ordered anticlockwise.

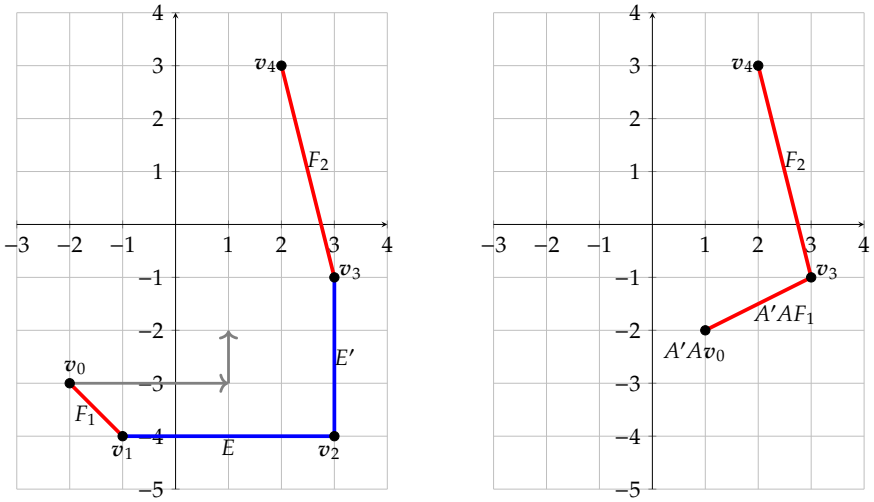

FIGURE 4.9: The situation of subcase (b) in the proof of Proposition 4.3.21. In this example, E and E' both have lengths equal to their heights; thus, $A = \left(\begin{smallmatrix} 1 & -1 \\ 0 & 1 \end{smallmatrix}\right)$ and $A' = \left(\begin{smallmatrix} 1 & 0 \\ 1 & 1 \end{smallmatrix}\right)$.

Consider the half space $\mathcal{H} = \{(x,y) \in N_{\mathbb{Q}} : x \geq y\}$. It is clear that $v_2 \in \mathcal{H}$. By assumption of subcase (b), note that P has at least 8 vertices. So, in order to not contradict Lemma 4.3.20, it follows that at least one of v_0 and v_4 lies in $\mathcal{H}$. Without loss of generality, we may assume that $v_0, v_1, v_2, v_3 \in \mathcal{H}$.

Let A and A' be the shears which map v_1 to v_2 and v_2 to v_3, respectively. We want to show that $A'Av_0$ satisfies the inequalities $-h_{F_2} < u_{F_2}(A'Av_0) \leq h_{F_2}$. Note that $v_0 = \lambda v_1 - (\mu, 0)$, for some $0 \leq \lambda < 1$ and $\mu > 0$. Thus, $A'Av_0 = \lambda v_3 - (\mu, n'\mu)$, where n' is the number of primitive singularities of E'. Since both $u_{F_2}(1,0)$ and $u_{F_2}(0,1)$ are strictly negative, the first inequality holds. On the other hand, $A'Av_0 = v_0 + (x, y)$, for some $x, y \in \mathbb{Z}$. Since v_0 lies in $\mathcal{H}$, it follows that $x, y \geq 0$. Furthermore, by the central symmetry of P, we have $u_{F_2}(v_0) \leq h_{F_2}$; thus, the second inequality holds.

Thus, we may apply Lemma 4.3.17 and transform Q so that its edges represented by H_k and S_{j+1} are $A'AF_1$ and F_2. But now, we still have $(-1,0)^t \in h'Q^*$, where h' is the height of the long edge E'. But by Proposition 4.3.8, the non-origin lattice points in $h'Q^*$ must be primitive inner normals to long edges; thus, we reach a contradiction. □

We are now ready to prove the main theorem of this section.

Proof of Theorem 4.3.1. Let P and Q be two symmetric Fano polygons which are mutation-equivalent. By Proposition 4.3.16, we may assume that P and Q have non-empty basket $\mathcal{B}$. By Proposition 4.3.21, we know that their edge data is equal. Finally, we apply Proposition 4.3.19 and we may conclude that P and Q are isomorphic. □

4.4 The behaviour of other Kähler–Einstein polygons under mutation

In this section, we aim to complete the proof of Theorem 4.1.3. Previously, in §4.3, we proved that there is at most one symmetric Fano polygon in each mutation-equivalence class. Equivalently, we proved that if two symmetric Fano polygons are mutation-equivalent, then they are isomorphic. So, in order to complete the proof of Theorem 4.1.3, we need to prove that (a) if two Kähler–Einstein Fano triangles are mutation-equivalent, then they are isomorphic and (b) if a symmetric Fano polygon is mutation-equivalent to a Kähler–Einstein triangle, then they are isomorphic. We prove (a) in Proposition 4.4.1. Since the arguments for centrally symmetric and 3-symmetric polygons will be different, we further split the proof of (b) into Proposition 4.4.4 and Proposition 4.4.5.

Proposition 4.4.1. *Let $P, Q \subset N_{\mathbb{Q}}$ be Kähler–Einstein Fano triangles. Suppose that P and Q are mutation-equivalent. Then P is isomorphic to Q.*

Before we do the proof of Proposition 4.4.1, we require the following lemma.

Lemma 4.4.2. *Let $P \subset N_{\mathbb{Q}}$ be a Kähler–Einstein Fano triangle of index k. Then k is odd.*

Proof. By Lemma 4.2.16, we may apply an appropriate transformation so that P has vertices $(-k, a-1)$, $(k, -a)$, and $(0,1)$, for some integers a and k. Suppose towards a contradiction that k is even. Now, since 2 divides either $a-1$ or a, it follows that either $(-k, a-1)$ or $(k, -a)$ is not primitive. So, P has a non-primitive vertex, which contradicts that P is Fano. □

We may now proceed with the proof.

Proof of Proposition 4.4.1. By Lemma 4.2.16, P is isomorphic to a triangle with primitive vertices $(-k, a-1)$, $(k, -a)$, and $(0,1)$, for some integers $a, k \geq 1$. Similarly, Q is isomorphic to a triangle with primitive vertices $(-k', a'-1)$, $(k', -a')$, and $(0,1)$, for some integers $a', k' \geq 1$. The dual polygons P^* and Q^* have normalised volumes $9/k$ and $9/k'$, respectively. Since P and Q are mutation-equivalent, these volumes coincide; thus, $k = k'$. It now remains to show that $a \equiv a' \mod k$.

Label the edges of P as E_0, E_1, E_2. We can write $k = \ell_i h_i$, where ℓ_i is the length of E_i and h_i is its height. We obtain the following system of linear congruences:

$$a \equiv -1 \mod \ell_0, \qquad a \equiv 2 \mod \ell_1, \qquad 2a \equiv 1 \mod \ell_2. \tag{4.3}$$

Thus, if m divides two of the lengths ℓ_i and ℓ_j for $i \neq j$, then m must divide 3.

If P does not have at least two long edges, then Q must be isomorphic to P. So, we assume otherwise. Thus, without loss of generality, E_0 and E_1 are long. This implies that $\ell_0, \ell_1 \geq \sqrt{k}$.

If $\gcd(\ell_0, \ell_1) = 1$, then $\ell_0\ell_1$ divides k. Since $\ell_0\ell_1 \geq k$, we obtain $\ell_0 = \sqrt{k} = \ell_1$. Thus, $k = 1$. But now, there is only one such triangle with index $k = 1$, so P and Q are isomorphic; in particular, $X_P = X_Q = \mathbb{P}^2$.

Now consider the case $\gcd(\ell_0, \ell_1) = 3$. Here, we have $\ell_0 = 3\widehat{\ell_0}$ and $\ell_1 = 3\widehat{\ell_1}$, where $\widehat{\ell_0}$ and $\widehat{\ell_1}$ are coprime. So, $k = 3\widehat{\ell_0}\widehat{\ell_1}\widehat{k} \leq 9\widehat{\ell_0}\widehat{\ell_1}$. So, $\widehat{k} \leq 3$. By Lemma 4.4.2, we have that $\widehat{k} \neq 2$. This leaves two possibilities for $\widehat{k}$.

If $\widehat{k} = 3$, then $\ell_0 = \ell_1 = \sqrt{k}$. Thus, $\widehat{\ell_0} = \widehat{\ell_1} = 1$, $\ell_0 = \ell_1 = 3$, and $k = 9$. Up to isomorphism, there is only one Fano triangle with weights $(1,1,1)$ and index $k = 9$. In fact, this is the triangle P' appearing in Example 4.5.9. Therefore, P and Q must be isomorphic.

If $\widehat{k} = 1$, then $k = 3\widehat{\ell_0}\widehat{\ell_1}$. Since $\widehat{\ell_0}$ and $\widehat{\ell_1}$ are coprime, we may assume without loss of generality that $\widehat{\ell_1}$ is not divisible by 3. Now, consider the system (4.3). We obtain $a \equiv -1 \mod 3\widehat{\ell_0}$ and $a \equiv 2 \mod \widehat{\ell_1}$. Since $3\widehat{\ell_0}$ and $\widehat{\ell_1}$ are coprime, we may apply the Chinese Remainder theorem. We obtain a unique solution for a modulo k, which determines P and Q up to isomorphism. Thus, P and Q are isomorphic. □

Now that we have shown the triangle/triangle case, it remains to show the triangle/symmetric case. It will be useful to have the following lemma as it allows us to verify the case when the basket of R-singularities is empty.

Lemma 4.4.3. *Let $P \subset N_{\mathbb{Q}}$ be a Kähler–Einstein Fano triangle. Then P is minimal.*

Proof. By Lemma 4.2.15, P has weights $(1,1,1)$. Let v_0, v_1, v_2 be the vertices of P and u_0, u_1, u_2 be the vertices of P^*, ordered so that $u_i(v_j) = -1$ if and only if $i \neq j$. In order to show minimality of P, it's enough to show that $u_i(v_i) \geq 1$, for all $i = 0, 1, 2$. To do this, we simply rearrange the identity $u_i(v_0 + v_1 + v_2) = 0$. We obtain $u_i(v_i) = 2 \geq 1$, and so we are done. □

We can now prove the remaining two propositions.

Proposition 4.4.4. *No Kähler–Einstein Fano triangle is mutation-equivalent to a centrally symmetric Fano polygon.*

Proof. Let P be a centrally symmetric Fano polygon and Q be a Kähler–Einstein triangle. Suppose towards a contradiction that P and Q are mutation-equivalent. Due to the central symmetry of P, the number of R-singularities in the basket must be even. Since Q has three edges, there are at most three R-singularities. Thus, there are either zero or two R-singularities in the basket.

First suppose that there are no R-singularities in the basket. By Lemma 4.4.3, the triangle Q will be minimal. Thus, the triangle Q appears in the list of [66]. The centrally symmetric P is also minimal and appears in that list. We see that there are no examples in the same mutation-equivalence class.

Otherwise, there are two copies of the same R-singularity in $\mathcal{B}$. Consider the edges of the triangle Q. Two of the edges F_1, F_2 host R-singularities and one edge F_0 is a pure T-singularity. It follows from Lemma 4.2.15 that the determinant of each edge is k, for some positive integer k. So, the edges F_1 and F_2 have the same number $m \geq 0$ of primitive T-singularities. Now, since P is centrally symmetric, it has an even number $2n$ of primitive T-singularities. Thus, the pure edge F_0 of Q has $2n-2m$ primitive T-singularities. Further, its determinant k must now be divisible by 2. But this contradicts Lemma 4.4.2. □

Proposition 4.4.5. *Let $P \subset N_{\mathbb{Q}}$ be a 3-symmetric Fano polygon and $Q \subset N_{\mathbb{Q}}$ be a Kähler–Einstein Fano triangle. Suppose that P is mutation-equivalent to Q. Then $P \cong Q$.*

Proof. First, we know that P and Q are minimal. So, if $\mathcal{B} = \varnothing$, then P and Q must appear in the list of minimal polygons in Theorem 5.4 of [66]. We see that there is at most one Kähler–Einstein triangle or 3-symmetric polygon for each number n of primitive T-singularities, which is a mutation-invariant. Therefore, $P \cong Q$.

Now, we have $\mathcal{B} \neq \varnothing$. Due to the symmetry of order 3 of P, the number of R-singularities of P is a multiple of 3. Further, since Q is a triangle and each edge has at most one R-singularity, the number of R-singularities of Q is at most 3. Since P and Q are mutation-equivalent, they have the same number of R-singularities, which must be 3. So, each edge of Q has an R-singularity. Further, these three R-singularities must be the same; in particular, they have the same height h. Therefore, each edge of Q has the same height h. Since each edge of Q must also be long, we may apply Lemma 4.2.17. So, we must have $X_Q = \mathbb{P}^2$ or $X_Q = \mathbb{P}^2/\mathbb{Z}_3$. In either case, Q now has no R-singularities, which is a contradiction. □

Now we simply put all these results together to derive the main theorem.

Proof of Theorem 4.1.3. The result straightforwardly follows from Theorem 4.3.1, Proposition 4.4.1, Proposition 4.4.4, and Proposition 4.4.5. □

4.5 Discussion of Kähler–Einstein polygons

Given Conjecture 4.1.2, it would follow that there is at most one Kähler–Einstein Fano polygon in each mutation-equivalence class. However, in the first part of this section,

we provide a counterexample to the conjecture. In particular, we show the existence of a Kähler–Einstein Fano polygon which is neither symmetric nor a triangle. This is enough to disprove the conjecture.

The second part of this section is dedicated to describing all Kähler–Einstein Fano quadrilaterals. In particular, we describe how quadrilaterals with barycentre as the origin must be constrained.

In the final part of this section, we construct a family of Kähler–Einstein Fano hexagons which are not minimal.

4.5.1 A Kähler–Einstein Fano quadrilateral

So, as stated above, we will prove that the quadrilateral in Proposition 4.1.4 is indeed Kähler–Einstein and non-symmetric.

Proof of Proposition 4.1.4. Since all of the vertices of P are primitive lattice points and the origin is contained in its strict interior, P is Fano. Using Magma [16], we find that P has a trivial automorphism group; thus, P is not symmetric. As P is clearly not a triangle, it only remains to show that the barycentre of P^* is the origin.

Again using Magma, we compute the dual P^* of P.

$$P^* = \operatorname{conv}\left\{\frac{1}{3149}(1,-28)^t, \frac{1}{1739}(151,2)^t, \frac{1}{481}(-31,4)^t, \frac{1}{871}(-43,-2)^t\right\} \subset M_{\mathbb{Q}}.$$

Label its vertices as u_1, u_2, u_3, u_4, respectively. Note that these are adjacent and given in anticlockwise order. To compute the barycentre, we subdivide P^* into two triangles $T_1 = \operatorname{conv}\{u_1, u_2, u_3\}$ and $T_2 = \operatorname{conv}\{u_3, u_4, u_1\}$. Let b_1 and b_2 be the barycentres of T_1 and T_2, respectively. Then, $b_1 = \frac{1}{1514669}(11461, 290)^t$ and $b_2 = \frac{1}{1514669}(-57305, -1450)^t$. The volumes of T_1 and T_2 are $\frac{3240}{1514669}$ and $\frac{648}{1514669}$, respectively. Thus, the barycentre of P^* is $\frac{1}{\operatorname{Vol}(P^*)}(\operatorname{Vol}(T_1)b_1 + \operatorname{Vol}(T_2)b_2) = (0,0)^t$.

So, P is a Kähler–Einstein Fano polygon which is not symmetric and not a triangle. Its existence thus disproves Conjecture 4.1.2. □

This means that it is still a wide-open question whether there is at most one Kähler–Einstein polygon per mutation-equivalence class.

Remark 4.5.1. We can ask whether the polygon P in the proof of Proposition 4.1.4 is mutation-equivalent to any other Kähler–Einstein polygon. Since the edges of P have lengths 1, 2, 7, 2 and heights 3149, 871, 481, 1739, respectively, it follows that none of its edges are long. Thus, the mutation-equivalence class consists only of P. So, in this case, P is not mutation-equivalent to any other other Kähler–Einstein polygon.

Having this example of a non-symmetric Kähler–Einstein quadrilateral allows us to test questions regarding barycentric transformations. These transformations were introduced in [53] as a way to measure how close a polytope is to being Kähler–Einstein. We recall the definition, specialised to dimension two.

Definition 4.5.2 ([53, Lemma 2.2])**.** Let P be a Fano polygon with vertices $v_1, v_2, \ldots, v_m$ written in anticlockwise order. Then the *barycentric transformation* $B(P)$ of P is defined as

$$B(P) := \operatorname{conv}\left\{\frac{v_{12}}{\gcd(v_{12})}, \frac{v_{23}}{\gcd(v_{23})}, \ldots, \frac{v_{m1}}{\gcd(v_{m1})}\right\},$$

where $v_{ij} = v_i + v_j$. We also write $B^1(P) := B(P)$ and $B^{k+1}(P) := B^k(B(P))$, for integer $k \geq 1$.

Note that the vertices of $B(P)$ are guaranteed to be primitive. However, it isn't certain that the origin is contained in the strict interior of $B(P)$. So, the barycentric transformation of a Fano polygon might not be Fano itself.

Definition 4.5.3 ([53, Definition 2.4])**.** A Fano polygon P is said to be of *type* B_k if $B^k(P)$ is also Fano. P is of *strict* type B_k if P is of type B_k but not of type B_{k+1}. P is of *type* B_∞ if $B^k(P)$ is Fano for all integer $k \geq 1$.

In [53], they expect that all smooth Kähler–Einstein (Fano) polytopes are of type B_∞. They show that this expectation holds in all dimensions less than 9, except for possibly one four-dimensional polytope [53, Theorem 1.3]. In two dimensions, they drop the smooth condition and prove that all Kähler–Einstein polygons are of type B_1 [53, Theorem 1.6]. They question whether Kähler–Einstein Fano polygons are all of type B_∞. If so, they also question whether the Kähler–Einstein property is preserved under barycentric transformation. We answer both questions in the negative.

Example 4.5.4. We compute iterated barycentric transformations of the polygon P from Proposition 4.1.4 to determine its strict type. Consider

$$B(P) = \operatorname{conv}\{(10, -163), (17, 70), (2, 225), (-11, -39)\}.$$

It contains the origin in its strict interior, so it is Fano. However, the barycentre of its dual is not the origin; thus, $B(P)$ is not Kähler–Einstein. Next, $B^2(P) = \operatorname{conv}\{(9, -31), (19, 295), (-3, 62), (-1, -202)\}$. Since it still contains the origin in its strict interior, it is Fano. But now, $B^3(P) = \operatorname{conv}\{(7, 66), (16, 357), (-1, -35), (8, -233)\}$. This polygon does not contain the origin in its strict interior; thus, $B^3(P)$ is not Fano. We can conclude that P is of strict type B_2.

4.5.2 The weight systems of quadrilaterals with barycentre as the origin

Proposition 4.5.5. *Let $P \subset N_{\mathbb{Q}}$ be a Kähler–Einstein quadrilateral. Then its dual polygon P^* is a quadrilateral with weight system*

$$W^* = \begin{pmatrix} \lambda_1 & \lambda_2 & 0 & \lambda_4 \\ 0 & \mu_2 & \mu_3 & \mu_4 \end{pmatrix},$$

for some positive integers $\lambda_1, \lambda_2, \lambda_4, \mu_2, \mu_4$ *and negative integer* μ_3 *which satisfy*

$$(\lambda_1 - \lambda_2) f \cdot \mu_3^2 = (\mu_3 - \mu_2) g \cdot \lambda_1^2 \tag{4.4}$$
$$(\lambda_1 - \lambda_4) f \cdot \mu_3^2 = (\mu_3 - \mu_4) g \cdot \lambda_1^2, \tag{4.5}$$

where $f = \lambda_1 + \lambda_2 + \lambda_4$ *and* $g = \mu_2 + \mu_3 + \mu_4$.

Before we prove Proposition 4.5.5, we must first prove the following lemma about triangles.

Lemma 4.5.6. *Let* $T \subset N_{\mathbb{Q}}$ *be a triangle with vertices* $\boldsymbol{v}_0, \boldsymbol{v}_1, \boldsymbol{v}_2$ *and weights* $(\lambda_0, \lambda_1, \lambda_2)$*, so that* $\sum_{i=0}^{2} \lambda_i \boldsymbol{v}_i = \boldsymbol{0}$*. Label the edges of* T *as* E_0, E_1, E_2 *so that* $\boldsymbol{v}_i \notin E_i$ *for* $i = 0, 1, 2$*. Suppose that the weights are* reduced*, i.e.* $\gcd(\lambda_0, \lambda_1, \lambda_2) = 1$*. Then, for all* $i = 0, 1, 2$*, the volume of* Δ_{E_i} *is* $k|\lambda_i|$*, for some positive* $k \in \mathbb{Q}$ *not depending on* i*.*

Proof. As in the remark under Definition 2.3 in [27], this result also follows in the non-integral case using Cramer's rule. □

We are now ready to prove the main result of this subsection.

Proof of Proposition 4.5.5. Let $\ell = \gcd(\lambda_1, \lambda_2, \lambda_4)$ and $m = \gcd(\mu_2, \mu_3, \mu_4)$. Consider (4.4). Since ℓ divides f, we see that ℓ^2 divides the left-hand side and the right-hand side. Further, since m divides g, we see that m^2 also divides both the left-hand and right-hand sides. The analogous statement holds for (4.5). Thus, we may divide the λ_i by ℓ and the μ_j by m. Hence, we may assume without loss of generality that $\ell = m = 1$.

Let $u_1, u_2, u_3, u_4 \in M_{\mathbb{Q}}$ be the vertices of P^*, given in anticlockwise order and aligned so that $W^*(u_1, u_2, u_3, u_4) = (0, 0)$. Then we obtain two triangles $T = \operatorname{conv}\{u_1, u_2, u_4\}$ and $T' = \operatorname{conv}\{u_2, u_3, u_4\}$ which partition P^*. The barycentres of T and T' are $b = \frac{1}{3}(u_1 + u_2 + u_4)$ and $b' = \frac{1}{3}(u_2 + u_3 + u_4)$, respectively.

Now, T has weights $(\lambda_1, \lambda_2, \lambda_4)$ and T' has weights (μ_2, μ_3, μ_4). Let the edges of T and T' be labelled as follows.

$$E_i = \operatorname{conv}\{u_n : n = 1, 2, 4 \text{ and } n \neq i\} \qquad E'_j = \operatorname{conv}\{u_n : n = 2, 3, 4 \text{ and } n \neq j\},$$

for $i = 1, 2, 4$ and $j = 2, 3, 4$. By Lemma 4.5.6, the triangles Δ_{E_i} have volumes $k_T \lambda_i$, for $i = 1, 2, 4$, and the triangles $\Delta_{E'_i}$ have volumes $k_{T'}|\mu_j|$, for $j = 2, 3, 4$, where $k_T, k_{T'} \in \mathbb{Q}$ are positive. But now, $\Delta_{E_1} = \Delta_{E'_3}$. In particular, $\operatorname{Vol}(\Delta_{E_1}) = \operatorname{Vol}(\Delta_{E'_3})$. It follows that the ratio between k_T and $k_{T'}$ is $(-\mu_3 : \lambda_1)$. Therefore, the ratio between the volumes of T and T' is $(-f\mu_3 : \lambda_1 g)$.

Since the barycentre of P^* is 0, it follows that $\operatorname{Vol}(T)b + \operatorname{Vol}(T')b' = 0$. Plugging in our expressions for the volumes and barycentres of T and T', we obtain that $-f\mu_3 \cdot u_1 + (\lambda_1 g - f\mu_3) \cdot u_2 + \lambda_1 g \cdot u_3 + (\lambda_1 g - f\mu_3) \cdot u_4 = 0$. Equivalently, $(-f\mu_3, \lambda_1 g - f\mu_3, \lambda_1 g, \lambda_1 g - f\mu_3)$ is a weight for P^*. So, it must be expressable as a $\mathbb{Q}$-linear combination of the rows of W^*:

$$(-f\mu_3, \lambda_1 g - f\mu_3, \lambda_1 g, \lambda_1 g - f\mu_3) = a \cdot (\lambda_1, \lambda_2, 0, \lambda_4) + b \cdot (0, \mu_2, \mu_3, \mu_4), \tag{4.6}$$

for some $a, b \in \mathbb{Q}$. Comparing the first coordinates in (4.6) gives $a = -f\mu_3/\lambda_1$ and comparing the third coordinates in (4.6) gives $b = \lambda_1 g/\mu_3$. Then, obtaining (4.4) is simply a matter of comparing the second coordinates in (4.6), substituting in the expressions of a and b, and rearranging. Equation (4.5) is obtained similarly from comparing the fourth coordinates in (4.6). □

Remark 4.5.7. We can create a nice parameterisation of the weight matrix in Proposition 4.5.5. First, we may assume that each row of the weight matrix is reduced, i.e. $\gcd(\lambda_1, \lambda_2, \lambda_4) = 1$ and $\gcd(\mu_2, \mu_3, \mu_4) = 1$. It follows from Equations (4.4) and (4.5) that λ_1^2 divides $f \cdot \mu_3^2$ and μ_3^2 divides $g \cdot \lambda_1^2$. So, let $a = \gcd(\lambda_1, \mu_3)$ and let ℓ and m be coprime integers such that $\lambda_1 = a\ell$ and $\mu_3 = am$. Now, let $d = \gcd(f, g)$ and let r and s be coprime integers such that $f = d\ell^2 s$ and $g = dm^2 r$. Finally, let $b = \gcd(\lambda_1 - \lambda_2, \mu_3 - \mu_2)$ and $c = \gcd(\lambda_1 - \lambda_4, \mu_3 - \mu_4)$. We can now express all λ_i and μ_j in terms of the parameters $a, b, c, d, \ell, m, r, s$. The weight matrix looks like the following.

$$W^* = \begin{pmatrix} a\ell & a\ell + br & 0 & a\ell + cr \\ 0 & am + bs & am & am + cs \end{pmatrix}.$$

Using the identities $f = \lambda_1 + \lambda_2 + \lambda_4$ and $g = \mu_2 + \mu_3 + \mu_4$, we eventually obtain the equations

$$b + c = -d\ell m \tag{4.7}$$
$$3a = d(mr + \ell s). \tag{4.8}$$

We can use this parameterisation to search for further examples of non-symmetric Kähler–Einstein Fano polygons.

Example 4.5.8. Let us fix $a = 48$. By (4.8), d divides 144. We choose $d = 36$. By (4.7), $b + c$ must be divisible by 36. Choose $b = 19$ and $c = 17$. Referring back to (4.7), we see that $36 = -36\ell m$. Thus, $\ell = 1$ and $m = -1$. Finally, (4.8) gives $4 = -r + s$. We may let $r = 1$ and $s = 5$.

This gives the following weight matrix

$$W^* = \begin{pmatrix} 48 & 67 & 0 & 65 \\ 0 & 47 & -48 & 37 \end{pmatrix},$$

which corresponds to a quadrilateral with barycentre zero. Taking the dual polygon and restricting to the lattice spanned by its vertices, we obtain the Kähler–Einstein Fano quadrilateral from Proposition 4.1.4.

4.5.3 Non-symmetric Kähler–Einstein polygons coming from symmetric polygons

In the previous subsection, we showed one way to construct non-symmetric Kähler–Einstein polygons which are not triangles. By construction, all previous examples were quadrilaterals. In this subsection, we will construct a different type of

non-symmetric Kähler–Einstein polygon. We first illustrate the main idea of the construction with the following example.

Example 4.5.9. Take the triangle P with vertices $(-1,-1)$, $(1,0)$, and $(0,1)$. This is Kähler–Einstein and symmetric, and has corresponding toric variety $X_P = \mathbb{P}^2$. Consider P with respect to the lattice $N+\frac{1}{9}(1,2)\mathbb{Z}$. This is isomorphic to the triangle P' with vertices $(-5,1)$, $(1,-2)$, and $(4,1)$, with respect to N, and whose corresponding toric variety is $X_{P'} = \mathbb{P}^2/\mathbb{Z}_9$. The weights of P' are the same as those of P, so P' is still Kähler–Einstein. However, the automorphism group of P' is now only generated by a reflection. Thus, P' is a Kähler–Einstein triangle which is not symmetric.

Remark 4.5.10. Note that a similar phenomenon was discussed in [54, Example 1.7]. They looked at a triangle P with $X_P = \mathbb{P}^2/\mathbb{Z}_{11}$. In this case, P had a trivial automorphism group.

We want to find more examples of non-symmetric Kähler–Einstein Fano polygons. To do this, we try to extend what we did in Example 4.5.9 to other symmetric polygons. In particular, we consider other symmetric polygons with respect to finer lattices in an attempt to destroy the symmetry but keep the Kähler–Einstein property. Of course, if a polygon is centrally symmetric with respect to one lattice, it will be centrally symmetric with respect to any other lattice. Thus, we restrict our attention to 3-symmetric polygons.

Proposition 4.5.11. *Let h,k be integers such that $h,k \geq 2$ and k is coprime to h, $h-1$, and $2h-1$. Then the polygon*

$$P_{h,k} := \operatorname{conv}\begin{pmatrix} -hk & (1-h)k & (2h-1)k & (2h-1)k & (1-h)k & -hk \\ 1-h & -h & -h & 1-h & 2h-1 & 2h-1 \end{pmatrix}$$

is a Kähler–Einstein Fano polygon which is not symmetric. Moreover, $P_{h,k}$ is of type B_∞. If we further suppose that $k \geq 2h-1$, then $P_{h,k}$ is not minimal.

Proof. We first show that the polygon is Kähler–Einstein. The polygon $P_{h,1}$ is 3-symmetric, and thus Kähler–Einstein. The polygon $P_{h,k}$ is isomorphic to $P_{h,1}$ with respect to the lattice $N+(1/k,0)\mathbb{Z}$. The weights of a polygon are the same, regardless of which lattice it is considered on. In particular, $P_{h,k}$ has the same weights are $P_{h,1}$. Thus, $P_{h,k}$ is also Kähler–Einstein.

Next, given the assumption that k is coprime to h, $h-1$, and $2h-1$, it easily follows that the vertices of $P_{h,k}$ are primitive. Thus, since the origin is still contained in the strict interior, the polygon is Fano. It remains to show that $P_{h,k}$ is not symmetric. To do this, we compare the lengths of its edges. Starting from the bottom-left edge of $P_{h,k}$ and going anticlockwise, the lengths are 1, $(3h-2)k$, 1, $3h-2$, k, and $3h-2$. Since $k \geq 2$, the lengths don't repeat three times. Thus, $P_{h,k}$ is not 3-symmetric. Since it's clearly not centrally symmetric, we may conclude that the polygon isn't symmetric.

Now, we determine the type of $P_{h,k}$. We compute its barycentric transformation and obtain that $B(P_{h,k})$ has vertices $\pm(k,-2)$, $\pm(2k,-1)$, and $\pm(k,1)$. In particular, $B(P_{h,k})$ is centrally symmetric. Thus, by [53, Theorem 1.6], $P_{h,k}$ is of type B_∞.

Finally, we show that if $k \geq 2h - 1$, then the polygon is not minimal. The bottom edge of $P_{h,k}$ has length $(3h - 2)k$ and height h, so it is a long edge. The top edge has length k and height $2h - 1$. Since $k \geq 2h - 1$, by assumption, it follows that it is also a long edge. Thus, $P_{h,k}$ is not minimal. □

So, we have found an infinite number of non-symmetric, non-triangle Kähler–Einstein Fano polygons.

Chapter 5

Generalised Flatness Constants

This chapter is based on joint work with Giulia Codenotti and Johannes Hofscheier, which appears in [26].

5.1 Introduction

Let $\mathbb{R}^d$ be the Euclidean space equipped with the Euclidean norm $|\cdot|$. The space of convex bodies, i.e., non-empty compact convex sets in $\mathbb{R}^d$ (note that some authors define convex bodies to be open, see, for instance, [93, Section 2]), is denoted by $\mathcal{K}^d$. Examples of convex bodies are polytopes, convex hulls of finitely many points in $\mathbb{R}^d$. (Lattice) polytopes are studied in a variety of mathematical areas such as algebraic geometry, commutative algebra, geometry of numbers, combinatorics and statistics.

Here we study the lattice width of convex bodies motivated by questions on lattice polytopes and symplectic manifolds. For a convex body $K \subset \mathbb{R}^d$, and a linear form $u \in \mathrm{Hom}(\mathbb{Z}^d, \mathbb{Z}) = (\mathbb{Z}^d)^*$, the *width of K along u* (or *with respect to u*) is given by

$$\mathrm{width}_u(K) \coloneqq \sup_{x,y \in K} |u(x) - u(y)|.$$

The *lattice width of K* (or simply *width of K*), $\mathrm{width}(K)$, is the minimum of its widths $\mathrm{width}_u(K)$ along all $u \in (\mathbb{Z}^d)^* \setminus \{0\}$. Khinchin's celebrated flatness theorem [68] guarantees that for every dimension d there exists a constant which bounds the width of convex bodies which are disjoint from the integer lattice $\mathbb{Z}^d$. This gives rise to the *classical flatness constant*

$$\mathrm{Flt}_d = \sup\left\{\mathrm{width}(K) : \ K \in \mathcal{K}^d, K \cap \mathbb{Z}^d = \varnothing\right\}.$$

It is conjectured that Flt_d is roughly proportional to d ([9, last paragraph in Section 8]). To the authors' knowledge, the best known upper bound at the time of writing is $\mathrm{Flt}_d \leq O(d^{4/3}\log^a d)$, where a is a constant [8]. Explicit values for Flt_d for low dimensions are scarce: clearly, $\mathrm{Flt}_1 = 1$, and Hurkens has shown that $\mathrm{Flt}_2 = 1 + \frac{2}{\sqrt{3}}$ [52]. However, already Flt_3 is not known: in [25, 6] the bounds $2 + \sqrt{2} \leq \mathrm{Flt}_3 \leq 3.972$ are shown and it is conjectured that $\mathrm{Flt}_3 = 2 + \sqrt{2}$.

In [7], Averkov, Hofscheier, and Nill introduced *generalised flatness constants* that provide a unifying approach to several questions on lattice polytopes and symplectic

manifolds. Generalised flatness constants $\mathrm{Flt}_d^A(X)$ depend on the choice of a ring $A \in \{\mathbb{Z}, \mathbb{R}\}$, and the choice of a fixed bounded subset $X \subset \mathbb{R}^d$ and its A-unimodular copies. An *A-unimodular transformation* $T\colon \mathbb{R}^d \to \mathbb{R}^d$ maps an $x \in \mathbb{R}^d$ to $Mx + b$, for some $M \in \mathrm{GL}_d(\mathbb{Z})$ and $b \in A^d$. We say $Y \subset \mathbb{R}^d$ is an *A-unimodular copy of* $X \subset \mathbb{R}^d$ if $Y = T(X)$ for some A-unimodular transformation $T\colon \mathbb{R}^d \to \mathbb{R}^d$. Then $\mathrm{Flt}_d^A(X)$ is the supremum over the widths of convex bodies in $\mathbb{R}^d$ that don't contain an A-unimodular copy of X:

$$\mathrm{Flt}_d^A(X) := \sup\left\{\mathrm{width}(K) : \ K \in \mathcal{K}^d, K \text{ contains no } A\text{-unimodular copy of } X\right\}.$$

By [7, Theorem 2.1], $\mathrm{Flt}_d^A(X)$ is a well-defined real number. By taking $A = \mathbb{Z}$ and X a lattice point, the usual flatness constant is recovered, i.e., $\mathrm{Flt}_d^{\mathbb{Z}}(\{\mathbf{0}\}) = \mathrm{Flt}_d$, justifying the definition of *generalised* flatness constants. A main result of this work is the computation of generalised flatness constants in dimension 2 when X is the 2-dimensional standard simplex $\Delta_2 = \mathrm{conv}(\mathbf{0}, e_1, e_2)$, where e_1, e_2 denotes the standard basis of $\mathbb{Z}^2$.

Theorem 5.1.1. *We have* $\mathrm{Flt}_2^{\mathbb{R}}(\Delta_2) = 2$ *and* $\mathrm{Flt}_2^{\mathbb{Z}}(\Delta_2) = \frac{10}{3}$.

A direct implication of the main theorem is that 2-dimensional convex bodies $K \subset \mathbb{R}^2$ whose width is larger than 2 contain an $\mathbb{R}$-unimodular copy of Δ_2. This bound is sharp in the sense that a convex body with lattice width 2 contains an $\mathbb{R}$-unimodular copy of Δ_2 (see Proposition 5.2.11). Similarly, any convex body whose width is larger than $\frac{10}{3}$ contains a $\mathbb{Z}$-unimodular copy of Δ_2. Again this bound is sharp (in the same sense as above). In particular, a convex body whose width is at least $\frac{10}{3}$ is spanning, i.e., the lattice points contained in the convex body affinely generate the ambient lattice. Spanning lattice polytopes turn out to have strong Ehrhart theoretical properties equivalent to ones of IDP polytopes, a much stronger combinatorial assumption on the polytope (see [50, 51]). The search for an effective and sufficient spanning test for lattice polytopes was one of the main motivations for the introduction of generalised flatness constants.

The proof of Theorem 5.1.1 relies on the study of A-X-free convex sets: if $X \subset \mathbb{R}^d$ is a fixed bounded set, then a convex set $K \subset \mathbb{R}^d$ is called *A-X-free* if the relative interior of K contains no A-unimodular copy of X. Here, we follow the convention that the relative interior of a point is the point itself. In Section 5.2, we show that the flatness constant $\mathrm{Flt}_d^A(X)$ is equal to the supremum over widths of A-X-free convex bodies. A key result in the study of generalised flatness constants is the following statement.

Theorem 5.1.2. *If $X \subset \mathbb{R}^d$ is a full-dimensional polytope, then every inclusion-maximal A-X-free convex body $K \subset \mathbb{R}^d$ is a polytope.*

Lemma 5.2.3 shows that, for any bounded X, to determine generalised flatness constants we can restrict our study to *inclusion-maximal* A-X-free convex sets. Precisely, we show that

$$\sup\left\{\text{width}(K) : \begin{array}{l}K \text{ is an}\\ \text{inclusion-}\\ \text{maximal}\\ A\text{-}X\text{-free}\\ \text{convex body}\end{array}\right\} \leq \text{Flt}_d^A(X) \leq \sup\left\{\text{width}(K) : \begin{array}{l}K \text{ is an}\\ \text{inclusion-}\\ \text{maximal}\\ A\text{-}X\text{-free}\\ \text{convex set}\end{array}\right\}.$$

It is straightforward to verify that in two dimensions, A-Δ_2-free, inclusion-maximal 2-dimensional convex sets which are unbounded are strips with rational slopes of sufficiently small width (see Proposition 5.3.3). Theorem 5.1.1 then follows from studying the inclusion-maximal A-Δ_2-free polygons. If $A = \mathbb{R}$, a theoretical argument shows that the width of inclusion-maximal $\mathbb{R}$-Δ_2-free convex polygons is bounded by 2. We further show that there are infinite families of inclusion-maximal $\mathbb{R}$-Δ_2-free convex polygons (see Section 5.5.1). Examples include the cross-polygon $\text{conv}(\pm e_1, \pm e_2)$ and the triangle $\text{conv}(e_1, e_2, -e_1 - e_2)$ which are both lattice polygons of width exactly 2. If $A = \mathbb{Z}$, we show that there is a unique $\mathbb{Z}$-Δ_2-free polygon which maximises the width, namely the triangle $\text{conv}(-2e_1 + 2e_2, \frac{4}{3}e_1 + \frac{1}{3}e_2, -\frac{1}{3}e_1 - \frac{4}{3}e_2)$, from which the result follows. Note that this unique maximiser isn't a lattice polygon.

For both $A = \mathbb{Z}$ and $A = \mathbb{R}$, we show that at least one of the A-Δ_2-free polygons with width equal to $\text{Flt}_2^A(\Delta_2)$ is a triangle. The same is true for the usual flatness constant in the plane, which is uniquely achieved at a triangle [52]. Further, the conjectured maximiser from [25] in three dimensions is a tetrahedron. It is thus natural to ask the following question.

Question 5.1.3. Is there always at least one A-X-free simplex among width maximisers of an A-generalised flatness constant? If $A = \mathbb{Z}$, are all maximisers simplices?

A positive answer to these questions would simplify the calculation of explicit values of the flatness constant greatly, since it would then no longer be necessary to check the width of the many inclusion-maximal A-X-free convex bodies that are not simplices.

We conclude the introduction by relating our results to the computation of the Gromov width of symplectic manifolds. Let (M, ω) be a $2d$-dimensional symplectic manifold. The *Gromov width* of M (denoted by $c_G(M)$) is the supremum over capacities πr^2 of balls with radius r that can be symplectically embedded in M (see [34]). We use the identification $S^1 = \mathbb{R}/\mathbb{Z}$ following the convention in [71, 74]. We are particularly interested in the case when M is a symplectic toric manifold with moment polytope Δ, i.e., a compact connected $2d$-dimensional symplectic manifold (M, ω) equipped with an effective Hamiltonian action of a torus $T \cong (S^1)^d$ and with a choice of a corresponding moment map $\mu\colon M \to \mathfrak{t}^*$ where $\mathfrak{t}$ denotes the lie algebra of T (so from now on we assume M to be toric). The explicit computation of Gromov width is still wide open; for example, even for symplectic toric manifolds it is not known how to read off the Gromov width from the moment polytope. Therefore there is a huge interest in finding effective upper and lower bounds for the Gromov width [4, 31, 61, 67, 74, 71, 77, 76, 91]. In particular, the result in [67, Corollary 11.4] (see

also [71, 74, 31]) can be restated in terms of generalised flatness constants as follows: the Gromov width of a symplectic toric manifold with moment polytope $P \subset \mathbb{R}^d$ is at least $\text{width}(P) \cdot \text{Flt}_d^{\mathbb{R}}(\Delta_d)^{-1}$. Here $\Delta_d \subset \mathbb{R}^d$ denotes the d-dimensional standard simplex. Combining this with Theorem 5.1.1 implies a lower bound on the Gromov width of 4-dimensional symplectic toric manifolds.

Theorem 5.1.4. *Let (M, ω) be a 4-dimensional symplectic toric manifold with moment polygon Δ. Then the Gromov width $c_G(M)$ of M accepts the following upper and lower bound:*

$$\frac{\text{width}(\Delta)}{2} \leq c_G(M) \leq \text{width}(\Delta).$$

The lower bound is a straightforward implication of [67, Corollary 11.4] and Theorem 5.1.1. The upper bound was conjectured in [7, Conjecture 3.12] and subsequently verified for 4-dimensional symplectic toric manifolds by Chaidez and Wormleighton [18, Corollary 4.19]. It is known that the upper bound is tight in the sense that there exist 4-dimensional symplectic toric manifolds whose Gromov width coincides with the lattice width of their moment polytopes (see, for instance, [7, Lemma 3.16]). There are also examples known where the Gromov width is strictly less than the width of the corresponding moment polygon (see, for instance, [55, Example 5.6]). However, to the authors' knowledge it is not known if the lower bound of Theorem 5.1.4 is also tight. That is, is there a 4-dimensional toric symplectic manifold whose Gromov width coincides with half of the width of its moment polygon?

The chapter is organised as follows. In Section 5.2, we show how to reduce the calculation of flatness constants to that of inclusion-maximal A-X-free bodies, and show some key properties of these bodies. Section 5.3 concerns the study of $\text{Flt}_d^A(\Delta_d)$ in one dimension and begins its study in two dimensions by analysing the unbounded case. Section 5.4 characterises inclusion-maximal $\mathbb{Z}$-Δ_d-free polytopes, leading to a proof of the case $A = \mathbb{Z}$ of Theorem 5.1.1. Section 5.5 proves the case $A = \mathbb{R}$ of Theorem 5.1.1.

Computations were carried out using Magma [16], polymake [32], Mathematica [57], and SymPy [78]. The code can be found at https://github.com/jhofscheier/gen-flat-const-dim2.

5.2 A general strategy to compute generalised flatness constants

In this section, we prove foundational observations on generalised flatness constants. We hope the approach introduced here provides an efficient framework for the study of generalised flatness constants in any dimensions and for various choices of X. At the end of the section we will outline a general strategy for the computation of generalised flatness constants which we will follow to determine $\text{Flt}_2^A(\Delta_2)$ for both $A = \mathbb{Z}$ and $A = \mathbb{R}$.

In our study, we will use the notion of Minkowski addition. It is well-known that if A and B are convex, compact, or polytopes, then the Minkowski sum will have the same properties. Furthermore, Minkowski addition is cancellative on the set of convex bodies, i.e., if $A, B, C \subset \mathbb{R}^d$ are convex bodies, then $A + C = B + C$ implies $A = B$. We will write $B^d \subset \mathbb{R}^d$ for the usual d-dimensional ball in Euclidean space with radius 1, i.e., the set of all points x in $\mathbb{R}^d$ whose Euclidean norm is bounded by 1, i.e., $|x| \leq 1$. Finally, let $B_\infty^d \subset \mathbb{R}^d$ be the (closed) unit ball with respect to the maximum norm $|\cdot|_\infty$. Note $B_\infty^d = [-1, 1]^d$ is a polytope.

Remark 5.2.1. The following are elementary but important observations. Their proofs are straightforward and are left to the reader. Let $X \subset \mathbb{R}^d$ be a bounded set. Then:

- $\mathrm{Flt}_d^A(X) = \mathrm{Flt}_d^A(\mathrm{conv}(X))$;
- $\mathrm{Flt}_d^A(X) = \mathrm{Flt}_d^A(\overline{X})$, where $\overline{X}$ denotes the closure of X with respect to the Euclidean topology.

5.2.1 A-X-free convex bodies

We begin by noticing that generalised flatness constants $\mathrm{Flt}_d^A(X)$ can equivalently be described via A-X-free convex bodies.

Lemma 5.2.2. *For a bounded set $X \subset \mathbb{R}^d$, we have:*

$$\mathrm{Flt}_d^A(X) = \sup\left\{\mathrm{width}(K) : K \in \mathcal{K}^d \text{ is an } A\text{-}X\text{-free convex body}\right\}.$$

Proof. The case $X = \varnothing$ can be straightforwardly verified, so suppose X is non-empty.

Since every convex body $K \subset \mathbb{R}^d$ that contains no A-unimodular copy of X is A-X-free, the inequality "$\leq$" straightforwardly follows.

For the reverse inequality, let $K \subset \mathbb{R}^d$ be an A-X-free convex body that contains an A-unimodular copy of X. If K were just a point, it would follow that X is A-unimodularly equivalent to K, so that, by our convention of relative interior of points, we would get $\mathrm{rel}(K) = K$ contained an A-unimodular copy of X, i.e., K is not A-X-free, a contradiction. Hence, the dimension of K is positive. By [92, Theorem 1.8.16], for any $\varepsilon > 0$, there exists a polytope $P \in \mathcal{K}^d$ such that $P \subset K \subset P + \varepsilon B^d$. Since $\dim(K) \geq 1$, it follows for sufficiently small $\varepsilon > 0$ that $\dim(P) \geq 1$ too. By moving the facets of P in by another $\varepsilon' > 0$ (clearly this is done inside the affine span of P), we obtain a polytope $P' \in \mathcal{K}^d$ whose width can be chosen to be arbitrarily close to the width of K and which doesn't contain an A-unimodular copy of X. So, $\mathrm{Flt}_d^A(X) \geq \mathrm{width}(K)$. The statement follows. □

The following lemma seems to be decisive for the explicit computation of generalised flatness constants in that it reduces the determination of an upper bound for $\mathrm{Flt}_d^A(X)$ to studying the width of inclusion-maximal A-X-free closed convex sets.

Lemma 5.2.3. *Let $X \subset \mathbb{R}^d$ be a non-empty bounded subset. Then every A-X-free convex body is contained in an inclusion-maximal A-X-free closed convex set.*

Proof. By Remark 5.2.1, we can assume that X is closed and convex. In particular, X is compact since it is bounded. Let $K \in \mathcal{K}^d$ be an A-X-free convex body.

Let $\mathcal{M}$ be the set of all A-X-free closed convex sets $C \subset \mathbb{R}^d$ that contain K (C not necessarily bounded). Note $\mathcal{M}$ is partially ordered with respect to inclusion. Our goal is to apply Zorn's Lemma. Therefore, we need to show that every totally ordered subset $S \subset \mathcal{M}$ has an upper bound in $\mathcal{M}$. We set $C_0 := \overline{\bigcup_{C\in S} C}$ which is a closed convex set in $\mathbb{R}^d$. It remains to verify that C_0 is also A-X-free. Assume towards a contradiction that C_0 contains an A-unimodular copy of X in its relative interior, say $Y \subset \operatorname{rel}(C_0)$ where Y is an A-unimodular copy of X. Since $\operatorname{rel}(C_0) \subset \bigcup_{C\in S} C$, it follows $Y \subset \bigcup_{C\in S} C$. Consider the "distance" between the boundary ∂C_0 of C_0 (considered as subset in the affine span $\operatorname{aff}(C_0)$) and Y:

$$d(\partial C_0, Y) := \inf\{|x - y| : x \in \partial C_0, y \in Y\}.$$

Since $\partial C_0 \cap Y = \emptyset$, ∂C_0 is closed, and Y is compact, a classical result from point set topology implies $d(\partial C_0, Y) > 0$. There exists an $\varepsilon > 0$ such that the Minkowski sum $Y + (\varepsilon B^d_\infty \cap \operatorname{aff}(C_0))$ is contained in the interior $\operatorname{int}(C_0)$. Then clearly

$$Y \subset Y + \left(\frac{\varepsilon}{2} B^d_\infty \cap \operatorname{aff}(C_0)\right) \subset Y + \left(\varepsilon B^d_\infty \cap \operatorname{aff}(C_0)\right) \subset \operatorname{rel}(C_0) \subset \bigcup_{C\in S} C.$$

Since $Y + (\frac{\varepsilon}{2} B^d \cap \operatorname{aff}(C_0))$ is compact, finitely many translations of $\varepsilon B^d_\infty \cap \operatorname{aff}(C_0)$ suffice to cover $Y + (\varepsilon B^d \cap \operatorname{aff}(C_0))$. Note the convex hull of these finitely many translates yield a polytope with vertices, say $v_1, \dots, v_n$. There exist $C_i \in S$ with $v_i \in C_i$. Since S is totally ordered, we conclude that there exists a $C \in S$ with $v_1, \dots, v_n \in C$, and thus $Y + (\frac{\varepsilon}{2} B^d \cap \operatorname{aff}(C_0)) \subset C$. Hence, $Y \subset \operatorname{rel}(C)$. A contradiction.

By construction $C_0 \in \mathcal{M}$ is an upper bound of S. The statement follows by Zorn's Lemma. □

Remark 5.2.4. The inclusion-maximal set from Lemma 5.2.3 might be unbounded: consider for example the rectangle with vertices $(\pm a, 1), (\pm a, 0)$, for any large $a \in \mathbb{R}$. This is a $\mathbb{R}$-Δ_2-free convex body and the only inclusion-maximal $\mathbb{R}$-Δ_2-free convex set containing it is the horizontal strip between height 0 and 1.

By Lemma 5.2.3, every A-X-free convex body is contained in an inclusion-maximal closed convex A-X-free set. Since the width is monotone with respect to inclusion, we have the following.

$$\sup\left\{\operatorname{width}(K) : \begin{array}{l}K \text{ is an}\\ \text{inclusion-}\\ \text{maximal}\\ A\text{-}X\text{-free}\\ \text{convex body}\end{array}\right\} \le \operatorname{Flt}^A_d(X) \le \sup\left\{\operatorname{width}(K) : \begin{array}{l}K \text{ is an}\\ \text{inclusion-}\\ \text{maximal}\\ A\text{-}X\text{-free}\\ \text{convex set}\end{array}\right\}. \quad (5.1)$$

That is, an upper bound on the width of inclusion-maximal A-X-free closed convex sets $C \subset \mathbb{R}^d$ (including the unbounded ones) gives an upper bound for $\operatorname{Flt}^A_d(X)$, while the width of any inclusion-maximal bounded A-X-free convex set yields a

lower bound. A strategy to determine the exact value of generalised flatness constants is to compute these upper and lower bounds and show they agree by studying the explicit values of the width in the two subcases: 1) C is unbounded; 2) C is a convex body.

In this work and with regard to the applications of generalised flatness constants to symplectic geometry, the case when the convex hull $\mathrm{conv}(X)$ is full-dimensional plays a crucial role. In this case, it suffices to consider full-dimensional A-X-free convex bodies, as the next lemma shows.

Lemma 5.2.5. *Let $X \subset \mathbb{R}^d$ be a bounded subset whose convex hull is full-dimensional. Then every A-X-free convex body is contained in a full-dimensional A-X-free convex body.*

Proof. By Remark 5.2.1, we may assume that X is a full-dimensional convex body. Let $K \subset \mathbb{R}^d$ be an A-X-free convex body of dimension $< d$. Then K is contained in an affine hyperplane $H \subset \mathbb{R}^d$. Let $U_H \subset \mathbb{R}^d$ be the unique linear subspace parallel to H. We first show that it suffices to consider the case $\dim(K) = d - 1$.

Suppose $\dim(K) < d - 1$. Let $B^{d-1} \subset U_H$ be the $d-1$-dimensional unit ball containing the origin. Then the Minkowski sum $K + B^{d-1}$ has dimension $d-1$ and is contained in H. Since X is full-dimensional, $K + B^{d-1}$ is A-X-free (it cannot contain an A-unimodular copy of X).

Hence, we may assume that K is $d-1$-dimensional contained in an affine hyperplane $H \subset \mathbb{R}^d$. Clearly, there exists a parallelepiped $\Pi^{d-1} \subset H$ which contains K. Let $v \in \mathbb{R}^d$ such that $\mathbb{R}v + U_H = \mathbb{R}^d$. Take $\varepsilon > 0$ such that the volume of the parallelepiped $\Pi^{d-1} + \varepsilon v$ is strictly smaller than the volume of X. Then $K \subset \Pi^{d-1} + \varepsilon v$ is full-dimensional and A-X-free (it cannot contain an A-unimodular copy of X). □

This guarantees that, whenever we work with a set X whose convex hull is full dimensional, the supremums on the left and right hand side of (5.1) can be taken over just the *full-dimensional* sets. A positive answer to the following question would confirm our suspicion that, once we restrict to full-dimensional sets, the width of the unbounded sets will always be strictly less than the widths of the bounded ones and thus that the inequalities in (5.1) above are in fact equalities.

Question 5.2.6. Do full-dimensional unbounded inclusion-maximal A-X-free sets always have "small" width, that is, they are never maximisers of width among all A-X-free bodies?

Remark 5.2.7. Let us provide more details why the restriction to full-dimensional inclusion-maximal A-X-free closed convex sets $C \subset \mathbb{R}^d$ is crucial. Consider the case that $X = \Delta_2$. Let $m \in \mathbb{R} \setminus \mathbb{Q}$ be an irrational real number. Then, for any closed interval $I \subset \mathbb{R}$, we have an A-Δ_2-free convex body $\{(x, m \cdot x) : x \in I\} \subset \mathbb{R}^2$. These convex bodies are contained in the inclusion-maximal A-Δ_2-free closed convex set $C = \{(x, m \cdot x) : x \in \mathbb{R}\} \subset \mathbb{R}^2$ (note C is inclusion-maximal A-X-free as otherwise it would contain a point outside the line $\{y = m \cdot x\}$, and thus would contain a 2-dimensional strip with irrational slope; now apply the argument from the proof of Proposition 5.3.3).

Since m is irrational, any $u \in (\mathbb{Z}^2)^* \setminus \{0\}$ induces a non-trivial linear form on the line $C = \{y = m \cdot x\}$, and thus $\mathrm{width}_u(C) = \infty$. It follows that $\mathrm{width}(C) = \infty$,

yielding the rather unhelpful upper bound $\mathrm{Flt}_2^A(\Delta_2) \leq \infty$. However, we shall see that considering full-dimensional inclusion-maximal A-Δ_2-free closed convex sets will provide exactly the bounds that we need to compute $\mathrm{Flt}_2^A(\Delta_2)$.

In dimension 2, the unbounded case is straightforward and will be done in Section 5.3. The study of inclusion-maximal A-X-free convex bodies is more intricate and the later sections of the chapter will be concerned with this investigation in dimension 2.

The following lemma is another important ingredient in the explicit computation of generalised flatness constants. Its significance lies in Corollary 5.2.10, which shows that an inclusion-maximal A-X-free convex body contains an A-unimodular copy of X. That will provide us with tools necessary to study those bodies yielding the exact numerical value of the respective generalised flatness constant.

Lemma 5.2.8. *Let $K, X \subseteq \mathbb{R}^d$ be d-dimensional convex bodies. If K does not contain an A-unimodular copy of X, there exists $\varepsilon > 0$ such that $K + \varepsilon B^d$ does not contain an A-unimodular copy of X.*

Proof. We split the proof into two cases. Suppose $A = \mathbb{R}$. We show the contrapositive, i.e., if for all (large enough) $n \in \mathbb{N}$, there exists an $\mathbb{R}$-unimodular transformation T_n with $T_n(X) \subseteq K + \frac{1}{n}B^d$, then K contains an $\mathbb{R}$-unimodular copy of X. We can represent T_n as a composition of a $\mathbb{Z}$-unimodular transformation A_n and a translation $\delta_n \in [0,1]^d$, i.e. $T_n(x) = A_n(x) - \delta_n$. Since $T_n(X) = A_n(X) - \delta_n \subseteq K + \frac{1}{n}B^d$, we get

$$A_n(X) \subseteq K + \frac{1}{n}B^d + \delta_n \subseteq K + B^d + [0,1]^d.$$

Since X is full-dimensional, there exists an affine $\mathbb{Z}$-basis $\mathcal{B} = \{b_0, \ldots, b_d\}$ of $\mathbb{Z}^d$ and a scaling factor $\eta > 0$ such that $\eta\mathcal{B} \subseteq X$. As a $\mathbb{Z}$-unimodular transformation, A_n is uniquely determined by the images of the b_i. We require that A_n maps $\eta\mathcal{B}$ onto an affine linearly independent subset of $\eta\mathbb{Z}^d \cap \left(K + B^d + [0,1]^d\right)$. Since $K + B^d + [0,1]^d$ is bounded and $\eta\mathbb{Z}^d$ is discrete, there are only finitely many choices for A_n. In particular, by restricting to an appropriate subsequence, we may assume that $A = A_n$ for all $n \in \mathbb{N}$.

Since $[0,1]^d$ is compact, there exists a convergent subsequence of $(\delta_n)_{n\in\mathbb{N}}$ with limit $\delta \in [0,1]^d$. To keep notation simple, we use the same symbol $(\delta_n)_{n\in\mathbb{N}}$ for this subsequence, i.e. δ_n converges to $\delta \in [0,1]^d$. Let T be the $\mathbb{R}$-unimodular transformation obtained by composing the $\mathbb{Z}$-unimodular transformation A with the translation δ. We show that $T(X) \subseteq K$.

Suppose $x \in X$. Since $A(x) - \delta_n \in K + \frac{1}{n}B^d$, there exists $z_n \in \frac{1}{n}B^d$ such that

$$y_n := A(x) - \delta_n - z_n \in K.$$

As n goes to infinity, we get that $y_n \to A(x) - \delta = T(x)$. Since K is compact, it follows that $T(x) \in K$.

If $A = \mathbb{Z}$, we repeat the argument above, however now there are no translations $\delta_n \in [0,1]^d$. ∎

The proof of Lemma 5.2.8 shows the following result which will be needed below.

Corollary 5.2.9. *Let $K, X \subseteq \mathbb{R}^d$ be d-dimensional convex bodies. If K does not contain an A-translate of X, then there exists an $\varepsilon > 0$ such that $K + \varepsilon B^d$ does not contain an A-translate of X.*

Furthermore, the following result follows from Lemma 5.2.8.

Corollary 5.2.10. *Let $K, X \subset \mathbb{R}^d$ be d-dimensional convex bodies. If K is inclusion-maximal A-X-free, then K contains an A-unimodular copy of X.*

Proof. Assume towards a contradiction K didn't contain an A-unimodular copy of X. By Lemma 5.2.8, K is contained in a strictly bigger convex body $K \subsetneq K' \subset \mathbb{R}^d$ with the same property. Since K' doesn't contain an A-unimodular copy of X, it is A-X-free. A contradiction to K being inclusion-maximal. □

By the definition of generalised flatness constants, given a convex body $K \subset \mathbb{R}^d$ with $\operatorname{width}(K) > \operatorname{Flt}_d^A(X)$, there exists an A-unimodular copy of X that is contained in K. However, a priori the case of equality $\operatorname{width}(K) = \operatorname{Flt}_d^A(X)$ is unclear, i.e., there could be such K that do not contain an A-unimodular copy or there could be such K that do. Lemma 5.2.8 implies the following complete answer to this question.

Proposition 5.2.11. *Let $K, X \subset \mathbb{R}^d$ be d-dimensional convex bodies with $\operatorname{width}(K) = \operatorname{Flt}_d^A(X)$. Then K contains an A-unimodular copy of X.*

Proof. Assume towards a contradiction K doesn't contain an A-unimodular copy of X. By Lemma 5.2.8, there exists $\varepsilon > 0$ such that $K + \varepsilon B^d$ also doesn't contain an A-unimodular copy of X. A contradiction since $\operatorname{width}(K + \varepsilon B^d) > \operatorname{width}(K)$. □

We conclude the section by proving Theorem 5.1.2 for the case $A = \mathbb{Z}$. Indeed, we show a more general version of Theorem 5.1.2 in that X just needs to be a bounded set. The case $A = \mathbb{R}$ is more involved and will be treated in Sections 5.2.2 and 5.2.3.

Proposition 5.2.12 (Case $A = \mathbb{Z}$ of Theorem 5.1.2)**.** *Let $X \subset \mathbb{R}^d$ be a bounded set. Then every inclusion-maximal $\mathbb{Z}$-X-free convex body is a polytope.*

Proof. Let $K \subset \mathbb{R}^d$ be an inclusion-maximal $\mathbb{Z}$-X-free convex body. There is a positive integer $N \in \mathbb{Z}_{>0}$ such that K is contained in $[-N, N]^d$. Set

$$A := \left\{ a \in [-N, N]^d \cap \mathbb{Z}^d \,:\, a \notin \operatorname{rel}(K) \right\},$$

and

$$\Delta := \bigcap_{a \in A} \left\{ H_a \text{ half-spaces such that } a \in \partial H_a,\ K \subset H_a \right\}.$$

Such choices of half-spaces exist due to the Separation Theorem. Since Δ is a finite intersection of half-spaces (note $|A| < \infty$), it's a polytope. Notice all lattice points of Δ are either in $\operatorname{rel}(K)$ or in $\partial\Delta$. Thus Δ is $\mathbb{Z}$-X-free. Since $K \subset \Delta$, we have that $K = \Delta$ is a polytope. □

5.2.2 Inclusion-maximal $\mathbb{R}$-X-free convex bodies

In this section we are going to prove Theorem 5.1.2 for the case $A = \mathbb{R}$.

Proposition 5.2.13 (Case $A = \mathbb{R}$ of Theorem 5.1.2)**.** *Let $X \subset \mathbb{R}^d$ be a polytope. Then every inclusion-maximal $\mathbb{R}$-X-free convex body is a polytope.*

Throughout $X \subset \mathbb{R}^d$ will be a fixed full-dimensional polytope and $K \subset \mathbb{R}^d$ a convex body. Notice that, by Lemma 5.2.5, we may assume that K is full-dimensional (a crucial assumption as explained in Remark 5.2.7). Then in the definition of $\mathbb{R}$-X-free "relative interior" can be replaced by just "interior".

We start by investigating the set of $\mathbb{R}$-unimodular copies S of X which are contained in K. In general, this is an infinite set (see Figure 5.1). We will identify

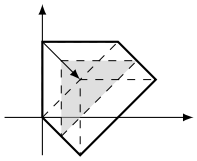

FIGURE 5.1: A polygon containing $\mathbb{R}$-unimodular copies of Δ_2 translated along a line segment.

two polytopes in this set if one is the translation of the other. The resulting set of equivalence classes will be denoted by $\mathcal{T}_K(X)$.

Lemma 5.2.14. *The set $\mathcal{T}_K(X)$ of $\mathbb{R}$-translation equivalence classes of $\mathbb{R}$-unimodular copies of X contained in K is finite.*

Proof. Clearly for every $\mathbb{R}$-unimodular copy S of X which is contained in K, there exists a $\mathbb{Z}$-unimodular copy S' of X such that $S' \subset K + [-1,0]^d$. Since $K + [-1,0]^d$ contains only finitely many lattice points, it follows that there can only be finitely many such S' contained in $K + [-1,0]^d$. The statement follows. □

In what follows, we will use a complementary operation to Minkowski addition usually referred to as Minkowski difference. We recall its definition and refer to [92] for further details and references. For subsets $A, B \subset \mathbb{R}^d$ the *Minkowski difference* $A \div B$ is the set of translation vectors that move B into A:

$$A \div B = \{x \in \mathbb{R}^d : B + x \subset A\} = \bigcap_{b \in B} (A - b).$$

From the last equality, it is clear that the Minkowski difference $A \div B$ of two convex bodies A, B in $\mathbb{R}^d$ is either empty or a are convex body too. Here is a justification why Minkowski difference can be regarded as a complementary operation to Minkowski addition.

Lemma 5.2.15 ([92, Lemma 3.1.11])**.** *Let $A, B \subset \mathbb{R}^d$ be two convex bodies. Then*

$$(A + B) \div B = A.$$

Furthermore, we have

$$(A \div B) + B = A$$

if and only if there exists a convex body $C \subset \mathbb{R}^d$ *such that* $A = B + C$.

From now on, let $S \subset \mathbb{R}^d$ be a fixed $\mathbb{Z}$-unimodular copy of X. We note that for any $\delta \in \mathbb{R}^d$, we have

$$K \div (S + \delta) = (K \div S) - \delta.$$

Furthermore, $K \div S$ is not empty if and only if K contains a translate of S. Studying the Minkowski difference $K \div S$ (also called *inner parallel body relative to* S) will be key to proving Proposition 5.2.13. In general, $K \div X$ will not be a polytope (see for instance

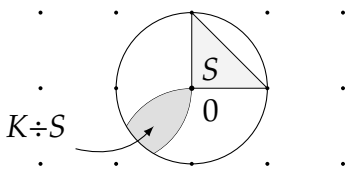

FIGURE 5.2: $K \div S$ for the unit disc K with centre at the origin and $S = \mathrm{conv}(\mathbf{0}, e_1, e_2) \subset \mathbb{R}^2$.

Figure 5.2). However, since X is a polytope there is an efficient way to determine the Minkowski difference $K \div X$:

Lemma 5.2.16. *Suppose* $K \div S \neq \emptyset$, *i.e., there exists* $\delta \in \mathbb{R}^d$ *such that* $S + \delta \subset K$. *Let* $v_1, \ldots, v_n$ *be the vertices of* $S + \delta$. *Then*

$$K \div (S + \delta) = \bigcap_{i=1}^{n} (K - v_i).$$

Proof. Let $v \in K \div (S + \delta)$. Then for all i, we have $v_i + v \in K$, and thus $v \in K - v_i$.

Suppose $v \in K - v_i$, i.e. $v_i + v \in K$, for all i. Since K is convex, it follows

$$\mathrm{conv}(v_1 + v, \ldots, v_n + v) = \mathrm{conv}(v_1, \ldots, v_n) + v = S + \delta + v \subset K.$$

Thus $v \in K \div (S + \delta)$ and the statement follows. □

The collection of inner parallel bodies $K \div S$ for $\mathbb{Z}$-unimodular copies S of X allows to characterise when exactly K is $\mathbb{R}$-X-free (see the next two statements).

Lemma 5.2.17. *An* $\mathbb{R}$*-translation of a* $\mathbb{Z}$*-unimodular copy* S *of* X *is contained in the interior of* K *if and only if* $\dim(K \div S) = d$.

Proof. Suppose there is a $\mathbb{Z}$-unimodular copy S of X and $\delta \in \mathbb{R}^d$ such that $S + \delta$ is contained in the interior of K. Since $(K \div (S + \delta)) + \delta = K \div S$, we may replace S by its translate $S + \delta$, so that $S \subset K$. We need to show that $\dim(K \div S) = d$. Consider small open neighbourhoods $B_1, \ldots, B_n$ around the vertices $v_1, \ldots, v_n$ of S. Choose B_i small enough such that it is contained in the interior of K. Move these neighbourhoods to the origin, i.e., consider $B_i - v_i$. The intersection $\bigcap_{i=1}^{n} (B_i - v_i)$ is an open neighbourhood of the origin which is contained in $K \div S$, and thus $\dim(K \div S) = d$.

For the reverse direction, suppose S is a $\mathbb{Z}$-unimodular copy of X with $\dim(K \div S) = d$. Like before, we may replace S by $S + \delta$ for some $\delta \in \mathbb{R}^d$ such that (after replacing) $S \subset K$. Denote the vertices of S by $v_1, \dots, v_n$. We claim there is an element w in $K \div S$ which is not contained in the translates $\partial K - v_i$ of the boundary of K for all $i = 1, \dots, n$. In other words, we claim that there is

$$w \in (K \div S) \setminus \left(\bigcup_{i=1}^{n} \partial K - v_i \right) = \left(\bigcap_{i=1}^{n} (K - v_i) \right) \setminus \left(\bigcup_{i=1}^{n} \partial K - v_i \right)$$

where the equality follows by Lemma 5.2.16. Before proving the claim, let us see how it implies the statement: $w + v_i \in K \setminus \partial K$, and thus $\operatorname{conv}(v_1, \dots, v_n) + w \subset K \setminus \partial K$, i.e. $S + w$ is contained in the interior of K.

It remains to show the claim. Suppose by contradiction $(K \div S) \setminus \left(\bigcup_{i=1}^{n} \partial K - v_i \right)$ is empty, i.e. $K \div S$ is contained in the union of the shifted boundaries $\partial K - v_i$ for $i = 1, \dots, n$. By our assumption $\dim(K \div S) = d$, there are linearly independent vectors $w_1, \dots, w_d \in \mathbb{R}^d$ such that the d-dimensional simplex $\Delta := \operatorname{conv}(\mathbf{0}, w_1, \dots, w_d)$ is contained in $K \div S$. We obtain a contradiction if we apply the d-dimensional Euclidean volume to the inclusion $\Delta \subset \bigcup_{i=1}^{n} (\partial K - v_i)$:

$$0 < \operatorname{Vol}(\operatorname{conv}(v_1, \dots, v_n)) \leq \operatorname{Vol}\left(\bigcup_{i=1}^{n} \partial K - v_i \right) \leq \sum_{i=1}^{n} \operatorname{Vol}(\partial K - v_i) = 0. \qquad \square$$

Corollary 5.2.18. *K is $\mathbb{R}$-X-free if and only if $\dim(K \div S) < d$ for all $\mathbb{Z}$-unimodular copies S of X.*

Proof. The contrapositive, i.e., $K \subset \mathbb{R}^d$ is not $\mathbb{R}$-X-free if and only if there is some affine $\mathbb{Z}$-unimodular copy S of X with $\dim(K \div S) = d$, straightforwardly follows from Lemma 5.2.17. $\square$

Fix an inclusion-maximal $\mathbb{R}$-X-free convex body $K \subset \mathbb{R}^d$. Recall that we want to show that K is a polytope. As a first step, we approximated K by a polytope $P \subset \mathbb{R}^d$ which contains K such that up to real translations K and P contain the same $\mathbb{Z}$-unimodular copies of X.

Lemma 5.2.19. *For a d-dimensional convex body $K \subset \mathbb{R}^d$, there exists a d-dimensional convex polytope $P \subset \mathbb{R}^d$ which contains K such that $\mathcal{T}_K(X) = \mathcal{T}_P(X)$.*

Lemma 5.2.19 follows from the following well-known result (see also [92, Theorem 1.8.16]).

Lemma 5.2.20. *If $K \subset \mathbb{R}^d$ is a d-dimensional convex body and $\varepsilon > 0$, then there exists a polytope $P \subset \mathbb{R}^d$ such that $K \subset P \subset K + \varepsilon B^d$.*

Proof. Recall the (closed) unit ball B_∞^d with respect to the infinity norm $|\cdot|_\infty$ is a polytope, namely $B_\infty^d = [-1, 1]^d$. Since any two norms on $\mathbb{R}^d$ are equivalent, there exists $\alpha > 0$ such that $\alpha B_\infty^d \subset \varepsilon B^d$.

Since the collection $\left\{x + \alpha B_\infty^d : x \in K\right\}$ covers the compact set K, already a finite subset of balls suffices to cover K. The polytope P obtained by taking the convex hull of these finitely many ∞-balls with radius α satisfies the statement, i.e., $K \subset P \subset K + \varepsilon B^d$. □

Proof of Lemma 5.2.19. Choose $N > 0$ large enough such that K is contained in the interior of $[-N, N]^d$. Then $\mathcal{T}_K(X) \subset \mathcal{T}_{[-N,N]^d}(X)$ and this inclusion is strict in general. Our strategy is to cut $[-N, N]^d$ with further half-spaces so that the resulting polytope P satisfies $\mathcal{T}_K(X) = \mathcal{T}_P(X)$.

Consider a $\mathbb{Z}$-unimodular copy Q of X such that $[-N, N]^d$ contains an $\mathbb{R}$-translate of Q but K doesn't, i.e. $[Q] \in \mathcal{T}_{[-N,N]^d}(X) \setminus \mathcal{T}_K(X)$. By Corollary 5.2.9, there exists $\varepsilon_Q > 0$ such that $K + \varepsilon_Q B^d$ does not contain an $\mathbb{R}$-translate of Q. Let $\varepsilon > 0$ be the minimum of the ε_Q over all Q with $[Q] \in \mathcal{T}_{[-N,N]^d}(X) \setminus \mathcal{T}_K(X)$ (note $\mathcal{T}_{[-N,N]^d}(X)$ is finite by Lemma 5.2.14). If necessary reduce $\varepsilon > 0$ such that $K + \varepsilon B^d \subset [-N, N]^d$. By Lemma 5.2.20, there exists a polytope $P \subset \mathbb{R}^d$ such that $K \subset P \subset K + \varepsilon B^d$. By our choice of ε, we have that $\mathcal{T}_{K+\varepsilon B^d}(X) = \mathcal{T}_K(X)$, and by the monotonicity of $\mathcal{T}_K(X)$ with respect to K, this polytope satisfies $\mathcal{T}_K(X) = \mathcal{T}_P(X)$. □

Remark 5.2.21. In Lemma 5.2.19, the polytope P, which contains K, isn't necessarily $\mathbb{R}$-X-free in general (see Figure 5.3). By intersecting P with further half-spaces

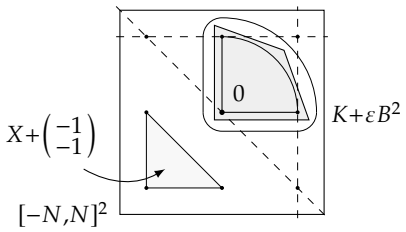

FIGURE 5.3: Illustration of Lemma 5.2.19. Here, K is a quarter of a disc and $X = \mathrm{conv}(\mathbf{0}, e_1, e_2) \subset \mathbb{R}^2$ the standard simplex. The polytope P might not be $\mathbb{R}$-X-free.

(e.g., the half-spaces indicated by the dashed lines), we get a new polytope which is $\mathbb{R}$-X-free. The proof of Proposition 5.2.13 will show this is always true.

The proof of Proposition 5.2.13 will make use of the following theorem, whose proof we postpone until Section 5.2.3.

Theorem 5.2.22. *Let $K_1, \ldots, K_n \subset \mathbb{R}^d$ be convex bodies such that $\dim(K) < d$ where $K := K_1 \cap \ldots \cap K_n$. Suppose $x \in K$ such that x is contained in the boundary of every K_i for $i = 1, \ldots, n$. Then there are (nonempty) finite collections of closed half-spaces $\{H^+(i, j)\}_{j \in J_i}$ for $i = 1, \ldots, n$ such that the boundary of $H^+(i, j)$ is a supporting hyperplane to K_i at x, and*

$$\dim\left(\bigcap_{j \in J_1} H^+(1, j) \cap \ldots \cap \bigcap_{j \in J_n} H^+(n, j)\right) < d.$$

Proof of Proposition 5.2.13. The idea is to construct an $\mathbb{R}$-X-free polytope P which contains K. Since K is inclusion-maximal with respect to this property, it follows that $K = P$ is a polytope. Lemma 5.2.19 yields a first approximation P' of this polytope P which satisfies $\mathcal{T}_K(X) = \mathcal{T}_{P'}(X)$. However, P' might not be $\mathbb{R}$-X-free in general (see Figure 5.3). We claim that P' can be cut with further half-spaces such that the resulting polytope still contains K and is $\mathbb{R}$-X-free. We prove this claim by induction on the number r of equivalence classes $[Q] \in \mathcal{T}_{P'}(X)$ with $\dim(K \div Q) = d$. By Lemma 5.2.14, the number r is finite.

In the base case, i.e. $r = 0$, we have $\dim(P \div Q) < d$ for all $[Q] \in \mathcal{T}_P(X)$, and thus by Corollary 5.2.18, the polytope P' is already $\mathbb{R}$-X-free.

Consider the case $r \geq 1$. Let Q be a $\mathbb{Z}$-unimodular copy of X with $\dim(P' \div Q) = d$. Note that by construction $[Q] \in \mathcal{T}_K(X)$. We want to intersect P' with finitely many half-spaces, so that the resulting polytope P'' contains K and $\dim(P'' \div Q) < d$. By Corollary 5.2.18, $\dim(K \div Q) < d$. Let $\delta \in K \div Q$. If $v_1, \ldots, v_n$ are the vertices of $Q + \delta$, then, by Lemma 5.2.16, $K \div (Q + \delta) = (K - v_1) \cap \ldots \cap (K - v_n)$. If the origin $\mathbf{0}$ is in the interior of $K - v_i$, then this convex body does not contribute to the dimension drop and we omit it. By abuse of notation, let us assume that the origin $\mathbf{0}$ is contained in the boundary of $K - v_i$ for $i = 1, \ldots, n$. By Theorem 5.2.22, there exist (nonempty) finite collections of closed half-spaces $\{H^+(i,j)\}_{j \in J_i}$ for $i = 1, \ldots, n$ such that the boundary $H(i,j)$ of $H^+(i,j)$ is a supporting hyperplane to $K - v_i$ at $\mathbf{0}$ and the dimension of the cone $C := \bigcap_{i=1}^n \bigcap_{j \in J_i} H^+(i,j)$ is at most $d - 1$. We define a new polytope:

$$P'' := P' \cap \bigcap_{j \in J_1} (H^+(1,j) + v_1) \cap \ldots \cap \bigcap_{j \in J_n} (H^+(n,j) + v_n).$$

Since $H(i,j)$ is a supporting hyperplane to $K - v_i$ at $\mathbf{0}$, the affine hyperplane $H(i,j) + v_i$ is a supporting hyperplane to K at v_i, and thus P'' contains K as well. Note that $Q + \delta$ is contained in P'', so that

$$P'' \div (Q + \delta) = (P'' - v_1) \cap \ldots \cap (P'' - v_n) \subset C.$$

Since $P'' \div Q$ is contained in C and C is not full-dimensional, it follows that $\dim(P'' \div Q) < d$. As the number of $[Q'] \in \mathcal{T}_{P''}(X)$ with $\dim(P'' \div Q') = d$ is at most $r - 1$, it follows by the induction hypothesis that we can intersect P'' with finitely many further half-spaces such that the resulting polytope P contains K and is $\mathbb{R}$-X-free. This completes the proof. □

5.2.3 Intersection of convex bodies

In this section, we prove Theorem 5.2.22 which played a key role in the proof of Proposition 5.2.13. The proof will be given at the end of the section, after some preliminary work. The key idea is to reduce the proof of Theorem 5.2.22 to the study of convex cones. More precisely, we consider the tangent cone to the individual convex bodies at the given common point. Recall the *support cone* (sometimes also

called *tangent cone* or *projection cone*) of a convex body $K \subset \mathbb{R}^d$ at a point x in K:

$$S_K(x) = \overline{\mathbb{R}_{>0}(K - x)}.$$

The dual notion is the *normal cone* to K at x:

$$N_K(x) := \left\{\ell \in (\mathbb{R}^d)^* \colon \ell\,(x' - x) \geq 0 \text{ for any } x' \in K\right\}.$$

It is a well-known fact that the support cone is a closed convex cone whose dual cone is the normal cone, i.e. $S_K(x) = N_K(x)^\vee$. Furthermore, note that the dimension of the convex body K coincides with the dimension of its support cone $S_K(x)$ at any point x in K.

In Theorem 5.2.22, we study an intersection of convex bodies whose dimension is strictly less than the ambient dimension, and by what we have just said, it suffices to consider the involved tangent cones. Note that the linear forms defining the half spaces of Theorem 5.2.22 are elements in the normal cones to the individual convex bodies. A key step in the proof of Theorem 5.2.22 will be to understand how the tangent cone to the intersection of the convex bodies relates to the individual tangent cones. To this end, we recall the following well-known statement which relates the dual of an intersection of closed convex cones to the individual dual cones.

Proposition 5.2.23. *Let $C_1, \ldots, C_n \subset \mathbb{R}^d$ be closed convex cones. Then we have*

$$(C_1 \cap \ldots \cap C_n)^\vee = \overline{C_1^\vee + \cdots + C_n^\vee}.$$

The following example shows that in general it is necessary to take the closure in Proposition 5.2.23:

Example 5.2.24. Let $C_1 = \{(x, y, z) \in \mathbb{R}^3 \colon x^2 + y^2 \leq z^2, z \geq 0\}$ and $C_2 = \mathbb{R}_{\geq 0}(1, 0, -1)$ (see Figure 5.4). Then $x_t := (-t, 1 + \frac{1}{t}, \sqrt{t^2 + (1 + \frac{1}{t})^2}) \in C_1$ and $y_t := (t, 0, -t) \in C_2$. It

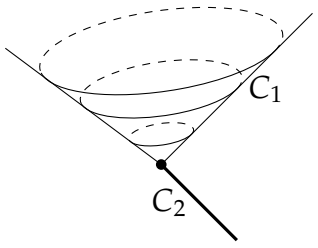

FIGURE 5.4: Illustration of the cones in Example 5.2.24.

is straightforward to verify that $\lim_{t\to\infty}(x_t + y_t) = (0, 1, 0)$ is contained in the closure of the sum of cones $C_1 + C_2$, but not in the sum.

Observe also that in this example, the line $\mathbb{R}(1, 0, -1)$ has one half-ray $\rho = \mathbb{R}_{>0}(-1, 0, 1)$ contained in C_1 and its other half-ray $-\rho$ contained in the other cone C_2. Waksman and Epelman [104] observed that such a line exists whenever the sum of two closed convex cones isn't closed:

Theorem 5.2.25 ([104, Theorem on p. 95]). *Suppose $d \geq 3$. Let $C_1, C_2 \subset \mathbb{R}^d$ be two closed convex cones. If the sum $C_1 + C_2$ is not closed, then there exists a straight line $L = \rho + (-\rho)$ where $\rho = \mathbb{R}_{>0}x$ for some $\mathbf{0} \neq x \in L$ such that $\rho \subset C_1$ and $-\rho \subset C_2$.*

Remark 5.2.26. Note that if the ambient dimension d is less than or equal to 2, then every closed convex cone is polyhedral. It is a well-known fact that the sum of two polyhedral cones is always closed. Indeed, if $x_1, \ldots, x_r, y_1, \ldots, y_s \in \mathbb{R}^d$ (any dimension d), then $\operatorname{cone}(x_1, \ldots, x_r) + \operatorname{cone}(y_1, \ldots, y_s) = \operatorname{cone}(x_1, \ldots, x_r, y_1, \ldots, y_s)$, and thus the sum is closed. In particular, Theorem 5.2.25 is an empty statement for $d \leq 2$, and Waksman and Epelman exclude these dimensions from their statement.

Corollary 5.2.27. *Suppose $d \geq 3$. Let $C_1, \ldots, C_n \subset \mathbb{R}^d$ be closed convex cones. If the sum $C_1 + \cdots + C_n$ is not closed, then there exists a straight line $L = \rho + (-\rho)$ where $\rho = \mathbb{R}_{>0}x$ for some $\mathbf{0} \neq x \in L$ such that $\rho \subset C_i$ and $-\rho \subset C_1 + \cdots + \widehat{C_i} + \cdots + C_n$ for some index $i = 1, \ldots, n$.*

Here, the notation $C_1 + \cdots + \widehat{C_i} + \cdots + C_n$ means that we omit the i-th summand.

Proof. We do induction on n. The base case $n = 2$ is Theorem 5.2.25. Suppose $n > 2$. If $C_2 + \cdots + C_n$ is not closed, by the induction hypothesis, there is a straight line $L = \rho + (-\rho)$ where $\rho = \mathbb{R}_{>0}x$ for some $\mathbf{0} \neq x \in L$ such that $\rho \subset C_i$ and $-\rho \subset C_2 + \cdots + \widehat{C_i} + \cdots + C_n$ for some $i \in \{2, \ldots, n\}$. The statement then follows, since $C_2 + \cdots + \widehat{C_i} + \cdots + C_n \subset C_1 + C_2 + \cdots + \widehat{C_i} + \cdots + C_n$. If instead $C := C_2 + \cdots + C_n$ is closed, it is a closed convex cone, and by Theorem 5.2.25, there exists a straight line $L = \rho + (-\rho)$ where $\rho = \mathbb{R}_{>0}x$ for some $\mathbf{0} \neq x \in L$ such that $\rho \subset C_1$ and $-\rho \subset C_2 + \cdots + C_n$. □

The following statement will be used in the proof of Theorem 5.2.22.

Lemma 5.2.28. *If $C \subset \mathbb{R}^d$ is a closed convex cone, then there are finitely many linear forms $\ell_1, \ldots, \ell_n \in C^\vee$ such that*

$$\dim\Big(\{x \in \mathbb{R}^d : \ell_1(x) \geq 0\} \cap \ldots \cap \{x \in \mathbb{R}^d : \ell_n(x) \geq 0\}\Big) = \dim(C).$$

Proof. Let $e_1, \ldots, e_r \in C$ be a basis of the $\mathbb{R}$-linear span of C. We extend these linearly independent vectors to a basis of $\mathbb{R}^d$, say $e_1, \ldots, e_r, e_{r+1}, \ldots, e_d$. Let $f_1, \ldots, f_d$ be the dual basis of $(\mathbb{R}^d)^*$. Then we have $\pm f_{r+1}, \ldots, \pm f_d \in C^\vee$, and thus

$$\dim\left(\bigcap_{i=r+1}^{d} \{x \in \mathbb{R}^d : f_i(x) \geq 0\} \cap \bigcap_{i=r+1}^{d} \{x \in \mathbb{R}^d : -f_i(x) \geq 0\}\right) = \dim(C).$$

□

We are now ready to prove Theorem 5.2.22.

Proof of Theorem 5.2.22. Note $\dim(K) = \dim(S_K(x))$. Furthermore, the set of supporting hyperplanes of the tangent cone $S_{K_i}(x)$ at x coincides with the set of supporting hyperplanes of K_i at x. We continue by investigating the tangent cones $S_K(x), S_{K_1}(x), \ldots, S_{K_n}(x)$ and their relations.

The following equality is straightforward to verify:

$$\mathbb{R}_{>0}(K-x) = \mathbb{R}_{>0}\left((K_1 \cap \ldots \cap K_n) - x\right) = \mathbb{R}_{>0}(K_1 - x) \cap \ldots \cap \mathbb{R}_{>0}(K_n - x).$$

Since the dimension of the closure of a convex set coincides with the dimension of the original set, we get

$$\dim(S_K(x)) = \dim\left(\mathbb{R}_{>0}(K-x)\right) = \dim\left(\mathbb{R}_{>0}(K_1 - x) \cap \ldots \cap \mathbb{R}_{>0}(K_n - x)\right) < d. \quad (5.2)$$

We claim that $\dim(S_{K_1}(x) \cap \ldots \cap S_{K_n}(x)) < d$ as well. Assume towards a contradiction that the dimension of the intersection of the support cones were d, i.e., the intersection of the support cones is full-dimensional. Then the intersection of the support cones contains an affine basis of $\mathbb{R}^d$, and thus a full-dimensional simplex Δ. Let y be the barycentre of Δ. Let $\Delta' \subset \Delta$ be the simplex obtained by shrinking Δ with respect to its barycentre, e.g. $\Delta' = \frac{1}{2}(\Delta - y) + y$. Then the smaller simplex Δ' is contained in the interior of every tangent cone $S_{K_i}(x)$ for $i = 1, \ldots, n$, and thus

$$\Delta' \subset \mathbb{R}_{>0}(K_1 - x) \cap \ldots \cap \mathbb{R}_{>0}(K_n - x),$$

which is a contradiction to inequality (5.2).

Hence $\dim(S_{K_1}(x) \cap \ldots \cap S_{K_n}(x)) < d$. By Proposition 5.2.23, we have

$$(S_{K_1}(x) \cap \ldots \cap S_{K_n}(x))^\vee = \overline{N_{K_1}(x) + \cdots + N_{K_n}(x)}.$$

We distinguish two cases, namely whether $N_{K_1}(x) + \cdots + N_{K_n}(x)$ is closed or not.

Suppose $N_{K_1}(x) + \cdots + N_{K_n}(x)$ is closed. By Lemma 5.2.28, there exist linear forms $\ell_1, \ldots, \ell_r \in (S_{K_1}(x) \cap \ldots \cap S_{K_n}(x))^\vee$ such that

$$\dim(\{y \in \mathbb{R}^d \colon \ell_1(y) \geq 0\} \cap \ldots \cap \{y \in \mathbb{R}^d \colon \ell_n(y) \geq 0\}) = \dim(S_{K_1}(x) \cap \ldots \cap S_{K_n}(x)) < d. \quad (5.3)$$

Since $(S_{K_1}(x) \cap \ldots \cap S_{K_n}(x))^\vee = N_{K_1}(x) + \cdots + N_{K_n}(x)$, every linear form ℓ_j can be expresses as a sum $\ell_j = \ell_{1,j} + \cdots + \ell_{n,j}$ for some linear forms $\ell_{i,j} \in N_{K_i}(x)$. We define $H^+(i,j) = \{y \in \mathbb{R}^d \colon \ell_{i,j}(y) \geq 0\}$. Then the intersection of all these closed half-spaces is a polyhedral cone C whose dual cone is given by $C^\vee = \operatorname{cone}(\{\ell_{i,j} \colon i = 1, \ldots, n; j = 1, \ldots r\})$. The dual cone $C^\vee$ contains the cone $D := \operatorname{cone}(\ell_1, \ldots, \ell_r) \subset (\mathbb{R}^d)^*$, and thus $C \subset D^\vee$. Since, by Equation (5.3), $\dim(D^\vee) < d$, we are done.

Suppose now $N_{K_1}(x) + \cdots + N_{K_n}(x)$ is not closed. Then by Corollary 5.2.27, there exists a straight line $L = \rho + (-\rho) \subset (\mathbb{R}^d)^*$ where $\rho = \mathbb{R}_{>0}\ell$ for some $\mathbf{0} \neq \ell \in L$ such that $\rho \subset N_{K_i}(x)$ and $-\rho \subset N_{K_1}(x) + \cdots + \widehat{N_{K_i}(x)} + \cdots + N_{K_n}(x)$ for some index $i = 1, \ldots, n$. There exist $\ell_j \in N_{K_j}(x)$ for $j \neq i$ such that $-\ell = \ell_1 + \cdots + \widehat{\ell_i} + \cdots + \ell_n$. We define $H_i^+ := \{y \in \mathbb{R}^d \colon \ell(y) \geq 0\}$ and $H_j^+ := \{y \in \mathbb{R}^d \colon \ell_j(y) \geq 0\}$ for $j \neq i$. Let C be the intersection of these closed half-spaces. Then the dual cone is given by $C^\vee = \operatorname{cone}(\ell, \ell_1, \ldots, \widehat{\ell_i}, \ldots, \ell_n)$ which contains the straight line L. Thus $C \subset L^\vee$ where $\dim(L^\vee) = d - 1$. □

Remark 5.2.29. Note the proof of Theorem 5.2.22 shows that the sets $\{H^+(i,j)\}_{j\in J_i}$ for $i = 1,\dots,n$ can be chosen such that $|J_i| \leq 2$.

5.3 Preliminary observations in dimensions 1 and 2

Let us begin our quest of determining $\mathrm{Flt}_d^A(\Delta_d)$ for $d = 1,2$ and $A \in \{\mathbb{Z},\mathbb{R}\}$. We first settle the one-dimensional case. By Remark 5.2.1, the flatness constants of bounded sets $X \subset \mathbb{R}$ whose convex hull is full-dimensional are completely characterised by the flatness constants of closed intervals $I = [x,y] \subset \mathbb{R}$.

Recall that the floor of a real number x, $\lfloor x \rfloor$, is the largest integer which is less than or equal to x. Similarly, the ceiling of a real number x, $\lceil x \rceil$, is the smallest integer that is greater than or equal to x.

Theorem 5.3.1. *Let $I = [x,y] \subset \mathbb{R}$, with $x \leq y$. Set $\delta := \lceil x+y \rceil$. Then*

$$\mathrm{Flt}_1^{\mathbb{Z}}(I) = \begin{cases} 1+2y-\delta & \text{if } \delta-(x+y) \leq \frac{1}{2}, \\ \delta - 2x & \text{otherwise.} \end{cases}$$

Proof. Let $\mathfrak{I}$ be the set of all transformed intervals under $\mathbb{Z}$-unimodular transformations, i.e., $\mathfrak{I} := \{T(I) : T \text{ a } \mathbb{Z}\text{-unimodular transformation}\}$. Note that $\mathfrak{I}$ comes equipped with a total ordering, namely $[x,y] < [x',y']$ if $x < x'$. In this proof, we will simply write "I-free" for "$\mathbb{Z}$-I-free".

We call two intervals $J < J'$ in $\mathfrak{I}$ *successive* if for any interval $J'' \in \mathfrak{I}$ such that $J \leq J'' \leq J'$ it follows that either $J = J''$ or $J' = J''$. It is straightforward to show that the inclusion-maximal I-free convex bodies are exactly the convex hulls of unions of two successive intervals in $\mathfrak{I}$.

It remains to determine the structure of $\mathfrak{I}$ with respect to its total order. As $\mathfrak{I}$ is the union of $I+\mathbb{Z}$ and $-I+\mathbb{Z}$, there can be at most one translate of $-I$ between I and $I+1$, say $I \leq -I+\delta < I+1$.

Set $\delta := \lceil x+y \rceil$. Then it's clear that $x \leq -y+\delta < x+1$, i.e. that $I \leq -I+\delta < I+1$.

Now, $I = -I+\delta$ if and only if $\delta = x+y$. In this case, every maximal I-free interval is a translation of $I \cup (I+1) = [x, y+1]$. This has width $1+y-x$, which also coincides with $1+2y-\delta$.

Finally, we consider the case $I \neq -I+\delta$. Here, every maximal I-free interval is a translation of either $(-I+\delta-1)\cup I = [-y+\delta-1, y]$ or $I \cup (-I+\delta) = [x, -x+\delta]$. These have respective widths $1+2y-\delta$ and $\delta-2x$. Thus, the flatness constant will be the maximum of the two. Further, it can be seen that the former width is the maximum of the two if and only if $\delta-(x+y) \leq \frac{1}{2}$.

□

Remark 5.3.2. Note that in the situation of Theorem 5.3.1, we have $\mathrm{Flt}_1^{\mathbb{R}}(I) = y-x$. Indeed, the maximal I-free convex bodies are exactly the translates of I.

Furthermore, Theorem 5.3.1 shows that in general $\mathrm{Flt}_1^{\mathbb{Z}}(nX) \neq n\mathrm{Flt}_1^{\mathbb{Z}}(X)$ $(n \in \mathbb{N})$. Indeed, using Theorem 5.3.1, we immediately find that $\mathrm{Flt}_1^{\mathbb{Z}}([0,\frac{4}{3}]) = 2$ while $2 \cdot$

$\mathrm{Flt}_1^{\mathbb{Z}}([0, \frac{2}{3}]) = \frac{8}{3}$. This answers the question in [7] whether $\mathrm{Flt}_d^{\mathbb{Z}}(\cdot)$ is linear with respect to positive dilations.

This gives a complete answer in 1 dimension for full-dimensional $X \subset \mathbb{R}$. Let us now turn to 2 dimensions. Recall from Section 5.2 our general strategy: considering inclusion-maximal A-Δ_2-free closed convex sets C, we obtain an upper bound for $\mathrm{Flt}_d^A(\Delta_2)$. Furthermore, recall that since Δ_2 is full-dimensional, it suffices to consider full-dimensional inclusion-maximal A-Δ_2-free closed convex sets C (see Lemma 5.2.5). Here, we will classify the unbounded C. Their widths will turn out to be strictly smaller than the maximal width of the bounded C's. Hence, the maximal width of the bounded C's will be then equal to the respective flatness constant.

Proposition 5.3.3. *Let $A \in \{\mathbb{R}, \mathbb{Z}\}$. Then up to A-unimodular transformations there exists exactly one unbounded inclusion-maximal A-Δ_2-free closed convex set $C \subset \mathbb{R}^2$ of dimension* 2*, namely*

- *if $A = \mathbb{Z}$, then $C = [-1, 1] \times \mathbb{R}$; and*
- *if $A = \mathbb{R}$, then $C = [0, 1] \times \mathbb{R}$.*

In particular, the width is 2 *in the first and* 1 *in the second case.*

For the proof of the previous statement, we need to recall the definition of the *tail cone* (or *recession cone*) of a closed convex set $A \subset \mathbb{R}^d$:

$$\mathrm{tail}(A) := \left\{ v \in \mathbb{R}^d : \ x + \lambda v \in A \text{ for all } x \in A \text{ and } \lambda \geq 0 \right\}.$$

Proof. Since $C \subset \mathbb{R}^2$ is an unbounded closed convex set, it follows by [89, Theorem 8.4] that $\mathrm{tail}(C) \neq \{\mathbf{0}\}$. Then $\mathrm{tail}(C)$ is a 1-dimensional closed convex cone. Hence $\mathrm{tail}(C)$ lies on a line $y = m \cdot x$ for a real number $m \in \mathbb{R}$. We claim $m \in \mathbb{Q}$ is rational.

Assume towards a contradiction that $m \in \mathbb{R} \setminus \mathbb{Q}$ were irrational. Since C is full-dimensional, it contains a small affine ball $v + \varepsilon B^2$ for $v \in \mathbb{R}^2$ and $\varepsilon > 0$. Indeed, by approximating v with a rational point and decreasing ε (if necessary), we may assume that $v \in \mathbb{Q}^2$. Then $v + \varepsilon B^2 + \mathrm{tail}(C)$ is contained in C where $v + \mathrm{tail}(C)$ lies on an affine line parallel to $y = m \cdot x$, say $\{y = m \cdot x + c\} \subset \mathbb{R}^2$ for $c \in \mathbb{R}$. Note $(v + \mathrm{tail}(C)) \cap \mathbb{Q}^2 = \{v\}$ as otherwise m would be a rational number (a contradiction). By Kronecker's theorem [70] (see also [39, Theorem 438] or [49, Theorem 1]), for every $\delta, N > 0$ there exist integers $x_\delta, y_\delta \in \mathbb{Z}$ with $|x_\delta| \geq N$ (where both $x_\delta > 0$ and $x_\delta < 0$ can be chosen) such that $|m \cdot x_\delta + c - y_\delta| < \delta$, i.e., (x_δ, y_δ) comes arbitrarily close to $v + \mathrm{tail}(C)$.

Let $x, y, z \in \mathbb{Z}^2$ be three lattice points that were chosen so that y lies strictly closer to $v + \mathrm{tail}(C)$ than x while z lies closer to $v + \mathrm{tail}(C)$ than y. We may assume that x, y, z lie in $v + \varepsilon B^2 + \mathrm{tail}(C)$, and thus in the interior of C. It follows that $\mathrm{conv}(x, y, z)$ is a lattice triangle contained in the interior of C. Triangulating this triangle into empty simplices yields a $\mathbb{Z}$-unimodular copy of Δ_2 that is contained in the interior of C. A contradiction. Note that this solves both cases $A = \mathbb{R}$ and $A = \mathbb{Z}$.

Hence $m \in \mathbb{Q}$ is rational, and thus up to a $\mathbb{Z}$-unimodular transformation, we have that $v + \mathrm{tail}(C)$ lies on the line given by $x = c$ for some $c \in \mathbb{R}$. Consider the

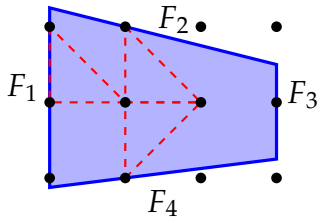

FIGURE 5.5: Facets F_1, F_2 and F_4 of this $\mathbb{Z}$-Δ_2-free polygon are locked, while F_3 is not. Dashed in red are $\mathbb{Z}$-unimodular copies of Δ_2 that are locking the respective facets. Note the polygon is indeed $\mathbb{Z}$-Δ_2-free since all interior lattice points are collinear.

projection $\pi\colon \mathbb{R}^2 \to \mathbb{R}; (a,b) \mapsto a$. Since C is convex, the closure of the image $\pi(C)$ is an interval, say $I = [r,s]$ for $r, s \in \mathbb{R}$. Note the tail cone $\operatorname{tail}(C)$ ensures that for any u in I there exists an affine ray $w + \operatorname{tail}(C) \subset C$ that projects down to u.

Suppose $A = \mathbb{Z}$. Then $s - r \leq 2$, as otherwise I would contain two integers in its interior which would imply that C contains a $\mathbb{Z}$-unimodular copy of Δ_2 in its interior. It straightforwardly follows that (up to a translation by a lattice point) $C = [-1,1]\times\mathbb{R}$.

Suppose $A = \mathbb{R}$. Then $s - r \leq 1$, as otherwise I would contain an $\mathbb{R}$-translate of the interval $[0,1]$ in its interior which would imply that C contains an $\mathbb{R}$-unimodular copy of Δ_2 in its interior. Then it is easy to see that (up to a real translation) $C = [0,1] \times \mathbb{R}$. □

It remains to study the bounded cases. The remaining sections of this manuscript will be concerned with this study.

5.4 The $\mathbb{Z}$-flatness constant of Δ_2

Let $K \subset \mathbb{R}^d$ be a convex body and let $X \subset \mathbb{R}^d$ be an arbitrary bounded set. By Proposition 5.2.12, inclusion-maximal $\mathbb{Z}$-X-free bodies are polytopes (a stronger version of Theorem 5.1.2 for the case $A = \mathbb{Z}$). The following definition is the key to characterising inclusion-maximal $\mathbb{Z}$-Δ_d-free polytopes.

Definition 5.4.1. A facet F of a full-dimensional polytope $P \subset \mathbb{R}^d$ is said to be $\mathbb{Z}$-Δ_d-*locked* if there exists a $\mathbb{Z}$-unimodular copy T of Δ_d contained in P such that $T \cap \operatorname{rel}(F) \neq \emptyset$ and $V(T) \setminus \operatorname{rel}(F) \subset \operatorname{int}(P)$, where $V(T)$ denotes the set of vertices of T. Notice that T gives rise to lattice points in the relative interior of F, namely $V(T) \cap \operatorname{rel}(F)$. Such lattice points are called *locking points*.

We will say simply *locked* instead of $\mathbb{Z}$-Δ_d-locked wherever it is clear from the context that we are discussing $\mathbb{Z}$-Δ_d-flatness. See Figure 5.5 for an illustration of the concepts of "locked facet" and "locking point". The definition of locked facet is crafted so that if a point is added beyond any locked facet, the resulting polytope is no longer a $\mathbb{Z}$-Δ_d-free polytope. Recall that a point x is *beyond* the facet F of a full-dimensional polytope P if it lies in the half-space which is defined by the supporting

hyperplane of F and which does not contain $\text{int}(P)$. Furthermore, x is *beneath* F if it lies in the same half-space as P.

The following proposition shows that being inclusion-maximal among $\mathbb{Z}$-Δ_d-free polytopes is equivalent to all facets being locked.

Proposition 5.4.2. *Let $P \subset \mathbb{R}^d$ be a $\mathbb{Z}$-Δ_d-free polytope. Then, P is inclusion-maximal if and only if all its facets are locked.*

Proof. Suppose that all facets of P are locked. Let F be a facet of P and $x \in \mathbb{R}^d \setminus P$ be a point beyond F. Since F is locked, there exists a $\mathbb{Z}$-unimodular copy T of Δ_d contained in P such that $T \cap \text{rel}(F) \neq \emptyset$ and $V(T) \setminus \text{rel}(F) \subset \text{int}(P)$. Let $Q = \text{conv}(P, x)$. The relative interior of the facet F lies in the interior of Q, and thus so does T. Hence P is inclusion-maximal with respect to the property of being $\mathbb{Z}$-Δ_d-free.

We prove the reverse implication by verifying the contrapositive, i.e., if there exists a facet of P that is not locked, then P isn't inclusion-maximal with respect to the property of being $\mathbb{Z}$-Δ_d-free. Let F be a facet of P that is not locked and let Q be the polytope obtained from P by moving the facet F outwards by a small amount, such that $P \subsetneq Q$ but no new lattice points are captured, that is, $P \cap \mathbb{Z}^d = Q \cap \mathbb{Z}^d$. In particular, the set of $\mathbb{Z}$-unimodular copies of Δ_d which are contained in P coincides with the set of such copies that are contained in Q. Note however that any lattice point in the relative interior of the facet F of P are in the interior of Q. From the assumption that F is not locked we will now deduce that Q is also a $\mathbb{Z}$-Δ_d-free polytope, and thus P is not inclusion-maximal.

Let H be the supporting hyperplane that defines the facet F of P, and let $H_{\geq 0}$ (resp. $H_{>0}$) be the closed half-space (resp. open half-space) with boundary equal to H such that $P \subset H_{\geq 0}$. Notice $Q \cap H_{\geq 0} = P$. It remains to show that any $\mathbb{Z}$-unimodular copy T of Δ_d that is contained in Q isn't contained in the interior of Q. Recall from above that T is also contained in P. We distinguish two cases:

- If $T \cap \text{rel}(F) = \emptyset$, then $T \subset Q \cap H_{>0} = P \setminus F$. Since $Q \cap H_{\geq 0} = P$ and $T \not\subset \text{int}(P)$, it straightforwardly follows that $T \not\subset \text{int}(Q)$.
- If $T \cap \text{rel}(F) \neq \emptyset$, then $V(T) \setminus \text{rel}(F) \not\subset \text{int}(P)$, i.e., there is another facet F' of P that contains a vertex of T. Since F' is contained in a facet of Q, it follows that $T \not\subset \text{int}(Q)$. □

We now focus on dimension $d = 2$, where our goal is to show the following theorem.

Theorem 5.4.3 (Case $A = \mathbb{Z}$ of Theorem 5.1.1)**.** $\text{Flt}_2^{\mathbb{Z}}(\Delta_2) = \frac{10}{3}$.

By Lemma 5.2.3, to prove the theorem it is enough to show that any inclusion-maximal $\mathbb{Z}$-Δ_2-free convex set has width at most $\frac{10}{3}$ and to provide an example of a $\mathbb{Z}$-Δ_2-free polygon of that width. Unbounded full-dimensional inclusion-maximal $\mathbb{Z}$-Δ_2-free convex sets were studied in Proposition 5.3.3 and have width 1. Thus we are left with determining the maximum width of inclusion-maximal $\mathbb{Z}$-Δ_2-free convex bodies, which are polygons by Theorem 5.1.2. The rest of the section is devoted to proving that this width is $\frac{10}{3}$.

Note Proposition 5.4.2 guarantees that any inclusion-maximal $\mathbb{Z}$-Δ_2-free polygon contains at least one interior lattice point, since otherwise it is impossible for its facets to be locked. The following proposition deals with (inclusion-)maximal $\mathbb{Z}$-Δ_2-free polygons containing exactly one interior lattice point. The case of polygons whose interior contains at least two lattice points will be treated afterwards.

Proposition 5.4.4. *If $P \subset \mathbb{R}^2$ is a maximal $\mathbb{Z}$-Δ_2-free polygon with $|\text{int}(P) \cap \mathbb{Z}^2| = 1$, then $\text{width}(P) \leq 3$.*

Proof. Let P be an inclusion-maximal $\mathbb{Z}$-Δ_2-free polygon with exactly one interior lattice point. By Proposition 5.4.2, each facet F of P is locked. Since there's a unique lattice point in the interior of P, for each facet F there is a $\mathbb{Z}$-unimodular copy T of Δ_2 contained in P such that two vertices of T are contained in the relative interior of F and the third vertex of T is in the interior of P. Up to an appropriate unimodular transformation, we may assume that there is a facet for which $T = \text{conv}(\mathbf{0}, e_1, e_2)$, and that $\mathbf{0}$ is the interior lattice point of P. By using the fact that $\mathbf{0}$ is the only interior lattice point of P, we can conclude that P is disjoint from the following regions (see Figure 5.6):

C_1 The affine cone $(-e_1 + e_2) + \text{cone}(-e_1, -e_1 + e_2)$ minus its apex $-e_1 + e_2$ (otherwise $-e_1 + e_2$ would be contained in the interior of P. Note that we include the open half-rays of the affine cone into C_1 because $\mathbf{0}$ is in the interior of P and e_2 is in the relative interior of F);

C_2 The affine cone $-e_1 + \text{cone}(-e_1, -e_1 - e_2)$ minus its apex $-e_1$ (otherwise $-e_1$ would be contained in the interior of P);

C_3 The affine cone $(-e_1 - e_2) + \text{cone}(-2e_1 - e_2, -e_1 - 2e_2)$ minus its apex $(-e_1 - e_2)$ (otherwise $-e_1 - e_2$ would be contained in the interior of P).

Let C_i' be the region obtained from C_i by reflecting along the line $\mathbb{R}(e_1 + e_2)$. Notice $C_3 = C_3'$. Since $\mathbf{0}$ is the only interior lattice point, it follows from Proposition 5.4.2 that every facet of P contains two lattice points in its relative interior. We already know that $\{x + y = 1\}$ cuts out a facet of P. For the remaining facets, the only candidates are lattice points disjoint from the regions C_i, C_i' and contained in the open half-plane $\{x + y < 1\}$, i.e., $-e_1+e_2$, $-e_1$, $-e_1-e_2$, $-e_2$, e_1-e_2, those drawn in Figure 5.6. It is easy to see that the possibility for P to have two other facets each containing two of these lattice points in the relative interior is if $P = \text{conv}(-e_1+2e_2, -e_1-e_2, 2e_1-e_2)$, which has width equal to 3. □

Now suppose the polygon P contains at least two interior lattice points. Clearly these interior lattice points are collinear, since any set of non-collinear points contains a triangle, and any lattice triangle can be triangulated into unimodular ones, and thus in particular contains a unimodular triangle.

The following theorem shows that polygons with at least two interior lattice points can have larger width than 3 and the maximum width is achieved by a triangle with exactly two interior lattice points.

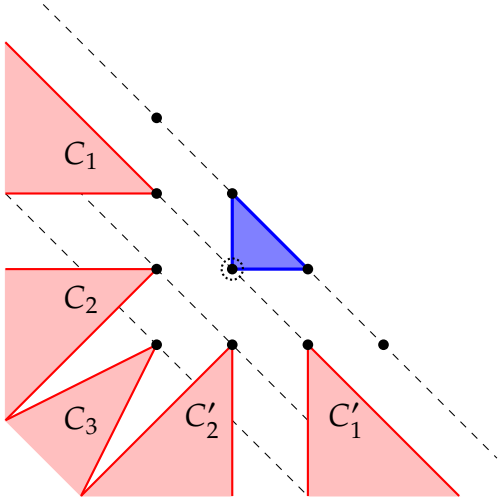

FIGURE 5.6: The regions C_i and C_i' which are disjoint from P.

Theorem 5.4.5. *If $P \subset \mathbb{R}^2$ is a $\mathbb{Z}$-Δ_2-free polygon with $|\text{int}(P) \cap \mathbb{Z}^2| \geq 2$, then $\text{width}(P) \leq \frac{10}{3}$. Equality is only achieved (up to $\mathbb{Z}$-unimodular transformations) by $\text{conv}\left(\frac{1}{3}e_1 + \frac{5}{3}e_2, -\frac{4}{3}e_1 - \frac{5}{3}e_2, 2e_1\right)$, which contains exactly 2 interior lattice points.*

In order to prove Theorem 5.4.5, it suffices to study inclusion-maximal $\mathbb{Z}$-Δ_2-free polygons which have at least two interior lattice points. Since in Proposition 5.4.4 we have already found a $\mathbb{Z}$-Δ_2-free triangle with width equal to 3, to find the polygons of largest width we can restrict our study to those whose width is greater than 3. The strategy for the proof is to use Proposition 5.4.2 and to distinguish polygons according to their locking lattice points.

Thus from now on we let P be a maximal $\mathbb{Z}$-Δ_2-free polygon with at least two interior lattice points and width strictly greater than 3. Up to an affine unimodular transformation, we may assume that

- the interior of P contains $\mathbf{0}$ and e_1,
- any lattice point which does not lie on the horizontal axis is not in the interior of P, and
- P contains a point $p_0 = xe_1 + ye_2$ with $0 < x < 1$ and $y > \frac{3}{2}$.

Indeed, there is a $\mathbb{Z}$-unimodular transformation that maps the lattice segment comprised by the interior lattice points of P (recall they are collinear) onto a lattice segment lying on the x-axis. Since this lattice segment has lattice length at least one, we can assume that both $\mathbf{0}$ and e_1 are contained in it. To simplify notation, let us use the same symbol P for the transformed polygon. Since the width of P is larger than 3, it cannot be contained in the strip $\left\{-\frac{3}{2} \leq y \leq \frac{3}{2}\right\}$. After possibly flipping along the x-axis, this shows that P contains a point p_0 whose y-coordinate is larger than $\frac{3}{2}$. Note the triangle with vertices $\mathbf{0}$, e_1 and p_0 intersects the line $\{y = 1\}$ in a segment of length less than 1 which does not contain lattice points (as otherwise such a lattice point would be in the interior of P). After applying an appropriate

horizontal shearing this segment lies in the strip $\{0 \leq x < 1\}$, and thus so does p_0. Recall that a linear unimodular transformation $\varphi\colon \mathbb{Z}^2 \to \mathbb{Z}^2$ of the form

$$\varphi(\lambda_1 b_1 + \lambda_2 b_2) = (\lambda_1 + k\lambda_2)\, b_1 + \lambda_2 b_2,$$

for a lattice basis b_1, b_2 of $\mathbb{Z}^2$ and an integer $k \in \mathbb{Z}$ is called a *shearing along the line* $\mathbb{R}b_1$.

Suppose P has been transformed to satisfy the conditions above. Let us determine the possible lattice points that can lock a facet of P. No lattice point on the x-axis can lock a facet, since they are collinear with the interior lattice points of P. Since the triangle $T := \operatorname{conv}(\mathbf{0}, e_1, p_0)$ is contained in P, it follows that the affine locally open rays $e_2 + \mathbb{R}_{<0}e_1$ and $e_1 + e_2 + \mathbb{R}_{>0}e_1$ are disjoint from P. Hence the only lattice points in the upper half-plane $\{y > 0\}$ that can be contained in P are e_2 and $e_1 + e_2$ (any other lattice point in $\{y > 0\}$ forces e_2 or $e_1 + e_2$ to be in the interior of P). Next we determine which lattice points in the lower half-space $\{y < 0\}$ can be contained in P. Since $p_0 \in P$, every lattice point in $\{y < 0\}$ which is in the upper closed half-space given by the line going through the two points e_2, $e_1 + \frac{3}{2}e_2$ is disjoint from P (otherwise e_2 is in the interior of P). Using the symmetry induced by reflecting about the vertical line $\left\{x = \frac{1}{2}\right\}$, it follows that $P \cap \{y < 0\}$ is also disjoint from the upper closed half-space given by the line through the two points $\frac{3}{2}e_2$, $e_1 + e_2$. Note the remaining lattice points at height $y = -1$ could be contained in P: $-3e_1 - e_2, -2e_1 - e_2, -e_1 - e_2, -e_2, e_1 - e_2, 2e_1 - e_2, 3e_1 - e_2$ or $4e_1 - e_2$. Let $q_k := ke_1 - e_2$ for $k \in \{-3, -2, -1\}$. Since q_k cannot be an interior lattice point of P, it follows that P is disjoint from the region C_k which is defined to be $\sigma_k \setminus \{q_k\}$ where σ_k is the affine cone having apex at q_k and supporting lines going through q_k and e_1 or $e_1 + \frac{3}{2}e_2$ respectively. For $q_0 = -e_2$, the respective region is $C_0 = \sigma_0 \setminus \{q_0\}$ where σ_0 is the affine cone having apex at q_0 and supporting lines the y-axis and the line going through $-e_2$ and e_1 (see Figure 5.7). By using the symmetry induced by reflecting

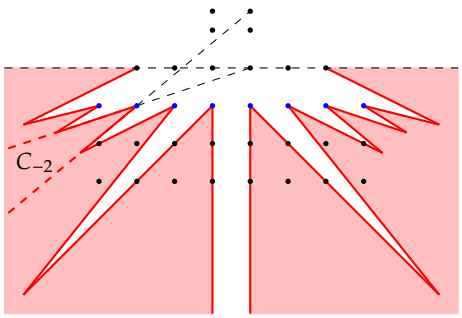

FIGURE 5.7: Possible locking points in the lower half-plane in blue. P is disjoint from the red regions as otherwise it would pick up interior lattice points away from the x-axis.

about the vertical axis $\left\{x = \frac{1}{2}\right\}$, it straightforwardly follows that the possible lattice points that can be contained in P and that lie in the lower half-plan $\{y < 0\}$ can only be those from above at height $y = -1$.

These ten lattice points (two at height $y = 1$ and eight at height $y = -1$; shown in red in Figure 5.8) are therefore the only lattice points away from the x-axis which

can be contained in P, and thus are the possible locking points. Next we show that the assumption width$(P) > 3$ implies that at most four of them can be in P, more precisely, at most two of the points at height $y = -1$ can be in P. Recall our (additional) assumption that the polygon P is inclusion-maximal $\mathbb{Z}$-Δ_2-free.

Lemma 5.4.6. *If $P \cap \{y = -1\}$ contains at least 3 lattice points, then* width$(P) \leq 3$.

In the following, let us denote the basis of $(\mathbb{Z}^2)^*$ dual to e_1, e_2 by e_1^*, e_2^*.

Proof. Suppose P contains at least 3 lattice points whose y-coordinate equals -1. Then P is contained in the half-space $\{y \geq -1\}$, since any point outside this half-space would force the middle lattice point to be in the interior of P, which is not allowed. In particular, there is a facet F supported by $\{y = -1\}$. All other facets of P are locked (see Proposition 5.4.2), and since they cannot be locked by points on $\{y = -1\}$, they can only be locked by e_2 and $e_1 + e_2$. Thus P is a triangle with one facet F, one facet through e_2 and another through $e_1 + e_2$. The latter two facets intersect in the vertex p_0 from above.

If P is contained within the strip $\{-1 \leq y \leq 2\}$, then width$(P) \leq 3$. If not, we have $p_0 \in \{y > 2\}$. Let us consider the facet F of length b as the base of the triangle P. With respect to this base, P has height $h > 3$. The triangle conv$(e_2, e_1 + e_2, p_0)$ is similar to P and has base of length 1 and height $h - 2$. From the assumption $h > 3$ and the equality (compare with the intercept theorem)

$$\frac{h-2}{1} = \frac{h}{b},$$

we obtain $b < 3$. Note b is the length of the facet F. Since p_0 lies in $\{0 < x < 1\}$ and the facets of P that intersect at p_0 pass through e_2 and $e_1 + e_2$ respectively, these facets must have positive and negative slope respectively. This means that the width of P with respect to the linear form e_1^* is b, the length of the facet F, and thus is less than 3. Hence P has width at most 3. □

We have narrowed down the possible lattice points of P that lie off the x-axis: up to two consecutive points from the set $\{-3e_1 - e_2, -2e_1 - e_2, -e_1 - e_2, -e_2, e_1 - e_2, 2e_1 - e_2, 3e_1 - e_2, 4e_1 - e_2\}$, and points from $\{e_2, e_1 + e_2\}$ (see the red points in Figure 5.8). Since P is a full dimensional polygon, it has at least three facets, and since each of these facets are locked, at least three points of the above are contained in P. Further, we have observed that we can pick at most four of the above points (see Lemma 5.4.6), and thus the polygon P is either a triangle (containing one lattice point on $y = -1$ and two on $y = 1$, or vice versa) or a quadrilateral (containing two lattice points at $y = 1$ and two at $y = -1$).

In the following sections we treat the two cases separately. In fact, we further subdivide the case where P is a quadrilateral into two subcases. The four facets of a quadrilateral P are locked by both lattice points e_2 and $e_1 + e_2$ on $y = 1$ and by two consecutive lattice points on $y = -1$. Since four is the maximum number of locking points the polygons under consideration can have, the relative interior of each facet of a quadrilateral P contains exactly one locking point. The convex hull P' of the

four locking points intersect the x-axis in a line segment $S = P' \cap \{y = 0\}$ of length 1, which implies that S contains a lattice point. Thus P' can either be unimodularly equivalent to a rectangle, if the endpoints of S are lattice points, or to a cross-polygon, if the endpoints of S are not lattice points, and therefore S contains exactly one lattice point in its interior. Recall that a cross-polygon is $\mathbb{Z}$-unimodularly equivalent to $\mathrm{conv}(\pm e_1, \pm e_2)$. Furthermore, the rectangle will always be $\mathbb{Z}$-unimodularly equivalent to $\mathrm{conv}(\pm e_2, e_1 \pm e_2)$. Figure 5.8 illustrates the possibilities for the convex hull P' of the locking points. In what follows, we will often say that "the polygon P is

FIGURE 5.8: The two lattice points required to be in the interior of P are denoted by "$*$". The red lattice points are the possible locking points of P. Possible convex hulls P' of locking points (when P is a quadrilateral) are drawn in blue. The left P' is unimodularly equivalent to a cross-polygon while the right P' is unimodularly equivalent to a rectangle. The red dashed polygons are examples of quadrilaterals circumscribed around P'.

circumscribed around P'". The precise definition is the following.

Definition 5.4.7. Let $P, P' \subset \mathbb{R}^2$ be polygons. We say that P is *circumscribed* around P' if each vertex of P' is contained in a facet of P, and each facet of P contains a vertex of P'.

5.4.1 Triangles

We first consider the case where P is a triangle. Since all facets of P are locked, there are at least three locking points. Thus, given three lattice points A, B and C, two on the line $y = 1$ and one on the line $y = -1$, or vice versa, we want to show that $\frac{10}{3}$ is an upper bound for the width of any $\mathbb{Z}$-Δ_2-free triangle P with facets locked by A, B and C. We do not require that the points A, B and C are the only locking points: a facet of P might contain another lattice point in its interior.

There are 22 possible triples (A, B, C): 8 have the two lattice points on the line $y = 1$ and one on $y = -1$, while 14 have one lattice point on $y = 1$ and two consecutive ones on $y = -1$. Reflecting along the line $x = \frac{1}{2}$ yields the same result, so only 11 triples need to be checked. In Table 5.1 (below), we record these 11 triples. The cases 8–11 are not admissible: P is assumed to contain a point p_0 in $\left\{y > \frac{3}{2}\right\}$, and thus two points of the triple (A, B, C) need to lock the two facets through this point. However, in cases 8–11 this is impossible while also guaranteeing that $\mathbf{0}$ and e_1 are in the interior of P. For the remaining cases, we relax our assumptions and only require that the facets of P are locked by the triple (A, B, C), P contains $\mathbf{0}, e_1$ and it does not contain any lattice points away from the x-axis in its interior. That is, we forget the requirement that P contains a point $p_0 = xe_1 + ye_2$ with $0 < x < 1$ and $y > \frac{3}{2}$, and we allow $\mathbf{0}, e_1$ to lie in the boundary of P. Note this relaxation is possible as long as $\frac{10}{3}$

is an upper bound for any P satisfying the relaxed conditions. Our computations show that this is the case. This relaxation comes with two advantages, namely 1) the constraints on the polygon P are simplified; 2) it allows further symmetry (unimodular transformations fixing the x-axis, such as reflection about or shearing along the x-axis) resulting into a reduction of cases. In particular, the second point allows us to treat the following pairs of cases as being equivalent: $1 \sim 7$, $2 \sim 6$, and $3 \sim 5$. Finally, because of this relaxation, Table 5.1 includes upper bounds that are smaller than 3: in these cases, the largest width in the relaxed conditions was only achieved by a triangle P with e_1 on the boundary.

In order to bound the width of polygons whose facets are locked by a fixed triple (A, B, C), we employ a computer assisted strategy together with an approach that Hurkens has used to compute the classical flatness constant in 2 dimensions [52]. Let X, Y and Z be the vertices of the triangle P. We consider A, B, C, X, Y, Z as row vectors and write:

$$\begin{bmatrix} A \\ B \\ C \end{bmatrix} = \begin{bmatrix} 0 & \lambda & \bar{\lambda} \\ \bar{\mu} & 0 & \mu \\ \nu & \bar{\nu} & 0 \end{bmatrix} \begin{bmatrix} X \\ Y \\ Z \end{bmatrix}$$

for some $\lambda, \mu, \nu \in [0, 1]$, with $\bar{\lambda} + \lambda = \bar{\mu} + \mu = \bar{\nu} + \nu = 1$. Inverting the matrix, we obtain

$$\begin{bmatrix} X \\ Y \\ Z \end{bmatrix} = \frac{1}{\lambda\mu\nu + \bar{\lambda}\bar{\mu}\bar{\nu}} \begin{bmatrix} -\mu\bar{\nu} & \bar{\lambda}\bar{\nu} & \lambda\mu \\ \mu\nu & -\bar{\lambda}\nu & \bar{\lambda}\bar{\mu} \\ \bar{\mu}\bar{\nu} & \lambda\nu & -\lambda\bar{\mu} \end{bmatrix} \begin{bmatrix} A \\ B \\ C \end{bmatrix}.$$

Since A, B and C are fixed, these are formulas for X, Y and Z in terms of the parameters λ, μ, and ν. In fact, the coordinates of the pairwise differences of the vertices X, Y and Z are rational functions with a *linear* numerator and denominator equal to $\lambda\mu\nu + \bar{\lambda}\bar{\mu}\bar{\nu}$:

$$\begin{bmatrix} X - Y \\ Y - Z \\ Z - X \end{bmatrix} = \frac{1}{\lambda\mu\nu + \bar{\lambda}\bar{\mu}\bar{\nu}} \begin{bmatrix} -\mu & \bar{\lambda} & -1 + \lambda + \mu \\ -1 + \mu + \nu & -\nu & \bar{\mu} \\ \bar{\nu} & -1 + \lambda + \nu & -\lambda \end{bmatrix} \begin{bmatrix} A \\ B \\ C \end{bmatrix}. \tag{5.4}$$

Thus the slopes of the facets of P are rational functions with linear numerator and linear denominator in terms of the parameters λ, μ, and ν. The conditions $\mathbf{0}, e_1 \in P$ and that the interior $\mathrm{int}(P)$ of P is disjoint from the lattice points off the x-axis constrain the possible slopes. In terms of the parameters λ, μ, and ν, these constraints are linear. We thus obtain a polytope $Q \subset [0, 1]^3$ of admissible λ, μ, and ν.

Next, we express the width of P in a chosen direction in terms of the parameters λ, μ, and ν. Clearly, for a fixed direction, the width can be achieved on any pair of vertices depending on λ, μ, and ν. Wherever it is achieved by the same two vertices, the width is a linear function (in λ, μ, and ν) divided by $\delta := \lambda\mu\nu + \bar{\lambda}\bar{\mu}\bar{\nu}$. Our strategy includes choosing directions "ad hoc" such that:

1) The width in one such direction is achieved on the same pair of vertices for all

parameters $\lambda, \mu, \nu \in Q$, so that the width of P accepts an upper bound of the form

$$\frac{\min\{\ell_1(\lambda,\mu,\nu),\ldots,\ell_r(\lambda,\mu,\nu)\}}{\delta}$$

where the ℓ_i's are linear forms in terms of λ, μ, and ν.

2) The maximum over Q of this function is at most $\frac{10}{3}$. The actual computations are carried out with polymake [32] and Mathematica [57].

For the cases where the upper bound of $\frac{10}{3}$ is achieved, we determine the respective extremal points $(\lambda, \mu, \nu) \in Q$ and show that these parameters correspond to triangles P which are unimodularly equivalent to conv $\left(\frac{1}{3}e_1 + \frac{5}{3}e_2, -\frac{4}{3}e_1 - \frac{5}{3}e_2, 2e_1\right)$.

	conv$(\mathbf{0}, e_1, A, B, C)$	width	width directions	vertices of maximiser
1	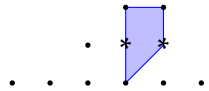	$\leq \frac{10}{3}$	$e_1^*, e_2^*, e_1^* - e_2^*$	$\frac{1}{3}\begin{bmatrix}-4 & 1 & 6\\ -5 & 5 & 0\end{bmatrix}$
2	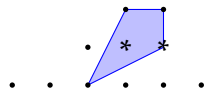	$\leq \frac{2}{\sqrt{7}-2}$	$e_1^*, e_2^*, e_1^* - e_2^*$	$\frac{1}{3\sqrt{7}}\begin{bmatrix}-6-3\sqrt{7} & 8+\sqrt{7} & 1+2\sqrt{7}\\ -9 & -2-\sqrt{7} & 5+4\sqrt{7}\end{bmatrix}$
3	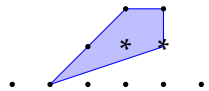	$< \frac{10}{3}$	$e_2^*, e_1^* - e_2^*$	$\frac{1}{3}\begin{bmatrix}-12 & 3 & 3\\ -5 & 5 & 0\end{bmatrix}$
4	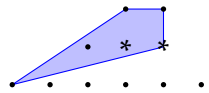	< 3	e_2^*	$\frac{1}{2}\begin{bmatrix}-10 & 2 & 2\\ -3 & 3 & 0\end{bmatrix}$
	Equivalent cases			
5	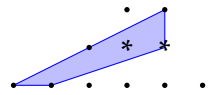 equivalent to case 3			
6	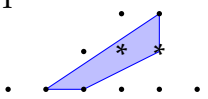 equivalent to case 2			
7	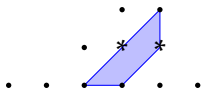 equivalent to case 1			
	Not admissible triples (A, B, C)			
8	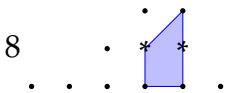			
9	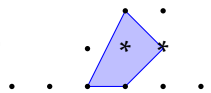			
10	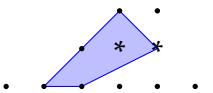			
11	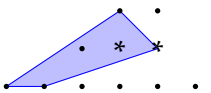			

TABLE 5.1: Up to symmetry, all possible triples of locking points (A, B, C); we list the largest possible width a triangle circumscribed around them can have, the directions in which this width is achieved, and the vertices of the triangle of largest width.

To illustrate our strategy, let us work out the details for one choice of locking points, namely $(A, B, C) = (e_1 + e_2, -e_2, e_2)$ (case 1 in Table 5.1). The other cases 2–4 work similarly. By (5.4), we have

$$X-Y = \left(-\frac{\mu}{\delta}, \frac{-2+2\lambda}{\delta}\right), \qquad Y-Z = \left(\frac{-1+\mu+\nu}{\delta}, \frac{2\nu}{\delta}\right), \qquad Z-X = \left(\frac{1-\nu}{\delta}, \frac{2-2\lambda-2\nu}{\delta}\right).$$

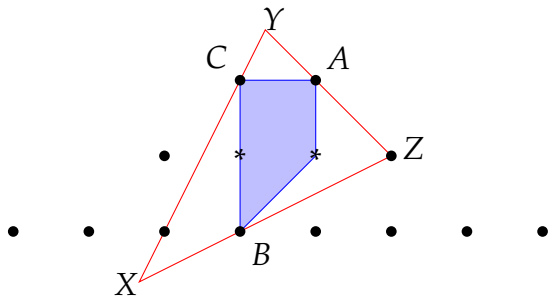

FIGURE 5.9: A triangle P (in red) with locking points $(A, B, C) = (e_1 + e_2, -e_2, e_2)$. This is the unique $\mathbb{Z}$-Δ_2-free triangle of width $\frac{10}{3}$.

First we determine the polytope Q of admissible parameters. The slopes m_{XY}, m_{YZ} and m_{ZX} of the facets of P through $\{X, Y\}$, $\{Y, Z\}$ and $\{Z, X\}$ respectively can be expressed in terms of λ, μ, and ν:

$$m_{XY} = \frac{2 - 2\lambda}{\mu}, \qquad m_{YZ} = \frac{2\nu}{-1 + \mu + \nu}, \qquad m_{ZX} = \frac{2 - 2\lambda - 2\nu}{1 - \nu}.$$

The position of the vertices X, Y, and Z of P is constrained by the two assumptions that P contains $\mathbf{0}, e_1$ and that no other lattice point away from the x-axis is in the interior of P. Since $\mathbf{0} \in P$, we have $m_{XY} \geq 0$, while $e_1 \in P$ yields $m_{YZ} \leq 0$ and $m_{ZX} \leq 1$. Since $e_1 - e_2$ is not in the interior of P, we have $m_{ZX} \geq 0$. Similarly, since $-e_1 - e_2$ is not in the interior of P, we have $m_{XY} \geq 2$. In a similar way, any further lattice point off the x-axis would give us other constraints. Many will be redundant, but some might further restrict the polytope Q of admissible parameters. However, we do not need all constraints and we can stop once we have enough to obtain an upper bound not exceeding $\frac{10}{3}$. In this case, the following constraints on the slopes are enough:

$$m_{XY} \geq 2, \qquad m_{YZ} \leq 0, \qquad 0 \leq m_{ZX} \leq 1.$$

Arithmetic manipulation of these inequalities yields constraints on the parameters λ, μ, and ν which define the polytope of admissible parameters

$$Q = \left\{(\lambda, \mu, \nu) \in [0,1]^3 : \ 1 - \lambda - \mu \geq 0, 1 - \mu - \nu \geq 0, 1 - \lambda - \nu \geq 0, -1 + 2\lambda + \nu \geq 0\right\}.$$

We now determine the widths of P in the directions e_1^*, e_2^*, and $e_1^* - e_2^*$. On Q, these are achieved at $Z - X$, $Y - X$, and $Z - Y$ respectively:

$$\begin{aligned}
\text{width}_{e_1^*}(P) &= e_1^*(Z - X) = \frac{1 - \nu}{\delta} \\
\text{width}_{e_2^*}(P) &= e_2^*(Y - X) = \frac{2 - 2\lambda}{\delta} \\
\text{width}_{e_1^* - e_2^*}(P) &= (e_1^* - e_2^*)(Z - Y) = \frac{1 - \mu + \nu}{\delta}.
\end{aligned}$$

We thus obtain

$$\begin{aligned}\operatorname{width}(P) &\leq \min\left\{\operatorname{width}_{e_1^*}(P), \operatorname{width}_{e_2^*}(P), \operatorname{width}_{e_1^*-e_2^*}(P)\right\} \\ &= \frac{\min\{1-\nu, 2-2\lambda, 1-\mu+\nu\}}{\delta} =: \frac{f(\lambda,\mu,\nu)}{\delta}.\end{aligned}$$

We denote the numerator of the last expression $f(\lambda,\mu,\nu)$. To show that any admissible triangle P has width at most $\frac{10}{3}$, it suffices to verify

$$\max_{(\lambda,\mu,\nu)\in Q} f(\lambda,\mu,\nu) \leq \frac{10}{3}.$$

To do so, we note that $f(\lambda,\mu,\nu)$ is a tropical polynomial, and using polymake, we calculate its *regions of linearity*, which when intersected with Q gives polytopes Q_i over which f coincides with a linear function f_i (for further details on tropical geometry, we refer to [59]). Using Mathematica [57], for each i, we compute the maximum of the rational function $\frac{f_i}{\delta}$ over the region Q_i. In this way, we verify that in this case there is exactly one point in Q at which the maximum $\frac{10}{3}$ is achieved, namely at $(\lambda,\mu,\nu) = \left(\frac{2}{5}, \frac{1}{5}, \frac{4}{5}\right)$. For these values, the corresponding triangle P is exactly the triangle depicted in Figure 5.9, which will turn out to be the only $\mathbb{Z}$-Δ_2-free polygon of width $\frac{10}{3}$, as stated in Proposition 5.4.2.

5.4.2 Quadrilateral circumscribed around a rectangle

Next, we consider the case where P is a quadrilateral and the convex hull of its locking points P' is $\mathbb{Z}$-unimodularly equivalent to a lattice rectangle with area equal to two. Then, we can assume that $P' = \operatorname{conv}(\pm e_2, e_1 \pm e_2)$.

First, observe that the vertices of P are in the vertical strip $0 < x < 1$ or in the horizontal strip $-1 < y < 1$. Indeed, any point strictly outside of both strips forces one of the locking points to be in the interior of P, a contradiction. Furthermore, a vertex on the boundary of a strip forces two facets to coincide, and thus P to be a triangle, a case which was dealt with already in Section 5.4.1. Thus, one vertex of P lies in each of the four connected components of the union of the two strips minus the rectangle P'.

Note two vertices of P in, say, the horizontal strip, one on each side of P', completely determine P. Let us denote those two vertices by $-\kappa e_1 + \lambda e_2$ and $(\mu+1)e_1 + \nu e_2$, with $\kappa, \mu > 0$ and $-1 < \lambda, \nu < 1$. Then the lines supporting the edges of P are

$$y = \frac{1-\lambda}{\kappa}x+1, \qquad y = -\frac{1+\lambda}{\kappa}x-1, \qquad y = -\frac{1-\nu}{\mu}x+\frac{1-\nu}{\mu}+1, \qquad y = \frac{1+\nu}{\mu}x-\frac{1+\nu}{\mu}-1$$

and thus the two remaining vertices of P are given by

$$\left(\frac{(1-\nu)\kappa}{(1-\nu)\kappa+(1-\lambda)\mu}, \frac{(1-\nu)(1-\lambda)}{(1-\nu)\kappa+(1-\lambda)\mu}+1\right) \quad \text{and} \quad \left(\frac{(1+\nu)\kappa}{(1+\nu)\kappa+(1+\lambda)\mu}, \frac{-(1+\nu)(1+\lambda)}{(1+\nu)\kappa+(1+\lambda)\mu}-1\right). \tag{5.5}$$

Clearly the width in the horizontal direction is $\text{width}_h = \kappa + \mu + 1$, while from the previous formulae we obtain the width in the vertical direction: $\text{width}_v = 2 + \frac{(1+\lambda)(1+\nu)}{(1+\lambda)\mu+(1+\nu)\kappa} + \frac{(1-\lambda)(1-\nu)}{(1-\lambda)\mu+(1-\nu)\kappa}$.

We first show if κ, μ and λ are fixed, the maximum vertical width is attained for $\nu = \lambda$. To that end compute the partial derivative of width_v with respect to ν:

$$\frac{\partial}{\partial \nu}\text{width}_v = -\frac{4\kappa\mu\cdot(\lambda-\nu)\cdot(\kappa(\lambda\nu-1)+\mu(\lambda^2-1))}{((1-\nu)\kappa+(1-\lambda)\mu)^2\cdot((1+\nu)\kappa+(1+\lambda)\mu)^2}.$$

It is straightforward to verify that on our domain $\kappa, \mu > 0$ and $-1 < \lambda, \nu < 1$ this partial derivative only vanishes at $\nu = \lambda$. It is easy to check that this is indeed a maximum.

We can thus focus on the case where P has two horizontally aligned vertices (κ, λ) and (μ, λ). From Formulae (5.5), it readily follows that the top and bottom vertices are vertically aligned (see Figure 5.10). Let $\zeta + 1$ be the y-coordinate of the top vertex

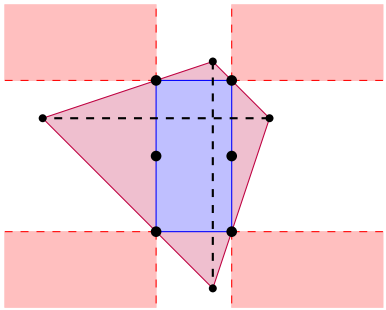

FIGURE 5.10: The maximum width in the vertical direction is achieved when the vertices of the circumscribed quadrilateral are horizontally and vertically aligned.

of P and $-\xi - 1$ be that of the bottom vertex. We calculate the area A of P in two different ways. Since the diagonals of P are orthogonal, we have $A = \frac{(\kappa+\mu+1)(\zeta+\xi+2)}{2}$ where $\kappa + \mu + 1$ respectively $\zeta + \xi + 2$ are the lengths of the horizontal and vertical diagonal. On the other hand, P can be decomposed into the union of P' and four triangles, each sharing an edge with P' and a vertex with P. The sum of the areas of these pieces gives $A = 2 + \kappa + \mu + \frac{\zeta+\xi}{2}$. These two expressions for the area A of P yield the equation $(\kappa + \mu)(\zeta + \xi) = 2$. Thus if $\kappa + \mu > 2$ then $\zeta + \xi < 1$. We conclude by observing that $\kappa + \mu > 2$ is equivalent to the horizontal width being greater than 3 and $\zeta + \xi > 1$ is equivalent to the vertical width being greater than 3. Since these conditions cannot happen at the same time, the width of P is at most 3.

5.4.3 Quadrilateral circumscribed around a cross-polygon

Let $\diamond_2 \subset \mathbb{R}^2$ be the 2-dimensional cross-polygon, i.e., $\diamond_2 = \text{conv}(\pm e_1, \pm e_2) \subset \mathbb{R}^2$. Here we are going to bound the width of inclusion-maximal $\mathbb{Z}$-Δ_2-free quadrilaterals P circumscribed around $\diamond_2$. As above, it suffices to consider such quadrilaterals whose width is greater than 3. We begin with some preliminary observations.

Switching to the 2-dimensional lattice generated by $f_1 := (1,1)$ and $f_2 := (1,-1)$ results in more manageable equations for the widths of P. Let us denote the basis dual to the basis f_1, f_2 of the new lattice by f_1^*, f_2^*. Explicitly, $f_1^* = \frac{1}{2}(e_1^* + e_2^*)$ and $f_2^* = \frac{1}{2}(e_1^* - e_2^*)$. In this lattice, the cross-polygon which P is circumscribed around has vertices $\pm f_1$ and $\pm f_2$.

Notice that P has a vertex in each of the four following regions

$$\pm\left\{(x,y) \in \mathbb{R}^2 : \ -1 < x < 1,\ y > 1\right\} \quad \text{and} \quad \pm\left\{(x,y) \in \mathbb{R}^2 : \ x > 1,\ -1 < y < 1\right\},$$

which we will refer to as the top, bottom, right, and left regions, respectively. We label the vertices of P in the top and bottom regions as $Z = (\kappa, \lambda)$, $W = (\mu, \nu)$, respectively, where $-1 < \kappa, \mu < 1$ and $\lambda, -\nu > 1$. The vertices in the right and left region are labeled Y, X respectively. Note that P is completely determined by the parameters $\kappa, \lambda, \mu, \nu$ defining Z and W.

By Proposition 5.4.4, P contains at least two interior lattice points since its width is assumed to be greater than 3. Clearly, $\mathbf{0}$ is one interior lattice point of P. The second interior point could be either $\pm(2,0)$ or $\pm(0,2)$. By symmetry, we may assume without loss of generality that $(0,2)$ is the other interior point. This implies $\lambda > 2$ and that the top vertex Z of P is extremal in the sense that the width with respect to the directions f_1^* and f_2^*, i.e., $\text{width}_{f_i^*}(P)$, is attained at Z. We can express the left and

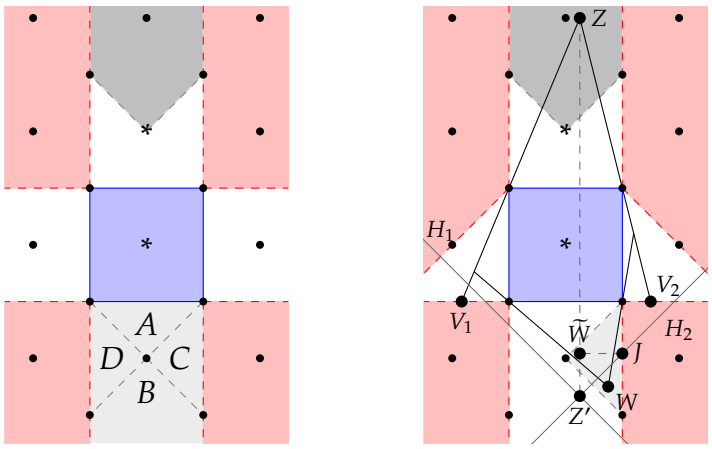

FIGURE 5.11: (left) The cross-polygon in the transformed lattice. The top vertex Z belongs to the dark grey region. The bottom vertex W belongs to one of the four light grey subregions, labelled A, B, C, D. (right) The case where W is in subregion C.

right vertices of P in terms of the parameters $\kappa, \lambda, \mu, \nu$ as follows:

$$X = -f_2 - \frac{2}{\frac{\lambda-1}{\kappa+1} - \frac{\nu+1}{\mu+1}}\left(1, \frac{\lambda-1}{\kappa+1}\right), \qquad Y = f_2 + \frac{2}{\frac{\nu+1}{\mu-1} - \frac{\lambda-1}{\kappa-1}}\left(1, \frac{\nu+1}{\mu-1}\right).$$

The width with respect to the horizontal functional $f_1^* + f_2^*$ is achieved at X and Y and can thus be expressed as follows.

$$w_0 \coloneqq \operatorname{width}_{f_1^*+f_2^*}(P) = \left(f_1^* + f_2^*\right)(Y - X) = 2 + \frac{2}{\frac{\nu+1}{\mu-1} - \frac{\lambda-1}{\kappa-1}} + \frac{2}{\frac{\lambda-1}{\kappa+1} - \frac{\nu+1}{\mu+1}}.$$

We are now ready to prove the following.

Proposition 5.4.8. *Let P be a maximal $\mathbb{Z}$-Δ_2-free quadrilateral circumscribed around a cross-polygon. Then* $\operatorname{width}(P) < \frac{10}{3}$.

Proof. We have four cases depending on which subregion the bottom vertex W lies in; these subregions are denoted by A, B, C and D in the left part of Figure 5.11. Since the setup is symmetric about the y-axis, it suffices to consider the cases A, B, and C as case D is equivalent to case C.

Let's start with case A. It turns out that it is enough to find the largest possible width of P with respect to the directions f_1^*, f_2^*, and $f_1^* + f_2^*$. Notice that the bottom vertex W of P is not extremal with respect to any of those three width directions. Moving W upwards increases all three of those widths. Thus, we may move W to the line $y = -1$, in which case P degenerates to a triangle. We can consider this triangle to be circumscribed around the *three* points f_1, f_2, and $-f_2$, and thus it can be regarded as circumscribed around case 1 from Table 5.1 (one needs to apply a shearing to arrive at case 1), which has width less than or equal to $\frac{10}{3}$ with respect to those same three width directions. Hence, $\operatorname{width}(P) < \frac{10}{3}$.

Let's now deal with case B. Here, the widths with respect to f_1^* and f_2^* are achieved at the vertices Z and W:

$$w_1 \coloneqq \operatorname{width}_{f_1^*}(P) = f_1^*(Z - W) = \frac{\kappa - \mu}{2} + \frac{\lambda - \nu}{2},$$

$$w_2 \coloneqq \operatorname{width}_{f_2^*}(P) = f_2^*(W - Z) = \frac{\mu - \kappa}{2} + \frac{\lambda - \nu}{2}.$$

The partial derivative of w_1 with respect to μ is

$$\frac{\partial w_0}{\partial \mu} = \frac{8(\kappa-\mu)(\nu+1)(\lambda-1)\left((\lambda-1)(\kappa\mu-1) - (\nu+1)\left(\kappa^2+1\right)\right)}{\left(\left(\frac{\lambda-1}{\kappa+1}(\mu+1) - (\nu+1)\right)\left(\nu+1-\frac{\lambda-1}{\kappa-1}(\mu-1)\right)(\kappa^2-1)\right)^2}. \tag{5.6}$$

Within our constraints $-1 < \kappa, \mu < 1$, $\lambda > 2$, and $\nu < -1$, the above expression vanishes if and only if $\kappa = \mu$; it is positive for $\mu < \kappa$ and negative for $\mu > \kappa$. Thus, w_0 is maximal along $\kappa = \mu$, where it is equal to $2 + \frac{4}{\lambda-\nu-2}$. By looking at the first summands of w_1 and w_2, it can be seen that $\min\{w_1, w_2\}$ is also maximal along $\kappa = \mu$. We obtain $\operatorname{width}(P) \leq \min\{2 + \frac{4}{\lambda-\nu-2}, \frac{\lambda-\nu}{2}\}$. Since $2 + \frac{4}{\lambda-\nu-2}$ decreases when $\frac{\lambda-\nu}{2}$

increases, and vice versa, the maximum is achieved when those expressions coincide, which occurs at $\nu = \lambda - 6$. Hence, $\operatorname{width}(P) \leq 3$.

Finally, we deal with case C; see the right part of Figure 5.11. The width with respect to f_1^* is achieved at Z and X, while the width with respect to f_2^* is achieved at W and Z. Assume towards a contradiction that the widths with respect to the directions $f_1^* + f_2^*$, f_1^*, and f_2^* are greater than or equal to $\frac{10}{3}$, i.e., $w_0, w_1, w_2 \geq \frac{10}{3}$. Let $Z' := Z - \left(0, \frac{20}{3}\right)$ so that

$$f_1^*(Z - Z') = f_1^*\left(0, \frac{20}{3}\right) = \frac{10}{3} \qquad \text{and} \qquad f_2^*(Z' - Z) = f_2^*\left(-\left(0, \frac{20}{3}\right)\right) = \frac{10}{3}.$$

Since w_1 (resp. w_2) is assumed to be at least $\frac{10}{3}$, there is a point of P below the line H_1 (resp. H_2) passing through Z' with slope -1 (resp. 1). In particular, vertex X is below the line H_1 and vertex W is below the line H_2, since they are the vertices maximising the width along the respective directions.

We will use the following inequalities:

$$\lambda \leq 4 \qquad \text{and} \qquad \kappa \geq 0. \tag{5.7}$$

We first prove $\lambda \leq 4$. An upper bound for w_0 is given by the width with respect to $f_1^* + f_2^*$ of the triangle T circumscribed around the cross-polygon with vertex Z and opposite edge supported by the line $y = -1$. The bottom vertices of T are $V_1 := (-1 - \frac{2(\kappa+1)}{\lambda-1}, -1)$ and $V_2 := (1 - \frac{2(\kappa-1)}{\lambda-1}, -1)$. Thus, $\operatorname{width}_{f_1^*+f_2^*}(T) = 2 + \frac{4}{\lambda-1}$. Since by assumption $w_0 \geq \frac{10}{3}$, so is this larger width. We obtain $\lambda \leq 4$.

To prove that $\kappa \geq 0$, consider the bottom-left vertex V_1 of the triangle T defined in the previous paragraph. Since the vertex X of P lies below H_1, so does V_1, and thus $-2 - \frac{2(\kappa+1)}{\lambda-1} \leq \kappa + \lambda - \frac{20}{3}$, which is equivalent to $\frac{20}{3} + \kappa - \frac{17}{3}\lambda + \kappa\lambda + \lambda^2 \geq 0$. Consider the left side of the previous inequality as a family of functions $f_\kappa \colon [2,4] \to \mathbb{R}$ on the closed interval $[2,4]$ for parameters $\kappa \in [-1,1]$. Observe that $\kappa \in [-1,1]$ is admissible if and only if there exists $\lambda \in [2,4]$ such that $f_\kappa(\lambda) \geq 0$ (we include the case $\lambda = 2$). Then $\kappa \in [-1,1]$ is admissible if the maximum of f_κ on $[2,4]$ is non-negative. It is straightforward to show

$$\max_{\lambda \in [2,4]} f_\kappa(\lambda) = \begin{cases} 5\kappa & \kappa > -\frac{1}{3} \\ 3\kappa - \frac{2}{3} & \text{otherwise} \end{cases} \qquad \text{at } \lambda = \begin{cases} 4 & \kappa > -\frac{1}{3} \\ 2 & \text{otherwise} \end{cases}$$

Hence, $\kappa \geq 0$ are the only admissible parameters.

Next, we aim to bound w_0 from above by considering a different quadrilateral $\widetilde{P}$ circumscribed around the cross-polygon, with top vertex Z and bottom vertex $\widetilde{W} := (\kappa, \lambda - \kappa - \frac{17}{3})$ (note that the inequalities from (5.7) guarantee that $\lambda - \kappa - \frac{17}{3} < -1$). It is straightforward to compute that $\widetilde{w}_0 := \operatorname{width}_{f_1^*+f_2^*}(\widetilde{P}) = 2 + \frac{4}{\kappa + \frac{11}{3}}$. Since $\kappa \geq 0$, we get that $\widetilde{w}_0 \leq 2 + \frac{12}{11} < \frac{10}{3}$.

To reach a contradiction, we show that $w_0 \leq \widetilde{w}_0$. Consider the partial derivatives of w_0 with respect to μ and ν, the coordinates of the vertex W. The first was

already computed in Equation (5.6), and we observed that the maximum is achieved along $\mu = \kappa$. The second is computed here.

$$\frac{\partial w_0}{\partial \nu} = \frac{2}{(1-\mu)\left(\frac{\nu+1}{\mu-1} - \frac{\lambda-1}{\kappa-1}\right)^2} + \frac{2}{(1+\mu)\left(\frac{\lambda-1}{\kappa+1} - \frac{\nu+1}{\mu+1}\right)^2} \tag{5.8}$$

Since $-1 < \mu < 1$, Equation (5.8) shows that $\frac{\partial w_0}{\partial \nu} > 0$. Now, consider the intersection point J of the lines H_2 and $\{x = 1\}$. It's straightforward to compute $J = (1, \lambda - \kappa - \frac{17}{3})$. The point J has largest y-coordinate of all points in C on or below H_2 (see Figure 5.11). Thus, $\nu \leq \lambda - \kappa - \frac{17}{3}$. So, moving W horizontally to the line $x = \kappa$ and then vertically to the line $y = \lambda - \kappa - \frac{17}{3}$ increases the width w_0, and thus $w_0 \leq \widetilde{w}_0$. Combined with $\widetilde{w}_0 < \frac{10}{3}$, we get that $\text{width}(P) \leq w_0 < \frac{10}{3}$, a contradiction. □

This concludes the proof of Theorem 5.4.3.

5.5 The $\mathbb{R}$-flatness constant of Δ_2

This section focuses on the $\mathbb{R}$-flatness constant. The first goal is to prove the following theorem (case $A = \mathbb{R}$ of Theorem 5.1.1).

Theorem 5.5.1 (Case $A = \mathbb{R}$ of Theorem 5.1.1)**.** $\text{Flt}_2^{\mathbb{R}}(\Delta_2) = 2$.

It is straightforward to verify that the cross-polygon $\diamond_2 := \text{conv}(\pm e_1, \pm e_2)$ is $\mathbb{R}$-Δ_2-free and has width 2, and hence $\text{Flt}_2^{\mathbb{R}}(\Delta_2) \geq 2$. To prove Theorem 5.5.1, we thus need to bound the $\mathbb{R}$-flatness constant of Δ_2 from above by 2. By Lemmas 5.2.5 and 5.2.3, it suffices to bound the lattice width of inclusion-maximal $\mathbb{R}$-Δ_2-free closed convex sets C by 2. By Proposition 5.3.3, if C is unbounded, its lattice width is bounded by 1. Hence, it remains to study the width of the bounded C's which, by Theorem 5.1.2, are polygons. Our strategy is to show that any polygon $P \subset \mathbb{R}^2$ with width greater than 2 is not $\mathbb{R}$-Δ_2-free. A key ingredient in the proof is the notion of rational diameter:

Definition 5.5.2. Let $K \subset \mathbb{R}^d$ be a convex body. The *rational diameter of K* is the largest dilation of an $\mathbb{R}$-unimodular copy of the unit segment $[0, 1]$ which is contained in K, i.e.

$$l(K) := \max\left\{l \in \mathbb{R}_{\geq 0} : \ lS \subseteq K \text{ for some } \mathbb{R}\text{-unimodular copy } S \text{ of } [0,1]\right\}.$$

Notation 5.5.3. In what follows, we will always assume that the rational diameter of P is achieved with a horizontal line segment. This we can do without loss of generality, because, were this not the case, we could apply an $\mathbb{R}$-unimodular transformation mapping the rational diameter into a horizontal segment. We thus use the following shorthand notation for horizontal line segments $S \subset \mathbb{R}^d$: $[x, y] := \text{conv}(xe_1, ye_1)$.

The following lemma shows that for polygons the width is bounded from above by twice the rational diameter, i.e., $\text{width}(P) \leq 2l$ where l is the rational diameter of P.

Lemma 5.5.4. *Let $P \subset \mathbb{R}^2$ be a polygon with rational diameter $l = 1 + 2a > 0$ (that is, $a > -\frac{1}{2}$), achieved with $S = [-a, 1+a] \subseteq P$. Then $P \subset \{(x,y) \in \mathbb{R}^2 : \ -l \leq y \leq l\}$.*

Proof. The affine line $\{y = l\}$ is covered by segments $S_b := S + (lb, l)$ for $b \in \mathbb{Z}$. First, notice that we must have $(x,l) \notin \text{int}(P)$ for all $(x,l) \in S_0$, as otherwise the line segment with end points $(x,0)$ and (x,l) could be extended upwards and still be contained in P, contradicting that l is maximal. Now, the same argument holds for the points in the segments S_b for any $b \in \mathbb{Z}$ by applying an appropriate unimodular transformation (a shearing). Since the segments S_b cover the horizontal line at height l, all points (x,l) with $x \in \mathbb{R}$ must be disjoint from $\text{int}(P)$. Applying a reflection about the x-axis gives us that all $(x,-l)$ with $x \in \mathbb{R}$ must be disjoint from $\text{int}(P)$. Thus, $P \subset \{(x,y) \in \mathbb{R}^2 : \ -l \leq y \leq l\}$ as desired. □

Recall that for the proof of Theorem 5.5.1 we are only interested in polygons of width strictly larger than 2. Lemma 5.5.4 shows that we then only need to consider polygons with rational diameter $l > 1$. The following lemma will allow us to also bound the rational diameter from above.

Lemma 5.5.5. *Let $P \subset \mathbb{R}^2$ be an $\mathbb{R}$-Δ_2-free polygon with rational diameter $l = 1 + 2a > 1$ (that is, $a > 0$), achieved with $S = [-a, 1+a] \subseteq P$. Then $\text{int}(P)$ is disjoint from the segments $[-a,a] + (b, \pm 1)$, for all $b \in \mathbb{Z}$. In particular, if $a \geq \frac{1}{2}$ then $P \subset \{(x,y) \in \mathbb{R}^2 : \ -1 \leq y \leq 1\}$ and $\text{width}(P) \leq 2$.*

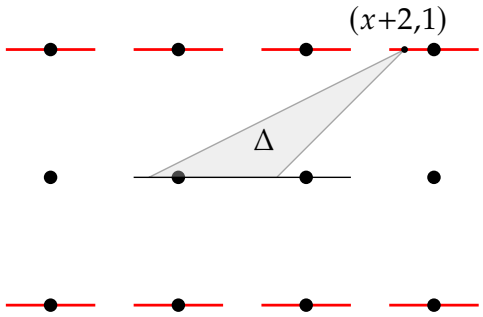

FIGURE 5.12: Forbidden segments from Lemma 5.5.5.

Proof. Consider the point $(x+b, 1)$, for some $-a < x < a$ and $b \in \mathbb{Z}$. The convex hull of this point and the points $(x,0), (x+1,0) \in P$ is an $\mathbb{R}$-unimodular copy Δ of Δ_2. If the point $(x+b,1)$ were contained in the interior of P, the Minkowski difference $P \div \Delta$ would be 2-dimensional. By Corollary 5.2.18, this contradicts P being $\mathbb{R}$-Δ_2-free. Therefore, $(x+b,1) \notin \text{int}(P)$, for all $x + b \in \text{int}([-a,a]) + \mathbb{Z}$. The same argument holds for all points $(x+b,-1)$. Thus, $\text{int}(P)$ is disjoint from the interiors of all segments $[-a,a] + (b, \pm 1)$.

In fact, $\text{int}(P)$ is disjoint from not just the interior, but from the whole segment $[-a,a] + (b, \pm 1)$ for all $b \in \mathbb{Z}$: suppose otherwise that one of the endpoints is contained in the interior of P. Then, there exists an open ball around that endpoint which is contained in the interior of P. This yields a contradiction, as the interiors of the segments must be disjoint from $\text{int}(P)$.

Suppose $l \geq 2$, that is, $a \geq \frac{1}{2}$. Then the interior of P is disjoint from all points $(x + b, \pm 1)$ with $-\frac{1}{2} \leq x \leq \frac{1}{2}$ and $b \in \mathbb{Z}$, which cover the entire horizontal lines at height 1 and -1. Thus P must be contained in the strip $\{(x, y) \in \mathbb{R}^2 : \ -1 \leq y \leq 1\}$, which has width 2. □

We are now ready to prove Theorem 5.5.1. We use the bounds on the lattice diameter from the previous lemmas and the lower bound on the width to show that certain areas of the plane are disjoint from the polygon P. Eventually this allows us to bound the polygon so tightly that we reach a contradiction.

Proof of Theorem 5.5.1. Let $P \subset \mathbb{R}^2$ be an $\mathbb{R}$-Δ_2-free polygon, with rational diameter l and assume towards a contradiction that $\text{width}(P) > 2$. We may assume without loss of generality that the rational diameter is achieved with $S = [-a, 1 + a]$, where $l = 1 + 2a$. By Lemma 5.5.4, we have $P \subset \{(x, y) \in \mathbb{R}^2 : \ -l \leq y \leq l\}$, and thus $2l \geq \text{width}(P) > 2$, that is, $l > 1$, i.e. $a > 0$. By Lemma 5.5.5, $\text{int}(P)$ is disjoint from all segments $[-a, a] + (b, \pm 1)$ with $b \in \mathbb{Z}$, and, since $\text{width}(P) > 2$, it follows that $a < \frac{1}{2}$.

Since $\text{width}(P) > 2$, there exists a point $(r, s) \in P$ with either $1 < s \leq l$ or $-l \leq s < 1$. Due to the symmetry about the x-axis, we may assume that $1 < s \leq l$. We may also assume that (r, s) is the point of P with largest y-coordinate. Furthermore, we may assume that $a \leq r \leq 1 - a$; otherwise, we apply a shearing so that the x-coordinate of our point would satisfy this condition. Let L_1 be the line through

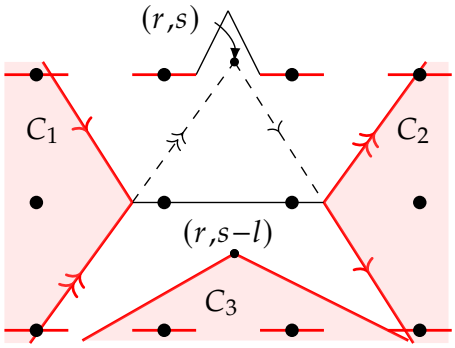

FIGURE 5.13: Regions C_1, C_2, C_3 from Claims 1 and 2.

the points (r, s) and $(1 + a, 0)$, and L_2 the line through (r, s) and $(-a, 0)$. We define affine pointed cones C_1 and C_2 with apex in $(-a, 0)$ respectively in $(1 + a, 0)$, and rays bounding them above and below, parallel to L_1 and L_2 for C_1, respectively L_2 and L_1 for C_2. Precisely, $C_1 := (-a, 0) + \text{cone}((r - 1 - a, s), (-r - a, -s))$ and $C_2 := (1 + a, 0) + \text{cone}((r + a, s), (-r + 1 + a, -s))$.

Claim 1. *The regions C_1 and C_2 are disjoint from* $\text{int}(P)$.

Proof of Claim 1. The arguments for the affine cones C_1 and C_2 are the same, so we conduct the proof for C_1.

Since the rational diameter is achieved at $S := [-a, 1 + a]$, no other point on the horizontal axis can be in P. If a point (x, y) in the interior of C_1 with $y < 0$ were

in P, the segment connecting it to (r, s) would also be in P, which is a contradiction as this segment intersects the horizontal axis outside of S.

Suppose now that a point (x, y) in the interior of C_1 with $0 < y < 1$ were in P. The horizontal segment S' with an endpoint in (x, y) and one in L_1 would then also be in P. Since S' intersects the boundary ray of C_1 parallel to L_1 in an interior point, S' strictly contains a segment congruent to S. Since S' has lattice length strictly larger than l, we obtain a contradiction to l being the rational diameter of P.

Finally, no point $(x, y) \in C_1$ with $y \geq 1$ can be in P because it would force P to contain the lattice point $(0, 1)$ in its interior, and thus a small translate of $\text{conv}((0, 0), (0, 1), (1, 0,))$ would be contained in the interior of P, a contradiction to the hypothesis that P is $\mathbb{R}$-Δ_2-free.

These three cases together show that no point in the interior of C_1 can be in P, which is equivalent to our claim that C_1 is disjoint from the interior of P. □

Let $C_3 := (r, s-l) + \text{cone}((r-1-a, s-l), (r+a, s-l))$ be the affine cone with apex in $(r, s-l)$, and two boundary rays lying on the two lines passing through $(r, s-l)$ and the two endpoints of S respectively.

Claim 2. *The region C_3 is disjoint from* $\text{int}(P)$.

Proof of Claim 2. Observe that the point $q := (r, s-1-2a)$ cannot be in $\text{int}(P)$, because if any point q' vertically below q were in P, the segment with endpoints q' and (r, s) would have lattice length strictly larger than S, a contradiction.

If any point $p \in \text{int}(C_3)$ were also in P, the triangle $\text{conv}(p, (-a, 0), (1 + a, 0))$ would be in P. However, this triangle contains q in its interior, a contradiction. □

Recall s is assumed to have the largest y-coordinate of all points of P. Let L_5 be the line parallel to the x-axis and going through the point $(0, s-2)$. Since P has width greater than 2, P intersects L_5 in a line segment $[a, b]$ of positive length which by the previous claims is not in $\text{int}(C_i)$ for $i = 1, 2, 3$. By symmetry, we may assume $[a, b]$ lies between C_1 and C_3. Furthermore, suppose a is to the left of b.

The key idea of the proof is to consider the family of quadrilaterals (see also Figure 5.14)

$$Q_x := \text{conv}((-a, 0), (1+a, 0), (r, s), (x, s-2)) \qquad \text{for } (x, s-2) \in \mathbb{R}^2 \text{ between } C_1 \text{ and } C_3.$$

Note x is the only free parameter of this family. We think of the elements of this family to be quadrilaterals where the bottom vertex can move. Indeed, $Q_{x'}$ is obtained from Q_x via a piecewise linear transformation $\psi_{x'-x} \colon \mathbb{R}^2 \to \mathbb{R}^2$ which is given as follows: below the x-axis, apply the shearing which maps $(x, s-2)$ to $(x', s-2)$; above, apply the identity. We want to show that every Q_x of this family contains an $\mathbb{R}$-translation of $\widetilde{\Delta} := \text{conv}(\mathbf{0}, -e_1, e_2)$. We do this in two stages: 1) show if $Q_{x'}$ is obtained from Q_x by moving the bottom vertex further to the left and Q_x contains an $\mathbb{R}$-translation of $\tilde{\Delta}$, then $Q_{x'}$ does so as well; 2) show that the quadrilateral $Q_{\bar{x}}$ for the largest possible $\bar{x}$ contains an $\mathbb{R}$-translation of $\tilde{\Delta}$.

Granting this statement for a moment, let us complete the proof of Theorem 5.5.1. There is an $x \in \mathbb{R}$ such that $Q_x = \text{conv}((-a, 0), (1 + a, 0), (r, s), b)$. Suppose Δ is

an $\mathbb{R}$-translation of $\tilde{\Delta}$ that is contained in Q_x. Our goal is to show that $P_x \div \Delta$ is 2-dimensional where P_x is the pentagon $\text{conv}(Q_x, a)$.

Consider the horizontal line segment B which forms the base of Δ. Note that B lies below the x-axis: otherwise, the vertex v of Δ which is a translation of e_2 would have y-coordinate at least 1, which forces its x-coordinate to be less than $1 - a$; this in turn forces the vertex of Δ corresponding to $-e_1$ to have x-coordinate less than $-a$, which is a contradiction since no such point lies in Q_x. Thus, if Δ intersects the boundary of the pentagon P_x, then it does it in a single point that is contained in the interior of the respective facet of P_x. Since the vertex of Δ corresponding to $-e_1$ lies in the interior of P_x, it follows that at most two vertices of Δ lie on the boundary of P_x. With Lemma 5.2.16 it's straightforward to show that $P_x \div \Delta$ is 2-dimensional. By Corollary 5.2.18, it follows that P_x isn't $\mathbb{R}$-Δ_2-free. A contradiction to the assumption $\text{width}(P) > 2$. Therefore, an $\mathbb{R}$-Δ_2-free polygon P has $\text{width}(P) \leq 2$. Thus, $\text{Flt}_2^{\mathbb{R}}(\Delta_2) = 2$.

It remains to prove the two claims from above.

Claim 3. *Suppose Q_x contains a translation Δ of $\widetilde{\Delta}$. Then $Q_{x'}$ also contains a translation Δ' of $\widetilde{\Delta}$, for $x' \leq x$ and $(x', s-2) \notin C_i$ for all $i = 1, 2, 3$.*

Proof of Claim 3. Consider the horizontal line segment B which forms the base of Δ. With the same argument as above, it follows that B lies below the x-axis.

Let $x' \leq x$. Clearly, the image of B under the transformation $\psi_{x'-x}$ is the segment $B' := B + (x' - x, 0)$, which is thus contained in $Q_{x'}$. In order to show that $\Delta' := \Delta + (x' - x, 0)$ is contained in $Q_{x'}$, it remains to prove that $v' := v + (x' - x, 0)$ is contained in $Q_{x'}$. Note v' and v are both above the x-axis. Since Q_x and $Q_{x'}$ coincide above the x axis, v lies in both. Since v' lies to the left of v, it must also lie to the left of L_1. Since L_2, the line through $(-a, 0)$ and (r, s), has slope greater than or equal to 1, v' must be to the right of it; otherwise, the left vertex of B', which lies on the line through v' with slope 1, would also be to the left of L_2, and thus contained in C_1, a contradiction. Thus Δ' is contained in $Q_{x'}$. □

We now want to show that, letting $(\bar{x}, s-2)$ be the right-most point between $\text{int}(C_1)$ and $\text{int}(C_3)$, $Q_{\bar{x}}$ contains an $\mathbb{R}$-translation of $\tilde{\Delta}$. Explicitly we have $\bar{x} = \frac{r(s-2)+(1+a)(1-2a)}{s-1-2a}$. Let L_1, L_2, L_3, L_4 be the lines defining the boundary of $Q_{\bar{x}}$: L_1 is the line through the points (r, s) and $(1 + a, 0)$, and the others are chosen to lie in counterclockwise order along the boundary of $Q_{\bar{x}}$. Explicitly,

$$\begin{aligned}
L_1 &= \{(1+a, 0) + t_1(r - 1 - a, s) : \ t_1 \in \mathbb{R}\}, \\
L_3 &= \{(\bar{x}, s-2) + t_3(-a - \bar{x}, 2 - s) : \ t_3 \in \mathbb{R}\}, \\
L_4 &= \{(1+a, 0) + t_4(r - 1 - a, s - 1 - 2a) : \ t_4 \in \mathbb{R}\} \\
&= \left\{(\bar{x}, s-2) + t_4'(1 + a - \bar{x}, 2 - s) : \ t_4' \in \mathbb{R}\right\}.
\end{aligned}$$

The lines $L_1 - e_2$ and L_4 intersect at $t_1 = t_4 = \frac{1}{1+2a}$ in the point $\beta = (\beta_1, \beta_2) = (1 + a + \frac{r-1-a}{1+2a}, \frac{s-1-2a}{1+2a})$. Both the points β and $\beta + e_2$ are in $Q_{\bar{x}}$. The intersection between L_4 and $L_3 + e_1$, obtained at $t_3 = t_4' = \frac{1}{1+2a}$, is the point $\alpha = (\alpha_1, \alpha_2) =$

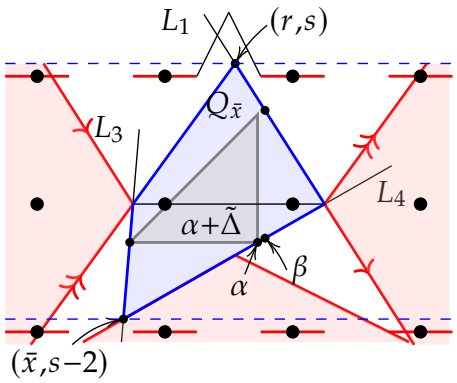

FIGURE 5.14: The quadrilateral $Q_{\bar{x}}$ and the lines L_1, L_3, L_4.

$(\bar{x} + \frac{1+a-\bar{x}}{1+2a}, \frac{(s-2)2a}{1+2a})$; and both α and $\alpha - e_1$ are in $Q_{\bar{x}}$. Since $s > 1$ and $0 < a < \frac{1}{2}$, we have $\beta_2 - \alpha_2 = \frac{(s-1)(1-2a)}{1+2a} > 0$, or equivalently $\alpha_2 \leq \beta_2$. Hence $\alpha + \tilde{\Delta}$ and $\beta + \tilde{\Delta}$ are both contained in $Q_{\bar{x}}$ (recall $\tilde{\Delta} := \text{conv}(\mathbf{0}, -e_1, e_2)$). □

5.5.1 Inclusion-maximal $\mathbb{R}$-Δ_2-free convex bodies in dimension 2

In the previous section, we have established the maximum width of $\mathbb{R}$-Δ_2-free convex bodies. We now devote our attention to inclusion-maximal $\mathbb{R}$-Δ_2-free convex bodies. We have seen in Theorem 5.1.2 that inclusion-maximal $\mathbb{R}$-Δ_2-free convex bodies are in fact always polytopes. It would be interesting to have a complete characterisation of these polytopes, in analogy to the classification of maximal hollow 2-bodies of Hurkens [52]. Note that hollow convex bodies are $\mathbb{Z}$-$\{\mathbf{0}\}$-free convex bodies.

Here, we will see that the situation for $\mathbb{R}$-Δ_2-free bodies is more intricate than for hollow ones. We construct infinite families of $\mathbb{R}$-Δ_2-free bodies but cannot classify all such bodies. It might thus be of particular interest to investigate the special class of those inclusion-maximal $\mathbb{R}$-Δ_2-free polygons which achieve the maximum width 2. Of these, we only know two examples (up to $\mathbb{R}$-unimodular equivalence): the cross-polygon $\text{conv}(\pm e_1, \pm e_2)$ and the triangle $\text{conv}(e_1, e_2, -e_1 - e_2)$, see Figure 5.15.

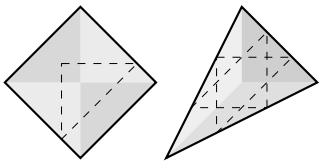

FIGURE 5.15: Maximal $\mathbb{R}$-Δ_2-free polygons of width 2, with inscribed $\mathbb{R}$-unimodular triangles.

To discuss examples of maximal $\mathbb{R}$-Δ_2-free polygons, we need the notion of *locked* facet. A facet F of a polygon P defines two half-planes, whose boundary is the affine line spanned by the facet F. We say that a point x is *beyond* the facet F of P if it lies in the half-plane defined by F which does not contain the interior $\text{int}(P)$, while x is *beneath* F if it lies in the same half-plane as P.

Definition 5.5.6. A facet F of an $\mathbb{R}$-Δ_2-free polygon P is *locked* if for any $x \in \mathbb{R}^2$ beyond F, an $\mathbb{R}$-unimodular copy of Δ_2 is contained in the interior of $\operatorname{conv}(P, x)$.

Clearly all facets of an $\mathbb{R}$-Δ_2-free polygon P are locked if and only if P is maximal. Indeed, any point outside of P must be beyond at least one facet, and thus the polygon obtained by adding this point to P would by the definition of locked facet contain an $\mathbb{R}$-unimodular triangle in its interior.

The following characterisation of locked facets will play an important role in our study of maximal $\mathbb{R}$-Δ_2-free polygons.

Proposition 5.5.7. *Let $P \subset \mathbb{R}^2$ be an $\mathbb{R}$-Δ_2-free polygon. Then a facet F of P is locked if and only if P contains an $\mathbb{R}$-unimodular copy Δ of Δ_2 such that the face $\mathcal{F} := F \cap \Delta$ of Δ is not empty, lies in the relative interior of F and the face ℓ of Δ that is opposite to $\mathcal{F}$ satisfies* $\dim(P \div \ell) = 2$.

In the proof of Proposition 5.5.7, we use the following statement which can be straightforwardly checked.

Proposition 5.5.8. *Let $\sigma_1, \sigma_2 \subset \mathbb{R}^2$ be two 2-dimensional polyhedral cones. Then* $\dim(\sigma_1 \cap \sigma_2) = 2$ *if and only if one of the following conditions are satisfied:*

1. *$\sigma_1 \subset \sigma_2$ or $\sigma_2 \subset \sigma_1$; or*
2. *there exists a ray ρ of σ_1 that is contained in the interior of σ_2 and vice versa.*

Proof of Proposition 5.5.7. Suppose the facet $F = [a, b]$ of P is locked ($a, b \in \mathbb{R}^2$). Let $\eta \in \mathbb{R}^2$ be an outer facet normal of F. The points $x_n := \frac{1}{2}(a + b) + \frac{1}{n}\eta$ for $n \in \mathbb{N}$ are beyond F. Hence for every $n \in \mathbb{N}$ there exists an $\mathbb{R}$-unimodular copy S_n of Δ_2 that is contained in the interior of $P_n := \operatorname{conv}(P, x_n)$. Note S_n is an $\mathbb{R}$-translation of a $\mathbb{Z}$-unimodular copy of Δ_2 that is contained in $P_1 + [0, 1]^2$. Since $P_1 + [0, 1]^2$ contains only finitely many $\mathbb{Z}$-unimodular copies of Δ_2, by restricting to an appropriate subsequence, we may assume that S_n is an $\mathbb{R}$-translation of exactly one fixed $\mathbb{Z}$-unimodular copy $\widetilde{\Delta}$ of Δ_2 for all n, i.e., $S_n = \widetilde{\Delta} + \delta_n$ for some $\delta_n \in \mathbb{R}^2$. Since there exists a (large enough) natural number $N \in \mathbb{N}$ such that δ_n is in the compact set $[-N, N]^2$ for all n, the sequence of δ_n's has a convergent subsequence. To simplify notation, we abuse notation and use the same notation $(\delta_n)_{n\in\mathbb{N}}$, $(S_n)_{n\in\mathbb{N}}$ for these subsequences. Then $\Delta := \lim_{n\to\infty} S_n$ is contained in P and intersects the facet F in a non-empty face $\mathcal{F} := F \cap \Delta$ of Δ.

Let ℓ be the face of Δ opposite to $\mathcal{F}$. Since an $\mathbb{R}$-translation of Δ is in the interior of P_n we have $\dim(P_n \div \Delta) = 2$ (see Lemma 5.2.17). We claim $\dim(P \div \ell) = 2$. Assume towards a contradiction $\dim(P \div \ell) \leq 1$. This is only possible if ℓ is an edge, say $[c_1, c_2]$ for $c_1, c_2 \in \mathbb{R}^2$ (as otherwise $P \div \ell$ is just a translation of P, and thus full-dimensional). By Lemma 5.2.16, $P \div [c_1, c_2] = (P - c_1) \cap (P - c_2)$. For sufficiently small $\varepsilon > 0$, we have $(c_i + \varepsilon B^2) \cap P = (c_i + \varepsilon B^2) \cap P_n$ for $i = 1, 2$ and $n \in \mathbb{N}$. Thus

$$(P_n \div \Delta) \cap \varepsilon B^2 = \bigcap_{v \in V(\Delta)} (P_n - v) \cap \varepsilon B^2 \subset \bigcap_{i \in \{1,2\}} (P - c_i) \cap \varepsilon B^2 = (P \div \ell) \cap \varepsilon B^2,$$

where $V(\Delta)$ denotes the set of vertices of Δ. Hence $\dim(P_n \div \Delta) \leq 1$, a contradiction.

If $\mathcal{F}$ is contained in the relative interior of F, the implication "$\Rightarrow$" follows. Suppose otherwise, i.e. $\mathcal{F}$ intersects F in an endpoint. Note it is not possible that $\mathcal{F}$ intersects F in both endpoints (since the end points a, b of F will remain vertices of P_n for sufficiently large $n \in \mathbb{N}$). Suppose $a \in \mathcal{F}$. In particular, a is a vertex of Δ. Let $a_1 := a$ and a_2 be the two vertices of Δ that are not contained in the relative interior of F. Call Δ's third vertex c. There exists a *fixed* $\varepsilon > 0$ such that $(P_n - a_i) \cap \varepsilon B^2 = \sigma_{a_i}^{(n)} \cap \varepsilon B^2$ and $(P - a_i) \cap \varepsilon B^2 = \sigma_{a_i} \cap \varepsilon B^2$ for some polyhedral cones $\sigma_{a_i}^{(n)}, \sigma_{a_i} \subset \mathbb{R}^2$ $(i = 1, 2)$. However, around c we might need to choose $\varepsilon_n > 0$ depending on $n \in \mathbb{N}$ such that $(P_n - c) \cap \varepsilon_n B^2 = \sigma_c \cap \varepsilon_n B^2$ for some polyhedral cone $\sigma_c \subset \mathbb{R}^2$. In addition, $(P - c) \cap \varepsilon B^2 = \sigma_c'$ for a possibly different cone $\sigma_c' \subset \mathbb{R}^2$ and we might need to decrease the ε from above. Note if ε_n needs to be adjusted with $n \in \mathbb{N}$, then $\varepsilon_n \to 0$ as $n \to \infty$. Furthermore, $\sigma_{a_2}^{(n)} = \sigma_{a_2}$ doesn't change for sufficiently small $\varepsilon > 0$. Indeed, only one ray of $\sigma_a^{(n)}$ changes, namely the ray $\rho_a^{(n)} := \mathbb{R}_{\geq 0}(\frac{1}{2}(b - a) + \frac{1}{n}\eta)$. Since $\dim(P_n \div \Delta) = 2$ for all $n \in \mathbb{N}$ (where $(P_n \div \Delta) \cap \varepsilon_n B^2 = \sigma_a^{(n)} \cap \sigma_{a_2} \cap \sigma_c \cap \varepsilon_n B^2$ for all sufficiently large $n \in \mathbb{N}$) and $\dim(P \div \Delta) \leq 1$, it follows with Proposition 5.5.8 that $\rho_a^{(n)}$ lies in the relative interior of $\sigma_{a_2} \cap \sigma_c$. Since $\dim(P \div \Delta) \leq 1$, one ray of $\sigma_{a_2} \cap \sigma_c'$ is $\rho_a = \mathbb{R}_{\geq 0}\frac{1}{2}(b - a)$. Hence, $\rho_a \cap \varepsilon B^2 \subset P \div \Delta$ for some sufficiently small $\varepsilon > 0$, and thus we can move Δ within P such that it intersects the facet F in its relative interior.

For the reverse implication suppose x is strictly beyond the facet F of P. Then the vertices of $\mathcal{F}$ lie in the interior of $\operatorname{conv}(P, x)$, and thus for sufficiently small $\varepsilon > 0$, it follows that $(P \div \ell) \cap \varepsilon B^2 \subset \operatorname{conv}(P, x) \div \Delta$. That is, $\dim(\operatorname{conv}(P, x) \div \Delta) = 2$, i.e., an $\mathbb{R}$-translation of Δ is contained in the interior of $\operatorname{conv}(P, x)$ by Lemma 5.2.17. □

Certainly, the previous proof heavily relies on properties of 2-dimensional geometry. It would be interesting to know a characterisation of locked facets similar to Proposition 5.5.7 in higher dimensions:

Question 5.5.9. Find a characterisation of $\mathbb{R}$-locked facets in d dimensions for $d \geq 3$ similar to the one in Proposition 5.5.7.

The following statements will be useful to prove that facets of our candidate maximal polygons are locked and follow by Proposition 5.5.7.

Corollary 5.5.10. *Let P be an $\mathbb{R}$-Δ_2-free polygon containing $\Delta = \operatorname{conv}(v_1, v_2, v_3)$, an $\mathbb{R}$-unimodular copy of Δ_2. Suppose that each vertex v_i lies in the relative interior of a distinct facet F_i of P. If the lines spanned by F_2 and F_3 meet at a point, then F_1 is locked. See Figure 5.16.*

Proof. By the assumption, Δ is an $\mathbb{R}$-unimodular copy of Δ_2 that is contained in P such that $F_1 \cap \Delta$ is a vertex of Δ that lies in the relative interior of F_1. Since the lines spanned by F_2, F_3 intersect in a point beneath F_1, it follows that $\dim(P \div \operatorname{conv}(v_2, v_3)) = 2$. The statement follows by Proposition 5.5.7. □

Remark 5.5.11. Note that in Corollary 5.5.10, the point where the two lines spanned by the facets F_2 and F_3 meet is beneath the facet F_1. It cannot be beyond the facet F_1, as

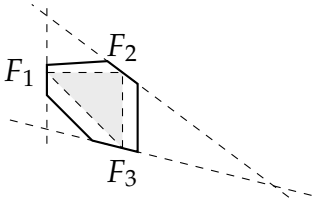

FIGURE 5.16: Facets F_1, F_2, F_3 are locked by Corollary 5.5.10.

otherwise $\dim(P \div \Delta) = 2$, and thus an $\mathbb{R}$-translation of Δ is contained in the interior of P.

Corollary 5.5.12. *If P is an $\mathbb{R}$-Δ_2-free polygon containing $\Delta = \operatorname{conv}(v_1, v_2, v_3)$, an $\mathbb{R}$-unimodular copy of Δ_2, with v_1, v_2 lying in the relative interior of two distinct parallel facets F_1, F_2 of P, while $v_3 \in \operatorname{int}(P)$, then the two parallel facets are locked.*

Proof. We show that F_1 is locked (a similar argument works for F_2). Note Δ is an $\mathbb{R}$-unimodular copy of Δ_2 contained in P such that $F_1 \cap \Delta$ is a vertex of Δ that is contained in the relative interior of F_1. Since $v_3 \in \operatorname{int}(P)$, we have $\dim(P \div \operatorname{conv}(v_2, v_3)) = 2$. The statement follows by Proposition 5.5.7. □

We now construct a family of maximal $\mathbb{R}$-Δ_2-free bodies consisting of all parallelograms circumscribed around a unit square $[0,1]^2$. An $\mathbb{R}$-unimodular copy of $[0,1]^2$ we call an $\mathbb{R}$-*unimodular parallelogram* (or simply *unimodular parallelogram* if it is clear from the context that we consider $\mathbb{R}$-unimodular copies).

Proposition 5.5.13. *If P is a parallelogram such that the relative interior of each of its facets contains one vertex of a fixed unimodular parallelogram, see Figure 5.17, then P is a maximal $\mathbb{R}$-Δ_2-free convex set.*

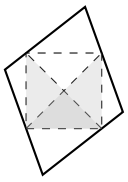

FIGURE 5.17: A parallelogram circumscribed around a unit square. Any such parallelogram is maximal $\mathbb{R}$-Δ_2-free, since each facet is locked.

Proof. We first show P is $\mathbb{R}$-Δ_2-free. Up to an $\mathbb{R}$-unimodular transformation, we can assume that the unimodular parallelogram is the standard unit square $Q = [0,1]^2$. Note P is contained in the union of the vertical and horizontal strip containing Q, and two vertices of P lie in each strip. Thus the parallel lines supporting facets of P through e_1 and e_2 have positive slope, while those through $\mathbf{0}$ and $e_1 + e_2$ have negative slope. We call the parallel lines through $\mathbf{0}$ and $e_1 + e_2$ respectively L and $L + e_1 + e_2$.

Let $v = (v_1, v_2) \in \mathbb{R}^2$ be a normal vector to L (which is not necessarily rational). Since L has negative slope, we can assume $v \in \mathbb{R}^2_{>0}$. The lattice segment $\operatorname{conv}(\mathbf{0}, e_1 + e_2)$ has endpoints on both lines, and thus the width of P with respect to v is $\langle v, e_1 + e_2 \rangle =$

$v_1 + v_2$. Any segment with width in direction v larger than this can't be between the two lines, and hence doesn't lie in P.

Our goal is to show that every segment that is contained in P and that is an $\mathbb{R}$-translation of a primitive lattice segment is contained in Q. Hence, the only $\mathbb{R}$-unimodular copies of Δ_2 that are contained in P are an $\mathbb{R}$-translation of one of the unimodular triangles contained in Q. For any primitive lattice segment ℓ there exists a $\mathbb{Z}$-translation such that $\ell \subset \mathbb{R}^2_{\geq 0}$ or $\ell \subset \mathbb{R}_{\geq 0} \times \mathbb{R}_{\leq 0}$. Note a segment parallel to the primitive lattice segment $\operatorname{conv}(\mathbf{0}, me_1 + ne_2)$, for integers m, n with $\gcd(m, n) = 1$, has width in direction v equal to $mv_1 + nv_2$. If $m, n \geq 1$ and $m + n > 2$, the segment cannot be contained in P. We have thus excluded all primitive lattice segments that are contained in $\mathbb{R}^2_{\geq 0}$ (up to a $\mathbb{Z}$-translation) and that can't be moved in the square Q via an $\mathbb{R}$-translation. An analogous argument using the other pair of parallel facets disqualifies all primitive lattice segments that are contained in $\mathbb{R}_{\geq 0} \times \mathbb{R}_{\leq 0}$ (up to a $\mathbb{Z}$-translation) and that can't be moved in the square Q via an $\mathbb{R}$-translation.

The only segments which are contained in P are therefore $\mathbb{R}$-translations of the lattice segments contained in Q. It follows that the only $\mathbb{R}$-unimodular copies of Δ_2 contained in P are those contained in Q. Since no translation of these is contained in the relative interior of P (see Lemma 5.2.17), P is $\mathbb{R}$-Δ_2-free.

We now wish to show that P is maximal with this property. To do so, we apply Corollary 5.5.10 for each facet of P: the square Q contains four unimodular triangles, each of which has one vertex in the interior of three of the four facets of P. Consider $\operatorname{conv}(\mathbf{0}, e_1, e_2)$: this triangle shows that the facet containing e_1 is locked, because the facets of P containing $\mathbf{0}$ and e_2 are consecutive and thus meet at a point beneath the facet containing e_1. Thus the conditions of Corollary 5.5.10 are satisfied and the facet is locked. The same triangle shows that the facet of P containing e_2 is locked, while applying the same arguments to the triangle $\operatorname{conv}(\mathbf{0}, e_1, e_1 + e_2)$ shows that the remaining two facets are also locked. As we have remarked earlier, when all facets of an $\mathbb{R}$-Δ_2-free polygon are locked, the polygon is maximal. □

We thus have a family of quadrilaterals with plenty of structure that are maximal $\mathbb{R}$-Δ_2-free. However, there are many examples of maximal $\mathbb{R}$-Δ_2-free quadrilaterals which we do not know how to characterise. On the left of Figure 5.18 we see one such example. That this quadrilateral Q is $\mathbb{R}$-Δ_2-free can be seen by checking that any unimodular triangle which fits within a box circumscribed to Q cannot be translated into Q (see the git-repository mentioned above for a Magma script that automates this verification). To prove that it is inclusion-maximal, we can again apply Corollary 5.5.10 to each facet: in Figure 5.18 the unimodular triangles corresponding to each locked facet are represented. There are also examples of maximal $\mathbb{R}$-Δ_2-free polygons with more facets. On the right side of Figure 5.18 is one such example. Again the fact that it is $\mathbb{R}$-Δ_2-free can be checked by testing all unimodular triangles which fit into an appropriate rectangle (see also the git-repository from above), while its maximality follows from applying Corollary 5.5.10 to each facet, with respect to the triangles inscribed to the hexagon in Figure 5.18.

In Section 5.5.1 we showed that maximal $\mathbb{Z}$-Δ_2-free polygons have at most 4 facets. It is natural to ask if there is also an upper bound on the facets of maximal $\mathbb{R}$-Δ_2-free polygons. In fact, Lovasz proved that maximal hollow convex bodies in any

FIGURE 5.18: The quadrilateral on the left with vertices $(-0.21, 0.11)$, $(0.46, 0.98)$, $(1.42, 1.02)$, $(0.82, -0.42)$ is maximal $\mathbb{R}$-Δ_2-free, as certified by the inscribed triangles.
On the right is a maximal $\mathbb{R}$-Δ_2-free hexagon with vertices $(0, 0.7)$, $(0, 1.25)$, $(0.4, 1.45)$, $(1.37, 0.72)$, $(1.2, -0.05)$, $(0.6, 0.1)$. The inscribed triangles certify that each facet is locked, relying on the fact that no two facets are parallel.

dimension d have at most 2^d facets (see [5] for a complete proof). This suggests the following questions.

Question 5.5.14. Is there an upper bound on the number of facets of maximal $\mathbb{R}$-Δ_d-free polytopes in $\mathbb{R}^d$? For maximal $\mathbb{Z}$-Δ_d-free polytopes?

Bibliography

[1] Mohammad Akhtar and Alexander Kasprzyk. "Mutations of fake weighted projective planes". In: *Proceedings of the Edinburgh Mathematical Society* 59.2 (2016), pp. 271–285.

[2] Mohammad Akhtar et al. "Minkowski polynomials and mutations". In: *SIGMA Symmetry Integrability Geom. Methods Appl.* 8 (2012). doi:10.3842/SIGMA.2012.094, Paper 094, 17.

[3] Mohammad Akhtar et al. "Mirror symmetry and the classification of orbifold del Pezzo surfaces". In: *Proc. Amer. Math. Soc.* 144.2 (2016). doi:10.1090/proc/12876, pp. 513–527. ISSN: 0002-9939.

[4] C. Arezzo, A. Loi, and F. Zuddas. "Some remarks on the symplectic and Kähler geometry of toric varieties". In: *Ann. Mat. Pura Appl. (4)* 195.4 (2016), pp. 1287–1304. ISSN: 0373-3114. DOI: 10.1007/s10231-015-0516-9. URL: https://mathscinet.ams.org/mathscinet-getitem?mr=3522347.

[5] G. Averkov. "A proof of Lovász theorem on maximal lattice-free sets". In: *Beiträge zur Algebra und Geometrie* 54 (2013), pp. 105–109. DOI: 10.1007/s13366-012-0092-8.

[6] G. Averkov et al. "A local maximizer for lattice width of 3-dimensional hollow bodies". In: *Discrete Appl. Math.* 298 (2021), pp. 129–142. ISSN: 0166-218X. DOI: 10.1016/j.dam.2021.04.009. URL: https://mathscinet.ams.org/mathscinet-getitem?mr=4248373.

[7] Gennadiy Averkov, Johannes Hofscheier, and Benjamin Nill. "Generalized flatness constants, spanning lattice polytopes, and the Gromov width". In: *manuscripta mathematica* 170.1 (2023), pp. 147–165.

[8] W. Banaszczyk et al. "The flatness theorem for nonsymmetric convex bodies via the local theory of Banach spaces". In: *Math. Oper. Res.* 24.3 (1999), pp. 728–750. ISSN: 0364-765X. DOI: 10.1287/moor.24.3.728. URL: https://mathscinet.ams.org/mathscinet-getitem?mr=1854250.

[9] A. Barvinok. *A course in convexity*. Vol. 54. Graduate Studies in Mathematics. American Mathematical Society, Providence, RI, 2002, pp. x+366. ISBN: 0-8218-2968-8. DOI: 10.1090/gsm/054. URL: https://mathscinet.ams.org/mathscinet-getitem?mr=1940576.

[10] Victor Batyrev. "Lattice polytopes with a given h^*-polynomial". In: *Algebraic and geometric combinatorics*. Amer. Math. Soc., Providence, RI, 2006.

[11] Victor Batyrev and Benjamin Nill. "Combinatorial aspects of mirror symmetry". In: *Contemporary Mathematics* 452 (2008), pp. 35–66.

[12] Victor V. Batyrev. "Dual polyhedra and mirror symmetry for Calabi-Yau hypersurfaces in toric varieties". In: *J. Algebraic Geom.* 3.3 (1994), pp. 493–535. ISSN: 1056-3911.

[13] Victor V. Batyrev and Elena N. Selivanova. "Einstein-Kähler metrics on symmetric toric Fano manifolds". In: *J. Reine Angew. Math.* 512 (1999). doi:10.1515/crll.1999.054, pp. 225–236. ISSN: 0075-4102.

[14] Robert J. Berman, Sébastien Boucksom, and Mattias Jonsson. "A variational approach to the Yau–Tian–Donaldson conjecture". In: *J. Amer. Math. Soc.* 34.3 (2021). doi:10.1090/jams/964, pp. 605–652. ISSN: 0894-0347.

[15] Harold Blum, Yuchen Liu, and Chenyang Xu. "Openness of K-semistability for Fano varieties". In: *Duke Math. J.* 171.13 (2022). doi:10.1215/00127094-2022-0054, pp. 2753–2797. ISSN: 0012-7094.

[16] Wieb Bosma, John Cannon, and Catherine Playoust. "The Magma algebra system. I. The user language". In: vol. 24. 3-4. doi:10.1006/jsco.1996.0125. 1997, pp. 235–265.

[17] Daniel Cavey and Edwin Kutas. "Classification of minimal polygons with specified singularity content". In: *Interactions with lattice polytopes*. Vol. 386. Springer Proc. Math. Stat. doi:10.1007/978-3-030-98327-7_5. Springer, Cham, 2022, pp. 115–134.

[18] J. Chaidez and B. Wormleighton. "ECH embedding obstructions for rational surfaces". In: (Aug. 2020). eprint: 2008.10125. URL: https://arxiv.org/pdf/2008.10125.pdf.

[19] Xiuxiong Chen, Simon Donaldson, and Song Sun. "Kähler-Einstein metrics on Fano manifolds. I: Approximation of metrics with cone singularities". In: *J. Amer. Math. Soc.* 28.1 (2015). doi:10.1090/S0894-0347-2014-00799-2, pp. 183–197. ISSN: 0894-0347.

[20] Xiuxiong Chen, Simon Donaldson, and Song Sun. "Kähler-Einstein metrics on Fano manifolds. II: Limits with cone angle less than 2π". In: *J. Amer. Math. Soc.* 28.1 (2015). doi:10.1090/S0894-0347-2014-00800-6, pp. 199–234. ISSN: 0894-0347.

[21] V Chvátal. "On certain polytopes associated with graphs". In: *J. Combin. Theory, Ser. B* 18 (1975), pp. 138–154.

[22] Tom Coates et al. "Maximally mutable Laurent polynomials". In: *Proceedings of the Royal Society A* 477 (2021), p. 20210584.

[23] Tom Coates et al. "Mirror symmetry and Fano manifolds". In: *European Congress of Mathematics*. doi:10.4171/120. Eur. Math. Soc., Zürich, 2013, pp. 285–300.

[24] Tom Coates et al. "Quantum periods for 3-dimensional Fano manifolds". In: *Geom. Topol.* 20.1 (2016). doi:10.2140/gt.2016.20.103, pp. 103–256. ISSN: 1465-3060.

[25] G. Codenotti and F. Santos. "Hollow polytopes of large width". In: *Proc. Amer. Math. Soc.* 148 (2020), pp. 835–850. DOI: 10.1090/proc/14721. URL: https://doi.org/10.1090/proc/14721.

[26] Giulia Codenotti, Thomas Hall, and Johannes Hofscheier. "Generalised Flatness Constants: A Framework Applied in Dimension 2". In: *arXiv:2110.02770* (2021). URL: https://arxiv.org/abs/2110.02770.

[27] Heinke Conrads. "Weighted projective spaces and reflexive simplices". In: *Manuscripta Math.* 107.2 (2002). doi:10.1007/s002290100235, pp. 215–227. ISSN: 0025-2611.

[28] Alessio Corti and Liana Heuberger. "Del Pezzo surfaces with $\frac{1}{3}(1,1)$ points". In: *Manuscripta Mathematica* 153 (2017), pp. 71–118.

[29] D.A. Cox, J.B. Little, and H.K. Schenck. *Toric Varieties*. Graduate studies in mathematics. American Mathematical Society, 2011. ISBN: 9780821848197. URL: https://books.google.co.uk/books?id=AoSDAwAAQBAJ.

[30] Simon Donaldson. "Scalar curvature and stability of toric varieties". In: *J. Differential Geom.* 62.2 (2002). doi:10.4310/jdg/1090950195, pp. 289–349. ISSN: 0022-040X.

[31] X. Fang, P. Littelmann, and M. Pabiniak. "Simplices in Newton-Okounkov bodies and the Gromov width of coadjoint orbits". In: *Bull. Lond. Math. Soc.* 50.2 (2018), pp. 202–218. ISSN: 0024-6093. DOI: 10.1112/blms.12130. URL: https://mathscinet.ams.org/mathscinet-getitem?mr=3830114.

[32] E. Gawrilow and M. Joswig. "polymake: a framework for analyzing convex polytopes". In: *Polytopes—combinatorics and computation (Oberwolfach, 1997)*. Vol. 29. DMV Sem. Birkhäuser, Basel, 2000, pp. 43–73. URL: https://mathscinet.ams.org/mathscinet-getitem?mr=1785292.

[33] Israel M Gelfand et al. "Combinatorial geometries, convex polyhedra, and Schubert cells". In: *Advances in Mathematics* 63.3 (1987), pp. 301–316.

[34] M. Gromov. "Pseudo holomorphic curves in symplectic manifolds". In: *Invent. Math.* 82.2 (1985), pp. 307–347. ISSN: 0020-9910. DOI: 10.1007/BF01388806. URL: https://mathscinet.ams.org/mathscinet-getitem?mr=809718.

[35] Christian Haase and Jan Hofmann. "Convex-normal (pairs of) polytopes". In: *Canadian Mathematical Bulletin* 60.3 (2017), 510–521.

[36] Thomas Hall. "A New Mutation Invariant of Fano Polygons". In: *Preparation* (2024).

[37] Thomas Hall. "On the Uniqueness of Kähler-Einstein Polygons in Mutation-Equivalence Classes". In: *arXiv:2402.02832* (2024). URL: https://arxiv.org/abs/2402.02832.

[38] Thomas Hall et al. "Nearly Gorenstein Polytopes". In: *Electronic Journal of Combinatorics* (2023). URL: https://www.combinatorics.org/ojs/index.php/eljc/article/view/v30i4p42.

[39] G. H. Hardy and E. M. Wright. *An introduction to the theory of numbers*. Sixth. Revised by D. R. Heath-Brown and J. H. Silverman, With a foreword by Andrew Wiles. Oxford University Press, Oxford, 2008, pp. xxii+621. ISBN: 978-0-19-921986-5. URL: https://mathscinet.ams.org/mathscinet-getitem?mr=2445243.

[40] Jürgen Herzog, Takayuki Hibi, and Hidefumi Ohsugi. *Binomial ideals*. Vol. 279. Springer, 2018.

[41] Jürgen Herzog, Takayuki Hibi, and Dumitru I Stamate. "Canonical trace ideal and residue for numerical semigroup rings". In: *Semigroup Forum*. Vol. 103. Springer. 2021, pp. 550–566.

[42] Jürgen Herzog, Takayuki Hibi, and Dumitru I Stamate. "The trace of the canonical module". In: *Israel Journal of Mathematics* 233 (2019), pp. 133–165.

[43] Jürgen Herzog, Fatemeh Mohammadi, and Janet Page. "Measuring the non-Gorenstein locus of Hibi rings and normal affine semigroup rings". In: *Journal of Algebra* 540 (2019), pp. 78–99.

[44] Takayuki Hibi. "Distributive lattices, affine semigroup rings and algebras with straightening laws". In: *Commutative algebra and combinatorics* 11 (1987), pp. 93–109.

[45] Takayuki Hibi. "Dual polytopes of rational convex polytopes". In: *Combinatorica* 12 (1992), pp. 237–240.

[46] Takayuki Hibi and Dumitru I Stamate. "Nearly Gorenstein rings arising from finite graphs". In: *The Electronic Journal of Combinatorics* (2021), P3–28.

[47] Takayuki Hibi et al. "Gorenstein graphic matroids". In: *Israel Journal of Mathematics* 243.1 (2021), pp. 1–26.

[48] Akihiro Higashitani and Koji Matsushita. "Conic divisorial ideals and non-commutative crepant resolutions of edge rings of complete multipartite graphs". In: *Journal of Algebra* 594 (2022), pp. 685–711.

[49] E. Hlawka, J. Schoissengeier, and R. Taschner. *Geometric and analytic number theory*. Universitext. Translated from the 1986 German edition by Charles Thomas. Springer-Verlag, Berlin, 1991, pp. x+238. ISBN: 3-540-52016-3. DOI: 10.1007/978-3-642-75306-0. URL: https://mathscinet.ams.org/mathscinet-getitem?mr=1123023.

[50] J. Hofscheier, L. Katthän, and B. Nill. "Ehrhart theory of spanning lattice polytopes". In: *Int. Math. Res. Not. IMRN* 19 (2018), pp. 5947–5973. ISSN: 1073-7928. DOI: 10.1093/imrn/rnx065. URL: https://mathscinet.ams.org/mathscinet-getitem?mr=3867398.

[51] J. Hofscheier, L. Katthän, and B. Nill. "Spanning Lattice Polytopes and the Uniform Position Principle". In: (Nov. 2017). eprint: 1711.09512. URL: https://arxiv.org/pdf/1711.09512.pdf.

[52] C. A. J. Hurkens. "Blowing up convex sets in the plane". In: *Linear Algebra Appl.* 134 (1990), pp. 121–128. ISSN: 0024-3795. DOI: 10.1016/0024-3795(90)90010-A. URL: https://doi.org/10.1016/0024-3795(90)90010-A.

[53] DongSeon Hwang and Yeonsu Kim. "On barycentric transformations of Fano polytopes". In: *Bull. Korean Math. Soc.* 58.5 (2021). doi:10.4134/BKMS.b200928, pp. 1247–1260. ISSN: 1015-8634.

[54] DongSeon Hwang and Yeonsu Kim. "On Kähler–Einstein Fano polygons". arXiv:2012.13373 [math.AG]. 2020.

[55] T. Hwang, E. Lee, and D. Y. Suh. "The Gromov width of generalized Bott manifolds". In: *Int. Math. Res. Not. IMRN* 9 (2021), pp. 7096–7131. ISSN: 1073-7928. DOI: 10.1093/imrn/rnz066. URL: https://mathscinet.ams.org/mathscinet-getitem?mr=4251298.

[56] Nathan Owen Ilten. "Mutations of Laurent polynomials and flat families with toric fibers". In: *SIGMA Symmetry Integrability Geom. Methods Appl.* 8 (2012). doi:10.3842/SIGMA.2012.047, Paper 047, 7.

[57] Wolfram Research, Inc. *Mathematica, Version 12.3*. Champaign, IL, 2021. URL: https://www.wolfram.com/mathematica.

[58] Chen Jiang. "Boundedness of $\mathbb{Q}$-Fano varieties with degrees and alpha-invariants bounded from below". In: *Ann. Sci. Éc. Norm. Supér. (4)* 53.5 (2020). doi:10.24033/asens.2445, pp. 1235–1248. ISSN: 0012-9593.

[59] M. Joswig. *Essentials of tropical combinatorics*. Graduate Studies in Mathematics. Providence, RI: American Mathematical Society, 2022.

[60] R. Kannan and L. Lovász. "Covering minima and lattice-point-free convex bodies". In: *Ann. of Math. (2)* 128.3 (1988), pp. 577–602. ISSN: 0003-486X. DOI: 10.2307/1971436. URL: https://mathscinet.ams.org/mathscinet-getitem?mr=970611.

[61] Y. Karshon and S. Tolman. "The Gromov width of complex Grassmannians". In: *Algebr. Geom. Topol.* 5 (2005), pp. 911–922. ISSN: 1472-2747. DOI: 10.2140/agt.2005.5.911. URL: https://mathscinet.ams.org/mathscinet-getitem?mr=2171798.

[62] Alexander M. Kasprzyk and Mohammad Akhtar. "Singularity content". arXiv:1401.5458 [math.AG]. 2014.

[63] Alexander M. Kasprzyk, Maximilian Kreuzer, and Benjamin Nill. "On the combinatorial classification of toric log del Pezzo surfaces". In: *LMS J. Comput. Math.* 13 (2010). doi:10.1112/S1461157008000387, pp. 33–46.

[64] Alexander M. Kasprzyk and Benjamin Nill. "Fano polytopes". In: *Strings, gauge fields, and the geometry behind*. World Sci. Publ., Hackensack, NJ, 2013, pp. 349–364.

[65] Alexander M. Kasprzyk and Benjamin Nill. "Reflexive polytopes of higher index and the number 12". In: *Electron. J. Combin.* 19.3 (2012). doi:10.37236/2366, Paper 9, 18.

[66] Alexander M. Kasprzyk, Benjamin Nill, and Thomas Prince. "Minimality and mutation-equivalence of polygons". In: *Forum Math. Sigma* 5 (2017). doi:10.1017/fms.2017.10, Paper No. e18, 48.

[67] K. Kaveh. "Toric degenerations and symplectic geometry of smooth projective varieties". In: *J. Lond. Math. Soc. (2)* 99.2 (2019), pp. 377–402. ISSN: 0024-6107. DOI: 10.1112/jlms.12173. URL: https://mathscinet.ams.org/mathscinet-getitem?mr=3939260.

[68] A. Ya. Khinchine. "A quantitative formulation of the approximation theory of Kronecker". In: *Izvestiya Akad. Nauk SSSR. Ser. Mat.* 12 (1948), pp. 113–122. ISSN: 0373-2436. URL: https://mathscinet.ams.org/mathscinet-getitem?mr=0024925.

[69] Max Kölbl. "Gorenstein graphic matroids from multigraphs". In: *Annals of Combinatorics* 24.2 (2020), pp. 395–403.

[70] L. Kronecker. "Näherungsweise ganzzahlige Auflösung linearer Gleichungen". German. In: *Berl. Ber.* 1885 (1885), pp. 1271–1300.

[71] J. Latschev, D. McDuff, and F. Schlenk. "The Gromov width of 4-dimensional tori". In: *Geom. Topol.* 17.5 (2013), pp. 2813–2853. ISSN: 1465-3060. DOI: 10.2140/gt.2013.17.2813. URL: https://mathscinet.ams.org/mathscinet-getitem?mr=3190299.

[72] Chi Li, Gang Tian, and Feng Wang. "The uniform version of Yau–Tian–Donaldson conjecture for singular Fano varieties". In: *Peking Math. J.* 5.2 (2022). doi:10.1007/s42543-021-00039-5, pp. 383–426. ISSN: 2096-6075.

[73] Chi Li, Xiaowei Wang, and Chenyang Xu. "On the proper moduli spaces of smoothable Kähler-Einstein Fano varieties". In: *Duke Math. J.* 168.8 (2019). doi:10.1215/00127094-2018-0069, pp. 1387–1459. ISSN: 0012-7094.

[74] G. Lu. "Symplectic capacities of toric manifolds and related results". In: *Nagoya Math. J.* 181 (2006), pp. 149–184. ISSN: 0027-7630. URL: https://mathscinet.ams.org/mathscinet-getitem?mr=2210713.

[75] George Mackiw. "Finite groups of 2×2 integer matrices". In: *Math. Mag.* 69.5 (1996). doi:10.2307/2691281, pp. 356–361. ISSN: 0025-570X.

[76] A. Mandini and M. Pabiniak. "On the Gromov width of polygon spaces". In: *Transform. Groups* 23.1 (2018), pp. 149–183. ISSN: 1083-4362. DOI: 10.1007/s00031-017-9430-0. URL: https://mathscinet.ams.org/mathscinet-getitem?mr=3763945.

[77] A. Marinković and M. Pabiniak. "Every symplectic toric orbifold is a centered reduction of a Cartesian product of weighted projective spaces". In: *Int. Math. Res. Not. IMRN* 23 (2015), pp. 12432–12458. ISSN: 1073-7928. DOI: 10.1093/imrn/rnv066. URL: https://mathscinet.ams.org/mathscinet-getitem?mr=3431626.

[78] Aaron Meurer et al. "SymPy: symbolic computing in Python". In: *PeerJ Computer Science* 3 (Jan. 2017), e103. ISSN: 2376-5992. DOI: 10.7717/peerj-cs.103. URL: https://doi.org/10.7717/peerj-cs.103.

[79] Sora Miyashita. "Levelness versus nearly Gorensteinness of homogeneous rings". In: *J. Pure Appl. Algebra* (2024).

[80] Sora Miyashita. "Nearly Gorenstein projective monomial curves of small codimension". In: *J. Comm. Alg.* (to appear).

[81] Mitsuhiro Miyazaki. "Gorenstein on the punctured spectrum and nearly Gorenstein property of the Ehrhart ring of the stable set polytope of an h-perfect graph". In: *arXiv:2201.02957* (2022).

[82] Mircea Mustaţa and Sam Payne. "Ehrhart polynomials and stringy Betti numbers". In: *Math. Ann.* 333 (2005), pp. 787–795.

[83] Benjamin Nill and Andreas Paffenholz. "Examples of Kähler-Einstein toric Fano manifolds associated to non-symmetric reflexive polytopes". In: *Beitr. Algebra Geom.* 52.2 (2011). doi:10.1007/s13366-011-0041-y, pp. 297–304. ISSN: 0138-4821.

[84] Hidefumi Ohsugi and Takayuki Hibi. "Convex polytopes all of whose reverse lexicographic initial ideals are squarefree". In: *Proc. Amer. Math. Soc.* 129.9 (2001), pp. 2541–2546.

[85] Hidefumi Ohsugi and Takayuki Hibi. "Normal polytopes arising from finite graphs". In: *Journal of Algebra* 207.2 (1998), pp. 409–426.

[86] Hidefumi Ohsugi and Takayuki Hibi. "Special simplices and Gorenstein toric rings". In: *J. Combin. Theory Ser. A* 113 (2006), 718–725.

[87] Alessandro Oneto and Andrea Petracci. "On the quantum periods of del Pezzo surfaces with $\frac{1}{3}(1,1)$ singularities". In: *Adv. Geom.* 18.3 (2018). doi:10.1515/advgeom-2017-0048, pp. 303–336. ISSN: 1615-715X.

[88] Miles Anthony Reid. "Surface cyclic quotient singularities and Hirzebruch–Jung resolutions". In: 2003. URL: https://api.semanticscholar.org/CorpusID:10811346.

[89] R. T. Rockafellar. *Convex analysis*. Princeton Landmarks in Mathematics. Reprint of the 1970 original, Princeton Paperbacks. Princeton University Press, Princeton, NJ, 1997, pp. xviii+451. ISBN: 0-691-01586-4. URL: https://mathscinet.ams.org/mathscinet-getitem?mr=1451876.

[90] Gerhard Rosenberger. "Über die Diophantische Gleichung ax2 + by2 + cz2 = dxyz". In: *Journal für die reine und angewandte Mathematik* 305 (1979), pp. 122–125. URL: http://eudml.org/doc/152079.

[91] F. Schlenk. *Embedding problems in symplectic geometry*. Vol. 40. De Gruyter Expositions in Mathematics. Walter de Gruyter GmbH & Co. KG, Berlin, 2005, pp. x+250. ISBN: 3-11-017876-1. DOI: 10.1515/9783110199697. URL: https://mathscinet.ams.org/mathscinet-getitem?mr=2147307.

[92] R. Schneider. *Convex bodies: the Brunn-Minkowski theory*. expanded. Vol. 151. Encyclopedia of Mathematics and its Applications. Cambridge University Press, Cambridge, 2014, pp. xxii+736. ISBN: 978-1-107-60101-7. URL: https://mathscinet.ams.org/mathscinet-getitem?mr=3155183.

[93] C. L. Siegel. *Lectures on the geometry of numbers*. Notes by B. Friedman, Rewritten by Komaravolu Chandrasekharan with the assistance of Rudolf Suter, With a preface by Chandrasekharan. Springer-Verlag, Berlin, 1989, pp. x+160. ISBN: 3-540-50629-2. DOI: 10.1007/978-3-662-08287-4. URL: https://mathscinet.ams.org/mathscinet-getitem?mr=1020761.

[94] Aron Simis, Wolmer V Vasconcelos, and Rafael H Villarreal. "On the ideal theory of graphs". In: *Journal of Algebra* 167.2 (1994), pp. 389–416.

[95] Richard P Stanley. *Combinatorics and commutative algebra*. Vol. 41. Springer Science & Business Media, 2007.

[96] Richard P Stanley. "Two poset polytopes". In: *Discrete Comput. Geom.* 1 (1986), pp. 9–23.

[97] Nawaz Sultani and Rachel Webb. "Some applications of abelianization in Gromov–Witten theory". arXiv:2208.07439 [math.AG]. 2023.

[98] Felix Tellander and Martin Helmer. "Cohen-Macaulay property of Feynman integrals". In: *Communications in Mathematical Physics* (2022), pp. 1–17.

[99] Gang Tian. "K-stability and Kähler-Einstein metrics". In: *Comm. Pure Appl. Math.* 68.7 (2015). doi:10.1002/cpa.21578, pp. 1085–1156. ISSN: 0010-3640.

[100] Gang Tian. "Kähler-Einstein metrics with positive scalar curvature". In: *Invent. Math.* 130.1 (1997). doi:10.1007/s002220050176, pp. 1–37. ISSN: 0020-9910.

[101] Klaus Truemper. *Matroid decomposition*. Vol. 6. Citeseer, 1992.

[102] N Viêt, Joseph Gubeladze, and W Bruns. "Normal polytopes, triangulations, and Koszul algebras." In: *Journal für die reine und angewandte Mathematik* 485 (1997), pp. 123–160.

[103] Rafael H Villarreal. *Monomial algebras*. Vol. 238. Marcel Dekker New York, 2001.

[104] Z. Waksman and M. Epelman. "On point classification in convex sets". In: *Math. Scand.* 38.1 (1976), pp. 83–96. ISSN: 0025-5521. DOI: 10.7146/math.scand.a-11619. URL: https://doi.org/10.7146/math.scand.a-11619.

[105] Neil L White. "The basis monomial ring of a matroid". In: *Advances in Mathematics* 24.2 (1977), pp. 292–297.

[106] Chenyang Xu. "K-stability of Fano varieties: an algebro-geometric approach". In: *EMS Surv. Math. Sci.* 8.1-2 (2021). doi:10.4171/emss/51, pp. 265–354. ISSN: 2308-2151.

[107] Günter Ziegler. *Lectures on Polytopes*. Springer, 1995.